# Investigating the innate and adaptive immune response in patients with metastatic colorectal cancer

**By Rosemary Millen**

Submitted in total fulfillment of the requirements of the degree of

**Doctor of Philosophy**

April 2019

Peter MacCallum Cancer Centre and Sir Peter MacCallum Department of Oncology Faculty of Medicine, Dentistry, and Health Sciences, The University of Melbourne

# ABSTRACT

The immune response is strongly associated with outcome in CRC (stages I-III). Cytotoxic CD8+ T-cells are the most important subset of immune cells positively associated with outcome, in most solid malignancies and especially CRC. However, in the advanced stage of CRC, this is not always the case. Stage-IV CRC metastasises (mCRC) commonly to the liver, which this thesis addresses. The gold standard for treatment of colorectal liver metastasis (CRLM) is surgical liver resection. Indeed, improvements in surgical techniques have greatly improved the 5-year survival of these patients; however, up to 60% of patients still recur following surgical liver resection. Understanding the progression of mCRC in the context of the immune response is the main focus of this thesis.

To investigate the immune response at the primary site of CRC, a unique retrospective cohort of *de novo* or synchronous mCRC patients (n=109) was explored. Included in this cohort were patients that had microsatellite unstable tumours (MSI) (n=12), which in the metastatic setting have a reduced overall survival (OS) and have been found to respond to checkpoint blockade inhibition (CBI). I analysed the primary tumours of these patients in the context of tumour infiltrating lymphocytes (TILs), immune escape mechanisms and oncogenic potential of these primary tumours, where the patients had synchronous metastatic disease. Despite high frequencies of cytotoxic CD8+ T-cells in some tumours, there was no association with OS, indicating the tumour had surpassed immune control. Expression of PD-L1 >1% on tumour cells was independently correlated with OS in multivariate analysis suggesting that tumour cells have the ability to progress in part at least by evading the immune response.

To evaluate the immune response at the metastatic site in the liver, a prospective cohort of CRLM patients was recruited (n=11) to examine the immune context in these tumours. Patients undergoing liver resection were included in the study, and freshly isolated lymphocytes from the tumour; normal liver and peripheral blood were analysed by flow cytometry. These tumours were found to have a reduced infiltration of cytotoxic CD8+ T-cells and increased infiltration of CD4+ T-cells, including T-regulatory cells that are known to suppress immune responses. This immune milieu in these tumours alludes to a reduced cytotoxic and increased immunosuppressive environment. To investigate the functional capacity of these immune cells, a novel immune cytotoxic assay was developed. This assay involved co-culturing patient-derived tumouroids with expanded autologous TILs to assess dynamic interaction of function of these cells. TILs expanded from these tumours were able to kill matched tumouroids, further indicating that when removed from the immunosuppressive TME these cells have functional ability to kill tumouroids. To assess if these TILs respond to CBI, addition of anti-PD-1

antibody was included in the co-culture assays where no improvement in killing was observed. Further investigation of other immune cell subsets in CRLM tumours was undertaken to gain an insight into other immune cell populations that may contribute to the tumour microenvironment (TME).

One population of unconventional T-cells abundant in the liver are mucosal-associated invariant T-cells (MAIT cells). These cells play a role in bacterial infections and bridge a gap between innate and adaptive immune responses, and their role in tumour immunity is less defined. These cells are of interest in the context of the TME as they have cytotoxic capability and rapid produce cytokine. When assessing MAIT cell presence in CRLM (n=25) by flow cytometry, MAIT cell frequency was reduced in the tumour compared to surrounding normal liver. The phenotype of MAIT cells in the tissue was phenotypically distinct compared to the periphery, with high expression of PD-1 and CD69, both markers of activation. To assess the potential of MAIT cells, peripheral MAIT cells were isolated from healthy donors and co-cultured with patient-derived tumouroids in an unstimulated and stimulated state. MAIT cells in both states were able to kill patient-derived tumouroids. This is the first documentation of MAIT cell killing with patient-derived material. Despite PD-1 expression on these cells, addition of anti-PD-1 antibody did not enhance this killing. Even though at reduced frequency in the tumour, MAIT cells are activated and may contribute to the tumour microenvironment (TME) in CRLM.

Patients with advanced-stage CRC have a reduced survival compared to earlier stage CRC patients. In the context of the immune response, it is evident that these tumours have evaded the immune response to progress to metastasis. The work of this thesis highlights that at the primary tumour site of patients with *de novo* mCRC, despite high frequencies of cytotoxic CD8+ T-cells, there is an inability at controlling tumour progression. This has likely arisen through immune evasive mechanisms. Therefore there should be a focus on improving the immunogenicity of these tumours to again be recognised by the immune cells. Secondly, at the metastatic site, the TME is immunosuppressed and reinvigorating the function of cytotoxic immune cells present may restore improved immune responses. Importantly, understanding the immune biology of these tumours will provide greater guidance to improve potential immune therapies for these patients into the future.

This declaration is to certify that:

i) This thesis comprises only my original work towards the PhD except where indicated in the Preface section.

ii) Due acknowledgements have been made in the text to all other material used.

iii) The thesis is fewer than 100,000 words in length, exclusive of tables, maps, bibliography and appendices.

Rosemary Millen

Peter MacCallum Cancer Centre Melbourne, Australia and Sir Peter MacCallum Department of Oncology Faculty of Medicine, Dentistry, and Health Sciences The University of Melbourne Parkville, Australia.

17th April 2019

## PREFACE

I would like to acknowledge those who directly contributed to the work presented in this thesis:

• Dr. Shona Hendry for scoring CD8+ T-cells, PD-L1 expression and MMR protein expression on tumour cells, which contributed to **Figures: 3.1-3.10** in **Chapter 3.**

• Dr David Byrne for staining CD8+ T-cells, PD-L1 and MMR proteins, which contributed to **Figures: 3.1-3.10** in **Chapter 3.**

• Dr. Vignesh Narasimhan for completing the univariate and multivariate analysis, which contributed to **Figures 3.1, 3.4, 3.10, 3.12, 3.14, 3.15, 3.16** and **Table 3.3** in **Chapter 3**.

• Dr. Joseph Kong for undertaking and compiling the data in **Figure 4.5, 4.9, 4.10, 4.12, 4.13** and **4.14** in **Chapter 4**.

• Ms Shienny Sampurno for undertaking and compiling the data in **Figure 4.7** in **Chapter 4**.

• Dr. Cori Behrenbruch and Dr. Momeneh Foroutan for undertaking and compiling the data in **Figure 5.1** in **Chapter 5**.

# PUBLICATIONS

1. *****Kong, J.C.^, Guerra, G.R^, **Millen, R^.** Roth, S., Xu, H..L., Neeson, P.N., Darcy, P.K., Kershaw, M.H., Sampurno, S., Malaterre, J., Liu, D.S., Pham, T., Wang, M., Huang, Y., Visvanathan, K., McCormick, J., Lynch, A.C., Warrier, S., Michael, M., Desai, J., Murray, W., Mitchell, C., Ngan, S., Phillips, W.A., Heriot, A.G., Ramsay, R.G. *Tumor Infiltrating Lymphocyte Function Predicts Response to Neoadjuvant Chemoradiotherapy in Locally Advanced Rectal Cancer*, Journal of Precision Oncology, 2018
   **^Equal First Author**

2. Bolther, M., Lise Dahl Andersen, K., Tolstrup, M., Visvanathan, K., Woolley, I., Skinner, N., **Millen, R**., Warner, N., Østergaard, N., Jensen-Fange, S. *Levels of regulatory B cells do not predict serological responses to hepatitis B vaccine,* Human Vaccines & Immunotherapeutics, 2018.

3. Carpinteri, S., Sampurno, S., Malaterre, J., **Millen, R**., Dean, M., Kong, J., Chittleborough, T., Heriot, A., Lynch A. C. and Ramsay, R.G. *Experimental study of delivery of humidified-warm carbon dioxide during open abdominal surgery*, British Journal of Surgery, 2018.

4. Hiller, J.G., Sampurno, S., **Millen, R**.,Kuruvilla, N., Ho, K.M., Ramsay, R.G., Riedel, B. *Impact of celecoxib on inflammation during cancer surgery: a randomized clinical trial*, Canadian Journal of Anesthesia, 2017.

5. Chen Yi Mei SL, Burchell J, Skinner N, **Millen R**, Matthews G, Hellard M, Dore GJ, Desmond PV, Sundararajan V, Thompson AJ, Visvanathan K, Sasadeusz J. *Toll-like Receptor Expression and Signaling in Peripheral Blood Mononuclear Cells Correlate With Clinical Outcomes in Acute Hepatitis C Virus Infection*. The Journal of Infectious Diseases, 2016.

6. **Millen, R.,** Malaterre, J., Cross, R.S., Carpinteri, S., Desai, J., Tran, B., Darcy, P., Gibbs, P., Sieber, O., Zeps, N., Waring, P., Fox, S., Pereira, L., Ramsay, R.G. (2016) *Immunomodulation by MYB is associated with Tumour Relapse in Patient with Early Stage Colorectal Cancer*. Oncoimmunology, 2016.

7. Malaterre, J., Pereira, L., Putoczki, T., **Millen, R**., Paquet-Fifield, S., Germann, M., Liu, J., Cheasley, D., Sampurno, S., Stacker, S., Achen, M., Ward, R., Waring, P., Mantamadiotis, T. and Ramsay, R.G. (2015) *Intestinal-specific activatable-Myb initiates colon tumorigenesis in mice*. Oncogene, 2015.

## ACKNOWLEDGEMENTS

The cumulative work of the last four years has not been solely achieved by myself but has included a range of people in my life to pull me through. First and foremost, I would like to thank my supervisor Rob Ramsay for taking me in as a work experience student eight years ago. I was lucky enough to meet Rob through his daughter Georgia, who is a dear friend of mine from school. Without Georgia's help I wouldn't be here today. Rob trained me to be the scientist I am today. He taught me presentation skills, how 'the data never lie', how to be on first-name basis with almost every person in the hospital regardless of whether they are the CEO or the cleaner. He armed me with these skills, which changed me as a person, to have complete confidence in myself and truly attempt to improve the outcome of cancer patients.

I would like to thank my second supervisor, Kumar Visvanathan for teaching me my foundations in immunological research, an area where I really found my passion. Kumar was always so willing to let me pursue scientific questions that were out of the box. I would like to thank both Rob and Kumar for giving me a lot of autonomy throughout my PhD and also backing me with my ideas. I would especially like to thank both of them for financially supporting me to complete my PhD, because I would now not be in the position of having an incredible opportunity that awaits me for my post-doc.

To my lab at Peter Mac, especially those who are past-lab members including Jordane Malatarre, Huiling Xu and Sandra Carpinteri for always supporting me through my science. To Sara Roth for teaching me strong foundations of immunology and preciseness of science, and stepping into my project later in the scene, I wish you had of been there from the start! To Lloyd Pereira, for training me from when I was just an honours student, to keep immaculate lab records and always think about the question. To Shienny Sampurno for being so integral to the lab and always saying yes to any task I needed help with. To Rebecca Abbott for giving me an opportunity to semi-supervise you as a student and all of your hard work in tissue culture, especially helping with all of my work that also contributed to this thesis. To my clinical PhD peers: Tim Chittleborough, Vignesh Narasimhan, Toan Pham, Kasmira Wilson, Jiasian Teh and Atan Das you have all added so much clinical wealth to my scientific knowledge and have become great friends. To Cori Behrenbruch for your assistance with sample collection and always being there to talk about what the future holds.

To my fellow two Musketeers: Glen Guerra and Joe Kong, it was such a hard time in the lab when we embarked on our journey and we achieved so much. The clinical aspect you taught me

as part of science is priceless and something, I will carry through with me my entire career. We had so much fun together and still managed to divide and conquer.

To all of Cancer Immunology Research, especially Paul Neeson, Paul Beavis, Jeanne Butler, Pasquale Petrone, Heloise Halse, Melissa Henderson, Amanda Oliver, Jess Michie, Andrew Freeman, *et al*. All of you have played such a significant role in very different ways. To Emma Petley, my best mate and MAIT, thank you for your friendship and guidance in all parts of my life. To Caroline Owen for mentoring me throughout my PhD and always backing me in leadership endeavours thank you, and Niranga Nawagamuwa for always saying yes. Thank you to Jane Oliaro and Sarah Ellis as my two mentors, who I could rely on getting a coffee with at anytime and getting great advice from.

To my St. Vincent's Hospital lab, that always felt like a family home when I would come over. A very special thank you to Jackie Yu, who has been on alongside the journey of my scientific career for 6 years, you are such a patient and meticulous scientist and such a good friend. To Julie Nigro for your ideas and support, especially assistance with writing applications. To Immunology Research Centre: Evelyn Salvaris, Nella Fisicaro, Jenny McRae, Veena Roberts, Doreen Fang, Neil Wilson and Peter Cowan for giving me advice and getting me through. A special thank you to Billy Nguyen and Christine Lancaster for all of your administrative help.

Thankyou to the hepatobiliary teams at Peter MacCallum Cancer Centre, St. Vincent's Hospital and Royal Melbourne Hospital. A special thank you to Associate Professor Ben Thomson, Mr Brett Knowles and Mr Simon Banting for always welcoming me into the operating theatre to collect samples. Without these samples I could not have achieved this body of work

I would like to thank my parents, Genie and Frank, for giving me many incredible opportunities, of which they sacrificed parts of their life and career to get me here. Thank you for always being so supportive in whatever I chose to do. For always supporting me financially when needed and always having a strong interest in what I was doing with my science. I really wouldn't be here without you both and although it is sad for me to leave to The Netherlands, it has been so special being back with you both and spending this time with you before I depart. Thank you to my sister Virginia, her husband Troy and their children: Eleanor and Henry for brightening up my life amidst thesis writing, and being so supportive of everything that has happened in the last 12 months. Thank you to my brother Hugh and his partner Marguerite for always being happy and asking me how the thesis is tracking. Thank you to my sister Clare for being my best friend and the one I call when I want to give up, and you talk me through to soldier on.

Finally, to my partner, Sean Cameron, who has known me for a few years, but has been my rock the last few months. Thank you for your patience in me writing this thesis. Thank you for cheering me up when I needed it and always telling me to GID. Thank you for always putting a smile on my face, grinning ear to ear, when I see you. We have still managed to have the best time during this hectic period, and I cannot wait for our adventure to Europe in 2019 that will really be once in a lifetime opportunity.

# LIST OF ABBREVIATIONS

5-FU -5-fluorouracil
5-OP-RU - 5-(2-oxo propylideneamino)-6-D-ribitylaminouracil
6-FP - 6-formyl pterin
AJCC - American joint committee on cancer
APC - Antigen presenting cell
CAR - Chimeric antigen receptor
CBA - Cytometric bead array
CBI - Checkpoint blockade inhibition
cCR - clinical Complete response
CD - Cluster of Differentiation
CRC - Colorectal cancer
CRLM-Colorectal liver metastasis
CT - Central tumour
CTLA-4 - Cytotoxic T-lymphocyte associated protein-4
DC - Dendritic cells
DFS - Disease-free survival
DL - Distant liver
dMMR - deficient mismatch repair
DN - Double negative
DP - Double positive
DSS - Disease specific survival
FACS - Fluorescent activated cell sorting
FFPE - Formalin-fixed paraffin embedded
FOLFIRI - FU/LV with irinotecan
FOLFOX - FU/LV with oxaliplatin
FULV - leucovorin
GMF - Geometric mean fluorescence
IFNγ - Interferon gamma
IHC - Immunohistochemistry
IL- Interleukin
IM - Invasive Margin
MAIT - Mucosal associated invariant T-cells
mCRC - metastatic Colorectal cancer
MDOTS/PDOTS - Murine- and Patient-derived organotypic tumour spheroids
MDSC - Myeloid-derived suppressor cells
MFI - Mean fluorescent intensity
MHC - Major histocompatibility complex
mIHC - multispectral Immunohistochemistry
MMR - Mismatch repair
MR1 - MHC-related 1
MSI - H - Microsatellite instability high
MSI - Microsatellite instability
MSS - microsatellite stable
NACRT - Neoadjuvant chemoradiotherapy

NHMRC - National health and medical research council
NIH - National Institutes of Health
NK - Natural Killer cell
NKT - Natural killer T-cells
NSCLC - Non-small cell lung cancer
OS - Overall survival
PBMC - Peripheral blood mononuclear cell
pCR - pathological Complete response
PD-1 - Programmed cell death protein -1
PD-L1 - Programmed death ligand-1
PFS - Progression-free survival
PI - Propidium iodide
PMA - Phorbol 12-myristate
pMMR - proficient mismatch repair
RC - Rectal cancer
RCC -Renal cell carcinoma
RCT - Randomised controlled trial
SD - Standard deviation
SEM - Standard error of the mean
T-regs - T-regulatory cells
TCR - T-cell receptor
Th - helper T-cells
TIL - Tumour infiltrating lymphocyte
TME - Tumour microenvironment
TNFα - Tumour necrosis factor alpha
TNM - Tumour Node Metastasis
UICC TNM - Union for international cancer control Tumour Node and Metastasis staging
VELIPI - Vascular emboli, lymphatic invasion, and perineural invasion
WES - Whole exome sequencing

# TABLE OF CONTENTS

# LIST OF FIGURES

# LIST OF TABLES

# 1. LITERATURE REVIEW

## 1.1 Cancer

Cancer is responsible for approximately 8.2 million cancer-related deaths and approximately 17 million new cases worldwide arising in 2018 (UK, 2019). The incidence of cancer cases is estimated to rise up to 70% over the next two decades (Stewart, 2014b). The broad term 'cancer' is used to describe a variety of diseases that can affect different organs within the body. The pathology involves abnormal growth of cells uncontrollably, in most cases forming a malignant tumour. These tumours can invade surrounding tissue and spread to distal sites, often-another organ in the body, a process referred to as metastasis. Metastasis to the liver is a primary cause of death from colorectal cancer (CRC) and is referred to as metastatic CRC (mCRC).

## 1.2 Colorectal Cancer

CRC is a form of cancer that develops in the colon or rectum. It is the third most common tumour worldwide, with 1.4 million cases reported and 694, 000 deaths recorded in 2012 (Stewart, 2014a). In Australia CRC is projected to account for 13.5% of new cancer cases in 2015. The number of new CRC cases in 2018 is 17,004 including 9,294 males and 7,709 females. The number of deaths due to CRC in 2018 is projected to surpass 4,129. However, the prospect of five-year relative survival has improved from 51% in the years 1985-89 to 69% in the years 2010-2014 (Welfare, 2014). CRC and its metastases are the focus of this thesis.

### 1.2.1 Risk Factors

Approximately 85-90% of CRC cases arise sporadically, due to chromosomal instability (CIN) (Grady & Carethers, 2008). The risk factors associated with CRC include increasing age and previous polyps or previous CRC. A number of environmental factors also influence the risk of developing CRC. Diet is one factor where high fat, high intake of red meat and lack of fibre may increase the risk of developing CRC (Boyle & Langman, 2000). Other environmental factors include smoking, high alcohol consumption and a sedentary lifestyle. Further, diagnosis of inflammatory bowel disease (IBD) including Crohn's disease and ulcerative colitis (UC) make up approximately 60% of the risk incidence for CRC, with severity and duration of IBD increasing risk (Jess, Rungoe, & Peyrin-Biroulet, 2012; von Roon *et al*., 2007). After initial diagnosis of IBD, the risk of developing CRC may occur within eight to 10 years. Crohn's disease affects the ilium and the colon, whereas UC affects the colon and rectum only (Abraham & Cho, 2009).

Hereditary diseases associated with CRC include Lynch syndrome (also collectively called Hereditary Non-Polyposis CRC (HNPCC)) and Familial Adenomatous Polyposis (FAP), which

account for 10-15% of CRC cases (Kinzler & Vogelstein, 1996). Lynch syndrome is characterised by a younger onset of CRC, average age 45, compared to the general population average age onset of 63. The tumours are predominantly right-sided, proximal to the splenic flexure in the colon. Adenomas can develop rapidly into carcinomas within two to three years, compared to eight-10 years in the general population (Vasen, Watson, Mecklin, & Lynch, 1999). The pathology of these tumours is poorly differentiated, with a higher infiltration of lymphocytes, and has a better prognostic outcome compared to patients with non-HNPCC CRC (Dolcetti *et al*., 1999). The diagnosis of Lynch syndrome typically involves the genetic screening for defects in DNA mismatch repair (MMR) genes that have a germline mutation in the DNA MMR genes including PSM2, MLH1, MSH2 and MSH6 (Dinh *et al*., 2011). Such cases are referred to as microsatellite instability (MSI) cases and may lead to different treatment approaches in the clinic, explained subsequently in this review.

### 1.2.2 Diagnosis

CRC is diagnosed by taking a biopsy of the primary tumour during a colonoscopy or sigmoidoscopy, which is then confirmed as adenocarcinoma by a pathologist. Subsequent whole body examination using imaging techniques including: computated topography (CT), magnetic resonance imaging (MRI) and fluorine-18 (F-18) fluorodeoxyglucose (FDG)-positron emission tomography (FDG-PET) of the chest, abdomen and pelvis is undertaken to rule out metastatic disease (Kekelidze, D'Errico, Pansini, Tyndall, & Hohmann, 2013). Not only do these imaging techniques help diagnosis but also guide the approach for appropriate treatment and surgical procedures. An effective way of determining diagnosis, prognosis and the appropriate treatment plan is a multidisciplinary team approach which includes a consensus between surgeons, medical oncologists, radiologists, pathologists and, increasingly, researchers (Morris *et al*., 2010).

### 1.2.3 Prognosis

The prognosis of CRC is determined (most commonly) by the American Joint Committee on Cancer (AJCC) Tumour Node Metastasis (TNM) staging system, which classifies the primary tumour growth (T), the number of lymph nodes affected (N) and the degree of metastatic spread (M). The prognosis of the CRC disease classified by the AJCC and compared to Duke's staging is outlined in **Table 1**. Progression of primary tumour describes invasion of the tumour into surrounding structures. $T_{is}$: Tumour *in situ*: intraepithelial or invasion of lamina propria; T1: Tumour invades sub-mucosa; T2: Tumour invades muscularis propria; T3: Tumour invades through the muscularis propria; T4a: Tumour penetrates to the surface of the visceral peritoneum; T4b: Tumour directly invades or is adherent to other structures.

When regional lymph nodes become involved the following classification describes the presence and number of lymph nodes affected, confirmed by a pathologist. Nx: Node cannot be assessed; N0: No regional lymph node metastasis; N1: Metastasis in one to three regional lymph nodes that may include; N1a: metastasis in one regional lymph node; N1b: metastasis in two to three regional lymph nodes; N1c: Tumour deposit(s) in the sub-serosa, mesentery, or non-peritonealised peri-colic or perirectal tissues without regional nodal metastasis; N2: Metastasis in four or more regional lymph nodes; N2a: Metastasis in four to six regional lymph nodes; N2b: Metastasis in seven or more regional lymph nodes.

Grading of metastases involves the following classification, which is based on the location and site of metastatic spread. M0: No metastasis; M1: Distant Metastasis; M1a: Metastasis confined to one organ or site (for example, liver, lung, ovary, non-regional node); M1b: Metastases in more than one organ/site or the peritoneum (Cancer, 2010).

**Table 1.1. Anatomic stage/prognostic groups (AJCC, 7th Edition)**

| ANATOMIC STAGE/PROGNOSTIC GROUPS | | | | | |
|---|---|---|---|---|---|
| Stage | T | N | M | Dukes* | MAC* |
| 0 | Tis | N0 | M0 | – | – |
| I | T1 | N0 | M0 | A | A |
| | T2 | N0 | M0 | A | B1 |
| IIA | T3 | N0 | M0 | B | B2 |
| IIB | T4a | N0 | M0 | B | B2 |
| IIC | T4b | N0 | M0 | B | B3 |
| IIIA | T1–T2 | N1/N1c | M0 | C | C1 |
| | T1 | N2a | M0 | C | C1 |
| IIIB | T3–T4a | N1/N1c | M0 | C | C2 |
| | T2–T3 | N2a | M0 | C | C1/C2 |
| | T1–T2 | N2b | M0 | C | C1 |
| IIIC | T4a | N2a | M0 | C | C2 |
| | T3–T4a | N2b | M0 | C | C2 |
| | T4b | N1–N2 | M0 | C | C3 |
| IVA | Any T | Any N | M1a | – | – |
| IVB | Any T | Any N | M1b | – | – |

### 1.2.4 Primary Colorectal Cancer Treatment

#### 1.2.4.1 Surgery

Surgical resection of the primary tumour is required with adequate margins to ensure there is no residual disease left behind. For primary colon carcinoma, the margins recommended are at least five cm or more. Adherent T4 tumours adjacent to other structures require en-bloc resection to obtain a resection margin of R0 (no gross or microscopic tumour remains in the primary tumour bed) (Nahas *et al*., 2017). If the disease has progressed, with lymph node involvement, a lymphadenectomy is performed with at least 12 nodes required for appropriate nodal staging (Ong & Schofield, 2016).

#### 1.2.4.2 Chemotherapy

Local disease at the primary site in the colon or rectum is typically treated by surgical removal of the tumour and any regional lymph nodes that are involved (Chang, Rodriguez-Bigas, Skibber, & Moyer, 2007). Adjuvant chemotherapy regimens may also be administered including: 5-fluorouracil (5-FU) and leucovorin (FU/LV), FU/LV with irinotecan (FOLFIRI) or FU/LV with oxaliplatin (FOLFOX) or, more recently, a combined regimen of 5-FU, irinotecan and oxaliplatin (FOLFOXFIRI) for metastatic disease.

#### 1.2.4.3 Radiotherapy

In the context of locally advanced rectal cancer, neoadjuvant chemoradiotherapy (NACRT) is offered prior to planned rectal cancer total mesorectal excision (rcTME). There have been previous reports in patients where the residual tumour is undetectable through imaging and endoscopy that are monitored for a ‘watch and wait approach (no surgery but with intensive follow up). In a study by Habr-Gama *et al*, patients who demonstrated a complete clinical response (cCR) with no follow-up surgery were monitored for a minimum of 60 months. Five-year overall survival (OS) was 93% and disease-free survival (DFS) was 85% (Habr-Gama *et al*., 2004). In addition to this, approximately 15-20% of patients who underwent NACRT and subsequent surgery had a pathological complete response (pCR), where no tumour is detected histologically post-resection (Maas *et al*., 2011). Theoretically, these patients did not require the morbid operation of rcTME. Identifying ways to predict which patients will present with a pCR is a current challenge in the field, and it is likely that randomised controlled trials (RCTs) will be required to predict this. We have developed an assay to assist in the prediction of patient response to NACRT, which will be discussed further in this review.

## 1.3 Metastatic Colorectal Cancer (mCRC)

The most common site of mCRC is the liver, followed by lung and peritoneum, and up to 40% of patients with CRC will develop systemic recurrence following curative treatment for the primary colorectal tumour (Manfredi *et al*., 2006). The accepted standard of care for liver metastases is surgical resection for patients with deemed resectable disease (Koh, 2017). Based on current guidelines by the National Health and Medical Research Council (NHMRC), patients

presenting with colorectal liver metastasis (CRLM) are stratified into three groups of either: definitively resectable disease, 'borderline' resectable and unresectable disease (Koh, 2017).

### 1.3.1 Surgery for Synchronous Disease

Patients may present with synchronous disease, where the primary and the metastatic tumours are both detected *in situ* at the time of diagnosis. Traditional strategies for treatment of synchronous CRC have been staged resections, where the primary tumour is resected with subsequent resection of the hepatic metastases. This traditional approach is mostly because synchronous resections are viewed as too challenging for the health of these patients, with a perception of higher morbidity and mortality risk. However in more recent years surgical strategies for mCRC have developed, due to safety improvements of surgical and anaesthetic procedures (Silberhumer *et al*., 2015).

Synchronous mCRC resections are becoming more common in selected patients. In a systematic review by Hillingsø & Wille-Jørgensen assessing 16 studies, it was found that there was no difference in terms of five-year survival between synchronous and staged surgical resections. Additionally, it was found that synchronous resections had a shorter hospital stay with lower perioperative morbidity. However, synchronous resection patients had a higher mortality rate than in the staged resections, although this does not appear to affect OS rates (Hillingso & Wille-Jorgensen, 2009). The flaws of this systematic review are that there is considerate heterogeneity between studies, and there is bias affecting the endpoints of the analysis, therefore a RCT would be required to settle this issue. Nevertheless, this systematic review supports the notion that a combined approach is safe in selected patients with synchronous disease with access to specialist colorectal and hepatobiliary surgeons (Hillingso & Wille-Jorgensen, 2009; Vassiliou *et al*., 2007; Weber, Bachellier, Oussoultzoglou, & Jaeck, 2003).

### 1.3.2 Surgery for Metachronous Disease

Metachronous disease presentation is where the first and second malignant transformation is variable. This means that the primary tumour may develop and be resected and a distant metastatic tumour develops consequently (Tziris *et al*., 2008). If the hepatic metastases are deemed resectable with curative intent, surgical resection offers improved long-term survival (Padman *et al*., 2013). A retrospective population-based study by Morris *et al*, demonstrated patients who presented with stage IV disease at diagnosis survived one year following primary colorectal tumour resection. Subsequent five-year survival was 42.5 per cent and 18.5 per cent for those who did and did not have liver resection respectively, as seen in **Figure 1.1** (Morris *et al*., 2010).

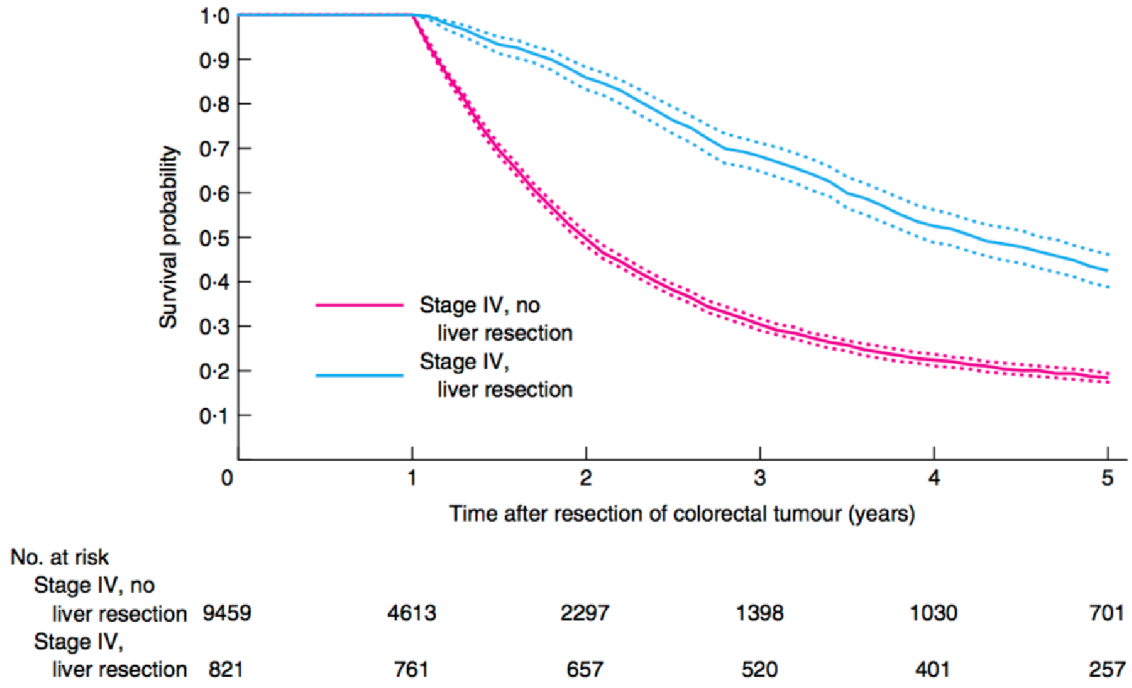


**Figure 1.1 Kaplan-Meier curves for study population overall and patients with Stage III or IV CRC with and without liver resection** (Morris *et al*, 2010)

### 1.3.3 Hepatectomy for CRLM

The standard of care for resectable hepatic metastases is surgical resection of the liver and this is associated with improved survival outcomes. Five-year survival rates post surgical resection average 40% (Choti *et al*., 2002). Studies that span 10-year follow up periods have reported that 20% of patients who underwent liver resection have shown benefit from the resection and are considered to be cured (Luca Vigano, 2012; Tomlinson JS1, 2007). Technical considerations for liver resection include the remnant volume of functional liver tissue after resection and whether vasculature is involved, to proceed with the surgery.

Surgical resection margins of the liver have an influence on prognosis and are described as the border of the tissue removed in cancer surgery (Tranchart *et al*., 2013). A positive margin indicates that tumour cells are found at the edge of the tissue and that the tumour has not been entirely resected (R1). Negative margins (>1cm) have an improved DFS (R0), however R1 margins (<1cm) have decreased DFS. The accepted gold standard is 1cm, yet more recent studies have claimed that negative margins of <1mm are associated with significantly improved five-year survival (Cady *et al*., 1998; Vandeweyer *et al*., 2009). Additional prognostic considerations include the number of liver metastases present, the response to treatment at the primary site and the degree (if any) of extra-hepatic disease (Bilchik, Poston, Adam, & Choti, 2008; Folprecht *et al*., 2010).

Observational studies reported by Morris *et al* have suggested that surgical resection of hepatic tumours either with, or without, adjuvant therapy have improved survival, compared to non-interventional therapy options (Morris *et al*., 2010; Padman *et al*., 2013; Zeman, Maciejewski, Poltorak, & Kryj, 2013). However patients that are deemed 'borderline resectable' require perioperative chemotherapy treatment to obtain any survival benefit to be eligible for liver resection (Padman *et al*., 2013).

### 1.3.4 Chemotherapy for mCRC

Unfortunately, not all patients with metastasis will have the option of a liver resection, with curative intent. The majority of patients will have disease that is either borderline resectable or unresectable (Manfredi *et al*., 2006). For patients with borderline resectable disease, perioperative chemotherapy is offered in both the neoadjuvant and adjuvant setting. Patients with potentially resectable disease should be discussed at a multidisciplinary meeting, with the treatment plan taking into consideration co-morbidities and suitability for aggressive treatment (Nott, 2017). Furthermore, in all cases, patients must be considered to be able to tolerate intensive chemotherapy (Benson *et al*., 2018; Nott, 2017; Padman *et al*., 2013; Van Cutsem *et al*., 2016).

### 1.3.5 Chemotherapy in the Neoadjuvant and Perioperative Setting

Combination of surgical resection and chemotherapy reduces the risk of relapse in mCRC patients. Down staging chemotherapy in the neoadjuvant setting provides the opportunity to reduce the size of 'borderline' resectable disease to be resectable, by debulking tumours. It can also guide adjuvant treatment, following assessment of tumour responsiveness to the chemotherapy (Nordlinger *et al*., 2008). Oxaliplatin is a third-generation platinum derivative, and the doublet combination as FOLFOX makes it the current most effective chemotherapeutic reagent for mCRC (Andre *et al*., 1999; Andre *et al*., 2004). In a RCT comparing FU/LV and FOLFOX, the latter provided a beneficial response rate of 50% with a prolonged progression-free survival (PFS) in patients with advanced CRC (de Gramont *et al*., 2000).

In line with the aforementioned study, Nordlinger *et al* adopted the FOLFOX4 regimen (Day 1: oxaliplatin, Day 2: Leucovorin) in a RCT known as the European Organisation for Research and Treatment of Cancer (EORTC) 40983 study to assess perioperative FOLFOX compared to surgery alone. Patients were randomly assigned to FOLFOX4 six weeks pre and six weeks post-surgery or surgery alone. Compared to surgery alone, perioperative FOLFOX reduced progression-free survival (PFS) by 25% in patients with mCRC. It also demonstrated that perioperative chemotherapy treatment is complementary with surgery, and this formed the basis of FOLFOX4 perioperatively as current standard practice (Nordlinger *et al*., 2008). A population-based study assessed three-year survival rates comparing chemotherapy alone

(19.5%), surgery alone (73.8%), and surgery with perioperative chemotherapy (73.7%). A very important finding of this study was that the combination therapy significantly improved resection margins compared to surgery alone, 86.2% versus 95.9% in the group treated with resection alone (p=0.038) (Padman *et al*., 2013). Collectively these studies all demonstrate the survival benefit of chemotherapy in the perioperative and adjuvant setting.

### 1.3.6 Chemotherapy in the Adjuvant Setting

Following surgical liver resection, relapse occurs in 75% of patients, with five-year relapse-free survival between 15-35% (Fong, Fortner, Sun, Brennan, & Blumgart, 1999; Nordlinger *et al*., 1996). Recurrences tend to occur within the first two years following resection, which are often confined to the liver (Fong *et al*., 1997). Therefore, using chemotherapy in the adjuvant setting may reduce the risk of hepatic recurrence and improve survival. Current NHMRC guidelines indicate that patients with a higher risk of recurrence following liver resection should receive adjuvant chemotherapy (Koh, 2017). In a pooled analysis of two multicentre randomised control phase III trials, the efficacy of systemic adjuvant chemotherapy with bolus FU/LV following liver resection was investigated. Patients were randomly assigned surgery alone or surgery followed by adjuvant chemotherapy. By combining the studies as a pooled analysis, Mitrey *et al* reasoned that this would improve statistical power. Adjuvant chemotherapy improved both PFS and overall survival (OS) in multivariate analysis, with five-year survival rates of 52.8% in the chemotherapy group and 39.6% in the surgery alone group (Mitry *et al*., 2008). These studies again confirm that adjuvant chemotherapy improves survival, with oxaliplatin-based doublet chemotherapy used as the most common regimen (Padman *et al*., 2013).

## 1.4 Biological Agents

Biological agents are used in first-line therapy for patients with mCRC. The first is bevacizumab (Avastin®) a humanised monoclonal antibody that targets the Vascular Endothelial Growth Factor-A (VEGF-A) inhibiting binding to its receptors. The second includes cetuximab (Erbitux®) and panitumumab (Vectibix®) humanised monoclonal antibodies that target the Epidermal Growth Factor Receptor (EGFR).

VEGF-A is a glycoprotein produced by neoplastic and normal cells. It is an important regulator of pathogenic and physiological angiogenesis (Ferrara, Gerber, & LeCouter, 2003; Hurwitz *et al*., 2004). Pre-clinical studies in human xenograft models demonstrated that a monoclonal antibody against VEGF-A has the ability to inhibit tumour growth *in vivo* (K. J. Kim *et al*., 1993). Initial Phase II trials investigated the efficacy of bevacizumab with FU/LV at high and low doses compared to FU/LV alone in patients with mCRC. It was reported that the addition of bevacizumab at both high and low doses increased median survival (control arm, 13.8 months; 95% confidence interval (CI), 9.1 to 23.0 months; low-dose arm, 21.5 months, 95% CI, 17.3 to

undetermined; high-dose arm, 16.1 months; 95% CI, 11.0 to 20.7 months) (Kabbinavar *et al*., 2003). Subsequently, a phase III RCT was established for patients with mCRC, to determine if combination chemotherapy folinic acid, fluorouracil and irinotecan (FOLFIRI) with addition of bevacizumab improves survival. Herwitz *et al* found that the median OS was 20.6 months with the addition of bevacizumab compared to 15.6 months with placebo alone. There was a modest increase in side effects, including thrombosis, bleeding, proteinuria, and hypertension, which were usually managed easily (Hurwitz *et al*., 2004).

Epidermal growth factor receptor (EGFR) is commonly unregulated in mCRC through receptor dimerisation by Epidermal growth factor (EGF)-like ligands (of which six have been characterised). Downstream signaling pathways are then activated, the most common being the MAP/ERK and PI3K-PTEN-AKT pathways, involved in cell survival and proliferation (Alroy & Yarden, 1997; Mendelsohn & Baselga, 2000). Therefore, it is important that tumours treated with anti-EGFR therapies are RAS-wild type (WT) so determining the RAS mutational status of the tumour is a requirement for treatment with anti-EGFR therapies. Targeted therapies of this pathway in mCRC include cetuximab and panitumumab. Cetuximab synergies with FOLFIRI and FOLFOX, improving response rate, median PFS and OS (Maughan *et al*., 2011; Van Cutsem *et al*., 2015). Cetuximab induces pro-apoptotic mechanisms and inhibits the proliferative capacity of tumour cells. Interestingly, there have been pre-clinical *in vitro* studies demonstrating an immunogenic response via the Fc receptor on immune cells, particularly natural killer (NK) cells through antibody dependent cell-mediated cytotoxicity (ADCC) (Roda *et al*., 2007; Veluchamy *et al*., 2016). This highlights multi-faceted targeting of tumour-intrinsic molecular pathways and extrinsic immune cell responses by this therapy. These targeted therapies demonstrate the importance of understanding molecular pathways involved in tumour progression, so that they can be targeted therapeutically to improve patient outcome.

### 1.5 Colorectal Carcinogenesis

The molecular carcinogenic steps for CRC mostly arise through the adenoma-carcinoma sequence in the normal colon mucosa, which occurs over decades. This is a sporadic pathway that accounts for 85-90% of CRC cases and is due to mutational inactivation of tumour suppressor genes and mutational activation of oncogenes within the genome (Vogelstein *et al*., 1988). The model of colorectal carcinogenesis was first proposed by Vogelstein & Fearon, and described the genetic ‘hits’ required for an adenoma to progress to carcinoma (E. R. Fearon & Vogelstein, 1990).

In the normal colonic mucosa, adenoma formation is the benign beginning of this sequence. Adenoma formation arises from a small pocket of epithelial stem cells following inactivation of

the adenomatous polyposis coli (*APC*) gene. Subsequently mutations in the *KRAS* gene are important somatic alterations, which leads to a conversion of a small adenoma to a larger dysplastic one. Approximately 30-50% of CRC patients harbour a KRAS mutation, and such mutations can be the initiating event in a subset of colorectal tumours (Vogelstein *et al*., 1988). Other oncogene mutations may be activated through amplification or rearrangement including *MYC* and *MYB* (Alitalo *et al*., 1984; Finley *et al*., 1989). Additionally, loss-of-function mutations including tumour suppressor genes such as TP53 occur frequently in CRC. Accordingly by the common region of loss of chromosome 17p in CRC was found to harbour the TP53 tumour suppressor gene (Baker *et al*., 1989). This Vogelgram model has been useful to understand carcinogenesis, but it is important to note that only a few of CRCs strictly develop by this sequence (Wood *et al*., 2007).

Shortly after the proposition of the adenoma-carcinoma sequence, researchers began investigating the genome for novel tumour suppressor genes. During this time Perucho *et al* observed that in approximately 130 colorectal tumours, deleted DNA bands were found. In 12% of cases these DNA bands were not deleted but were shortened in length. When analysing these sequences they contained simple repetitive sequences (microsatellites), with an estimate of approximately $10^5$ somatic mutations per tumour (Boland & Goel, 2010). These tumours were also noted to be pathologically and clinically distinct. Typically these tumours arose in the proximal colon, were less invasive, unlikely to have mutations in KRAS and TP53, were poorly differentiated and more common in younger patients (Ionov, Peinado, Malkhosyan, Shibata, & Perucho, 1993). The authors concluded that these deletions represented a unique pathway of tumour development that was likely to be hereditary, although this was not proven.

At the same time Thibodeau *et al* were investigating another type of microsatellite known as dinucleotide repeat sequences. They observed deletion mutations in sequences in these regions and coined the term *microsatellite instability* (MSI). A type I MSI mutation had large deletions or insertions into the sequences, whereas a type II MSI mutation involved a two-base-pair repeat change. Similarly to Perucho *et al*, 90% of these tumours were found in the proximal colon, and it was also concluded that these tumours represented a unique tumour progression pathway that 'does not involve loss of heterozygosity' (Thibodeau, Bren, & Schaid, 1993).

It has since been determined that the 12-17% of CRC cases have a unique mechanism of pathogenesis and these tumours are collectively described as microsatellite unstable. MSI is associated with defective DNA MMR genes. These MMR genes in mammals are: MLH1, MLH3, PMS1 and PMS2. Loss of MLH1 results in total loss of MMR activity, while loss of

PMS2 can be partially compensated by retention of MLH3 (Boland & Goel, 2010). Therefore, determining which MMR genes are lost is important in diagnostic confirmation of MSI.

The most common hereditary condition is HNPCC or Lynch syndrome, an autosomal dominant genetic condition, with a high risk of multiple tumours. Conversely, most CRCs with MSI are sporadic and methods to detect this defect include immunohistochemistry (IHC) or by polymerase chain reactions (PCR) that amplify microsatellite regions using the Bethesda panel (Murphy *et al*., 2006). Most of these tumours have loss of MLH1 and PMS2 proteins. Alternatively, Kane *et al* showed that MSH2 was silenced by methylation in most of these tumours (Kane *et al*., 1997). The features of sporadic MSI colorectal tumours include the absence of significant familial clustering, biallelic methylation of the MLH1 promoter, loss of MLH1 and PMS2 protein expression and frequent mutations in BRAF (V600E) (Valine substituted by glutamic acid driver mutation) (Sinicrope *et al*., 2006). The tumours are often diploid (74%) and patients with sporadic MSI colorectal tumours have a better prognosis than tumours that are microsatellite stable in earlier stages of disease, but this is not the case in advanced mCRC.

It is well known that HPNCC-associated and sporadic colorectal tumours (stage I-III) with high MSI have an improved five-year survival of up to 10-20% compared to MSS, which is independent of other prognostic factors (Gryfe *et al*., 2000; Wright *et al*., 2000). The presence of tumour infiltrating lymphocytes (TILs) within primary colorectal tumours has been associated with this improved DFS (Galon *et al*., 2006). It has also been observed in MSI-high (MSI-H) colorectal tumours with a higher infiltration of cytotoxic CD8+ T-cells are associated with a more favourable prognostic outcome (Dolcetti *et al*., 1999; House & Watt, 1979). Recent studies demonstrate patients with MSI-H tumours respond to checkpoint blockade inhibition (CBI) including anti-Programmed cell death protein 1 (PD-1) therapy compared to microsatellite stable (MSS) tumours (Le *et al*., 2015).

### 1.6 Tumour Immunity

Due to the nature of tumour progression, the mutational status of a tumour is dynamic with both genetic and epigenetic mutations acquired over time. A process known as “immunoediting” can lead to altered antigenic peptide profiles on tumour cells that are selectively recognised by immune cells. MacFarlane Burnett & Paul Ehrlich initially coined the term ‘immunosurveillance’ stating that the immune system could suppress carcinoma (Dunn, Bruce, Ikeda, Old, & Schreiber, 2002). This arose from the idea that mutations acquired in tumours are mostly somatic, due to errors in DNA replication and repair. The immune cells can detect peptides encoded by these mutations as foreign, which results in an immune response.

Therefore aberrant expression of mutated proteins as peptides presented on major histocompatibility complex (MHC)-I molecules is confined to tumour cells only and not normal tissue (Segal *et al*., 2008). The dynamic nature of acquiring such mutations therefore continually exposes the immune system to neoantigens (Gilboa, 1999; Wortzel, Philipps, & Schreiber, 1983). Two forms of mutations can occur: the first is a passenger mutation, where there is no positive or negative advantage to the tumour cells, but are retained through cell division and clonal expansion. Conversely, a driver mutation is one that provides the cell with a selective advantage that is necessary in promoting survival and tumourogensis. (Greenman *et al.*, 2007). As the tumour evolves in parallel with the immune response, the tumour can reduce its immunogenicity through immune-resistance mechanisms. Over time the tumour can therefore evade the immune response and continue progression, which will be expanded upon below.

### 1.6.1 Innate Immunity

The immune system is composed of an innate and adaptive arm, which traditionally has been viewed separately. However, it is becoming more apparent that these two arms of the immune system work in concert. The innate immune system is an archaic response of host defence against infection. It occurs rapidly and involves innate leukocytes including NK, NK T-cells (NKT), γδ T-cells and mucosal associated invariant T-cells (MAIT) as well as phagocytic cells such as macrophages, dendritic cells (DCs) and neutrophils (D. T. Fearon & Locksley, 1996). These cells become activated during an inflammatory response often due to the presence of a pathogen causing an infection (Janeway & Medzhitov, 2002). However we also know that most innate immune cells are involved in tumour control, as tumourogenesis can also create an inflammatory environment.

Natural killer (NK) cells were first identified for their ability to kill tumour cells independent of deliberate activation (Wu & Lanier, 2003). This mechanism was later realised to be due to a lack of MHC-I recognition on tumour cells, resulting in NK-cell mediated cytotoxicity. Unlike adaptive immune cells that require specific recognition of antigen, NK cells express a variety of unspecific activating (CD94-NKG2 receptors) and inhibitory (KIR receptors) receptors (Pegram, Andrews, Smyth, Darcy, & Kershaw, 2011). Upon activation NK cells have the ability to rapidly secrete cytokines including IFNγ, TNFα, MIP-1α, GM-CSF and RANTES (Biron, Nguyen, Pien, Cousens, & Salazar-Mather, 1999; Dorner *et al*., 2004). NK cells can also produce cytolytic molecules including granzyme B and perforin, without the requirement for transcription and proliferation (Gismondi, Stabile, Nisti, & Santoni, 2015; Pegram *et al*., 2011).

Natural Killer T-cells (NKT) share some common phenotypic and effector properties with NK cells and are CD1d-restricted. There are two subsets of NKT cells: invariant NKT cells (iNKT), which play a significant role in tumour immunosurveillance and 'non-invariant' NKT cells (Coquet *et al*., 2008; Gumperz, Miyake, Yamamura, & Brenner, 2002). iNKT cells recognise lipid antigens presented by the monomorphic MHC-like molecule CD1d, which is expressed on antigen presenting cells (APC), predominantly DCs. These cells recognise microbial and endogenous antigens such as glycolipids and play an important role in infection control. Upon T-cell receptor (TCR) stimulation and CD1d activation, iNKT cells can secrete regulatory cytokines including IL-4, IL-10 and IL-13 and inflammatory cytokines including IL-2, IFNγ and IL-17 (Stolk, van der Vliet, de Gruijl, van Kooyk, & Exley, 2018). Through production of IFNγ and cross-presentation to DCs, iNKT cells have the ability to boost and activate CD8+ T-cells in the tumour microenvironment (TME) (Brennan, Brigl, & Brenner, 2013; S. Fujii, Shimizu, Smith, Bonifaz, & Steinman, 2003). They have cytotoxic function through mediation of granules including perforin, granzymes and Fas/FasL dependant killing. In the context of tumour immunity iNKT cells have been found to control IL-6 producing CD1d+ CD68+ tumour associated macrophages (TAMs) and control regulatory myeloid derived suppressor cells (MDSCs) (Altman, Benavides, Das, & Bassiri, 2015; Song *et al*., 2009). In these indirect ways, iNKT cells have the ability to influence the TME.

### 1.6.2 Mucosal-Associated Invariant T-cells (MAIT cells)

MAIT cells are a recently defined subset of innate-like T-cells. MAIT cells are characterised by an invariant TCR that recognises bacterial vitamin B metabolites presented via MHC-related molecule, MR1 (Gherardin, McCluskey, Rossjohn, & Godfrey, 2018; Kjer-Nielsen *et al*., 2018; Kjer-Nielsen *et al*., 2012). MAIT cells express Vα7.2-Jα33 chain with an almost near invariant α chain that is paired with a limited diversity β chain (Vβ2 and Vβ13) (Tilloy *et al*., 1999). This TCR is restricted by the highly conserved molecule MR1 that captures a novel class of antigens that are released into the extracellular environment or can be found in the lumen of phagosomal compartments following microbe engulfment (McWilliam *et al*., 2016). This unique class of ligands belong to vitamin B antigens, and MAIT cell activation depends on recognition of the ligands bound to MR1. Therefore MAIT cells are recruited to the site of infection of microbial organisms that synthesise components of the riboflavin pathway. The specific ligand discovered to activate MAIT cells was recently found to be 5-(2-oxo-propylideneamino)-6-D-ribitylaminouracil (5-OP-RU) that is a derivative of the riboflavin biosynthesis pathway (Kjer-Nielsen *et al*., 2012). Synthesis of 5-OP-RU is strictly limited to certain strains of bacteria including *E. coli* as well as by some yeast (Gherardin, McCluskey, *et al*., 2018). Mammals cannot synthesise this metabolite, obtaining vitamin B2 (riboflavin) from dietary sources. Vitamin B2 (folate) derivatives including 6-formyl pterin (6-FP) can also be captured by MR1

however when presented it inhibits binding and does not activate the MAIT TCR (McWilliam *et al*., 2016). Bacteria and yeasts therefore specifically activate MAIT cells.

Recent studies have documented indirect MAIT cell activation through the cytokines IL-12 and IL-18, due to MAIT cells expressing these receptors (Shaler, Choi, *et al*., 2017). In a pathological state, it is evident that viruses are able to induce activation through this mechanism in a bystander cytokine-dependent fashion (Loh *et al*., 2016; van Wilgenburg *et al*., 2016). Upon microbial and mitogeneic stimulation, MAIT cells have the ability to secrete IFNγ and TNFα (Gold *et al*., 2010; Le Bourhis *et al*., 2013). MAIT cells also have the ability to produce IL-17 however this is independent of TCR ligation. IL-17 secretion has largely been demonstrated when stimulated via phorbol 12-myristate (PMA) and ionomycin and other mechanisms via IL-7 in hepatic MAIT cells (Dusseaux *et al*., 2011; X. Z. Tang *et al*., 2013). Direct and optimal stimulation of MAIT cells induces their cytotoxic potential with production of a granzyme B and perforin to induce cell death against MR1+ cells, typically those that have been infected by pathogens (Gold *et al*., 2010; Kurioka *et al*., 2015). Consistent across most studies, MAIT cells are reported to be predominantly CD8αα+, double negative (DN) (CD8-CD4-) with some CD4+ or double positive (DP) (CD8+CD4+) populations (Gherardin, Loh, *et al*., 2018; Gherardin, Souter, *et al*., 2018). As their name suggests, MAIT cells are often confined to mucosal-barrier surfaces including the gut, peripheral blood (5-10% of T-cells) and in the liver (up to 45% of T-cells) (E. Martin *et al*., 2009).

The role of MAIT cells in various pathogenic diseases is still unclear and understanding if they are involved in tumour immunosurveillance, specifically CRC has been explored over the last five years. This interest is mainly due to their presence in sites where inflammatory processes can drive carcinogenesis such as the colon and the liver. More recent studies demonstrate that MAIT cells are also present within primary human CRC tumours. Sundström *et al* were the first to document the presence of MAIT cells within these CRC tumours and their functionality. A higher percentage of MAIT cells accumulated in the tumour compared to surrounding unaffected mucosa, however CD8+ MAIT cells in the tumour were reduced. MAIT cells from the tumour produced significantly less IFNγ compared to those from the normal tissue, but produced similar amounts of Granzyme B. Analysis of MR1 mRNA expression by real-time PCR revealed MR1 was present within both the tumour and unaffected tissues, suggesting that both tumour cells and epithelial cells have the ability to present and activate MAIT cells via MR1. Reduced IFNγ production indicates that their effector function may also be suppressed in the TME.

Validating these above studies, Zabijack *et al* found a higher frequency of MAIT cells in CRC tumours compared to the healthy mucosa (Zabijak *et al*., 2015). When stratifying patients based on their MAIT infiltrate and TNM score (II-IV), there were no statistical differences observed. However there were statistical differences observed when comparing DFS and OS. Using a cut-off MAIT score whereby the number of MAIT cells within the tumour were three times higher than in the healthy tissue, it was concluded that a higher infiltration of MAIT cells within the tumour was associated with a poor prognosis. This was the first study to document MAIT cell correlation and prognosis.

Ling *et al* found that MAIT cells were significantly reduced in the peripheral blood of CRC patients compared to healthy donors (Ling *et al*., 2016). MAIT cells within the total tumour infiltrating lymphocyte (TIL) population were significantly increased compared to MAIT cells in the surrounding healthy tissue, validating both findings from Sundström and Zabijack. Interestingly, the Ling *et al* study had a prospective cohort of patients that had been treated with FOLFOX4. When tracking MAIT cell frequency in peripheral blood, there was an increase of 2% after six-cycles of FOLFOX4, indicating MAIT cells might be chemoresistant.

It is well known that MAIT cells are highly abundant within the human liver. A recent paper by Shaler *et al* investigated the role of MAIT cells in colorectal liver metastasis (CRLM) and found a reduced infiltration of MAIT cells within the tumour compared to surrounding normal liver (Shaler, Choi, *et al*., 2017). To investigate their functional capacity cells were stimulated using TCR/MR1-dependent and -independent stimuli. They found that upon stimulation, MAIT cells isolated from the tumour produced low amounts of IFNγ compared to distant liver. Following stimulation, granzyme B in hepatic MAIT cells was substantially higher than tumour and tumour margin MAIT cells. This highlights a potential tumour suppressive TME similar to that in the primary tumour. Shaler *et al* also investigated MAIT cell susceptibility to chemotherapy, in the context of FOLFOX and Avastin. There was no difference in MAIT frequency in the chemotherapy versus treatment naïve group. In addition, MAIT cell function was investigated by their ability to produce IFNγ, which was also not affected by chemotherapy. Whether this is a good or bad phenomenon in terms of CRC therapy is unknown.

The most recent study by Duan *et al*, investigated MAIT cells in in 50 patients with hepatocellular carcinoma (HCC). It was found that MAIT cells were reduced in the tumour compared to the normal surrounding liver. MAIT cells from the tumour had significantly upregulated inhibitory molecules including cytotoxic T-lymphocyte associated protein-4 (CTLA-4), PD-1 and T-cell immunoglobulin and mucin-domain containing-3 (TIM-3). MAIT cells had a reduced capacity to produce IFNγ and minimal granzyme B and perforin. In this

study MAIT cells significantly correlated with an unfavourable clinical outcome, and it was therefore concluded that MAIT cells had tumour-promoting capacity (Duan *et al*., 2019).

MAIT cells bridge the continuum area of innate versus adaptive immunity, similar to iNKT cells. The intriguing observation across all studies is that most MAIT cells are CD8+, which has prognostic implications in a range of solid tumours, including CRC. Therefore, it is likely that MAIT cells are pooled with conventional CD8+ T-cells and may account for up to 40% of TILs even though they are clearly not conventional cytotoxic T lymphocytes (CTLs). This matter warrants further investigation, which will be addressed in this thesis.

### 1.6.3 Adaptive Immunity

Unlike the innate immune response, the adaptive immune response is highly specific. Helper T-cells (Th) are classified as CD3+CD4+ effector cells and upon stimulation have the ability to produce IFNγ and IL-2 that favour cellular immunity. This influences the microenvironment and affects cytotoxic CD8+ T-cells, macrophages and NK cells. Th1 cells favour humoral immunity by producing IL-4, IL-5 and IL-15, acting on B-cells. Th17 cells produce IL-17A, IL-17F, IL-21 and IL-22, which has direct antimicrobial effects on tissue inflammation including epithelial, fibroblasts and immune cells (Fridman, Pages, Sautes-Fridman, & Galon, 2012).

T-regulatory cells (T-regs) are classified as CD3+CD4+Foxp3+ T-cells and have regulatory effector functions. T-regs have the ability to secrete immunosuppressive cytokines including Transforming growth factor beta **(**TGF-β) and IL-10. These cells are important in maintaining immune cell homeostasis and reducing autoimmunity (Fridman *et al*., 2012). However, in the TME these cells have the ability to influence tumour progression by suppressing the effector cells including Th1 and cytotoxic T-cells. CRC has the ability to secrete TGF-β, which can see conversion of infiltrating CD4+ T-cells to T-regs (Zdanov *et al*., 2016). This shows how potential mechanisms of the tumour cells may have extrinsic effects in the TME.

Cytotoxic CD3+CD8+ T-cells are effector T-cells that contain cytotoxic granules including granzymes and perforin. When a CD8+ T-cell interacts with a target cell through cognate antigenic MHC-I/TCR complex along with the immune synapse, cytotoxic granules are released. This causes subsequent death of the target cell through apoptosis. This is the mechanism by which CD8+ T-cells recognise and eliminate pathogen-infected cells as well as tumour cells. The infiltration of CD8+ T-cells in solid tumours, particularly CRC tumours, has now been strongly correlated with prognosis (Galon *et al*., 2006; Pages *et al*., 2005; Pages *et al*., 2009; Pages *et al*., 2018).

## 1.7 Immune Escape

We now know the host immune system can play both a tumour-protective and tumour-enhancing role. Therefore, as the original concept of immunosurveillance focused only on the protective role of the host immune system, this idea is no longer accurate. Instead, the broader term 'cancer-immunoediting' is more widely accepted to address these dual concepts (Dunn *et al*., 2002).

There are three main steps to the proposed framework of cancer-immunoediting that involve elimination, equilibrium and escape, also known as the "*3 E's*" of cancer immunoediting". The initial elimination step does encompass the original concept of immunosurveillance, whereby immune cells are successful in destroying the developing tumour. Tumour growth results in inflammation, with an influx of innate immune cells including NK, NKT and γδ T-cells to the site of the tumour resulting in IFNγ production (Girardi *et al*., 2018; Matzinger, 1994; Smyth & Trapani, 2001) and leading to IFNγ induced tumour cell death and release of chemokines, with an influx of APCs. In the draining lymph node DCs prime tumour specific CD4+ T-cells, which causes activation and accumulation of CD8+ and CD4+ T-cell infiltrate into the tumour site (Ferlazzo *et al*., 2002; Gerosa *et al*., 2002). Tumour destruction occurs via cytolytic T-cells, as the tumour bears antigens that have been immunogeneically enhanced (MHC-I) by exposure to local IFNγ production (Shankaran *et al*., 2001).

In the equilibrium state, remaining tumour and immune cells that have survived the elimination phase now experience a dynamic equilibrium. Lymphocytes continue to control the tumour and IFNγ production is exerted towards tumour cells, but the TILs do not eradicate the tumour. This scenario results in "*Darwinian-like*" selection of tumour cells, that become resistant to immune-mediated destruction. This process may span years, and could be the longest process of immunoediting (Dunn *et al*., 2002). The final phase is escape by the tumour cells to this immune cell-mediated killing. These tumour cells are insensitive to detection and elimination by immune cells and have undergone genetic or epigenetic mechanisms, to progress in an uncontrolled growth manner. Thus resulting in a clinically detectable tumour. The next section of this review will highlight the immune response in the context of CRC.

## 1.8 The Immune Response in Colorectal Cancer

In the past decade it has become strikingly apparent that the immune response in CRC tumours plays a major role. Most importantly measure of immune activity have been found to have greater prognostic significance than current AJCC and UICC TNM tumour staging (Pages *et al*., 2018). Conversely, the TNM staging system, explained earlier in this review, fails to take into account additional factors including the immune cell infiltrate that is known to affect prognosis. Other new technologies such as molecular pathway analysis, mutational status and tumour

gene-expression based stratification are important contributors to disease stage and treatment response but have moderate prediction accuracy and limited clinical utility (Guinney *et al*., 2015; Pages *et al*., 2018).

The concept of the host immunological reaction in CRC is not a new one. Studies conducted by House & Watt in 1979 first documented functional immune cell inhibition by tumour antigen. In functional migration studies of TILs, patients with sera that inhibited cancer cell migration *in vitro* had a high risk (50%) of developing recurrence or death, indicating systemic immune suppressive factors that can influence tumour progression (House & Watt, 1979).
In the mid 1980s, Jass investigated the prognostic significance of TILs in a large retrospective cohort of 447 rectal cancer formalin-fixed paraffin embedded (FFPE) sections with follow-up data of 15 years, using H&E staining to define lymphocytes (Jass, 1986). Fifteen-year survival was 90%, 60% and 40% when graded as pronounced, moderate and little to none, respectively. This study was one of the first to observe TILs at the margin of the tumour in rectal cancer specimens a feature that has now become prominent in current assessment of TIL.

In the 1990s, Ropponen *et al* and Naito *et al* investigated TILs in primary CRC to determine if this correlates with prognosis. Ropponen *et al* found a linear association between TIL infiltrate and Duke's stage A-B, however TILs were absent or weak in the stroma of large invasive Duke's stage C and D tumours. Reduced TILs were observed in later stages of disease demonstrating immune escape by the tumour and resulting in shorter survival. Naito *et al* defined the T-cell subsets and found that high cytotoxic CD8+ T-cell scores were associated with earlier Duke's A and B stages of disease (Naito *et al*., 1998). Collectively both of these studies show quantification of TILs as a prognostic measure and more importantly stratification of patients according to disease stage.

To address this question of ongoing immunoediting, Pages *et al* investigated the role of the immune system in early metastatic phases of tumour progression including vascular emboli, lymphatic invasion, and perineural invasion (collectively referred to as "VELIPI") (Pages *et al*., 2005). This was done in a large cohort of 959 CRC patients. Tumours that had features of VELIPI had a reduced five-year survival than those with no VELIPI. When assessing TIL subsets for prognosis and VELIPI, the presence of a strong immune infiltrate correlated with VELIPI-negative tumours. This was an interesting finding, as it may be assumed that with a more vascularised tumour, there would be a higher immune infiltrate, but this is not the case. Some tumours "hijack" the inflammatory response to promote invasiveness, proliferation and survival (Liotta & Kohn, 2001). However, in this study it was found that VELIPI-negative

tumours had a higher lymphocyte infiltrate, which indicates the host immune response is providing a protective role, perhaps by inhibiting VELIPI progression.

The seminal study by Galon *et al* defined the different immune subsets as well as the spatial location of immune cells within primary colorectal tumours. It was found that typing these tumours with immunological markers was a better predictor of patient survival compared to current TNM staging used for CRC (Galon *et al*., 2006). Assessing of CD3+ infiltrate at both the central tumour (CT) and invasive margin (IM), increased prediction of DFS and OS. Adding the immune memory marker CD45RO strengthened DFS, stratifying patients into long and short-term survivors, regardless of traditional TNM stage. Thus, although immunoediting occurs over time, the favourable adaptive immune response likely persists throughout tumour progression.

Since these studies, many investigations of TIL in primary CRC have been published (Fridman *et al*., 2012; Galon, Angell, Bedognetti, & Marincola, 2013; Mlecnik *et al*., 2010; Pages *et al*., 2009). For instance, we reported on the importance of an immune cell infiltrate in early stage node-negative microsatellite stable (MSS) CRC. We found that patients who had a high infiltration of cytotoxic CD8+ T-cells had a better relapse-free survival, as shown in **Figure 1.2**. We did not find statistical significance when assessing CD45RO+ infiltrate and this could indicate that the memory response is not as crucial in the early development of tumours as the cytotoxic response of the CD8+ T-cells (Millen *et al*., 2016). This study highlighted the importance of the immune response in the early stages of disease progression, and how this can affect relapse-free survival.

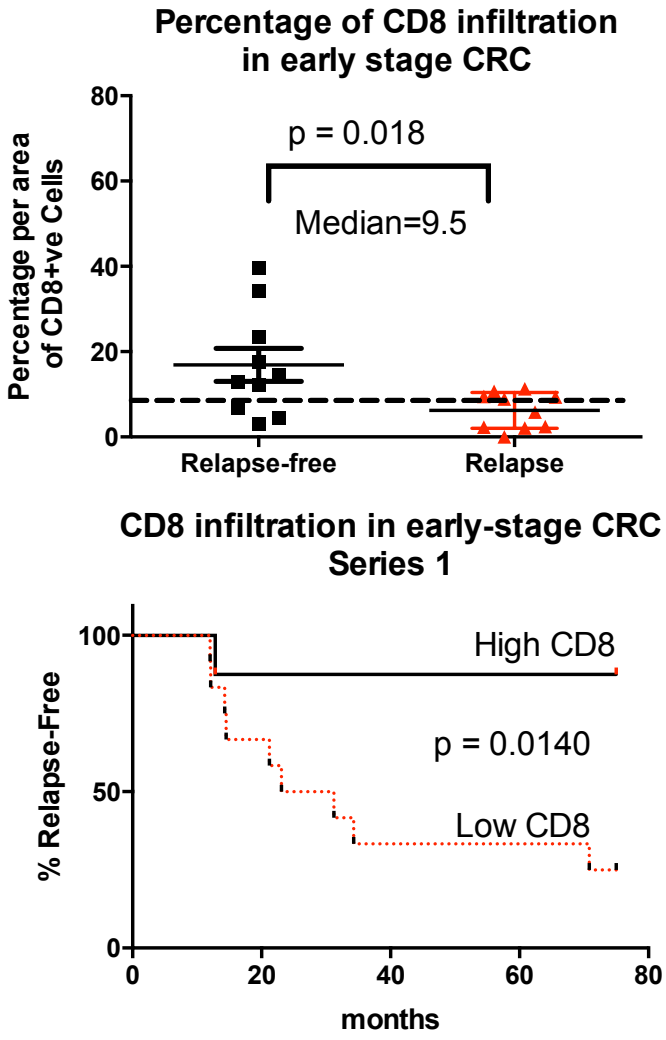


**Figure 1.2 Abundance of tumor infiltrating lymphocytes (TILs) in early stage MSS colorectal cancers track with relapse-free survival. (A)** CD8+ cells were evaluated in patients that had tumor relapse (n =10) and those who did not relapse (n = 10). Infiltrating CD8+ T-cells were found to be significantly higher in relapse-free patients (two-way T-test) (**B**) Data from (**A**) were used to calculate the statistical median, which was used to partition with an area above 9.5% and those 9.5% and below. Relapse-free patients were found to have significantly higher CD8C cells that tracked with relapse-free survival (Log-rank, Mantel–Cox test).

The latest reiteration of TILs in CRC has been an international validation of the Immunoscore, developed by Galon & Pages *et al* (Pages *et al*., 2018). The "*Immunoscore*" was found to predict the clinical outcome of patients with early and advanced stage CRC (Mlecnik *et al*., 2018; Pages *et al*., 2009). In a three-category "Immunoscore" analysis, a 0–25% density was scored as low, 25-70% intermediate and 70-100% was scored as high as shown in **Figure 1.3** (Pages *et al*., 2018). There was a significant positive correlation between survival and the

densities of CD3+ and CD8+ immune cells in each tumour region, in the training set. The lowest risk of recurrence and longest survival was seen in patients with a high Immunoscore. This was validated in the internal and external validation sets: overall patients with high Immunoscore had the lowest risk of recurrence and also a significantly longer risk to recurrence, OS and DFS.

This study also assessed immune infiltrates in MSI and MSS tumours and found when stratified using the three-category (low, intermediate and high) analysis, 45% of MSI tumours were associated with a high Immunoscore compared to 21% in the MSS cohort. However, when comparing the groups using the two-category (low and high [intermediate plus high]) analysis, patients with a high Immunoscore had prolonged DFS, time to recurrence and OS, regardless of microsatellite status. In addition to this, patients with MSI tumours with weak lymphocyte infiltrate did not have a survival advantage compared to MSS tumours against the overall trend for MSI-H versus MSS more generally.

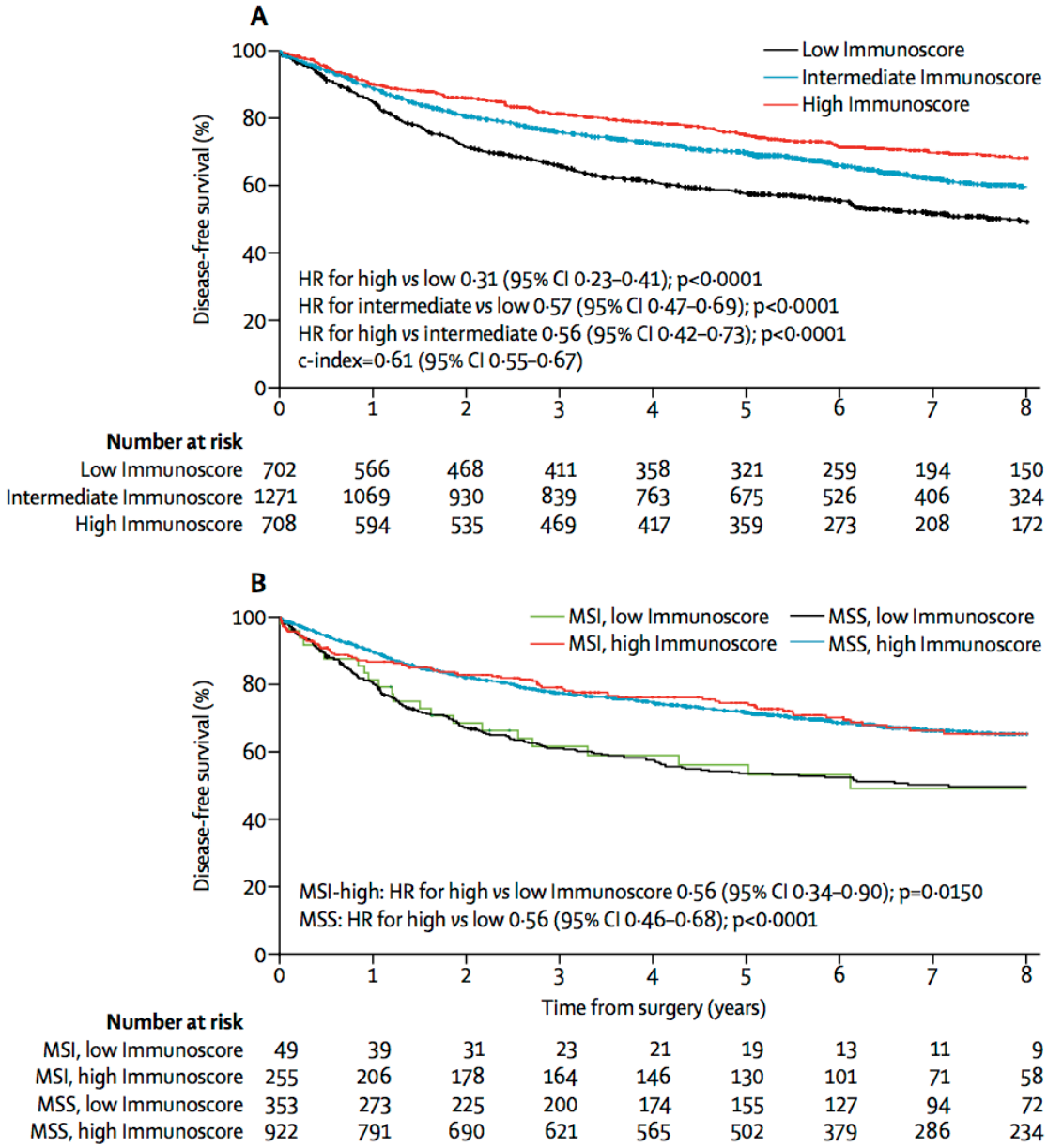


**Figure 1.3 Kaplan-Meier estimates of disease-free survival . (A)** Kaplan-Meier curves for disease-free survival according to the Immunoscore in all cohorts of patients with AJCC/UICC TNM stage I–III colon cancers. (**B**) Disease-free survival according to the Immunoscore and MSI status in 1579 patients with known MMR status. The Immunoscore is based on two categories (low Immunoscore vs. intermediate plus high Immunoscore). Five-year survival: 56% (95% CI 43−73) for patients with low Immunoscore and MSI (green), 75% (69−80) for patients with high Immunoscore and MSI (red), 53% (48−59) for patients with low Immunoscore and MSS (black), and 72% (69−74) for patients with high Immunoscore and MSS (blue). MSI=microsatellite instability. MMR=mismatch repair. MSS=microsatellite stable (Pagés *et al*, 2019)

## 1.9 The Immune Response in Metastatic Colorectal Cancer

TIL presence is well established in primary CRC tumours, but is the immune response the same at the metastatic site? Most studies that have focused on TILs in CRLM have defined TILs using either Haematoxylin & Eosin (H&E) or immunohistochemistry (IHC). Okano *et al* found an association between weak TIL infiltrate and reduced survival (one, three, five-year: 73, 26 and 19% respectively). They also reported an association between weak TILs and portal vein invasion, thus indicating the immune response is unable to control the tumour growth and spread in the liver (Okano *et al*., 2003).

Most studies describe CRLM tumours with a high number of TILs namely CD3+ and CD8+ cells, typically along the margin between the tumour and liver parenchyma, as being associated with a better OS (Halama *et al*., 2011; Kwak *et al*., 2016; Maker *et al*., 2015). There have been studies that also look into the difference of immune infiltrate between the primary colorectal tumour and the metastatic site. Shibutani *et al* report the density of the CD8+ and CD4+ T-cells in the primary tumour as being similar to the metastatic site. They found that Foxp3+ T-cells were higher in the primary than the metastasis. Due to this immunosuppressive TME, it may be advantageous for tumour growth and progression leading to subsequent metastasis through escape mechanisms (Shibutani *et al*., 2018).

Although metastatic tumours are thought to be poorly immunogenic and more immunosuppressed following escape from the primary site, these data collectively highlight the importance of accurately determining the immune response at the metastatic site. Therefore, such an assessment of the axis between the immune cells and the tumour cells is likely ongoing. Still, we can observe the strong importance of cytotoxic CD8+ T-cells in CRLM, and that this cytotoxic function is clearly important in tumour control. Despite these correlations of good immune response in the metastatic lesion and survival, immunotherapy responses in these tumours are still low. Therefore, establishing models to better understand this functional relationship is the next step to assess the quality of these immune cells.

Yoong & Adams questioned if TILs from CRLM were functionally impaired and if this could be reversed *in vitro* or *in vivo* by manipulating the defects (Yoong & Adams, 1998). Collectively they found that T-cells freshly isolated from CRLM have incomplete cellular activation, reduced proliferative capacity and impaired cytotoxic effector function likely due to a reduced CD3γ expression. This could be restored *in vitro* with rIL-2 however tumour-specific activity was not detected in any of the freshly isolated TILs. This phenotype is likely due to the

poor immunogenicity of the tumour cells, with lack of expression of MHC antigens and co-stimulatory molecules and reflects immunosuppressive factors in the TME (Bubenik, 2003).

A deeper functional study of TILs in CRLM was undertaken by Wagner *et al* who investigated tumour reactive T-cells and their subsequent function. Although the sample size of this study was small (n=16) it was the first study to document *in situ* tumour reactive T-cells. It assessed using freshly isolated TILs and Elispot to determine production of IFNγ specific to tumour antigen function MUC1. Interestingly there was no difference in frequency of CD3+ T-cells in the tumour and the liver. Higher frequencies of activated CD4+ T-cells and reduced cytotoxic CD8+ T-cells were also found. These activated CD8+ T-cells correlated with high CD4+ infiltrate, indicating T-helper cell effects in the TME (Wagner *et al*., 2008).

Therefore the assessment of immune cells using the Immunoscore is likely to have a profound impact on the clinic in the context of prognosis, however how might this information be employed? This is important in the era of immunotherapies, where the immune response needs to be considered. Collectively scoring TILs provides a quantitative measure of the immune response and how this affects clinical outcome. Nevertheless, what this system lacks is a measure of qualitative function. Although we know these TILs are present, and in cases at high frequencies, we don't know the quality of the TILs and how tumour specific these TILs are. The aforementioned functional assays are from over a decade ago and are surrogate measures. Currently, there is a real need for the development of assays that assess functionality of TILs in terms of active tumour control.

### 1.10 Modelling Responses to Immunotherapy *In Vitro* and *In vivo*

It is known that CRC is a heterogeneous disease, defined by significant inter-patient differences in response to therapy, perhaps due to the molecular diversity of the tumour (Linnekamp *et al*., 2018). Traditional *in vitro* models depended upon patient-derived cell lines that are commercially available. Almost all of these cell lines have been established decades prior with continial use in research laboratories and have therefore been cultured for years since they were initially derived from patients (Medico *et al*., 2015). There is an ongoing debate as to whether or not cell lines maintain tumour heterogeneity *in vitro*. Medico *et al* interrogated 152 CRC cell lines, using gene expression-based hierarchical clustering and short tandem repeat (STR) analysis. It was reported that cell lines with identical genetic background consistently clustered together, indicating that the genotype maintained strong control over the transcriptome, although all of these cells are essentially homogeneous (Medico *et al*., 2015).

To account for heterogeneity, patient-derived xenograft (PDX) models have been established to investigate the biology of the tumour in an *in vivo* system. They are developed by surgically implanting a section of patient-derived tumour into an immunodeficient mouse, to ensure the tumour is not rejected (Hidalgo *et al*., 2014). Such a model provides a platform to test therapeutics for drug safety and efficacy as well as investigating the biology of the tumour (S. A. Williams, Anderson, Santaguida, & Dylla, 2013). PDX models can be arduous, slow to establish and require further validation to ensure the graft is the true tumour type that was implanted. This may therefore not be the best model to use in clinical decision-making, as the replicative pace of these tumours in mice is not necessarily reflective of the tumour in humans and can take several months (Aparicio, Hidalgo, & Kung, 2015). Along with these factors, a critical component that PDX models lack is an immune system. Therefore, there is a need to develop less expensive and rapid models to accurately model the patient's functional immune response, which may potentially provide platforms for screening response to immunotherapies. Perhaps more comparatively such a platform needs to be effective in a clinically relevant time frame.

### 1.11 Organoid Culture

One such system that may have the capacity to model functional immune responses includes organoid cultures. Almost a decade ago, organoid culture was developed by Sato *et al* to study the stem-cell compartment of intestinal crypts (Sato *et al*., 2011). Crypts and villi are located in the small intestine, and allow the self-renewal capacity of the epithelium to be replaced every five days in the mouse. The stem-cell niche exists at the bottom of the crypt, where $Lgr5^+$ cells reside and give rise to the rapidly proliferating transient amplifying (TA) cells. The number of estimated stem cells per crypt is four to six, where enterocytes, goblet cells and enteroendocrine cells develop from the TA cells, and continuously move in coherent bands along the crypt-villus axis. Paneth cells are the fourth most differentiated cell type in the crypt structure, and reside at the base of the small intestine crypts (Sato *et al*., 2009). In 2009, Sato *et al*, developed a technology where one $Lgr5^+$ cell could be enriched in growth factor medium and produce an entire crypt-like structure *in vitro,* as seen in **Figure 1.4**. This study demonstrated that $Lgr5^+$ cells are indeed the stem cells within the intestinal epithelium that give rise to progenitor cells. This study also pioneered the *in vitro* culture of organoids, optimising the ideal growth factors used in tissue culture media to establish long-term culture of normal intestinal epithelia.

To grow normal intestinal organoids the following growth factor combination was developed by Sato & Clevers *et al* to sustain long-term passaging *in vitro*. It was long known that Wingless/integrated (Wnt) signalling is important for proliferation of crypts, and therefore the Wnt agonist R-spondin 1 was used to induce crypt hyperplasia (K. A. Kim *et al*., 2005). To

enhance intestinal proliferation Epidermal Growth Factor (EGF) was used and Noggin was used to induce crypt proliferation by blocking TGF-β. Finally, crypts undergo anoikis outside the normal tissue context and a rho kinase (ROCK) inhibitor was used to inhibit anoikis. Laminin (α1 and α2)-enriched matrigel was used in the culture systems to support intestinal epithelial growth. Matrigel is a commercially available product, which forms the collagen-like matrix for the intestinal crypts to grow in three-dimensional structures, recapitulating native tissue architecture (Sato *et al*., 2009; Stingl, Eaves, Zandieh, & Emerman, 2001). However, due to the nature of colorectal tumours, some of these GFs were not required for growth of tumouroids.

### 1.11.1 Co-Culture of Tumouroid and Immune Cells

To address the lack of organoid-immune cell co-culture systems, we hypothesised that immune cells could be co-cultured with organoids to assess cell-to-cell interactions. We focused only on the growth of cancer cells as organoids, rather than normal intestinal structure, and therefore called tumour-derived organoids *tumouroids*. At the time (2015), no other studies to our knowledge had been undertaken to address this concept. However since 2015 there have been several contributions to the field, including our own.

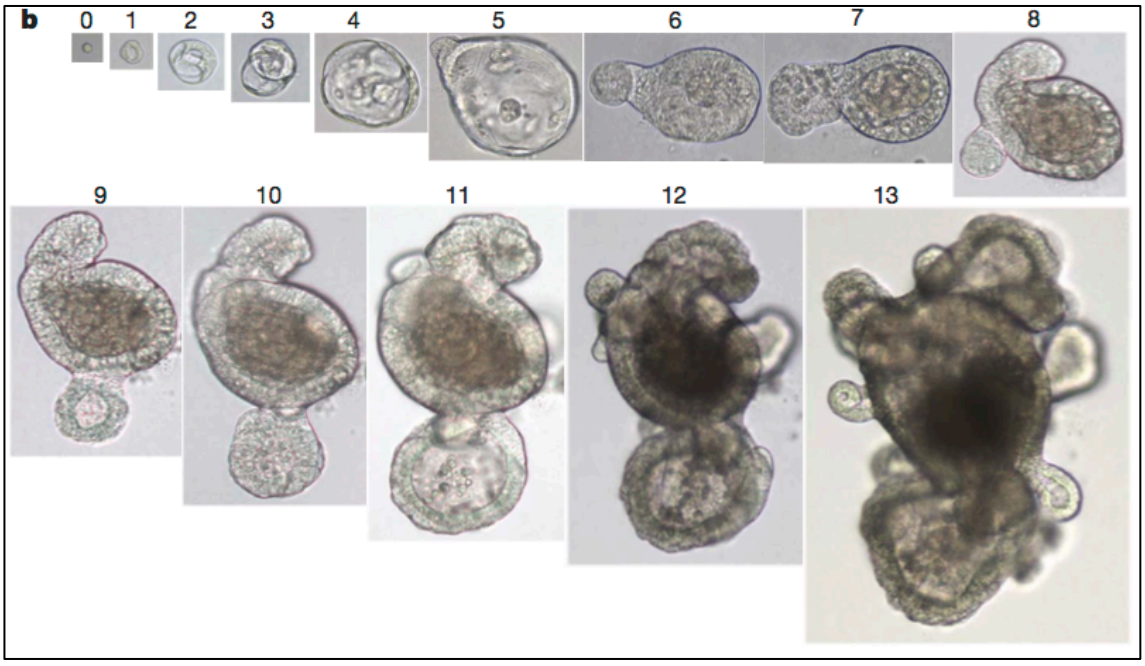


**Figure 1.4 Colony-forming efficiency of single cells sorted in individual wells.** An example of a successfully growing single $GFP^{hi}$ cell. Numbers above the images are the days of growth: days zero to four, five to seven, eight to eleven, 12 and 13 (Sato *et al*, 2009).

To this end, Nozaki *et al* investigated intestinal intraepithelial lymphocytes (IELs) and their interaction with intestinal epithelial cells (IECs), however models to study such interactions

were limited. This is partly due to IELs undergoing apoptosis following isolation, but this has been overcome with the recognition that growth factors required were to maintain growth *in vitro*. Intestinal mouse organoids were established and IELs were subsequently isolated from mice and added as a co-culture. These were cultured for seven days using whole-mount analysis and time-lapse live imaging was used to study the interactions. They showed that IELs are motile in this system, changing their contact status with epithelial organoids. This was the first study demonstrating lymphocyte interaction with epithelial cells in an *ex vivo* system. It proved that such a system could be used to study dynamic interactions using organoids (Nozaki *et al*., 2016).

To understand response to immunotherapy, namely checkpoint blockade inhibition (CBI), Jenkins *et al* used murine- and patient-derived organotypic tumour spheroids (MDOTS/PDOTS). Their system utilized a 3D-microfluidic-culture device, in which single-cell suspension of tumour were first fractionated to different sizes and then embedded in a collagen-based matrix, added to the device and cultured for a further six days. This device was viewed on a microscope to assess live/dead analysis of cells and supernatant was also assessed for cytokine production. Murine-derived tumours from the colon adenocarcinoma line MC38 and the melanoma line B16F10 were grown as MDOTS *ex vivo*. MDOTS were able to retain autologous immune contexture and short-term culture. To test CBI, MDOTS were treated with anti-PD-1 antibody in the device and sensitivity to treatment was assessed with live/dead microscopy imaging. The MC38 MDOTS were sensitive to anti-PD-1 in a dose-dependent manner. To validate the murine studies, PDOTS from cancers responsive to anti-PD-1 tumours including melanoma and merkel cell carcinoma (MCC) were assessed using flow cytometry. When compared to the original tumour tissue, immune cell populations were retained validating the use of PDOTS to assess function of immune cells from patient-derived material. Together these data describe the functional utility of MDOTS/PDOTS to model *ex vivo* responses to CBI (R. W. Jenkins *et al*., 2018).

Another recent study employed more traditional organoid culture without using a 3D-microfluidic-culture device. Dijkstra *et al* designed a platform to study tumour-reactive T-cells from patients with CRC and non-small cell lung cancer (NSCLC). To do this, patient-derived tumouroids were established and autologous peripheral blood mononuclear cells (PBMCs) were isolated and co-cultured with the tumouroids to select for tumour-specific T-cells. In the colorectal cohort, only deficient MMR (dMMR) patients were recruited, as these patients are known to respond to CBI. As 60% of dMMR colorectal tumours lose MHC-I, tumouroids were screened for MHC-I loss, by stimulating with IFNγ, with 62% of the tumouroid samples being proficient for MHC expression. Importantly it was found that tumouroids classified as MHC-I

deficient were also MHC-I deficient in the native tumour, confirming that MHC-I loss is not a result of organoid culture. To select for tumour-reactive T-cells, MHC-I and programmed death liand-1 (PD-L1) expression was induced on tumouroids using IFNγ stimulation and autologous PBMCs co-cultured for two weeks. An anti-PD-1 antibody was included in the co-culture to avoid immune inhibition by the tumouroids. In four out of eight samples, IFNγ and CD107a expression was detected in and on CD8+ cells. In one particular patient there were tumour reactive T-cells detected pre-stimulation and following co-culture with tumouroids the CD8+ tumour-reactive T-cells increased 10-fold, implying that a tumour-specific T-cell pool was already present. To ensure these responses were tumour-specific, autologous T-cells were co-cultured with matched normal organoids from dMMR, proficient-MMR (pMMR) CRC tumours and NSCLC, with no reactive T-cells detected.

Occasionally, CD4+ reactive T-cells were observed against normal organoids, and it was hypothesised that this may be directed against foreign antigens from the extracellular matrix, as this is a murine-basement membrane matrix. It was noted that this matrix (Geltrex) does have the ability to induce a CD4+ T-cell response, which is not tumour reactive and this could be bypassed by using other alternative synthetic products. Finally to test the cytotoxicity of these cells, after three days of co-culture with tumour-reactive T-cells, the number of live cells was quantified by flow cytometry. Substantial reduction of live cells was observed across all samples. This was further validated with live imaging microscopy. It was found that after the addition of tumour-reactive T-cells, tumouroid size was reduced and widespread apoptosis was observed. To confirm specificity, tumouroids were cultured without T-cells or in the presence of blocking MHC-I and –II antibodies, where the tumouroids continued to proliferate indicating MHC-mediated mechanism. Together these data validate and demonstrate the use of this platform to understand immune cell reactivity to autologous tumour cells, *ex vivo*. It opens up the possibility of the utility of this platform to test drugs, especially in the field of immune-oncology, as current patient-derived model systems are lacking (Dijkstra *et al*., 2018).

Contemporaneously with this study, our group investigating the co-culture of autologous TILs and tumouroids was accepted for publication (Kong, 2018). Our platform will be subsequently explained in this thesis, and was used to investigate TIL function against autologous tumouroids. I was involved in the establishment of the assay and the assay was subsequently employed in a controlled prospective trial where patients with rectal cancer were assessed using the assay. Subsequently, these patients underwent definitive NACRT prior to surgical resection. As explained earlier in this review, there is a need for a robust individualised pre-treatment test that predicts pCR with high concordance with outcome (Ryan, Warrier, Lynch, & Heriot, 2015; Smith, Wiland, Mace, Pai, & Kalady, 2014). We found functionality of patient specific

cytotoxic TILs to be highly predictive of pCR to NACRT. It is instructive that this assay is performed before the effects of the tumor cell damage are induced by NACRT. Because this implies that the quality of the endogenous TILs impact upon the multiple actions of NA. Like the previous studies described, we were also able to highlight the utility of assessing TIL function and response to CBI using patient-derived material that will hopefully lead to better treatment stratification of patients.

### 1.12 Checkpoint Blockade Inhibition (CBI)

The concept of CBI as a therapy has only been employed clinically for the past decade, however the mechanism underpinning these pathways has been investigated since the 1970s. The initial work reporting on T-cell anergy by Mueller, Jenkins & Schwartz, where they discovered that some T-cells entered a state of reduced responsiveness when encountering processed antigen presented by MHC-Ia molecules in the absence of functional accessory cells (Mueller, Jenkins, & Schwartz, 1989). In these studies, murine Type I CD4 T-cells were investigated in the presence of antigen and purified Ia molecules in a planar membrane of fixed APCs. The cells failed to stimulate proliferation and instead induced a state of "*proliferative non-responsiveness"*: where there was neither proliferation nor production of IL-2. This was TCR-dependent as it happened in the context of both antigen and APCs. (Quill & Schwartz, 1987). This state was likened to T-cell tolerance *in vivo*; a phenomenon that has been explored in the context of viral and tumour immunity.

It was later discovered that these stimulatory pathways were independent of TCR-CD3 signalling but occurred dependant upon CD28 expressed on T-cells. The ligands for CD28 were discovered as B7-1 (CD80) and B7-2 (CD86), both can be expressed on professional APCs including macrophages, DCs and activated B-cells, which provided the second co-stimulation signal for T-cell activation (Linsley *et al*., 1991; Linsley, Clark, & Ledbetter, 1990). Indeed this is the dominant co-stimulatory signal required for T-cells to elicit a strong immune response (June, Bluestone, Nadler, & Thompson, 1994).

Allison & Townsend postulated that tumours have the ability to activate T-cells through antigen-specific signals, but the lack co-stimulatory mechanisms necessary to render T-cell medicated immunity effective. When B7 was expressed on melanoma cells, it was demonstrated that tumour rejection could occur *in vivo*; this was CD8+ T-cell mediated (Townsend & Allison, 1993). A homolog of CD28 is CTLA-4, which has a stronger affinity for B7-1 and B7-2 than CD28. This interaction has the ability to down regulate T-cell responses *in vivo*. It was subsequently found that blocking these inhibitory T-cell receptors can potentially enhance co-

stimulatory receptors whereby anti-tumour immunity is improved (Leach, Krummel, & Allison, 1996).

Ipilimumab is a humanised monoclonal antibody that targets CTLA-4 that was developed following the successful use in controlling solid tumours in murine models. The mechanism of action of Ipilimumab is thought to occur through binding to the CTLA-4 receptor, expressed on activated CD4+ and CD8+ T-cells. This ensures that CTLA-4 cannot bind to its inhibitory receptor, B7 that can be expressed by APCs or tumour cells, to inhibit effector functions of activated T-cells and thus results in enhanced endogenous immune responses (Peggs, Quezada, Korman, & Allison, 2006). Initial phase I clinical trials investigated safety and response rates of Ipilimumab as a monotherapy in melanoma and renal cell carcinoma (RCC) reporting objective response rates of 7-15% (Blansfield *et al*., 2005; Ribas *et al*., 2005). Multiple subsequent trials in patients with advanced melanoma; advanced NSCLC and RCC have shown Ipilimumab to work in some patients as a monotherapy as measured according to the World Health Organization (WHO) criteria imaging assessment. More recent studies have reported that a combination of Ipilimumab plus Nivolumab, a humanised monoclonal antibody targeting PD-1, results in better response rates than monotherapy alone (Hellmann *et al*., 2018; Motzer *et al*., 2018).

The second group of antibodies used in CBI targets the PD-1 receptor (CD274) and PD-L1 (CD27) ligand axis are transmembrane proteins that are transcriptionally activated and expressed on activated immune cells including Myeloid cells, NK, T- and B-cells (Terme *et al*., 2011). This regulatory checkpoint pathway is employed by the immune system to dampen the immune response in peripheral tissues to maintain immune homeostasis. Following T-cell activation, immune dampening occurs at the time of an inflammatory response thus reducing the risk of autoimmunity whilst maintaining immune tolerance (Pardoll, 2012).

Ishida *et al* first discovered the PCDC1 gene in the early 1990s*;* when investigating lymphoma cells lines undergoing cell death and that in these cells PD-1 transcription was activated (Ishida, Agata, Shibahara, & Honjo, 1992). The ligands for the PD-1 receptor are PD-L1 or PD-L2, which can be expressed on placental cells, activated APCs and parenchymal cells that are involved in inflammation (Freeman *et al*., 2000). Freeman *et al* proved that binding of PD-1 by PD-L1 inhibits TCR mediated proliferation of T-cells, resulting in a strong inhibitory signal (Freeman *et al*., 2000).

Tumour cells have adapted mechanisms to exploit this pathway and evade the immune response with the ability to express PD-L1 or –L2. In murine model studies, Blank *et al* found that PD-

L1 expression could be induced by IFNγ treatment in the poorly immunogenic B16-F10 melanoma line. When testing the function of the B16-F10 cells, engaging transgenic CD8+ T-cells expressing a high-affinity TCR, had reduced effector function with minimal cytokine production and cytolysis. By eliminating PD-1 engagement, effector function could be restored. This was one of the first studies to demonstrate the potential effects of targeting anti-PD-1/PD-L1 interactions in a tumour system (Blank *et al*., 2004). Blocking the interaction of PD-1 and PDL1 therefore results in restoration of T-cell activation signals and subsequent effector functions of T-cells including cytokine production (Barber *et al*., 2006). However, it is still unknown how to predict which patients will respond to this therapy. PD-L1 expression on tumour cells is heterogeneous and is variable, so understanding PD-L1 inhibitors needs to be understood in greater detail (Alsaab *et al*., 2017). Patient characteristics including the tumour type, gender, mutational status of genes (EGFR and KRAS) and metastases of tumours have varying affects in response to PD-1 and PD-L1 inhibitors (D'Incecco *et al*., 2015).

Topalian *et al* was the first to report on safety and activity of anti-PD-1 therapy (Nivolumab) tested in advanced melanoma, NSCLC, castration-resistant prostate cancer, RCC and CRC. They found that treatment with anti-PD-1 antibody produced objective response rates in 20-25% of patients with advanced melanoma, RCC and NSCLC. Cumulative response rates were 18%, 28% and 27% in NSCLC, melanoma and RCC respectively. In patients that had positive PD-L1 expression on the tumour, 36% had an objective response (Topalian *et al*., 2012). More recently studies have been conducted investigating Nivolumab in the neoadjuvant setting in NSCLC. In this study, few immediate adverse events were reported, and a major pathological response was observed in 45% of tumours that could be evaluated (Forde *et al*., 2018). These studies demonstrate that targeting immune checkpoints provides survival benefits, particularly when used in combination. It is an exciting time in the field with the emergence of using CBI in the neoadjuvant setting.

### 1.12.1 Checkpoint Blockade in Colorectal Cancer

Although CBI therapies have proven efficacious in multiple solid malignancies, they have only been effective in select CRC patients. In initial reports of CBI, only one of 33 CRC patients treated with anti-PD-1 antibody responded, and this patient was found to have a microsatellite unstable tumour (Topalian *et al*., 2012).

Le *et al* conducted a subsequent phase 2 clinical trial to evaluate the clinical activity of anti-PD-1 (Pembrolizumab) in patients with progressive metastatic carcinoma, including CRC, with or without mismatch repair deficiency. The study found that colorectal tumours with dMMR had

objective response rates of 40% and PFS of 78%. Conversely CRC tumours that were pMMR had 0% objective response rate and 11% PFS rates, as seen in **Figure 1.5**.

This was the first study to definitively demonstrate that tumours with dMMR are more responsive to anti-PD-1 therapy than pMMR tumours. The hypothesis that dMMR tumours have an enhanced immune response is not a new concept, with many previous reports observing a strong immune presence in these tumours (Dolcetti *et al*., 1999; Young *et al*., 2001).

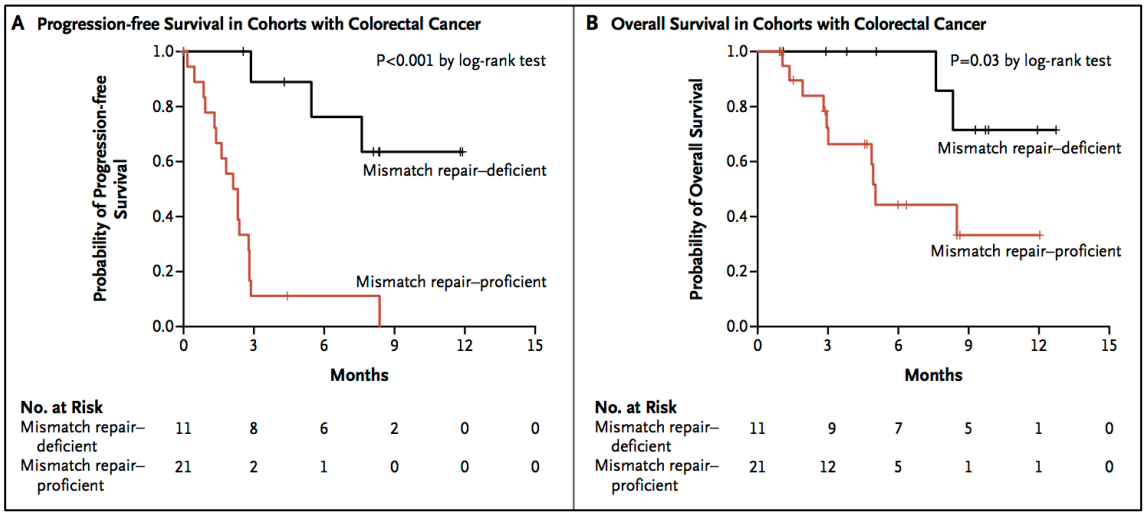


**Figure 1.5 Clinical benefit of anti-PD-1 therapy demonstrates response in patients with mismatch-repair deficiency. (A)** Kaplan–Meier curves are shown for PFS and (**B**) OS in the cohorts with colorectal cancer (Le *et al*, 2015). This was one of the first studies to show response to anti-PD-1 therapy in CRC.

Patients with MSI tumours have an improved prognosis stage-for-stage except those who have advanced Stage IV disease (Goldstein *et al*., 2014). This subset of patients typically does not respond to conventional chemotherapy and have a shorter OS compared to advanced stage IV microsatellite stable tumours. A recent multicentre phase 2 trial investigated the safety of Nivolumab as a monotherapy in this subset of MSI-H mCRC patients (Overman *et al*., 2017). In this study Nivolumab provided durable responses and disease control in previously treated mCRC patients that were microsatellite unstable. Understanding the disease progression in the context of the immune response in advanced stage IV mCRC will be addressed in this thesis. It will be important to understand in these responsive patients if they have high TIL densities compared to the non-responders mCRC-MSI high cases.

## 1.13 Overview, Hypothesis and Aims

Patients with advanced stage IV mCRC have a reduced survival compared to patients with earlier stages of CRC. In those patients who have CRLM, if left untreated, patients succumb to the disease within 12-24 months. Surgical intervention has certainly improved five-year survival in these patients, but recurrence is still common. We know that the immune response plays a role in CRC patients, and this is highlighted by the myriad studies that report tumours with high TIL presence have an improved OS and PFS at the primary site. This immune response in CRLM continues to be affective with improved survival correlated with increased cytotoxic CD8+ T-cells presence in these tumours. However in almost all studies, these TILs are only present on the invasive margin (IM) of the tumour indicating that there may be immunosuppressive factors at play.

The "Immunoscore" provides strong prognostic significance of patient outcome, however it only documents immune cell presence and not function. Developing novel strategies to additionally assess function of TILs is an area that requires further development in the field of tumour immunity. This thesis seeks to investigate the innate and adaptive immune responses involved in the progression of advanced stage IV CRC.

To investigate the immune responses in tumour progression at the primary site of advanced stage IV CRC, primary tumours of *de novo* mCRC stage IV patients were evaluated in **Chapter 3**. This was done in a retrospective cohort of these patients, a proportion of which have dMMR/MSI-H tumours. Understanding the biology of the immune infiltrate, tumour escape mechanisms together with clinical outcome in patients with advanced mCRC of both microsatellite stable and unstable tumours will be important contribution for potential treatment strategies of these patients.

Understanding the progression of metastasis to the liver in the context of the immune response may also provide insight into the mechanisms of tumour progression, in this setting. Additionally, determining not only immune cell presence but also immune function is an important property that warrants attention when assessing TILs. Therefore, **Chapter 4** describes the process of development of a novel cytotoxic immune assay that can be utilised to assess TIL function from patient-derived material *ex vivo*. The frequency, location and function of immune cells within CRLM tumours were evaluated. Additional investigation into the responsiveness of these CRLM TILs to CBI is assessed to determine if the cells are in a functional state and respond to CBI.

Finally, novel subsets of CD8+ T-cells, namely MAIT cells that are abundant in the liver were evaluated in the context of CRLM in **Chapter 5**. These cells may be of therapeutic interest in cancer immunotherapy as they have rapid effector functions and act independently of MHC-I, meaning they can be allogeneic. Their role in disease pathogenesis and cancer is starting to be understood and further investigation is required for their role in CRLM.

Therefore the following aims and hypotheses are in this thesis:

**Aim 1:** Determine immune escape mechanisms at the primary site that leads to metastatic progression in primary tumours of patients with advanced stage IV *de novo* mCRC.
**Hypothesis:** Patients with microsatellite unstable tumours will have a poor prognosis despite an increased infiltration of TILs.

**Aim 2:** Develop a novel method to determine the effector function of TILs from CRLMs in patients with mCRC.
**Hypothesis:** The presence and frequency of immune cells *in situ* alone does not always reflect their effector function.

**Aim 3:** Investigate a novel subset of cytotoxic CD8+ T-cells to determine their purpose in tumour immunity in the context of CRLM.
**Hypothesis:** MAIT cells are present within CRLM tumours due to their abundance in the liver.

## 2. METHODS

### 2.1 Human Participants

Patients undergoing surgical liver resection for their CRLM or synchronous resection for their primary colorectal and hepatic metastases were prospectively enrolled to the study following informed consent between October 2015-October 2018. This took place across three hospitals including St. Vincent's Hospital Melbourne, Peter MacCallum Cancer Centre and Royal Melbourne Hospital, all located in Melbourne, Australia. In total n=23 patients with CRLM were recruited, n=7 were treatment naïve and n=16 had neoadjuvant chemotherapy prior to liver resection. Inclusion criteria were radiological Magnetic Resonance Imaging (MRI) and $^{18}$Fluoro Deoxy-Glucose Positron Emission Tomography/Computerised Tomography ($^{18}$FDG PET/CT), confirmed diagnosis of CRLM and surgical resection with curative intent. Patients <18 years old were excluded from the study. Patients were discussed at the colorectal and hepatobiliary multidisciplinary team meeting whereby treatment decisions are made between the oncology, radiation oncology and surgical teams.

All work involving human participants was conducted according to ethical guidelines; using a protocol approved by the St. Vincent's Hospital Melbourne Human Research Ethics Committee (HREC) across all three hospitals (reference HREC/15/SVHM/54). Subsequent governance approval was obtained at each site.

**Table 2.1. Clinical and demographic characteristics of patients recruited to this study**

| **Demographic Attributes** | |
|---|---|
| Total patients, *n* | **23** |
| Female gender, *n (%)* | 9 (39) |
| Male gender, *n (%)* | 14 (61) |
| Mean age, years (±SD) | 58±10 |
| Median age (Range) | 60 (40-77) |
| **Oncologic Attributes** | |
| Liver Segment Involvement | |
| ≤3, *n (%)* | 18 (82) |
| >3, *n (%)* | 4 (18) |
| Extrahepatic Disease, *n (%)* | 6 (26) |
| Chemotherapy, *n (%)* | |
| Neoadjuvant Chemotherapy | 16 (70) |
| Chemotherapy Naïve | 7 (30) |
| Progression free survival (PFS) | |
| Recurrence, *n (%)* | 8 (40) |
| No recurrence, *n (%)* | 14 (60) |

## 2.2 Human Sample Processing

**Blood Collection: SepMateTM tubes**

Following general anesthesia, 40-50 mL of peripheral blood was drawn through an arterial line into ethylenediaminetetraacetic acid (EDTA)-blood collection tubes (Sarstedt AG & Co, Nümbrecht Germany). Tubes were centrifuged at 300 x g, 5 minutes to collect plasma, which was subsequently stored at -80°C.

PBMCs were obtained by density gradient centrifugation using SepMateTM-50 tubes (Stemcell Technologies, Vancouver, Canada) containing 15 mL low-endotoxin (<0.12 EU/mL) Ficoll-Paque PLUS (GE health care life sciences, Massachusetts, USA). Blood was diluted 1:2 with Phosphate Buffered Saline (PBS) and 25 mL were layered onto SepMateTM tubes. Tubes were centrifuged at 1200 x g, 10 minutes with the break on at room temperature (RT). Mononuclear cell layer was poured off and cells were washed with PBS at 300 x g, 8 minutes. Red blood cells were treated with ammonium chloride lysis (ACK) solution for 3 minutes and subsequently washed with PBS at 300 x g, 8 minutes. Cells were suspended in RPMI 1640 (Gibco, Thermo fisher Scientific, Massachusetts, USA) supplemented with 10% (v/v final) human AB-serum (Valley Biomedical, Inc., Virginia, USA), 100 U/mL penicillin and 100 µg/mL streptomycin (Sigma-Aldrich, Missouri, USA), glutamax (=2mM L-glutamine) (Gibco, Thermo fisher Scientific, Massachusetts, USA), 25mM HEPES, 10 µg/mL gentamycin and 0.25 µg/mL fungizone (Gibco, Thermo fisher Scientific, Massachusetts, USA) herein referred to as Complete Medium (CM). Cells were counted in 0.4% trypan blue (Gibco, Thermo fisher Scientific, Massachusetts, USA) using a haemocytometer and were either used immediately or were cryopreserved.

**Blood Collection: BD Vacutainer® CPT™ Cell Preparation Tube with Sodium Citrate**

Blood was collected by venepuncture in BD Vacutainer® CPT™ Cell Preparation Tubes (BD Biosciences, New Jersey, USA), stored upright and processed within 2 hours of collection. Tubes were centrifuged for 20 minutes, 1700 x g, at RT in a horizontal rotor (swing-out head). After centrifugation, whole plasma was removed by transfer pipette and stored at -80°C if required or discarded. Mononuclear cell and platelet layer was gently transferred into falcon tube (maximum 2 CPT tubes per falcon) using a transfer pipette. Cell suspension was washed with 30 mL of PBS, inverted 5-10 times and centrifuged for 10 minutes, 300 x g, RT. Supernatant was gently removed without disturbing the pellet. To remove red blood cells, 1-2 mL of ACK buffer was added at RT for 2-3 minutes and the reaction was stopped by adding 30 mL PBS and consequent centrifugation for 10 minutes, 120 x g, RT. Supernatant was discarded, and one final wash step completed, by adding PBS and centrifuging again for 10 minutes, 300 x g, RT. Cells were counted in 0.4% trypan blue (Gibco, Thermo fisher Scientific, Massachusetts, USA) using a haemocytometer and

were used immediately or cryopreserved for future experiments.

**Storage of Clinical Samples**

For snap frozen material, tissue was dissected and placed in a cryotube (Thermo fisher Scientific, Massachusetts, USA) and placed immediately on dry ice and subsequently transferred to -80°C. For cryopreservation, cells were resuspended in 10% Dimethyl sulfoxide (DMSO) (Sigma Aldrich, Missouri, USA) in fetal bovine serum (FBS) (Gibco, Thermo fisher Scientific, Massachusetts, USA) and immediately transferred to -80°C in Mr Frosty containers (Thermo fisher Scientific, Massachusetts, USA). After 24 hours vials were removed from the Mr Frosty containers and stored long term at -80°C.

**Fresh Tissue Preparation**

Following surgical resection of primary and/or hepatic metastases, fresh tumour and liver specimens were collected in RPMI 1640 (Gibco, Thermo fisher Scientific, Massachusetts, USA) supplemented with 5% (v/v) fetal bovine serum (FBS) (Gibco, Thermo fisher Scientific, Massachusetts, USA), 100 U/mL penicillin and 100 µg/mL streptomycin (Sigma Aldrich, Missouri, USA), and placed on ice. Tissue was initially dissected to remove necrotic regions and adjacent liver to expose a viable tumour margin and divided into four pieces: 1) snap-freezing tissue was immediately frozen on dry ice, 2) to cryo-preserve tissue, tissue pieces were added to 10% DMSO (Sigma Aldrich, Missouri, USA) in FBS (Gibco, Thermo fisher Scientific, Massachusetts, USA) and immediately transferred to -80°C in Mr Frosty containers, 3) formalin-fixing tissue was placed in 10% Neutral-Buffered Formalin (NBF) (Australian Biostain, Traralgon, Australia). Formalin-fixed tissues were transferred to 70% Ethanol (EtOH) after 24 hours and subsequently embedded in paraffin. FFPE blocks were stored at RT and slides were cut fresh prior to use for heamatoxylin and eosin (H&E) staining, Immunohistochemistry (IHC) and multiplex immunohistochemistry (mIHC), as detailed in **Immunohistochemistry** section. The fourth tissue piece was further divided and this margin was used to establish tumouroids and expansion of TILs.

**2.3 Expansion of Lymphocytes**

**Tumour Infiltrating Lymphocyte (TIL) Expansion**

To establish TIL expansion, small pieces of viable tumour (1 $mm^3$) were divided and each placed in 48-well plate containing CM supplemented with 6000 IU/mL recombinant human interleukin-2 (IL-2) (NCI, Charles River Laboratories, Massachusetts, USA). Media was changed twice weekly; by removing half of the CM and replacing with fresh CM supplemented with 12,000 IU/mL IL-2. Once cells reached 100% confluency, wells were transferred to a T25 flask and maintained at

$1.5x10^6$ cells/mL of CM supplemented with IL-2 (6000 IU/mL). When in culture, expanded TILs were used for downstream assays or cryopreserved for long-term storage at -80°C.

**MAIT Cell Expansion Protocol**

To expand MAIT cells from peripheral blood, PBMCs were isolated by Ficoll-Plaque density gradient using the SepMate protocol and sorted by FACS as described in **Cell Separation: Fluorescent Activated Cell Sorting (FACS)**. Primary human MAIT cells were stimulated for 48 hours on 96 well plates with 10 μg/mL plate-bound anti-human CD3 (OKT3; BD Biosciences, New Jersey, USA) and 1:40 dilution of Immunocult™ (Stemcell Technologies, Vancouver, Canada) in CM supplemented with 100 U/mL recombinant human IL-2 (NCI, Charles River Laboratories, Massachusetts, USA), 10 ng/mL rhuIL-7 (NCI, Charles River Laboratories, Massachusetts, USA), 50 ng/mL rhuIL-12 (Lonza, Basel, Switzerland), 50 ng/mL rhuIL-15 (NCI, Charles River Laboratories, Massachusetts, USA) and 50 ng/mL rhuIL-18 (R&D Technologies, Rhode Island, USA). After 48 hours, cells were removed from anti-CD3, anti-CD28 and PHA stimulation and maintained in human T cell media and supplemented cytokines.

## 2.4 Tumouroids

**Establishment of Patient-Derived Tumouroid Cultures**

To establish tumouroids, viable tumour was minced and enzymatically digested using Advanced DMEM F-12 (Gibco, Thermo fisher Scientific, Massachusetts, USA) supplemented with 100 U/mL penicillin and 100 μg/mL streptomycin (Sigma Aldrich, Missouri, USA), glutamax (=2mM L-glutamine) (Gibco, Thermo fisher Scientific, Massachusetts, USA), 25mM HEPES, 10 μg/mL gentamycin (Pfizer, New York, USA) and 0.25 μg/mL amphotericin B (Gibco, Thermo fisher Scientific, Massachusetts, USA), 1mg/mL collagenase type IV (Worthington, Biochemical Corporation, New Jersey, USA), 125 μg/mL dispase (Gibco, Thermo fisher Scientific, Massachusetts, USA), 25 μg/mL hyaluronidase (Sigma Aldrich, Missouri, USA) and 0.1 μg/mL DNAse (Sigma Aldrich, Missouri, USA), in a water bath, 37°C for 30-60 minutes. Tumour pieces were then titurated using a p-1000 pipette, media was added and homogenate was passed through a 70 uM filter. Cells were centrifuged at 400 x g, supernatant discarded and cell pellet resuspended in matrigel. 50 uL of the matrigel-cell suspension was seeded in corning 24-well plate, and maintained in 500 uL OB Media supplemented with: 5mM A8301 (Torcis Bioscience, Bristol, UK), 1 X B27™ (Gibco, Thermo fisher Scientific, Massachusetts, USA), 500 μg/mL Epidermal Growth Factor (Sigma Aldrich, Missouri, USA), 1 mg/mL Gastrin (Sigma Aldrich, Missouri, USA), 612.78 mM N-acetylcysteine (Sigma Aldrich, Missouri, USA), 10 mM SB202190 (Sigma Aldrich, Missouri, USA), 10 mM Y27632 (Sigma Aldrich, Missouri, USA), herein referred to as CRC media. Tumouroids were passaged every 7-10 days, or as required depending on growth rate.

Tumouroids that did not grow within 14-21 days were deemed stunted and were subsequently discarded.

**Passaging of Patient-Derived Tumouroid Cultures**

When tumouroids had reached 100-200 μm in diameter, tumouroids were considered suitable for passaging. A minimum of 2 wells would be cryopreserved for future use, by aspirating the media in the well and adding 1 mL of cold 10% DMSO in FCS, which was storage at -80°C.

The remaining wells to be passaged would be aspirated and cold Advanced DMEM-F/12 (Gibco, Thermo fisher Scientific, Massachusetts, USA) supplemented with 100 U/mL penicillin and 100 μg/mL streptomycin (Sigma Aldrich, Missouri, USA), glutamax (2mM L-glutamine) (Gibco, Thermo fisher Scientific, Massachusetts, USA), 25 mM HEPES, 10 μg/mL gentamycin and 0.25 μg/mL amphotericin B (Gibco, Thermo fisher Scientific, Massachusetts, USA) herein referred to as organoid basal (OB) media, would be added and used to scratch off the matrigel. The resulting mixture was transferred to a falcon tube, which was incubated on ice to convert the matrigel into a liquid state before starting centrifugation at 300 x g, 5 minutes. Media was aspirated, 1 mL of Tryple (Gibco, Thermo fisher Scientific, Massachusetts, USA) was added and tumouroids were incubated in a waterbath, 37°C for 10 minutes. Tumouroids were then triturated using a p1000 pipette, 9 mL of OBM was added and tumouroids were centrifuged 300 x g, 5 minutes. Media was aspirated and ice-cold matrigel was added to cell pellet. Amount of matrigel added to pellet was determined by cell pellet size, as a general rule each well was split 1:2. 50 μL of tumouroid/matrigel suspension was seeded per well of a 24-well plate. Plates were incubated for 30-45 minutes at 37°C for matrigel to set, before 500 μL of tumouroid growth media was added to each well. Tumouroids were grown in hypoxic conditions (37°C, 5% $O_2$, 5% $CO_2$) and growth media was changed twice weekly, and growth was monitored until subsequent passaging was required.

## 2.5 Cytotoxic Assay Protocols

**Cytotoxic Assay: Preparation of Tumouroids**

Tumouroids were deemed suitable for cytotoxic assay co-culture by passage 2-3 (10-14 days post initial biopsy) and were plated at least 5-7 days prior to performing the assay. For optimal assay conditions, organoids were grown to >50 μm and checked morphological for viability using a light microscope on the day of assay, before proceeding. Retractile tumouroids were chosen for the assay.

**Cytotoxic Assay: Passaging of Tumouroids**

At passage 2-3, when tumouroids cultivated in 24-well plate were between 100-200 μm in size,

media was aspirated from each well. Wells were washed twice with ice-cold organoid basal (OB) media, using the tip of p1000 pipette to scratch Corning Matrigel® Matrix (Sigma Aldrich, Missouri, USA) from the well, and transferred to a falcon tube.

Aspirate was incubated on ice, for 5 minutes and centrifuged 5 minutes, 500 x g, 4°C. OB media was aspirated and cell/matrigel pellet was resuspended in 1-5 mL pre-warmed (37°C) TrypLE Express (Gibco, Thermo fisher Scientific, Massachusetts, USA), tubes incubated in 37°C water bath, 10 minutes. Following incubation, organoids were forcefully triturated by mechanical dissociation using a p1000 pipette. To ensure organoids were at the single cell level, suspension was checked under the light microscope and further incubation with fresh TrypLE Express was commenced, if necessary. Cells were washed with 15 mL of OB media and centrifuged 5 minutes, 500 x g, 4°C. Supernatant was aspirated and the cell pellet was resuspended in 100 µL of ice-cold liquid matrigel. To check cell density, a small aliquot of cell suspension was visualised under a light microscope and additional matrigel was added if required.

Organoids were plated on pre-warmed µ-Plate 96 Well (ibidi, GmbH Germany), by seeding 20 µL of matrigel/cell suspension into each well, and placed to set in 37°C incubator for 30-60 minutes. Following incubation, 350 µL of pre-warmed CRC media, was added to each well, and tumouroids were grown in hypoxic conditions (37°C, 5% $O_2$, 5% $CO_2$) for 7-10 days prior to running the cytotoxic assay.

**Cytotoxic Assay: Preparation of TILs**

Expanded TILs were harvested from either 24-well plate or T25 flask and filtered through 70uM filter. Cells were counted using a haemocytometer, and subsequent TIL concentrations were determined. To calculate Effector: Target (E: T) ratio of TILs: tumouroid, tumouroids per well were counted. TIL concentration was determined for 5000 TILs: one organoid, and did not exceed 300,000 TILs/well. TILs were then centrifuged, washed with CM, centrifuged again and resuspended in the required volume of pre-warmed CRC media and kept at 37°C until ready for addition to the cytotoxic assay.

**Preparing the Cytotoxic Assay Media**

The number of wells required for the cytotoxic assay was determined and multiplied by 344 uL of CRC media. Propidium Iodide (PI) (Sigma Aldrich, Missouri, USA) was added, for a final concentration of 17.1 µg/mL, TILs were then resuspended in this media.

Media from the cultivated organoids in µ-Plate 96 was aspirated. Wells were set up in duplicate per condition with the following conditions: organoids alone (negative control), organoids+TILs, organoids+TILs+anti-PD-1 antibody (Keytruda, Merck, New Jersey, USA).

For the negative control wells 350 µL of CRC media + PI was added. TIL suspension was then added to remaining wells and supplemented with 6,000 IU/mL of rh-IL-2. Anti-PD-1 antibody

(Keytruda, Merck, New Jersey, USA) was added to respective wells at final concentration of 142.86 µg/mL. Remaining empty wells within the plate were filled with sterile PBS to prevent evaporation.

**Imaging Acquisition**

The µ-Plate (96 wells) was mounted on a heated stage in a temperature controlled chamber, which was maintained at 37°C, 5% $CO_2$ ("The Brick"; ibidi). Using the cellSens software (Olympus), imaging of the plate was obtained on a 10x (NA 0.5) air objective, selecting 10 tumouroids at the periphery of the matrigel. Optical sections were acquired through sequential scans of brightfield and PI (excitation 493nm) every 2 hours for 48 hours.

Imaging series were analysed using ImageJ software (NIH, Maryland, USA) to obtain the mean fluorescence intensity (MFI) of PI uptake in tumouroids over time. The mean of 10 tumouroids per well was taken to analyse kinetics of TIL-induced killing over time. The maximum MFI per time point was also assessed to obtain the overall maximum killing threshold of each condition.

**Caspase 3/7 E:T Titration**

To assess TIL-mediated tumouroid death, generation of activated-caspase 3/7 was used to show induced apoptosis using CellEvent™ Caspase-3/7 Green ReadyProbes™ Reagent (Thermo fisher Scientific, Massachusetts, USA). One drop of CellEvent™ Caspase-3/7 Green ReadyProbes™ Reagent and 17.1 µg/mL PI (Sigma Aldrich, Missouri, USA) was added to 1mL of CRC media and subsequently aliquoted to wells containing tumouroids for the assay. As this results anticipated, as TIL number increased, rapid tumouroid death was observed. Caspase 3/7 was detected using the Olympus IX3 GFP filter.

**MAIT Cell Cytotoxic Assay Co-culture**

Patient-derived tumouroids were established and maintained as previously described. Approximately 7 days before running the co-culture experiment, tumouroids were passaged and 20 uL seeded into a 96-well ibidi plate, with 350 uL of CRC media added. Healthy donor whole blood was collected following the **Blood Collection: BD Vacutainer® CPT™ Cell Preparation Tube with Sodium Citrate**. Following isolation, cells were counted and stained following the **Cell Separation: Fluorescent Activated Cell Sorting (FACS)** protocol, using antibodies against: CD3 PE-CF594, Vα7-2 BV711, CD161 PE and DAPI as a cell viability marker. Once cells were collected, they were maintained in SM at RT and centrifuged 300 x g, 10 minutes. Supernatant was aspirated and cell pellet was resuspended in 0.5-1 mL CM, and subsequently counted in 0.4% trypan blue (Gibco, Thermo fisher Scientific, Massachusetts, USA) using a haemocytometer, to confirm cell count from flow cytometry sorter.

For stimulated MAIT cells on Day 0 (D0): MAIT cells were stimulated for 48 hours using the **MAIT Cell Expansion Protocol**, before being used in co-culture with tumouroids.
For unstimulated MAIT cells on Day 2 (D2): Freshly isolated MAIT cells were used immediately in co-culture with tumouroids.

For co-culture with tumouroids approximately 2-4x$10^5$ MAIT cells were added to each well. This would depend on the cell harvest of each individual donor; however, the same number of cells would uniformly be added to each condition. The co-culture followed the same protocol: **Preparing the Cytotoxic Assay Media**, with some amendments. In the MAIT co-culture 100 U/mL of IL-2 was used in all wells. 5-OP-RU was generously donated by Dale Godfrey and Paul Beavis and used at 10 nM final concentration. Anti-PD-1 antibody (Keytruda, Merck, New Jersey, USA) was used at final concentration of 50 ug/mL Anti-MR1 (Biolegend, California, USA) antibody was used at final concentration of 10 μg/mL.

### 2.6 Flow Cytometry

#### Tissue Processing for Flow Cytometry Phenotyping

Following surgical resection, tumour and normal liver tissue (>3 cm from tumour) were collected immediately in RPMI 1640 (Gibco, Gibco, Thermo fisher Scientific, Massachusetts, USA) supplemented with 5% FBS (Gibco, Thermo fisher Scientific, Massachusetts, USA), 100 U/mL penicillin and 100 μg/mL streptomycin (Sigma Aldrich, Missouri, USA) herein referred to as wash medium and kept on ice until processed. Tissue was initially divided for storage, tumouroid establishment and TIL expansion, as described above. Remaining tissue was then weighed and finely minced using a scalpel blade. Minced tissue was divided into 1g (maximum) and enzymatically digested with 5 mL of DMEM supplemented with 75 U/mL collagenase type IV (Worthington) and 0.1 μg/mL DNase (Sigma Aldrich, Missouri, USA) in gentleMACS c-tubes (Miltenyi Biotech, Bergisch Gladbach, Germany). GentleMACS c-tubes harbouring tissue was placed on a gentleMACS dissociator to achieve single cell suspension, by using the human tumour program 1, 2 and 3. Following this, tubes were incubated on at shaker at 37°C for 30-60 mins. The gentleMACS c-tubes were placed on the gentleMACS dissociator and tumour programs were repeated as before. To inhibit the enzymatic reactions, tissue homogenate was passed through a 100 μm filter into a 50 mL falcon tube, and the plunger of a 3 mL syringe was used to grind remaining whole tissue. The filter was rinsed with wash medium and the single cell suspension was then poured through 70 μm filter followed by a 40 μm filter, with subsequent washing in-between. Cells were centrifuged at 330 x g, 10 minutes, 4°C. Supernatant was aspirated and red blood cells were lysed by resuspending the cells in ACK buffer for 3 minutes, room temperature with constant agitation. Tubes were filled to 50 mL with PBS, centrifuged for 300 x g, 10 minutes,

4°C. Supernatant was aspirated and cells resuspended in 2-3 mL wash medium for counting. Cells were diluted 1:10 with 0.4% trypan blue (Gibco, Thermo fisher Scientific, Massachusetts, USA) and counted using a haemocytometer. Cells were kept at 4°C until ready for downstream applications including flow cytometry, fluorescent activated cell sorting (FACS) or *in vitro* assay.

**Surface Cell Staining for Flow Cytometry**

Following tissue digestion for tumour and liver tissue or isolation of PBMCs, cells were divided into 4 wells of a 96-well v-bottom plate (Nunc, Thermo scientific, Massachusetts, USA). For unstained (U/S) and Fixable Viability Stain (FVS) only controls, 0.5-1 $x10^5$ cells were added to respective wells. For stained and isotype control samples 0.5-1.0$x10^6$ cells were added to respective wells. Cells were washed twice with PBS and centrifuged 400 x g, 4 minutes, 4°C. Fixable Viability Stain 575 (BD Biosciences, New Jersey, USA) was thawed on ice and diluted 1:1000 with PBS, 200 µL diluted FVS575 was added to FVS-only and isotype controls and stained sample, U/S control was resuspended in PBS. Cells were incubated at room temperature, 10 minutes in the dark. Following incubation, plate was centrifuged 400 x g, 4 minutes, 4°C to pellet cells, supernatant was discarded and cells were washed in PBS. Human Fc Block (BD Biosciences, New Jersey, USA) was diluted 1:10 in Brilliant Stain Buffer (BD Biosciences, New Jersey, USA) and stain and isotype-control samples were resuspended in this medium. U/S and FVS-only controls were resuspended in RPMI, 4% FCS, 100 U/mL penicillin and 100 µg/mL streptomycin (Sigma Aldrich, Missouri, USA) herein referred to as Staining Media (SM), samples were incubated 10 minutes, 4°C in the dark. Following incubation, 100 µL of antibody cocktail was added to stain and isotype-control wells, SM was added to U/S and FVS-only controls and samples were incubated 30 minutes, 4°C in the dark. Samples were washed twice with SM and fixed with 100 µL 1% Paraformaldehyde (PFA) in SM and acquired on the BD LSRFortessa™ X-20 within 48 hours. Alternatively, cells used for intracellular cytokine staining (ICS) or transcription factor (TF) staining, were fixed with 100 µL 1x Cytofix/Cytoperm (BD Biosciences, New Jersey, USA) or 1x Transcription Factor Buffer (BD Biosciences, New Jersey, USA) working solution and incubated 20 minutes or 45 minutes, 4°C in the dark, respectively.

**Intracellular Cytokine Staining (ICS) for Flow Cytometry**

Following cytofixation/permeabilisation cells were washed twice with 1x Perm/Wash™ (BD Biosciences, New Jersey, USA) working solution and centrifuged 350 x g, 4 minutes, 4°C. Cell pellets were resuspended in 50 µL of intracellular cytokine antibody/isotype cocktail and incubated 30 minutes, 4°C in the dark. Cells were washed twice with 1x Perm/Wash and resuspended in 200 µL of SM. Cells were acquired on the BD LSRFortessa™ X-20 within 8 hours of intracellular staining.

**Transcription Factor Staining for Flow Cytometry**

Following cytofixation/nuclear permeabilisation, cells were washed twice with 1x TF Perm/Wash™ (BD Biosciences, New Jersey, USA) working solution and centrifuged 350 x g, 4 minutes, 4°C. Cell pellets were resuspended in 100 µL of transcription factor monoclonal antibody/isotype cocktail and incubated 30 minutes, 4°C in the dark. Cells were washed twice with 1x TF Perm/Wash and resuspended in 200 uL of SM. Cells were acquired on the BD LSRFortessa™ X-20 within 48 hours of transcription factor staining.

**Cell Separation: Fluorescent Activated Cell Sorting (FACS)**

Cells were counted using a haemocytometer and resuspended at 2 $x10^8$/mL in SM. Surface antibodies were added to the cell suspension and incubated for 20 minutes in the dark at RT. Cells were washed with 5-10 mL of SM, centrifuged 300 x g, 5 minutes. Cell pellet was resuspended in SM at 1-2 $x10^8$/mL and acquired on a BD FACSAria™ Fusion 3 or 5. Sorted T-cells were defined initially by double exclusion, DAPI negative, lymphocyte morphology (as gated by SSC-A versus FSC-H) that were subsequently CD3+.

**Expanded TIL FACS Sort**

On the day of the cytotoxic assay, expanded TILs were stained following **Cell Separation: Fluorescent Activated Cell Sorting (FACS)** protocol. Following doublet exclusion, lymphocyte morphology (as gated by SSC-A versus FSC-H) that were subsequently CD3+, the following cells were defined for the TIL subset cytotoxic assay: NK Cells: CD56+CD8-, NKT Cells: CD3+CD56+, CD8: CD3+CD8+, CD4: CD3+CD4+

**MAIT Cell FACS Sort**

MAIT cells were defined as CD161 high, Vα7.2 and 5-OP-RU tetramer positive. Conventional cytotoxic T-cells were gated as CD8+.

**Cell Separation: Magnetic Activated Cell Sorting (MACS)**

To obtain an enriched population of MAIT cells, PBMCs or freshly isolated tissue-lymphocytes were counted using a haemocytometer and resuspended to 1 x $10^7$/mL in PBS, pH 7.2, 0.5% BSA and 2 mM EDTA, herein referred to as MACS buffer. Cells were centrifuged 300 x g, 5 minutes and resuspended in 90 µL MACS buffer with 10 µL of anti-human Vα7.2-PE (clone REA179, Miltenyi Biotech, Bergisch Gladbach, Germany), cells were incubated 20 minutes in the dark, 4°C. Cells were washed and resuspended in 80 µL of MACS buffer and labelled with 20 µL of Anti-PE Microbeads (Miltenyi Biotech, Bergisch Gladbach, Germany) and incubated 15 minutes in the dark, 4°C. Cells were washed and resuspended in 500 µL of MACS buffer, which was then passed through a magnetic field using a MACS MS column (Miltenyi Biotech, Bergisch Gladbach, Germany). The column was washed 3 times, and removed from the magnetic field. One

millilitre of MACS buffer was then applied to the column and positively labelled cells were collected when pushed through, using a plunger. Cells were counted with a haemocytometer and cell purity was confirmed by subsequent surface staining and flow cytometry acquisition and analysis.

**Flow Cytometry Antibodies**

All antibodies were mouse anti-human monoclonal antibodies, unless otherwise stated. Viability dyes included the use of Fixable Viability Stain 575 and 620 (BD Biosciences, New Jersey, USA) and DAPI (Thermo Fisher Scientific).

**Table 2.2 Flow Cytometry List of Antibodies**

| Specificity | Clone | Fluorochrome | Company | Dilution |
|---|---|---|---|---|
| **CD3** | PE-Cy7 | SK7 | BD Biosciences | 1:50 |
| **CD3** | PE-CF594 | UCHT1 | BD Biosciences | 1:40 |
| **CD45** | FITC | HI30 | BD Biosciences | 1:25 |
| **CD45** | BV510 | HI30 | BD Biosciences | 1:40 |
| **CD4** | APC-H7 | RPA-T4 | BD Biosciences | 1:50 |
| **CD4** | BV650 | SK3 | BD Biosciences | 1:40 |
| **CD8α** | RPA-T8 | V500 | BD Biosciences | 1:50 |
| **CD8α** | SK1 | APC-H7 | BD Biosciences | 1:20 |
| **CD161** | DX12 | PE | BD Biosciences | 1:20 |
| **Vα7.2** | 3C10 | BV711 | Biolegend | 1:40 |
| **Vα7.2** | 3C10 | BV421 | Biolegend | 1:20 |
| **Vα7.2** | REA179 | PE | Miltenyi Biotech | 1:100 |
| **HLA-DR** | G46-6 | BB515 | BD Biosciences | 1:20 |
| **CD279/PD-1** | EH12.2H7 | BV785 | Biolegend | 1:20 |
| **CD69** | FN50 | PE-Cy7 | BD Biosciences | 1:100 |
| **CD45RO** | UCHL1 | PerCP-Cy5.5 | BD Biosciences | 1:20 |
| **Foxp3** | 259D/C7 | PE | BD Biosciences | 1:5 |
| **CD25** | M-A251 | PE-Cy7 | BD Biosciences | 1:20 |
| **CD107a** | H4A3 | APC | BD Biosciences | 1:20 |
| **CD56** | NCAM16.2 | FITC | BD Biosciences | 1:50 |
| **CD56** | NCAM16.2 | PE-CF594 | BD Biosciences | 1:20 |
| **HLA-DR** | G46-6 | BB515 | BD Biosciences | 1:66 |
| **CD11b** | ICRF44 | BV786 | BD Biosciences | 1:20 |
| **CD33** | WM53 | PE-Cy5 | BD Biosciences | 1:10 |
| **CD279/PD1** | MIH4 | BV421 | BD Biosciences | 1:20 |
| **CD274/PD-L1** | MIH1 | APC-R700 | BD Biosciences | 1:20 |
| **IFNγ** | 4S.B3 | BV786 | BD Biosciences | 1:20 |
| **TNFα** | MAb11 | PerCP-Cy5.5 | BD Biosciences | 1:100 |
| **Granzyme B** | GB-11 | PE | Pericluster | 1:200 |
| **MR1 Tetramer** | 5-OP-RU ligand | BV421 | NIH | 1:20 |

The MR1 tetramer technology was developed jointly by: Professors James McCluskey, Jamie Rossjohn, and David Fairlie; and the material was produced by the NIH Tetramer Core Facility as permitted to be distributed by the University of Melbourne.

**Flow Cytometry Analysis**

For analysis of clinical samples, analysis was performed using FlowJo, LLC, vX0.7 (BD Biosciences, New Jersey, USA). T-cells were defined initially by double exclusion, FVS575-, lymphocyte morphology (as gated by SSC-A versus FSC-H), CD45+ and were subsequently CD3+.

### 2.7 Multiplex Cytokine Analysis

**Twelve- and Eight-plex Cytokine**

Twelve-plex cytokine array was performed using the Cytometric Bead Array (CBA) Flex Sets: IL-1α, IL-1β, IL-2, IL-4, IL-10, IL-12p70/IL-23, IL-17F, IFNγ, TNFα, GM-CSF, MCP-1 and VEGF (BD Biosciences, New Jersey, USA) according to manufacturers instructions.

Eight-plex cytokine array was performed using the CBA Flex Sets: IL-2, IL-6, IL-10, TNFa, FasL/CD178, Granzyme-B, IL-12p70, IFNγ according to manufacturers instructions.

Top standards were prepared at 2500 pg/mL and were serially diluted 1:2 to 10 pg/mL, with a blank control at 0 pg/mL. Briefly, capture beads were plexed and mixed 1:2 with standard/sample duplicates in 96-well plate. Plate was incubated at room temperature, light protected, 1 hour. PE-detection reagent was added to standard/sample wells, incubated room temperature, light-protected, 1 hour. Wells were washed with wash buffer, centrifuged 200 x g, 5 minutes. Wells were resuspended in wash buffer and acquired on BD FACSVerse™. Acquisition of each analyte included 300 events. Results were analysed using FCAP Array™ unknown concentrations were determined from the standard curve of each analyte.

### 2.8 Microscopy, Histology & Immunohistochemistry

**Scanning Electron Microscopy (SEM)**

Morphological killing was also examined by scanning electron microscopy (SEM) (JCM-6000, Jeol, operated at 15 kV under high vacuum). Organoids were plated onto an Aclar film in a 12 well plate overnight and co-cultured with TILS for 2 hours the following 156 day. Organoid-TILS co-cultures were fixed with 2.5% glutaraldehyde, 2% PFA in 0.1M sodium cacodylate buffer for 1 hour at 37°C, followed by washes in 0.1M sodium cacodylate buffer. For SEM, the fixed organoid-TILS co- cultures were dehydrated through a series of increasing concentrations of ethanol, underwent critical point drying in Leica EM CPD300, sputter-coated with gold and imaged using a bench top scanning electron microscope (JCM-6000, Jeol), operated at 5 kV under high vacuum.

**Immunohistochemistry**

**Immunohistochemistry: Manual**

FFPE blocks were cut at 4 μm thickness and transferred onto Superfrost Plus slides (Thermo fisher Scientific, Massachusetts, USA) and melted in 60°C oven for 1 hour. Slides were dewaxed in histolene and subsequently rehydrated in graded EtOH. Antigen retrieval was achieved by incubating slides in antigen retrieval buffer (**Table 2.2**) in pressure cooker at 125°C, 3 minutes followed by 90°C, 10 seconds. Slides were subsequently cooled at RT for 30 minutes, and then blocked with 10% hydrogen peroxide ($H_2O_2$) (Merck-Millipore, Massachusetts, USA) for 10 minutes. Slides were washed with 1% Tri-Phosphate Buffer (TBS) Tween (Sigma Aldrich, Missouri, USA) and primary antibody was added to each slide covering tissue, and incubated either overnight at 4°C or 1 hour at room temperature in humidified chamber. Following incubation, slides were washed three times in TBS-Tween and ImmPRESS® (Vector laboratories, California, USA) secondary antibody was added to tissue sections and incubated 30 minutes, room temperature in a humidified chamber. Slides were washed and staining was developed using DAB solution (DAKO, Agilent Pathology, California, USA) visualised using a light microscope. Slides were counterstained using Meyer's haematoxylin, rehydrated in graded EtOH and cover-slipped using automated coverslip machine (DAKO, Agilent Pathology, California, USA). Slides were scanned using the Virtual Slide microscope VS120 (Olympus Life Sciences, Tokyo, Japan) and digital images were analysed on Olyvia (Olympus Life Science, Tokyo, Japan).

**Table 2.3. Immunohistochemistry Antibody List: Manual Staining**

| Specificity | Antigen Retrieval | Clone | Dilution | Secondary |
|---|---|---|---|---|
| MYB | EDTA (10 mM) pH: 8 | EP769Y | 1:500 | Anti-Rabbit |
| GRP78 | EDTA (1 mM) pH: 8 | N-20 | 1:800 | Anti-Goat |
| RAD21 | Tris (10 mM) pH | Ab42522 | 1:200 | Anti-Rabbit |

**Table 2.4. Immunohistochemistry Antibody List: Automated Staining using the Ventana Benchmark Ultra platform**

| Specificity | Clone | Dilution | Company |
|---|---|---|---|
| CD8 | 4B11 | 1:100 | Leica Biosystems |
| PD-L1 | SP263 | Pre-dilute | Ventana |
| PMS2 | EPR3947 | Pre-dilute | Cell Marque |
| MSH6 | 08-1374 | 1:800 | Invitrogen |

**Immunohistochemistry: Automated**

These 3□m serial sections of were stained on a Ventana Benchmark Ultra platform (Ventana Medical Systems Inc, Arizona, USA) for using anti-CD8+ clone 4B11 (NCL-CD8-4B11, Leica Biosystems, Wetzlar, Germany) at a working dilution of 1:100, anti-PDL1 SP263 (790-4905, Ventana Medical Systems Inc, Arizona, USA) pre-dilute, anti-PMS2 EPR3947 (288R-18-ADR, Cell Marque, California, USA) pre-dilute and anti-MSH6 44 (08-1374, Invitrogen, California, USA) at 1:800. FFPE human placental, tonsil, lymph node, normal colon and colorectal tumour and were used as controls.

**CD8+ and PD-L1 scoring**

A trained pathologist selected two 'hot spot' regions, defined as 740x540 pixels, at 1.181mm/pixel = 0.56mm$^2$. For our quantitation 2 x 0.5mm$^2$ hotspots were selected per region. The invasive margin (IM) was defined as 1mm wide region centered on the border separating the host tissue from malignant glands, the central tumour (CT) was defined as everything else.

Positive tumour cells (TC) were defined as percentage of tumour cells with any discernible membrane staining and immune cells (IC) defined as percentage of tumour area covered by PD-L1 positive immune cells. Areas excluded: surface necrosis, macrophages and neutrophils associated with necrotic areas, normal lamina propria in non-invasive component. Cutoff values of 1%, 5% and 50% were set for TC or IC expression.

**Histoscore for Nuclear and Cytoplasmic Staining**

Each tissue section selected a CT and IM as defined by a registered pathologist. A region of 1mm$^2$ was assessed for each area (CT or IM). IHC assessment for other antigens involved inspection of VS120 generated images and scoring on the basis of a 0-12 Histoscore, which was the product of staining intensity (0=none, 1=weak, 2=moderate, 3=strong) and extent (0=none, 1=5% or less, 2=6-15%, 3=51-75%, 4=>76%). Two investigators in a blinded fashion scored de-identified slides.

**Multiplex Immunohistochemistry (mIHC)**

Multiplex immunohistochemistry was performed on FFPE sections using the PerkinElmer Opal 6-colour kit (Massachusetts, USA) as per manufacturer's instructions using the automated Leica bond RX opal multiplex protocol (Leica Biosystems, Wetzlar, Germany) as per manufacturer's instructions. The list of reagents is detailed in **Table 2.5**.

**Table 2.5 Antibody list for multiplex immunohistochemistry**

| Marker | Primary Antibody | Dil$^{n}$ | Secondary Antibody | TSA Plus | Colour |
|---|---|---|---|---|---|
| **PD-1** | Cell Marque (NAT105) | 1:100 | Mouse (pre-dilute) | 690 | Red |
| **PD-L1** | Ventana (SP263) | re-dilute | Rabbit (pre-dilute) | 620 | Yellow |
| **CD8** | Thermo Fisher (4B11) | 1:100 | Mouse IgG (1:500) | 540 | Green |
| **CD4** | Spring Bioscience (SP35) | 1:100 | Rabbit IgG (1:1000) | 570 | White |
| **FOXP3** | BioSB (polyclonal) | 1:100 | Rabbit IgG (1:1000) | 650 | Orange |
| **AE1AE3** | Leica (AE1 and AE3) | 1:200 | Mouse IgG | 520 | Magenta |

**Multispectral Imaging and Spectral Unmixing and Phenotyping**

Multiplex stained slides were imaged using the Vectra Multispectral Imaging System version 2 (PerkinElmer, Massachusetts, USA). Areas of interest included tumour and high power multispectral images (20X) were acquired. A spectral library containing the emitting spectral peaks of all fluorophores was created with the Nuance Image Analysis software (PerkinElmer, Massachusetts, USA), using multispectral images obtained from single stained slides for each marker and associated fluorophore. This spectral library was then used to separate each multispectral image into its individual components (spectral unmixing) allowing for the colour-based identification of all six markers of interest in a single image using HALO image analysis software (PerkinElmer, Massachusetts, USA). Cells were phenotyped into one of six different classes according to our markers of interest as follows: tumour cells (AE1AE3+), cytotoxic T-cells ($CD8^{+}$), helper T cells (CD4+), regulatory T-cells (CD4+FOXP3+), double negative T cells (CD3+CD4-CD8-) and other cells (DAPI+). All phenotyping and subsequent quantifications were performed blinded to the sample identity and clinical outcomes.

## 2.9 Molecular Techniques

**Extraction of RNA from Tumour Tissue**

Preserved tissue either snap-frozen or cryopreserved as described in **storage of clinical samples** were thawed on ice. Cryopreserved tissue was washed in media to remove DMSO. The AllPrep DNA/RNA Mini (Qiagen, Hilden, Germany) kit was used to extract DNA and RNA simultaneously as per manufacturer's instructions. Briefly, tissue was homogenised and placed in RLT buffer, and added to an AllPrep DNA spin column. Flow-through is collected for RNA purification and added on a RNeasy column, washed in EtOH, subsequent buffers and eluted off the column as purified RNA. Quantification of RNA was analysed on a spectrophotometer. DNA captured on original column is washed with buffers and eluted off the column as purified DNA.

**RNAseq Analysis**

The FASTQ files of the whole transcriptomics data were analysed using bcbio-nextgen pipeline to obtain the count level data. The bcbioRNASeq and DESeq2 packages in R were used for quality control and down-stream analyses. Transcript-per-million (TPM) were calculated for visualising the expression of genes. The heatmap was generated using the ComplexHeatmap package in R. Data was visualised using heatmaps, as the data had some extent of variability and there was a low sample size, which partially masked some of the true differences seen between the primary and colorectal tumours.

## 2.10 Statistical Analysis

All statistical analyses in this study were performed using GraphPad Prism (version 6 and 7; California, USA). Data analyses were conducted using unpaired Student's *t* test to compare two data sets, or using one-way/two-way ANOVA when analyzing multiple sets of data (more than two sets). Data are presented in this thesis as mean ± standard error of the mean (SEM).

**Clinical Statistical Analysis**

Data was analysed with IBM SPSS version 22 and Microsoft Excel. Overall survival was calculated from date of surgery to date of last follow up or death. Kaplan- Meier analysis with log rank test were conducted to estimate the overall (OS). Cox univariate analysis was utilised to identify factors affecting overall survival. Cox multivariate Hazards ratio model was developed to identify factors independently associated with overall survival. A p value $< 0.05$ was considered statistically significant.

## 3. THE IMMUNE RESPONSE IN mCRC AT THE PRIMARY SITE

### 3.1 Introduction

Rudolf Virchow first observed the link between the immune system and cancer in 1863, where he noted that neoplastic tissue was infiltrated with leukocytes, essentially connecting inflammation with cancer (Balkwill & Mantovani, 2001). Almost two decades later, Virchow also proposed the 'seed and soil' theory of metastasis, where he believed that metastasis occurred due to arrest of tumour-cell emboli in the vasculature (Talmadge & Fidler, 2010). These two observations by Virchow set the stage for this chapter, where assessment of the immune response and its impact on metastasis was explored.

MacFarlane Burnett and Paul Ehrlich postulated that the immune system could suppress carcinoma, in the early 1900s (Dunn *et al*., 2002). Burnett & Thomas subsequently coined "cancer immunosurveillance" as a probable mechanism of an effective immune response by which accumulations of tumour cells might be controlled (M. Burnet, 1957). Burnett implied that somatic mutations would occur naturally in dividing cells and because of this; an evolutionary mechanism must exist for eliminating malignant cells. From this theory, Burnett & Thomas speculated it was lymphocytes that actively surveyed and eliminated transformed cells (F. M. Burnet, 1970). At the time, such a new concept was highly controversial.

With the progression over the last 50 years these original concepts that have become integral to the development of tumour immunity, have been scientifically addressed. We now know the host immune system can play both a tumour-protective and tumour-enhancing role. Therefore, as the original concept of "immunosurveillance" focused on the protective role of the host immune system, this concept is no longer entirely encompassing. Instead, the broader term 'cancer-immunoediting' is more widely accepted to address these concepts (Dunn *et al*., 2002). Cancer immunoediting occurs when the immune cells and tumour cells interact, which can be either protective or indeed assist the development of the tumour. In the second instance the tumour becomes less immunogenic, and is able to evade the immune response. Such mechanisms of immune escape include downregulation of MHC-I, so the tumour cannot be readily detectable by the adaptive arm of the immune system (Garcia-Lora, Algarra, & Garrido, 2003).

Tumours also have the ability to exploit immune checkpoints by up-regulating PD-L1 (*CD274*) that inhibits T-cell function upon binding to the inhibitory checkpoint receptor PD-1 expressed on immune cells (Tumeh *et al*., 2014). PD-L1 can be induced on tumour cells extrinsically in

the TME often by IFNγ secretion (Blank *et al*., 2004). Additionally, PD-L1 can be intrinsically upregulated by tumour cells through amplification of the PD-L1 locus (Green *et al*., 2010) and structural variation of the 3' region of the *CD274* gene leading to elevated expression (Kataoka *et al*., 2016). These immune inhibitory mechanisms also lead to immune escape and subsequent tumour progression.

Most cancer deaths occur as a result of metastatic disease, which may be present at initial diagnosis (*de novo* stage IV) or when the primary tumour has been treated with curative intent and subsequently recurs (Hassett *et al*., 2017). *De novo* or synchronous presentation of stage IV CRC, with metastasis confined to the liver, represents 13 to 25% of newly diagnosed CRC patients (R. Martin *et al*., 2003). Understanding the immune response in the primary CRC site was addressed in this chapter, in a unique cohort of *de novo* mCRC patients, including some that had MSI-H tumours.

Metastatic CRC patients with microsatellite unstable tumours are a subset of patients that warrant further investigation. Traditionally, patients with mCRC (stage IV) that are MSI-H have a worse outcome than patients with mCRC MSS tumours (Goldstein *et al*., 2014; Koopman *et al*., 2009). Microsatellite unstable tumours (stages I-III) generally have a better prognosis than MSS CRC, stage for stage, except in the metastatic setting (Goldstein *et al*., 2014). The CheckMate142 study recently showed durable responses to Nivolumab, an anti-PD-1 antibody, in a group of mCRC patients that had MSI-H tumours. This cohort accounts for 5% of all CRC patients, and is a biomarker-defined subset of patients who benefit less from conventional chemotherapy and have a worse OS than patients with MSS mCRC (Overman *et al*., 2017). In this open-label phase 2 trial, 69% of patients had disease control for 12 weeks or longer. The results of this study suggest that patients with MSI-H mCRC should be considered for Nivolumab therapy. Further investigations of Nivolumab with other combinations such as Ipilumumab (anti-CTLA-4) should be further pursued in this subgroup of patients.

The basis for microsatellite instability involves DNA mismatch repair (MMR) system defects, resulting from epigenetic silencing of *MLH1, PSM2* and *MLH6* or mutations to these genes. Furthermore, Lynch syndrome is a result of germline mutations of a DNA repair gene, followed by somatic inactivation of the second allele. This defect results in accumulation of insertions or deletions in DNA repeat sequences also called microsatellites (Mlecnik *et al*., 2016). Frameshift mutations can occur in genes containing coding repeats and this can be a potential source of immunogenic neoantigen generation (D. S. Williams *et al*., 2010). Typically, patients who have microsatellite unstable tumours have a favourable prognosis and improved outcome, we believe, due to a high frequency of TILs (Alexander *et al*., 2001; Dolcetti *et al*., 1999; Gryfe *et al*., 2000;

Timmermann *et al*., 2010). However, as mentioned previously, a favourable prognosis is not observed in those patients with metastatic disease.

It is now accepted that there is an association between clinical outcome and immune cell presence documented in CRC (Balch *et al*., 1990; Galon *et al*., 2013; Galon *et al*., 2006; Jass, 1986; Naito *et al*., 1998; Ropponen, Eskelinen, Lipponen, Alhava, & Kosma, 1997). Pagés & Galon *et al* showed strong correlations between patient outcome and immune cell presence in CRC. This has led to the development of the "Immunoscore", which prognosticates patient outcome based on the presence of TILs, the most significant population being cytotoxic CD8+ T-cells (Galon *et al*., 2006; Pages *et al*., 2005; Pages *et al*., 2009). A comprehensive study by Mlecnik *et al* found that the Immunoscore was a stronger predictor of patient survival than microsatellite status alone (Mlecnik *et al*., 2016). In this study, it was found that MSI-H tumours had a prominent immune gene expression profile, which was also noticed in a subgroup of MSS tumours. MSI-H tumours displayed genetic evidence of immunoediting and had a high degree of frameshift mutations. These tumours had PD-L1 expression and had a high infiltration of Th1 effector cells that also expressed PD-1. Interestingly, those MSS patients that had a high "Immunoscore" had a prolonged disease specific survival (DSS) and a higher expression of the PD-1 gene *PDCD1* than those tumours that were MSS with a low Immunoscore (Mlecnik *et al*., 2016). This demonstrates that microsatellite status alone should not be the sole factor when considering patients for immunotherapy, and that the Immunoscore should be as part of the treatment decision-making process.

Understanding the immune response within the TME can provide more insight into why some patients respond to CBI and others do not. Indeed tumours that are MSI have many more somatic mutations and likely result in immunoediting. However, there may be other factors involved that regulate the immune response. In 2016, we investigated the immune response in a cohort of patients that were MSS with stage B (T2-4N0M0) disease. In addition to determining the immune infiltrate by classifying cytotoxic CD8+ T-cells, the transcription factor (TF) *MYB* and its pro-oncogenic target gene *GRP78* were evaluated. Patients that had relapsed had a lower infiltrate of CD8+ T-cells than those patients who were relapse-free (Millen *et al*., 2016). MYB expression was associated with those patients who relapsed. This correlated with an inverse relationship of CD8+ T-cell infiltrate, this and other experiments, and indicated that *MYB* may modulate the immune response. *GRP78* is a target gene of *MYB* and is known to modulate both immune response and therapy responses in cancer (Sugawara, Takeda, Lee, & Dennert, 1993; Wang *et al*., 2007). The expression of GRP78 tracked with MYB expression, with high expression of GRP78 only found in those patients who had relapsed, and a reduction of TILs in these areas. Together these data are the first to implicate MYB and its target gene *GRP78* as

modulators of the immune response in CRC potentially, providing insight into prognostic markers and therapeutic targets.

This current chapter investigated the immune response in a retrospective cohort of *de novo* mCRC patients, where the primary tumour had been surgically resected and evaluated. This cohort included both microsatellite stable and unstable tumours, and is the largest cohort of *de novo* mCRC MSI-H patients, to our knowledge, publically known. FFPE sections of primary tumours were investigated for infiltration of CD8+ T-cells and PD-L1 expression by IHC. Expression of other markers known to modulate the immune response including MYB and GRP78 were assessed. Another marker, RAD21, known to be predictive of chemotherapy treatment responses in CRC was also investigated. The protein RAD21 forms part of the cohesion complex; that is integral to chromosome segregation and error-free DNA repair (Deb *et al.*, 2014). Deb *et al* found that patients with colorectal tumours expressing RAD21 had aggressive disease. Additionally, RAD21 expression was found to be associated with tumours that were mutant KRAS and resistant to chemoradiotherapy. Assessment of these parameters provided important insight into the immune modulation and tumour progression mechanisms at play when the primary tumour is *in situ* with synchronous metastatic disease.

**Hypothesis:**

Patients with microsatellite unstable tumours will have a poor prognosis despite an increased infiltration of TILs.

**Aims:**

**1.** Assess the immune environment in primary tumours of *de novo* mCRC patients.

**2.** Determine survival factors in *de novo* mCRC patients associated with tumour progression.

### 3.2 Immune Status in Primary Tumours of Patients With mCRC

One hundred and nine patients with *de novo* mCRC who underwent primary tumour resection and had available archival tumour specimens were included in this study. The median OS in the entire cohort was 19 months. Microsatellite status was defined as either: deficient MMR (dMMR)/MSI-H (n = 12, 11%) or proficient MMR (pMMR)/MSS (n = 97, 89%), as outlined in **Table 3.1**. In univariate hazard ratio analysis we found that patients who were 65 years and older had a significantly reduced OS as seen in **Table 3.3**. No significant difference in OS was seen between patients with MSI-H/dMMR and MSS/pMMR tumours, as shown **Figure 3.1**

(median 12 months; 95% CI: 6.13-17.87) MSI/dMMR vs. 19 months (95% CI 13.34-24.66) MSS/pMMR, log rank p=0.304). Defects in mismatch repair genes were defined by diagnostic pathology using a PCR panel to detect specific microsatellite repeats (MSI-H versus MSS). Those samples with unknown MSI status from diagnostic pathology were subsequently tested using IHC to determine loss of protein expression and therefore defective mismatch repair (dMMR) of PMS2 and MSH6 by a gastric pathologist. Retention of PMS2 and MSH6 was therefore defined as proficient MMR (pMMR). Subsequent confirmation and validation of high frequency microsatellite instability (MSI-H) and microsatellite stable definition (MSS) was determined by the Bethesda PCR panel that interrogated five microsatellite loci (Murphy *et al*., 2006).

**Table 3.1. Microsatellite status demographic**

| Clinical Characteristics | Overall | dMMR/MSI-H | pMMR/MSS |
|---|---|---|---|
| **Total, n** | 109 | 12 | 97 |
| **Age (years), median** | 28-89, 89 | 48-87, 74 | 28-89, 69 |
| **Female, n (%)** | 50 (46) | 8 (67) | 42 (43) |
| **Male, n (%)** | 59 (54) | 4 (33) | 55 (57) |
| **Pathology Tumor Stage** | | | |
| **T2, n (%)** | 2 (2) | 1 (8) | 1 (1) |
| **T3, n (%)** | 48 (44) | 5 (42) | 43 (44) |
| **T4, n (%)** | 59 (54) | 6 (50) | 53 (55) |
| **Colon, n (%)** | 99 (91) | 12 (100) | 87 (90) |
| **Rectum, n (%)** | 11 (10) | 0 (0) | 10 (10) |
| **Right-sided** | 45 (41) | 10 (83) | 46 (47) |
| **Left-sided** | 59 (54) | 1 (8) | 57 (59) |
| **Unknown sidedness** | 5 (5) | 1 (8) | 4 (4) |

Patients were first stratified into MSI-H/dMMR and MSS/pMMR there was no significant difference in OS as seen in **Figure 3.1** (median 12 months MSI/dMMR vs. 19 months MSS/pMMR). However, there was perhaps a trend for MSI-H/dMMR to have a reduced OS, in keeping with the current literature.

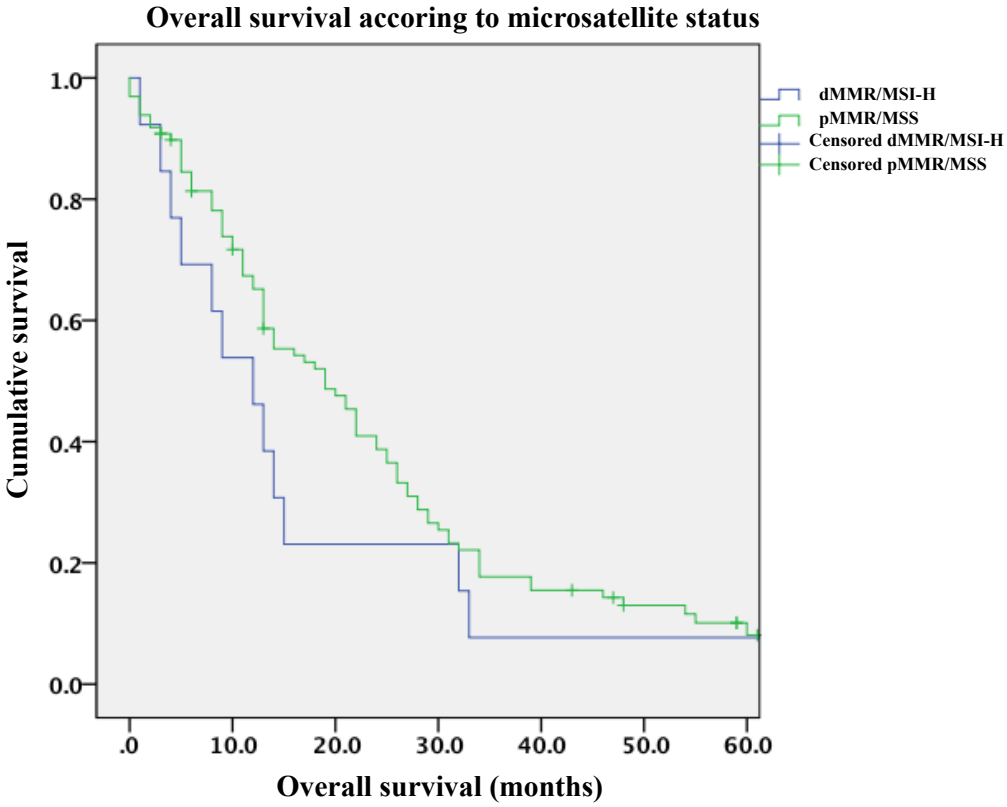


**Figure 3.1 Mismatch repair deficiency is not associated with a survival advantage in *de novo* mCRC tumours.** Kaplan-Meier survival curve showing OS stratified on microsatellite status of patients with *de novo* mCRC. Patients were stratified as MSI-H/dMMR (blue line) vs. MSS/pMMR (green line) against months. Median survival was 12 months (MSI-H/dMMR) and 19 months (MSS/pMMR), n=109 patients in total, MSI-H/dMMR n=12, MSS/pMMR n=97 Survival based on MSI status. Median survival for dMMR 12 months compared to 19 months for pMMR (log rank p=0.304).

To understand if survival was affected in some manner, by the immune response, TIL infiltrate was assessed. Cytotoxic CD8+ T-cells were quantified using IHC on whole tumour sections. In the earlier publications by Galon & Pagès *et al*, immune 'hot spots' were selected and quantified within the two tumour regions: CT and IM (Galon *et al*., 2006). We followed this approach in our cohort and a trained pathologist selected two 'hot spot' regions, defined as 740x540 pixels, at 1.181mm/pixel = 0.56mm$^2$. For our quantitation 2 x 0.5mm$^2$ hotspots were selected per region. The IM was defined as 1mm wide region centered on the border separating the host tissue from malignant glands, the CT was defined as other tumour region.

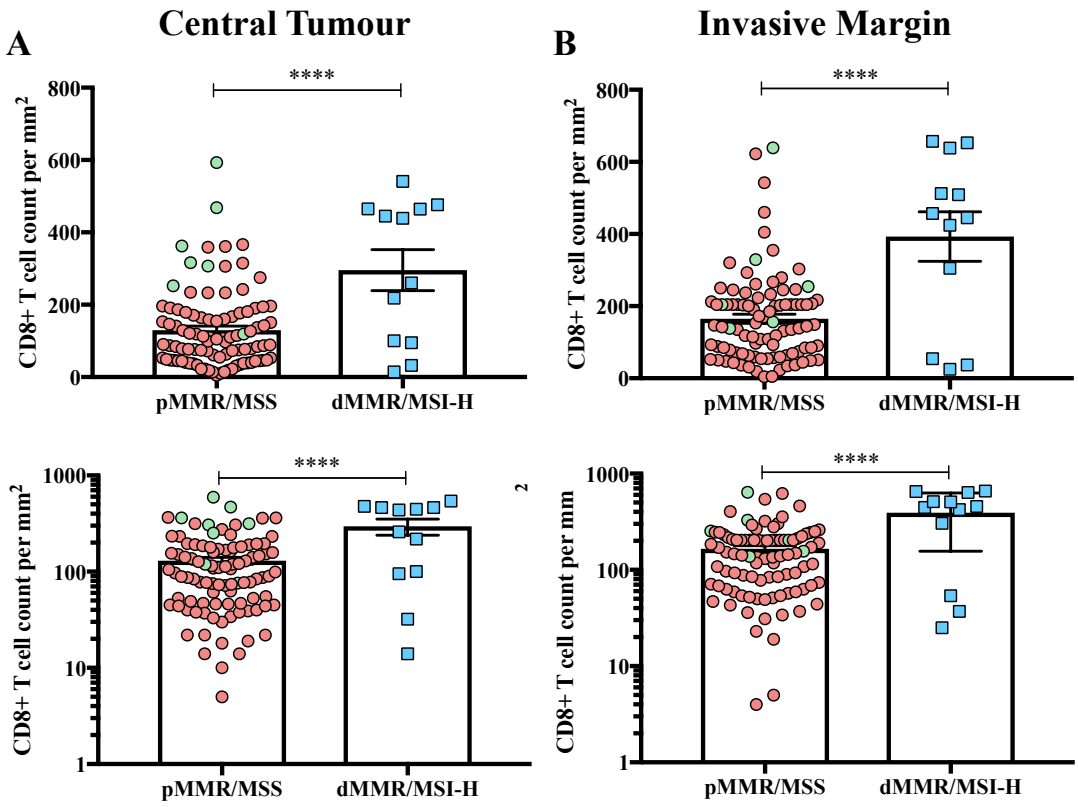


**Figure 3.2 Tumours that are dMMR/MSI-H have a higher immune infiltrate at both the CT and IM.** CD8+ T-cells were quantified as positive cells/mm$^2$ in each region of the tumour (**A**) shows CD8+ count/mm$^2$ in tumours that are pMMR/MSS (red) and dMMR/MSI-H (blue) in the CT and (**B**) IM using a linear scale (**C**) shows CD8+ count/mm$^2$ in the CT and (**D**) IM using a log scale to highlight the broad range of TIL. Green symbols represent patient outliers selected for additional microsatellite confirmation. Error bars represent SEM, n=96 (pMMR/MSS), n=12 (dMMR/MSS), two-tailed unpaired Mann-Whitney t-test, ****p<0.001.

When quantifying the CD8+ T-cell infiltrate as seen in **Figure 3.2**, it can be seen that microsatellite unstable tumours (dMMR/MSI-H) had a higher CD8+ T-cell infiltrate compared to microsatellite stable tumours (pMMR/MSS). This was observed at the CT (median 349.5 [95% CI 170.5, 421] MSI-H vs. 99 MSS, [95% CI 108.1,151.1]) as well as IM (median 451 MSI-H [95% CI 242.5, 543.5] vs. MSS 144 [95% CI 138.5, 191.7].

I also observed from this analysis that there was indeed an outlier group in the MSS/pMMR that had high CD8+ T-cell count/mm$^2$ (green symbols) in **Figure 3.2**. Those patients who were outliers in the MSS cohort were selected to have further confirmation of microsatellite status by PCR. These slides were retrieved and micro-dissected to extract DNA. The Bethesda gene panel was used to probe these samples to further define microsatellite status. All of the samples were found to be stable by the Bethesda panel as seen in **Table 3.2**, confirming that these patients had

authentic MSS tumours. High TIL infiltrate in tumours of MSS patient was an interesting observation because only CRC patients that have microsatellite unstable tumours are increasingly considered for checkpoint blockade therapy (CBI). This implies that despite TILs being present at high frequencies in tumours that are MSS, CBI does not rescue these TILs and these TILs may be dysfunctional. It may also imply that a small proportion of MSS patients may benefit from CBI, and quantifying TILs could be used as a measure to determine those who may benefit. These patients would not usually be considered based on their microsatellite stable status.

**Table 3.2. Microsatellite testing by PCR confirms stable microsatellite status in outlier MSS patients**

| Case Number | Tumour % | MSI |
|---|---|---|
| **1-21** | 60-90% | STABLE |

Quantitation of CD8+ T-cells in microsatellite stable and unstable tumours was assessed as depicted in **Figure 3.3** and this was used to determine the median cutoff as 124.5 CD8+ T-cells/mm$^2$ to assess OS. The combined region CT+IM (overall) CD8+ count/mm$^2$ was used to determine if CD8+ T-cell infiltrate affects OS. These data demonstrate that there was not a significant survival advantage offered with a high TIL score, as seen in **Figure 3.4**.

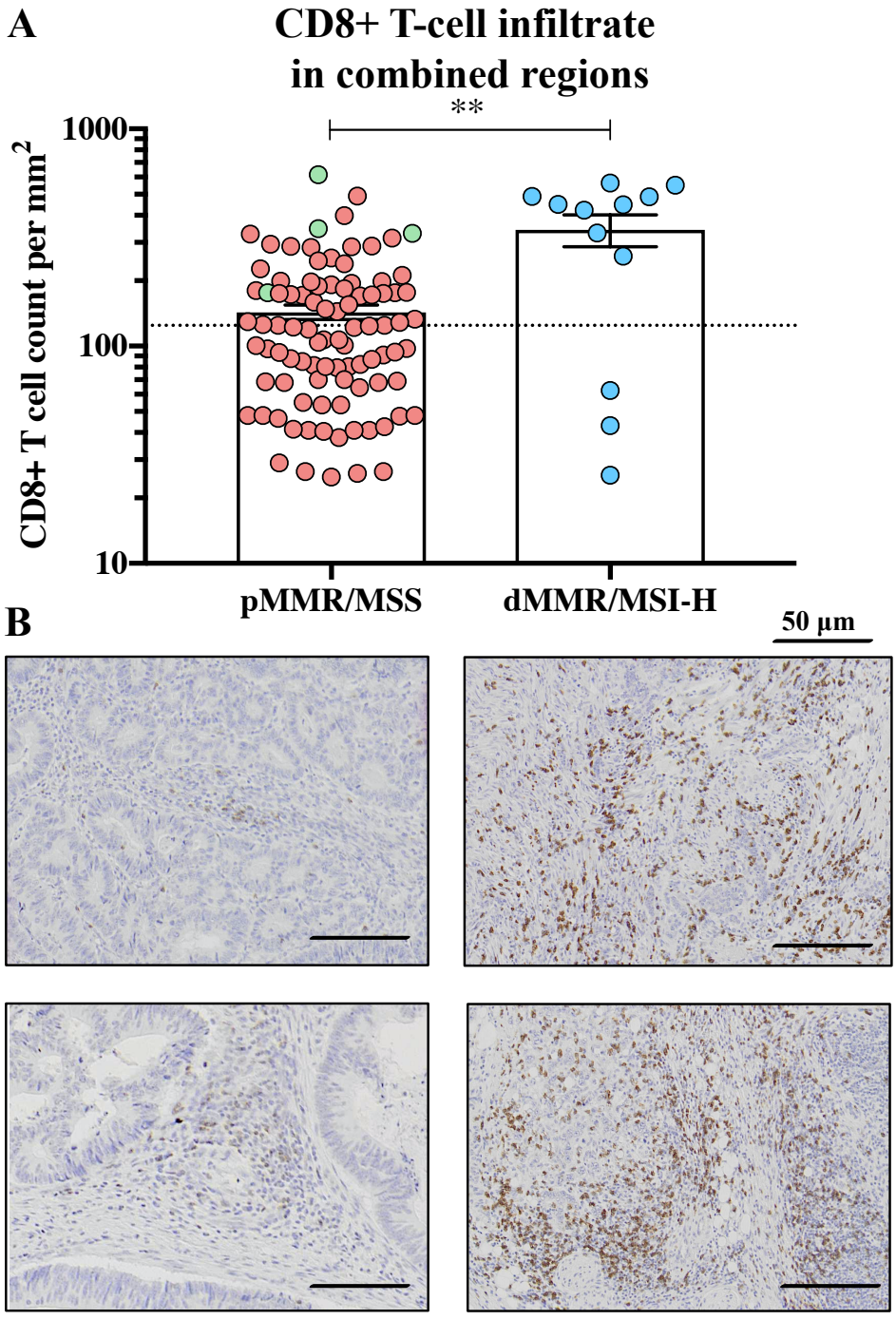


**Figure 3.3 Median cut-off of 124.5 CD8/mm$^2$ set for high and low TIL infiltrate in combined.** (**A**) Bar-plots showing overall CD8+ count/mm$^2$ in tumours that are pMMR/MSS (red) and dMMR/MSI-H (blue) in log-scale. Green symbols in microsatellite stable group were selected as outliers for further microsatellite testing; median cutoff for CD8+ infiltrate was 124.5 CD8+ T-cells/mm$^2$. (**B**) Representative images of CD8+ infiltrate in 2 patients that are MSS tumours (left panel) or microsatellite unstable tumours (right panel), scale bar=50 µm. Error bars represent SEM, n=93 (pMMR/MSS), n=12 (dMMR/MSS), two-tailed unpaired t test, **p=0.0034.

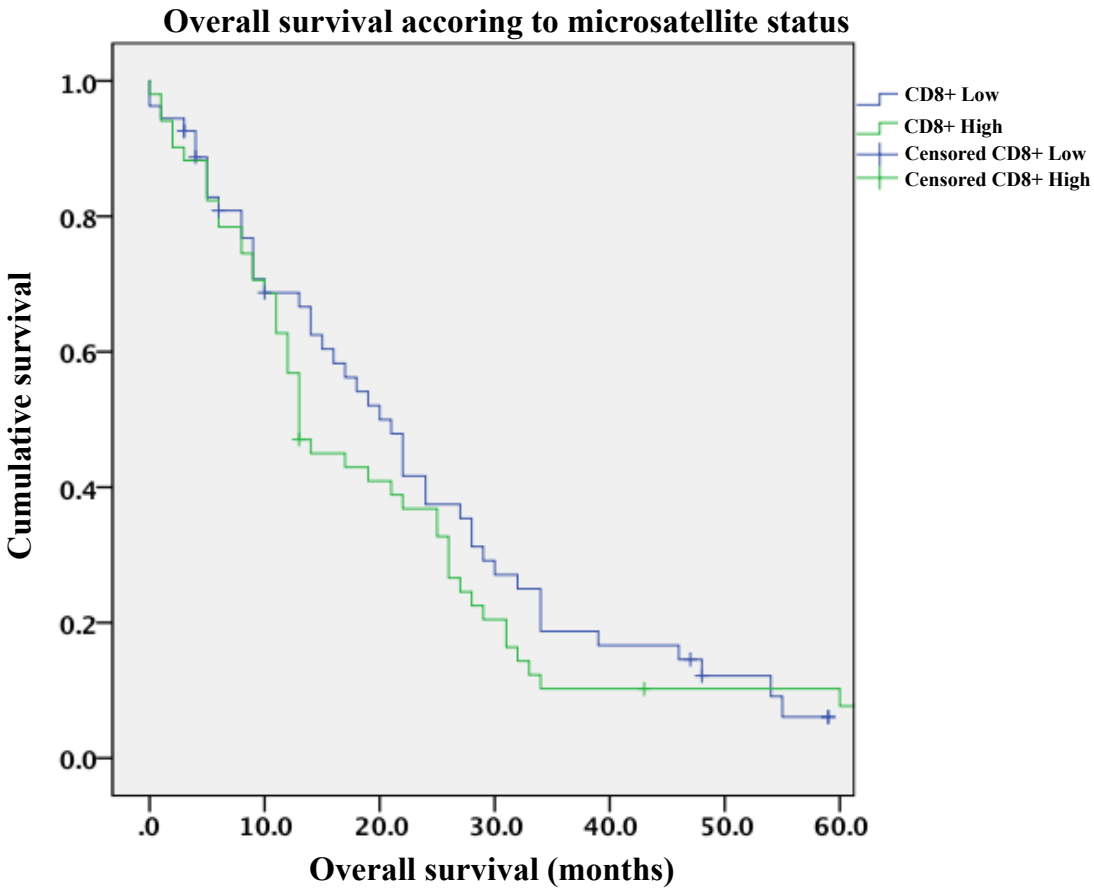


**Figure 3.4 No OS advantage when total CD8+ infiltrate was assessed in tumours of *de novo* mCRC patients.** Kaplan-Meier survival curve show OS stratified on median cutoff of CD8+ cells/mm$^2$ infiltrate to set CD8+ high (green line) and CD8+ low (blue line) infiltration within total count/mm$^2$ in patients with *de novo* mCRC. Cross symbols indicate date of last follow-up, n=103 patients in total. Median survival for low CD8+: 20 months and high CD8+: 13 months (log rank p = 0.426).

From these data it appeared that there was no survival advantage based on CD8+ infiltrate alone. Despite not influencing survival, the number of CD8+ T-cells infiltrating the tumour in MSI-H and some MSS patients was still high. This suggested that these TILs were present in numbers but may be in a state of dysfunction or are not tumour specific. Alternatively there might be immune-checkpoint mechanisms being exploited by the tumour resulting in immunosuppression. To investigate this in more depth, PD-L1 expression on tumour cells and infiltrating immune cells was assessed.

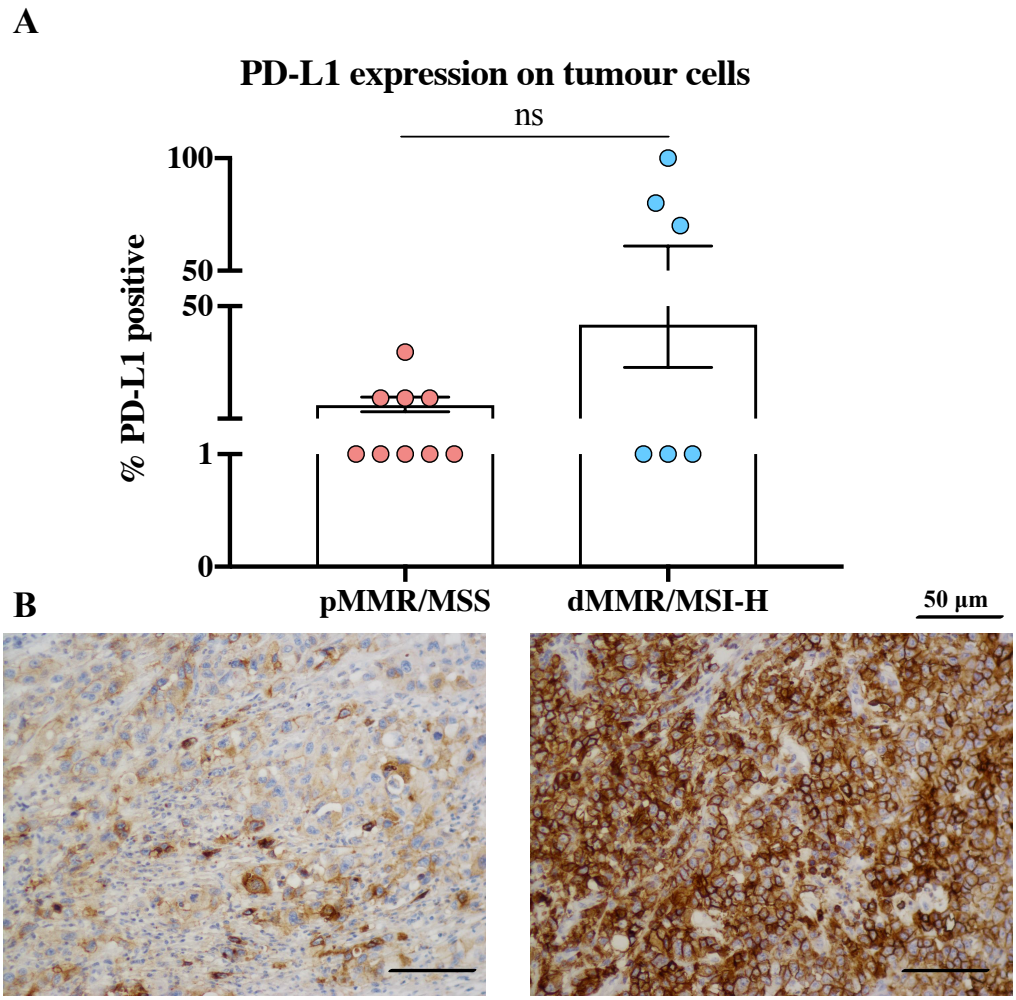


**Figure 3.5 PD-L1 expression on tumour cells is more prominent in dMMR/MSI-H than pMMR/MSS patients. (A)** Bar-plots representing percentage of tumour cells expressing PD-L1 in dMMR/MSS tumours (red symbols) and dMMR/MSI-H tumours (blue symbols). (**B**) Representative images of PD-L1 expression on tumour cells from MSS tumour (left panel) and dMMR (right panel), scale bar= 50 µM. Error bars represent SEM, n=9 (pMMR/MSS), n=6 (dMMR/MSS), Man-Whitney unpaired t-test, $p<0.05$.

As shown in **Figure 3.5** PD-L1 expression did not differ between microsatellite unstable and stable tumours. There was also no difference observed when PD-L1 expression was assessed on infiltrating immune cells, in **Figure 3.6A**.

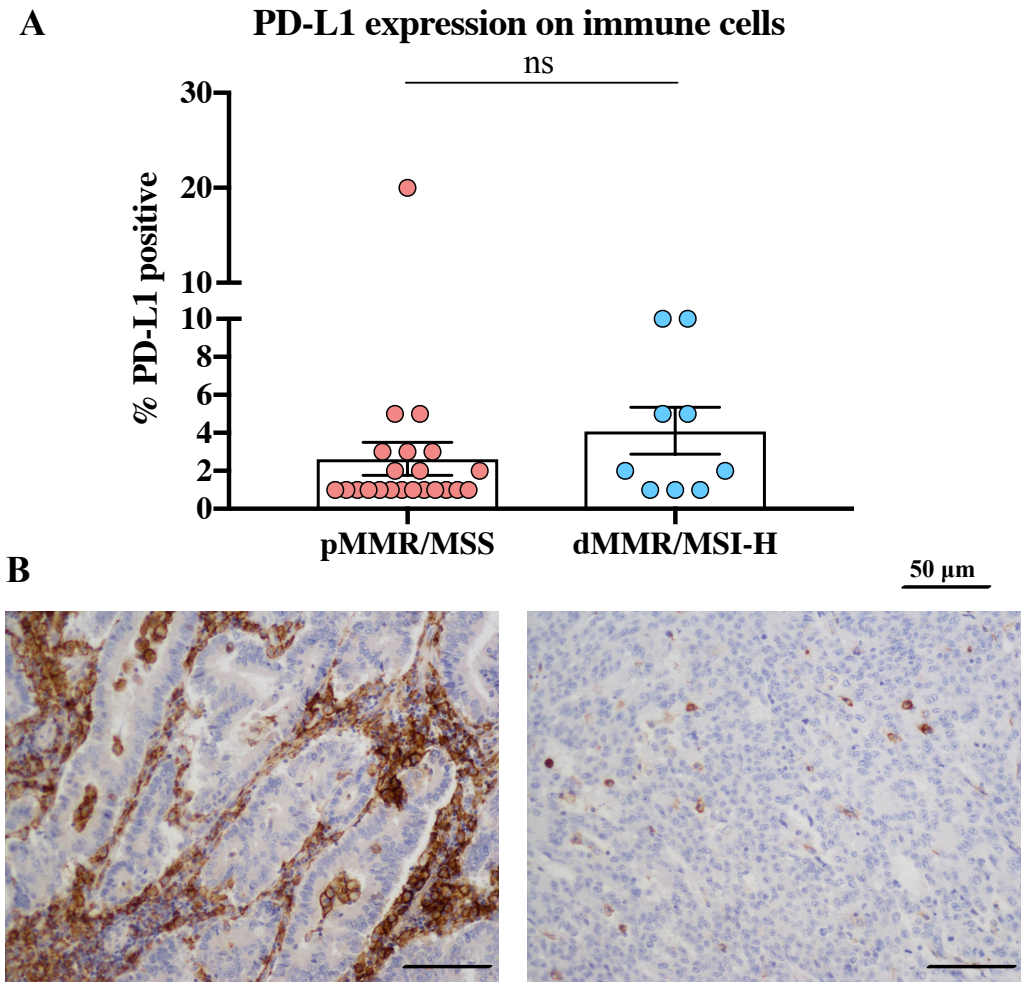


**Figure 3.6 PD-L1 expression on immune cells is more prominent in dMMR/MSI-H than pMMR/MSS patients. (A)** Bar-plots representing percentage of immune cells expressing PD-L1 in dMMR/MSS tumours (red symbols) and dMMR/MSI-H tumours (blue symbols). (**B**) Representative images of PD-L1 expression on stromal immune cells from dMMR tumour (left panel) and intra-epithelial immune cells in pMMR tumour (right panel), scale bar= 50 µm. Error bars represent SEM, n=22 (pMMR/MSS), n=9 (dMMR/MSS), Man-Whitney unpaired t-test, $p<0.05$.

Correlation analysis between positive PD-L1 expression, on tumour cells and immune cells, and CD8+ infiltrate was analysed, as seen in **Figure 3.7A-B**. There was a significant correlation found between PD-L1 expression on immune cells and CD8+ infiltrate, indicating that infiltrating immune cells could also be suppressing TIL effector function. This would need to be investigated further to determine what infiltrating immune cells were expressing PD-L1, such as T-regulatory cells or MDSCs.

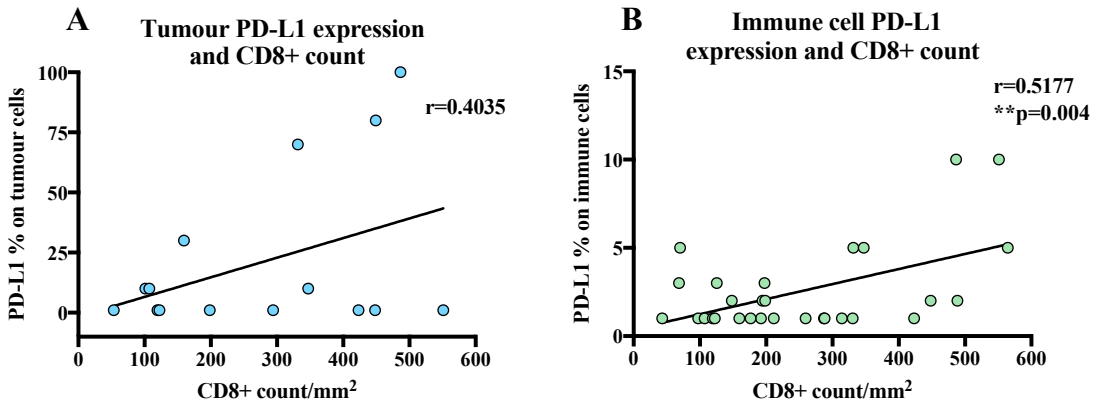


**Figure 3.7 Correlation between CD8+ infiltrate and PD-L1 expression on infiltrating immune cells, but not tumour cells.** XY-plots showing CD8+ count/mm$^2$ in combined regions and PD-L1 expression on (**A**) tumour cells for those patients with positive PD-L1 expression, n=15, correlation analysis, r=0.4035, ns and (**B**) immune cells for those patients with positive PD-L1 expression, n=31, correlation analysis, r=0.5177, **p=0.004.

The trained pathologist who scored these specimens observed direct lymph node involvement of invading tumour expressing PD-L1 as highlighted by the arrows in **Figure 3.8A-B**. Lymphovascular invasion (LVI) was also observed, as highlighted by arrows in **Figure 3.8C-D**, indicating escape mechanisms through micrometastases of tumour cells expressing PD-L1.

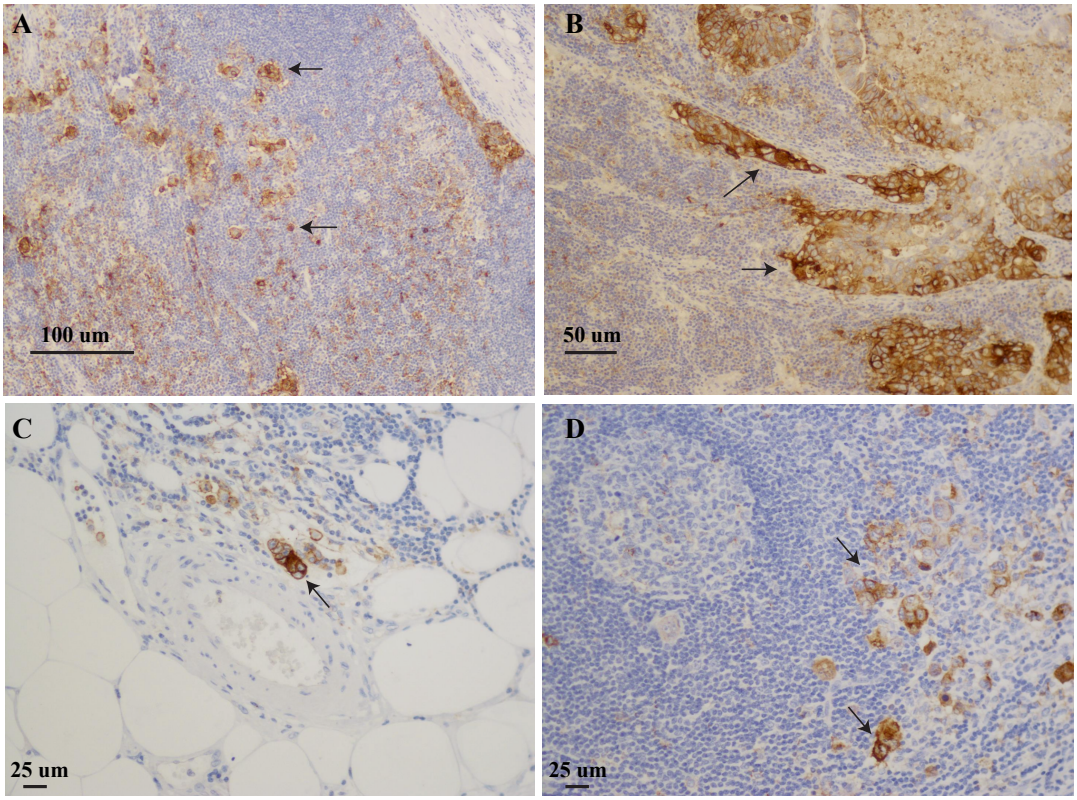


**Figure 3.8 Lymph node invasion occurs with tumour cell PD-L1 expression.** Representative images of tumour PD-L1 expression with (**A-B**) direct lymph node involvement (**C**) lymphovascular invasion and (**D**) lymph node metastasis by invading tumour cells expressing PD-L1 as indicated by the arrows. Scale bars represent 100, 50 and 25 μm.

The current pathological assessment of PD-L1 expression in clinical trials uses percentage "cut-offs" to stratify relatively high or low PD-L1 expression (Herbst *et al*., 2014; Patel & Kurzrock, 2015). To assess survival and PD-L1 expression, 1%, 5% and 50% cut-offs were adopted as shown in **Figure 3.9A**.

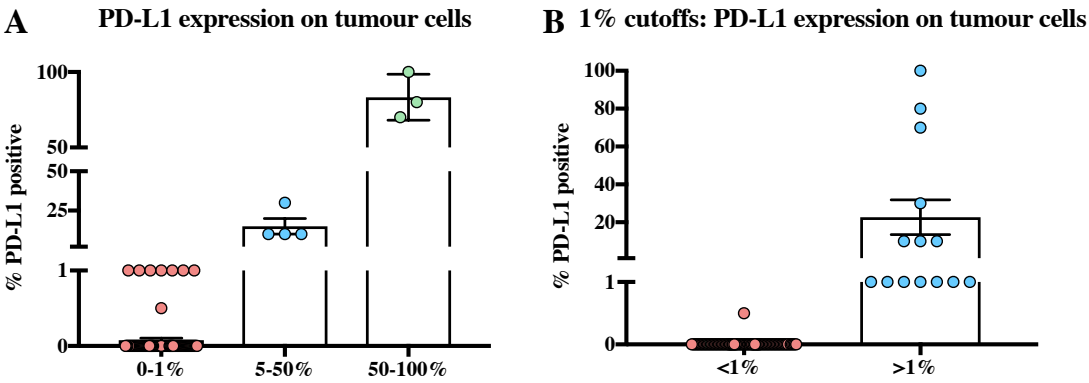


**Figure 3.9 PD-L1 expression on tumour cells.** (**A**) Pathologist scoring of: 0-1 (n=97), 5-50 (n=4) and 50-100% (n=3) and (**B**) <1% (n=90) and 1% or higher (n=14) PD-L1 expression on tumour cells from the primary tumour of patients with *de novo* mCRC, n=104.

When analysing OS based on surface expression of PD-L1 >1% on tumour cells, reduced OS was observed (median survival PD-L1 >1% 8 months and PD-L1<1% 19 months). No statistical differences were observed with this analysis, however in multivariate analysis PD-L1 expression on tumour cells was found to be significant as shown in **Table 3.3**. The no differences were seen when assessing cutoff scores of 5% and 50%, might reflect the small number of samples. Nevertheless, these data demonstrate immune evasion mechanisms at play in the primary tumours of *de novo* mCRC patients.

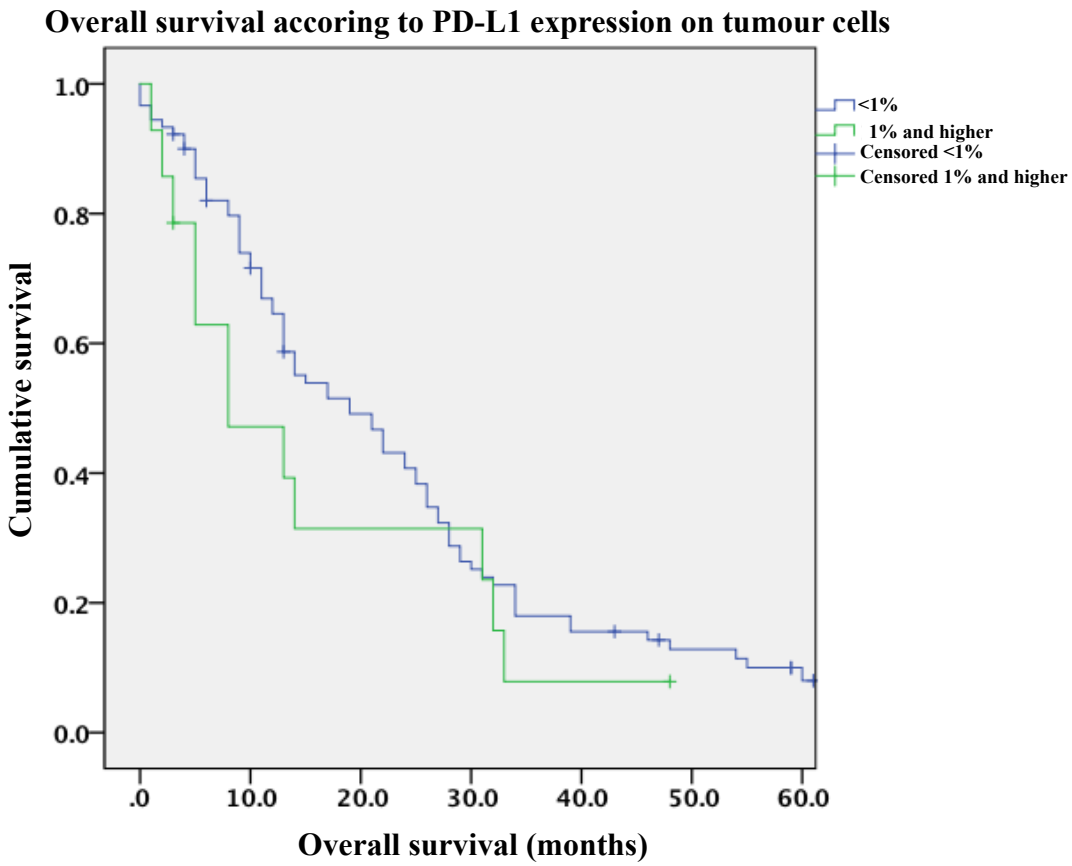


**Figure 3.10 Patients with tumour cells expressing 1% and higher PD-L1 have reduced OS.** Kaplan-Meier survival curve show OS stratified on tumour cells expressing <1% (blue line) or >1% PD-L1 (green line) on tumour cell surface. Survival based on PD-L1. Median survival for <1% 19 months compared to 8 months for 1% and higher (log rank p =0.253), n=98 patients in total.

Across both microsatellite stable and unstable tumours, CD8+ infiltrate did not influence OS, despite some tumours having a high frequency of CD8+ T-cells present. Additionally, expression on PD-L1 >1% on tumour cells affected OS but only in multivariate analysis. This may suggest that tumours are suppressing immune responses via exploitation of immune evasion. It also indicated "aggressive" tumour progression is likely to be in operation, perhaps through other oncogenic mechanisms.

### 3.3 Tumour Characteristics in Primary Tumours of Patients with *de novo* mCRC

To assess other tumour cell intrinsic mechanisms that may influence the TME, protein expression of MYB and GRP78 was assessed by IHC. This has been associated with a poor outcome in patients with Stage I-III CRC. It has also been associated with immune-modulation, where high MYB expression on tumour cells had an inverse relationship with CD8+ immune

infiltrate. Additionally MYB is known to regulate GRP78 that influences immune responses in cancer.

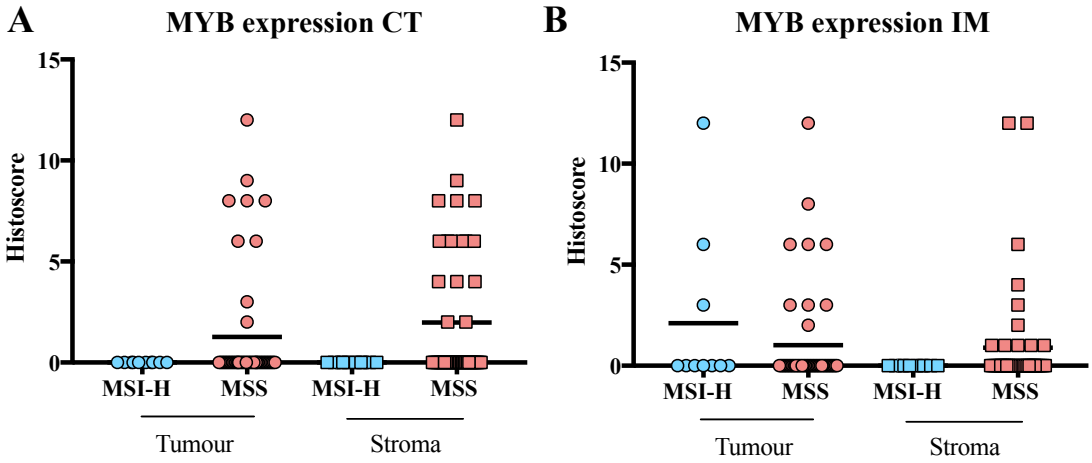


**Figure 3.11 Expression of MYB is more prevalent in MSS tumours. Scatter-plot represents tumours expressing MYB, using the histoscore that evaluates intensity x extent (0-12).** This was done at the (**A**) CT and (**B**) IM in both tumour and stromal cells. n=49, n=10 (MSI-H) and n=39 (MSS), black line represents mean ± SEM.

The areas at the CT and IM selected for MYB and GRP78 expression were matched with the areas originally selected by a pathologist for CD8+ T-cell analysis. The histoscore was utilised and assessed intensity of expression multiplied by extent of expression ranging from 0-12. As seen in **Figure 3.11** no detection of MYB expression was observed in the tumour or stromal cells at the CT in tumours that were MSI-H. Most expression was detected in MSS tumours at both the CT and IM.

To investigate the relationship between MYB and survival, the median histoscore value was used as a cut-off to define MYB high and low expression in the CT. As seen in **Figure 3.12**, no statistical difference was observed between MYB expression on tumour cells in the CT and OS.

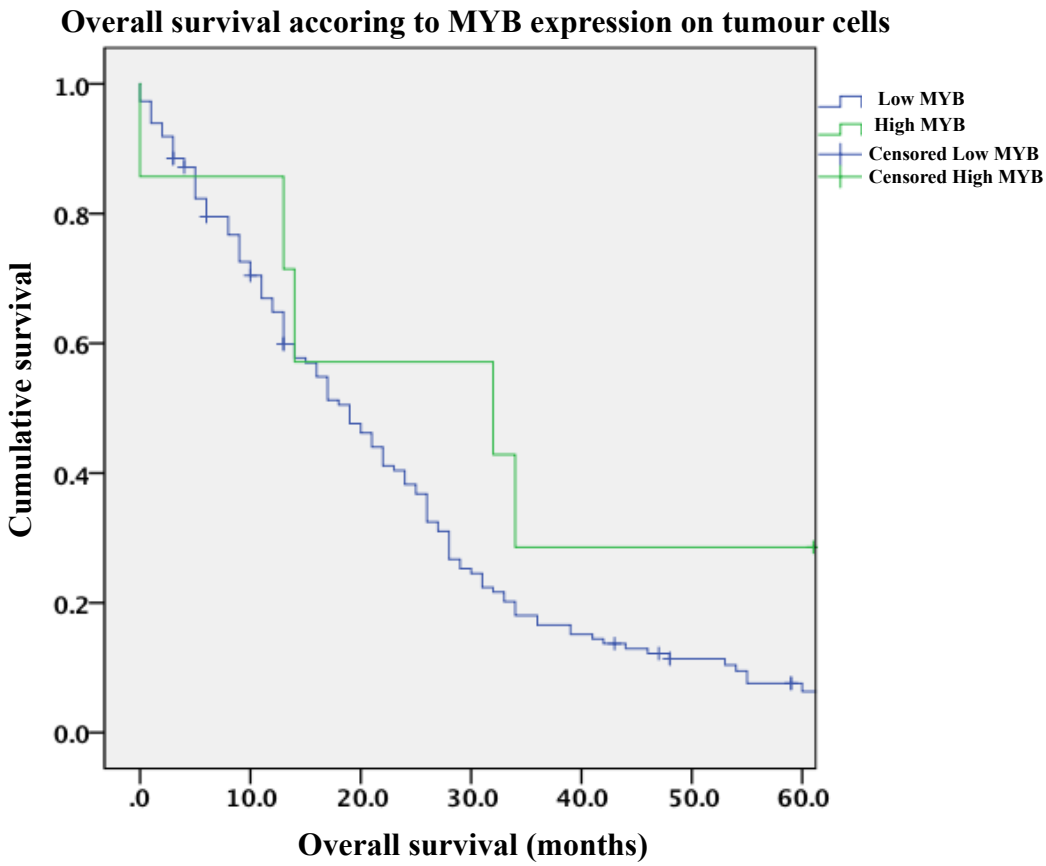


**Figure 3.12 Expression of MYB on tumour cells at the CT does not influence survival in Stage IV CRC patients.** Kaplan-Meier survival curve showing OS stratified on tumour cells expressing MYB. Low MYB (blue line) median survival 19 months, compared to high MYB (green line) 32 months (log rank p =0.222): n=109.

To investigate if GRP78 influenced the TME, samples were scored using the same histoscore as described for MYB expression. As seen in **Figure 3.11**, GRP78 expression is present across microsatellite unstable and stable tumours. In the microsatellite stable group, at both the CT and IM, GRP78 expression is higher on the tumour cells than stromal cells. Therefore assessment of GRP78 expression and survival was only done for tumour cell expression.

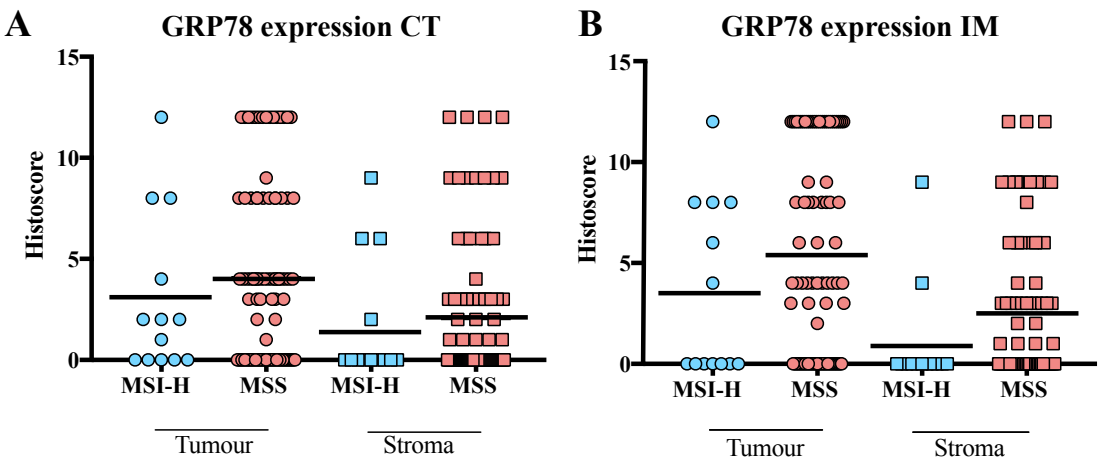


**Figure 3.13 Expression of GRP78 is more prevalent in MSS tumours, with greater expression on tumour cells than stromal cells.** Scatter-plot represents tumours expressing GRP78, using the histoscore that evaluates intensity x extent (0-12). This was done at the (**A**) CT and (**B**) IM in both tumour and stromal cells. n=111, n=13 (MSI-H) and n=85 (MSS), black line represents mean ± SEM.

Association between OS and GRP78 expression on tumour cells at the CT (**Figure 3.14**) and IM (**Figure 3.15**) was assessed. In both tumour areas, there was a trend, where patients with tumours expressing GRP78 had a reduced OS. However when evaluated in univariate and multivariate analysis, no statistical differences were observed.

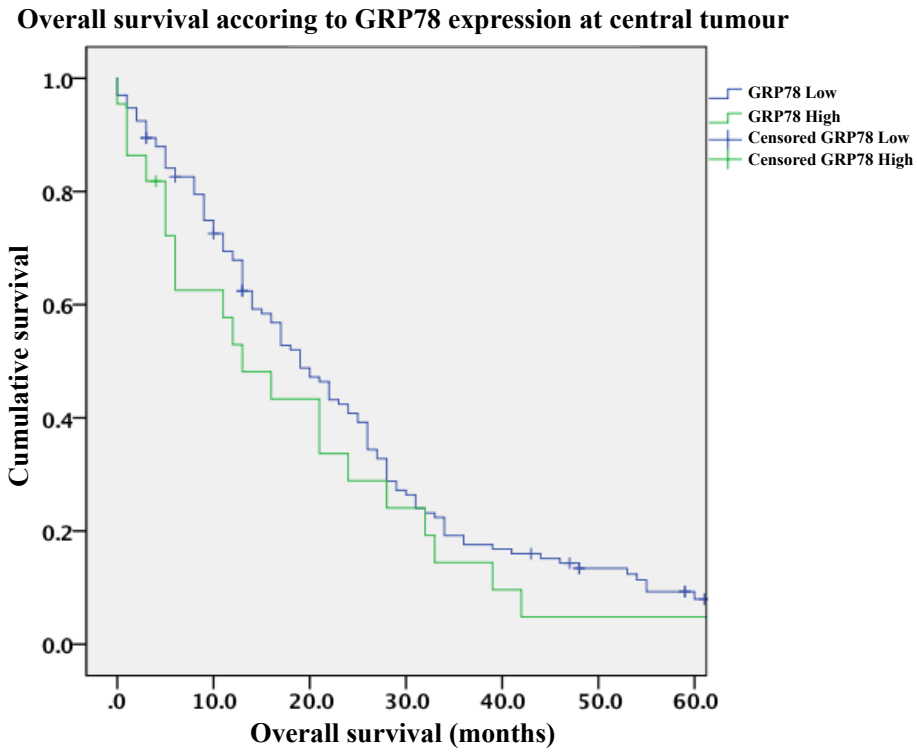


**Figure 3.14 Expression of GRP78 on tumour cells at the CT does not influence survival in Stage IV CRC patients.** Kaplan-Meier survival curve showing OS stratified on tumour cells expressing GRP78 at the CT, median survival 19 months for low, compared to 13 months for high (log rank p = 0.325) n=45.

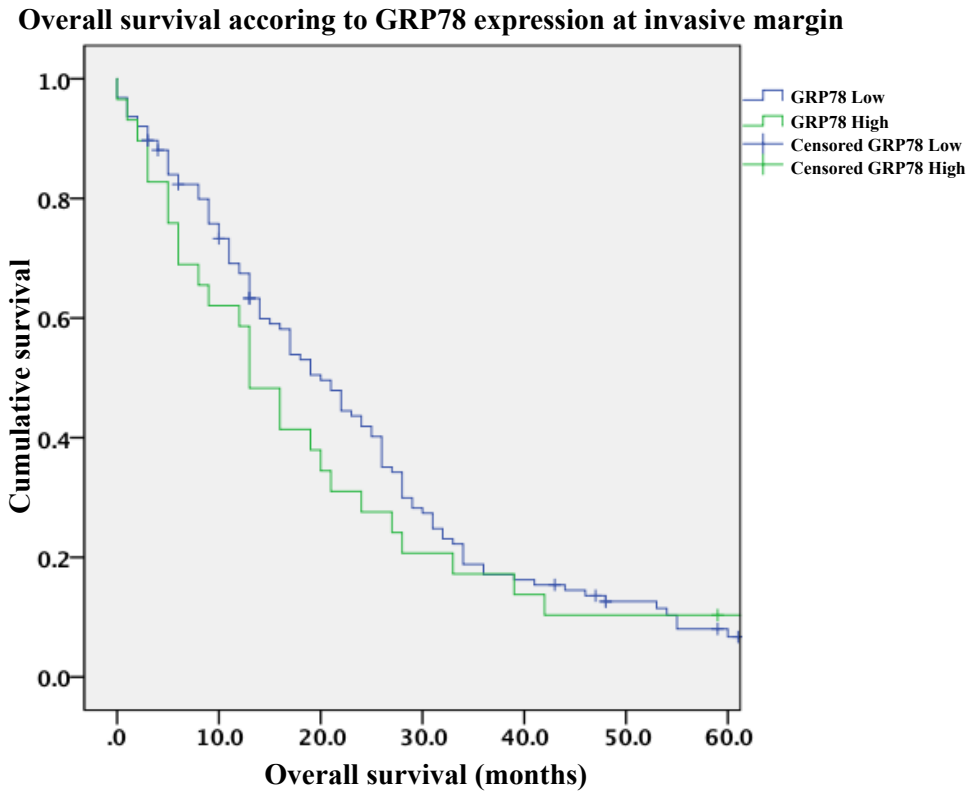


**Figure 3.15 Expression of GRP78 on tumour cells at the IM does not influence overall survival in Stage IV CRC patients.** Kaplan-Meier survival curve showing OS stratified on tumour cells expressing GRP78 at the IM. Median survival 20 months for low, compared to 13 months for high (log rank p = 0.596) n=36.

Finally, OS was interrogated based on RAD21 expression on tumour cells, as seen in **Figure 3.16**. There was a trend observed where tumours that had a high expression of RAD21, had an apparent improved OS, but this was not significant.

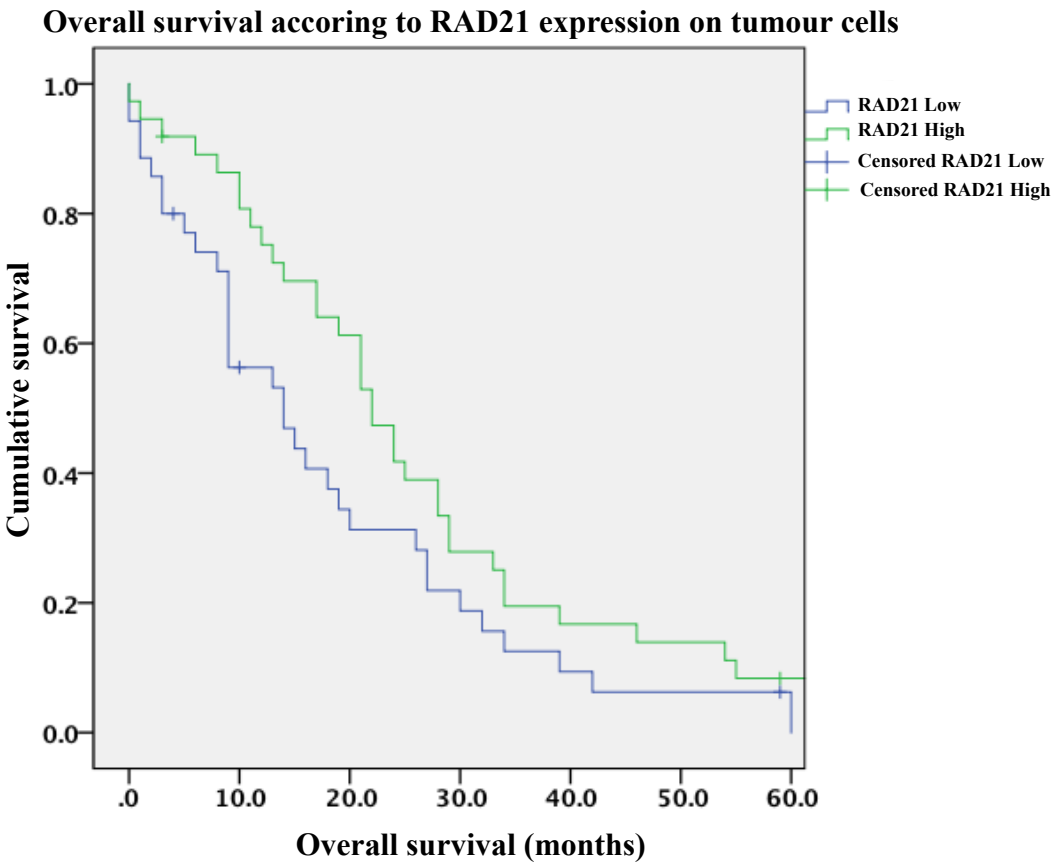


**Figure 3.16 Expression of RAD21 on tumour cells does not influence overall survival in Stage IV CRC patients.** Kaplan-Meier survival curve showing OS stratified on tumour cells expressing RAD21. (Log rank p = 0.08) n=36.

**Table 3.3. Univariate and Multivariate analysis for cumulative survival in *de novo* mCRC patients**

| | | Univariate HR (95% CI) | P value | Multivariate HR (95% CI) | P value |
|---|---|---|---|---|---|
| Gender | Female | | | | |
| | Male | 0.84 (.60-1.17) | 0.293 | 0.63 (0.31-1.28) | 0.20 |
| Site of original | Colon | | | | |
| | Rectum | 0.76 (0.42-1.37) | 0.362 | | |
| Age group | Up to 65 | | | | |
| | >65 | 1.61 (1.12-2.30) | **0.01*** | 1.09 (0.52-2.28) | 0.20 |
| T stage | T2 | | | | |
| | T3 | 0.38 (0.12-1.24) | 0.108 | | |
| | T4 | 0.75 (0.24-2.40) | 0.631 | | |
| Tumour PD-L1 | <1% | | | | |
| | 1% or more | 1.42 (.77-2.61) | 0.265 | 4.26 (1.46-12.45) | **<0.01**** |
| MYB CT | Low | | | | |
| | High | 0.61 (0.27-1.39) | 0.236 | 0.57 (0.20-1.65) | 0.30 |
| MYB IM | Low | | | | |
| | High | 0.90 (0.40-2.04) | 0.803 | 0.92 (0.23-3.71) | 0.91 |
| GRP78 CT | Low | | | | |
| | High | 1.26 (0.79-2.03) | 0.336 | 2.27 (0.57-9.00) | 0.24 |
| GRP78 IM | Low | | | | |
| | High | 1.12 (0.73-1.72) | 0.604 | 1.23 (0.47-3.22) | 0.67 |
| MSI | pMMR | | | | |
| | dMMR | 1.37 (0.74-2.51) | 0.315 | | |
| Overall CD8 | Low | | | | |
| | High | 1.18 (0.78-1.79) | 0.44 | 1.34 (0.70-2.58) | 0.38 |
| RAD21 | Low | | | | |
| | High | 0.65 (0.40-1.07) | 0.09 | 0.81(0.40-1.65) | 0.56 |

Univariate and multivariate analyses were carried out to determine additional factors that influenced OS as seen in **Table 3.3**. Patients who were 65 years and older had a significantly reduced OS in univariate analysis. Those patients who had tumour PD-L1 expression >1% had significantly reduced OS in multivariate analysis, indicating that PD-L1 expression independently affects OS in this cohort of *de novo* mCRC patients.

In summary microsatellite status alone did not affect OS in this cohort of *de novo* Stage IV mCRC patients. High CD8+ T-cell infiltrate was present in tumours that were both microsatellite stable and unstable but did not affect OS in these patients. This indicated that although T-cells are present within the TME, there are likely immunosuppressive mechanisms at play affecting the ability of the cytotoxic T-cells to elicit an effector response. Tumour expression of PD-L1 independently affected OS in multivariate analysis. Finally to assess if other tumour cell intrinsic factors played a role; MYB, GRP78 and RAD21 protein expression

was assessed. No significant difference was found with MYB, GRP78 or RAD21 expression and OS. These data provided insight into the immune response and the TME of these patients with *de novo* Stage IV mCRC.

### 3.4 Discussion

Approximately 15-25% of patients with CRC will present with synchronous metastatic disease at time of diagnosis (Leporrier *et al*., 2006). The traditional strategy for management of synchronous disease is a staged surgical approach, resecting the primary tumour first (Silberhumer *et al*., 2015). Surgical resection for cure is the only possibility to obtain long-term survival. However, despite surgical intervention, 5-year survival rates for CRC patients presenting with synchronous disease is only 30-37% (Fong *et al*., 1997; Fong *et al*., 1999; Gayowski *et al*., 1994).

CRC patients with microsatellite unstable tumours have an improved survival (Stage I-III) and are currently the only patients that are considered for CBI trials. However the circumstances are very different in the advanced stage of disease, and this needs to be understood in the context of the immune response. Metastatic stage IV CRC patients with MSI-H tumours represent a distinct subset of CRC patients that do not respond to conventional chemotherapy and have a reduced OS. In this study we employed a unique cohort of advanced stage IV *de novo* mCRC, including patients with microsatellite unstable tumours. OS was not significantly different when stratifying patients based on microsatellite status alone. However, there was a trend for patients with MSI-H tumours to have a reduced OS, reiterating the current view that this subset of mCRC patients has an overall poor prognosis. So why is this the case, and is it immune mediated?

To understand if the immune response influenced survival in these patients, cytotoxic CD8+ T-cells were quantified in the primary tumour. Although some tumours had a high number of CD8+ T-cell infiltrate, CD8+ T-cell presence alone did not influence survival. This is a very different scenario when compared to early-stage CRC. We reported that local early-stage CRC tumours infiltrating cytotoxic CD8+ T-cells correlated strongly with relapse-free survival (Millen *et al*., 2016). What this suggests is that in the early stages of disease; the immune response still plays a substantive role in tumour control. However, once the tumour progresses beyond immune control, into the advanced setting of disease, things are very different.

The fact that these patients have distant metastasis alludes to the concept that these primary tumours are: 1) aggressive with oncogenic potential to survive, proliferate and migrate and 2) these tumours have already evaded the immune response and have undergone immunoediting.

When contemplating the 'three E's' in the context of metastasis and within this cohort of patients, it is clear that tumour progression has reached the escape phase and beyond. Not only is the tumour able to escape locally through immunoediting, cell migration and invasion, but it has also escaped systemically to establish in a distant organ (Chambers, Groom, & MacDonald, 2002; Friedl & Wolf, 2003). It is likely that the primary tumour has undergone both genetic and epigenetic changes that provide oncogenic cell-intrinsic potential of the tumour cells and can influence cell-extrinsic properties such as affecting the TME. An example of this, in the context of CRC, is the *RAS* gene that is frequently mutated in tumours. The common *RAS* gene mutation in CRC is *KRAS* and is present in 30-50% of CRC tumours (Cox, Fesik, Kimmelman, Luo, & Der, 2014; Porru, Pompili, Caruso, Biroccio, & Leonetti, 2018). This mutation has the ability to extrinsically enhance the induction of T-reg cells (Zdanov *et al*., 2016), leading to an immunosuppressive environment that can promote tumour growth. Understanding immunoediting in the context of metastasis may provide insight into mechanisms of escape. Additionally other mechanisms of escape may include immune checkpoint mechanisms such as PD-L1 and CTLA-4, but there are certainly more.

Although no statistical difference was observed with OS and CD8+ T-cell infiltrate, high frequencies of CD8+ T-cells were present in most MSI-H tumours and interestingly, some patients that were MSS. Yet 50% of the entire cohort succumbed to the disease within 24 months, and so the immune system appears inefficient in tumour control. One reason this may occur is due to an immunosuppressive TME, with inhibition of cytotoxic CD8+ T-cells by tumour cells.

This immunosuppressive phenotype is reflected by the expression of PD-L1 on tumour cells. In multivariate analysis, PD-L1 expression on tumour cells did influence OS as an independent factor. The literature reports that selecting patients based on the expression of PD-L1 alone is not sufficient to predict response to CBI against PD1/PD-L1 (Dong *et al*., 2002; Gatalica *et al*., 2014; Patel & Kurzrock, 2015). It is likely that the expression of PD-L1 is dynamic, and capturing it using IHC alone may not demonstrate the fluctuating interplay between the immune response and tumour cells. The tumours analysed in this data set had all progressed to metastasis, as all patients had *de novo* mCRC. There was an interesting observation that tumour cells positive for PD-L1 expression were detected in the lymphovascular compartment. This highlighted a probable mechanism of tumour cells escaping the primary site and proceeding to metastasis. This observation clearly demonstrates how tumour cells have the ability to be undetectable to immune cell recognition and migrate to distant metastatic sites, via lymphatic's and the vasculature. When assessing PD-L1 expression on immune cells, there was a correlation between PD-L1 expression and CD8+ T-cell quantity. Cytotoxic CD8+ T-cells secrete IFNγ and

within the TME this can lead to up regulation of PD-L1 on tumour cells. The expression of PD-L1 on infiltrating immune cells likely reflects the IFNγ-induced adaptive regulation of infiltrating effector T-cells (Kowanetz *et al*., 2018). To counteract this, immune cells including MDSCs are known to express PD-L1 which also reflects an attempt to suppress immune responses occurring in the TME (F. Tang & Zheng, 2018). Additional immune evasion pathways to investigate in this cohort would be loss of MHC-I expression, to determine if the tumour cells down regulate this pathway to bypass immune control. As these tumours have progressed, the immune response has failed and this may also be attributed to additional oncogenic factors at play.

To assess if there were additional tumour-cell mechanisms influencing tumour growth and the immune response, MYB and its target GRP78 were quantified in this cohort. Expression of MYB in MSS tumours was more prominent than microsatellite unstable tumours. High MYB and GRP78 expression on tumour cells did not appear to affect the ability of CD8+ T-cells to infiltrate. Therefore these markers do not track with immune cells in the advanced setting of CRC. That is the opposite of what was observed in early-stage CRC, where high MYB expression had an inverse relationship to CD8+ T-cell infiltrate (Millen *et al*., 2016). This highlights the difference in progression of these tumours. In the early stage of tumour development including the equilibrium phase, where the T-cells may be in a more naïve/effector phase and can be influenced by tumour oncogenic factors such as *MYB* and *GRP78*. However, in the advanced stage of CRC, the tumour has evaded the immune response. If the CD8+ T-cells are terminally exhausted TILs within the TME, MYB and GRP78 may be important for tumour survival, but do no longer modulate the immune response.

Expression of *MYB* was not associated with survival. When assessing GRP78 expression on tumour cells and survival, no statistical difference in OS was observed in multivariate analysis. However, there was a trend to suggest that high expression of GRP78 in both regions of the tumour reduced OS. This was observed in our previous study that reported in early stage CRC, tumours with high expression of GRP78 was associated with relapse (Millen *et al*., 2016). Conversely, one study documented that high GRP78 expression was associated with an improved 5-year survival in CRC patients and improved response to adjuvant chemotherapy. Additionally, they found that cells were more resistant to 5-FU treatment when knocking down GRP78 expression, through mechanisms altering cell cycle (Thornton *et al*., 2013). All of the patients in this cohort had adjuvant chemotherapy, either 5-FU, FOLFOX or FOLFIRI, and whereby perhaps expression of GRP78 on tumour cells may have affected chemotherapy resistance.

It is known that RAD21 expression on tumour cells can influence resistance to DNA damaging agents such as chemotherapy, including 5-FU (Deb *et al*., 2014). RAD21 is a protein that has been previously reported to prognosticate and predict patients with CRC, and was investigated in this cohort. It has been found that tumours overexpressing RAD21 have a reduced OS (Deb *et al*., 2014). When assessing RAD21 expression in *de novo* mCRC tumours, there was a trend for high RAD21 expression being associated with an improved OS. It is known that the prognostic significance of RAD21 reduces when assessed in microsatellite unstable tumours (Deb *et al*., 2014), yet in other advanced primary tumours, including breast and endometrial cancer, it is associated with a poor prognosis (Supernat *et al*., 2012; Xu *et al*., 2010). In the current analysis of RAD21 expression, patients were stratified on expression alone and not stratified on microsatellite status. The other factor not taken into account in multivariate analysis was the chemotherapy regimen these patients underwent. Therefore accounting for previous chemotherapy treatment to determine if RAD21 expression influences survival in this cohort warrants further investigation.

In this unique cohort of patients, we identified that microsatellite status and cytotoxic T-cell infiltrate does not affect OS and this is likely due to the advanced stage of disease. Despite this, CD8+ T-cells are still present in high numbers in MSI-H tumours and some tumours that are MSS. As these tumours have progressed to metastasis, the anti-tumour immune response has been unable to control tumour progression and it is therefore probable that these TILs are dysfunctional or being inhibited in the TME. The current Checkmate142 open-label Phase II trial highlights the fact that TILs in mCRC MSI-H tumours are in a state of immune suppression because CBI can subsequently rescue TIL function. Understanding the quality of TILs in MSS tumours is also of interest, as it is known these patients do not respond to CBI and interrogating their biology may provide insight into why this is the case. Finally, additional focus should also be on interrogation of the TILs that are present at the distant metastatic site in CRLM, and this will be addressed in the **Chapter 4**.

# 4 DETERMINING THE FUNCTION OF IMMUNE CELLS AT THE METASTATIC SITE IN mCRC

## 4.1 Introduction

**Chapter 3** provided insight into the immune response at the primary site in patients with advanced stage IV mCRC. It was evident in these primary tumours that the immune response had failed, as the tumour had by definition escaped and progressed to a distant site. This chapter will focus on the immune response at the metastatic site in CRLM tumours to understand the mechanisms at play during tumour progression.

In humans, the presence of TILs generally indicates a favourable prognosis (Atreya & Neurath, 2008; Galon *et al*., 2006; Galon, Fridman, & Pages, 2007; Naito *et al*., 1998). The Immunoscore proposed by Pagès & Galon *et al* has contributed greatly to the field of immuno-oncology and will likely influence clinical decision-making in the future, as both a prognostic and predictive marker. Subsequent studies have investigated functional aspects of the immune infiltrate by looking at cytotoxic markers including granzyme B and proliferative markers such as Ki67 (Mlecnik *et al*., 2016).

Although these surrogate functional markers are instructive, the immune response remains highly dynamic and is multifaceted. The data obtained from assessing these markers using IHC only provides a "snapshot-in-time" of the tumour immune response and expression of these markers likely fluctuates over time and spatially. Although TILs are present in tumours, it is difficult to gauge their function using IHC alone. Understanding their dynamic activity is thus important to determine if these TILs are functional or dysfunctional; particularly in the era of immunotherapies. For instance, if the TILs are intrinsically dysfunctional, they may never be rescued by use of CBI. Therefore developing dynamic assays to assess cytotoxicity of TIL function has been of great interest to researchers in the field.

The current "gold standard" technique for measuring cytotoxic immune activity is the $^{51}$chromium release assay (CRA) (Biron *et al*., 1999; Verneris, Karimi, Baker, Jayaswal, & Negrin, 2004). This assay has the ability to measure the cytotoxicity of cytotoxic immune cells including NK cells and cytotoxic T lymphocytes (CTLs), it was developed in 1968 and is still a commonly used (Karimi *et al*., 2014). Both primary and clonal cell lines can be used as target cells, and these are loaded with radioactive chromium [$^{51}$Cr] prior to the co-culture. The cytotoxic cells of interest are then added at various ratios and the supernatant is collected at the endpoint of the co-culture, with a time-limitation of 4-16 hours. Cytotoxicity is measured

indirectly by measuring the amount of chromium that has been released (via cell lysate) into the supernatant, this is roughly relative to the amount of killing that has occurred (Brunner, Mauel, Cerottini, & Chapuis, 1968). However, there are some disadvantages of this assay; one of them is that only the endpoint of the assay can be measured for each test, and therefore understanding the kinetics of killing over time is not an easy option. This is also due to the time limitation of how long the target cells can spontaneously retain chromium (16-24 hours). Using 2D-cultures challenges the capacity of the assay and the use of 3D cultures including spheroids and organoids has not been routinely adopted either.

More recently, a non-labelling cell death assay utilises electrical impedance measurements of target cells. Adherent target cells attach to a matrix of microelectrodes on the bottom of the multi-well plate, causing an increase of impedance to an electric current. Conversely, when cells die and detach from the plate, impedance is reduced, and this is measured using the Xcelligence™ system. This can be used for cytotoxic drug screening of cancer cells and co-culture assays that include immune cells, as immune cells in the suspension do not substantially affect impedance (Peper *et al*., 2014). The main advantage of this system is that cells do not require labelling, which is often an issue of other assays including the CRA or the carboxyfluorescein succinimidyl ester (CSFE) assay that involves labelling of target cells to record cellular proliferation, using dye dilution. However, the limitation of this system is that it is currently confined to adherent 2D culture system. Nevertheless, there has been some progress in developing electrical cell–substrate impedance sensing (ECIS) for 3D cultures and matrices to investigate cell migration (Nguyen, Yin, Reyes, & Urban, 2013). Again, this system involves adherent cells covered by a 3D matrix and focuses on the ability of cancer cells to migrate. However, it lacks the ability to measure cell death within a 3D matrix, and investigating cytotoxic-mediated death of spheroids or organoids could not be employed in this assay. Thus there is a need to investigate other possibilities that allows researchers to test the capacity of cytotoxic immune cells particularly with 3D cultures.

This is apparent with very recent studies being published investigating immune cells and their interaction with patient-derived tumouroids, including our own, as detailed in **chapter 1**. Using this platform and other techniques, I sought to address the question of TIL function in CRLM, by isolating lymphocytes from the tissue and phenotyping these using fluorescent activated cell sorting (FACS), multiplex immunohistochemistry (Opal) and assessing TIL function using the assay developed in the Ramsay lab. In order to achieve this, we first had to design and establish the assay.

**Hypothesis:**

The presence and frequency of immune cells *in situ* alone does not always reflect their effector function

**Aims:**

**1.** Establish a platform to assess patient-derived TIL effector function *ex vivo*

**2.** Assess TILs isolated from CRLM tumours against matched patient-derived tumouroids

**3.** Investigate the proportion and phenotype of TILs in CRLM

## 4.2 Patient Characteristics

As part of this project I wrote the human ethics application and recruited patients with CRLM. Patients with CRLM were provided with informed consent and recruited to the study. On the day of the surgical operation, blood was drawn from the patients pre-incision for collection of PBMCs. After the specimen had been surgically removed from the patient, tumour and normal liver pieces were dissected in the operating theatre or by a registered pathologist (to ensure that the surgical margins were not compromised). The tissue was then placed in ice-cold media and transferred to the laboratory for immediate processing. The patient characteristics are listed in **Chapter 2**.

## 4.3 Establishment Of A Cytotoxic Assay

The initial learning curve of establishing tumouroids was steep, and this was due to the demanding technical aspects of organoid tissue culture. Only mouse-derived organoids had been successfully cultured in the lab prior to this project, and therefore human-derived organoids and tumouroid culture had not been routinely established. With the help of Dr. Jordane Maleterre in the laboratory, who had experience culturing mouse organoids, and alongside two other PhD students in the laboratory, Joe Kong and Glen Guerra, I successfully established and maintained tumouroid lines from patients with CRLM.

The idea to combine tumouroids and lymphocytes in a co-culture assay was extremely novel at the time, in 2015. This had not been reported in the literature, and with the success of establishing tumouroids in our lab; we had the ability to advance this concept. Initially I decided that microscopy would be the ideal method to visualise the interaction between the tumouroids and lymphocytes. The very first attempt to do this was in December 2015, using one of the CRLM tumouroid lines that I had established from the IM of the tumour. Central Tumour (CT), Invasive Margin (IM) and matched distant ‘normal’ liver (DL) lymphocytes were expanded

from the same tumour. Healthy donors PBMCs were used as a positive control for killing. Both the TILs and PBMCs were stained using a cell labelling dye; propidium iodide (PI) and organoids were stained with cell labelling dye CFSE that traces generations of cell division. This was imaged over time to visualise trafficking and immune cell homing towards the tumouroid as seen in **Figure 4.1 A-C**.

The images in **Figure 4.1 A-C** are "still-shots" from a live movie that was imaged over the course of every 1-minute following 24 hours of co-culture. The pink lines highlight 4 representative cells, of the many cells visualised that traffic towards the tumouroid. This was an informative observation because it depicts selective immune cells can actively migrate toward the tumouroid. In most cases, the immune cells stop and 'hover' in the area, and fail to progress or interact with the tumouroid. The distance travelled by each immune cell is quantified in **Figure 4.1D**. As can be seen, each cell migrates closer to the tumouroid, one cell more rapidly than the other three. This was the first documentation of lymphocytes having the ability to migrate through the 3D scaffolding matrix, matrigel, and also only selective lymphocytes migrating towards the tumouroid, perhaps indicative of chemotaxis. The rate of each immune cell was also calculated (**Fig. 4.1E**) which provided an indication of how far individual cells travelled.

In addition to fluorescent microscopy, a second plate was set up for measurement at the endpoint of the co-culture assay (24 hours). Cell trace violet (CTV) dye was added to the wells to stain the tumouroids, in order to visualise and assess the diameter of the tumouroids following exposure to immune cells. The plate was imaged on a wide field microscope and the diameter of each organoid was measured using Spotfire software (TIBCO), to quantitate the impact of TIL-induced damage to the tumouroids.

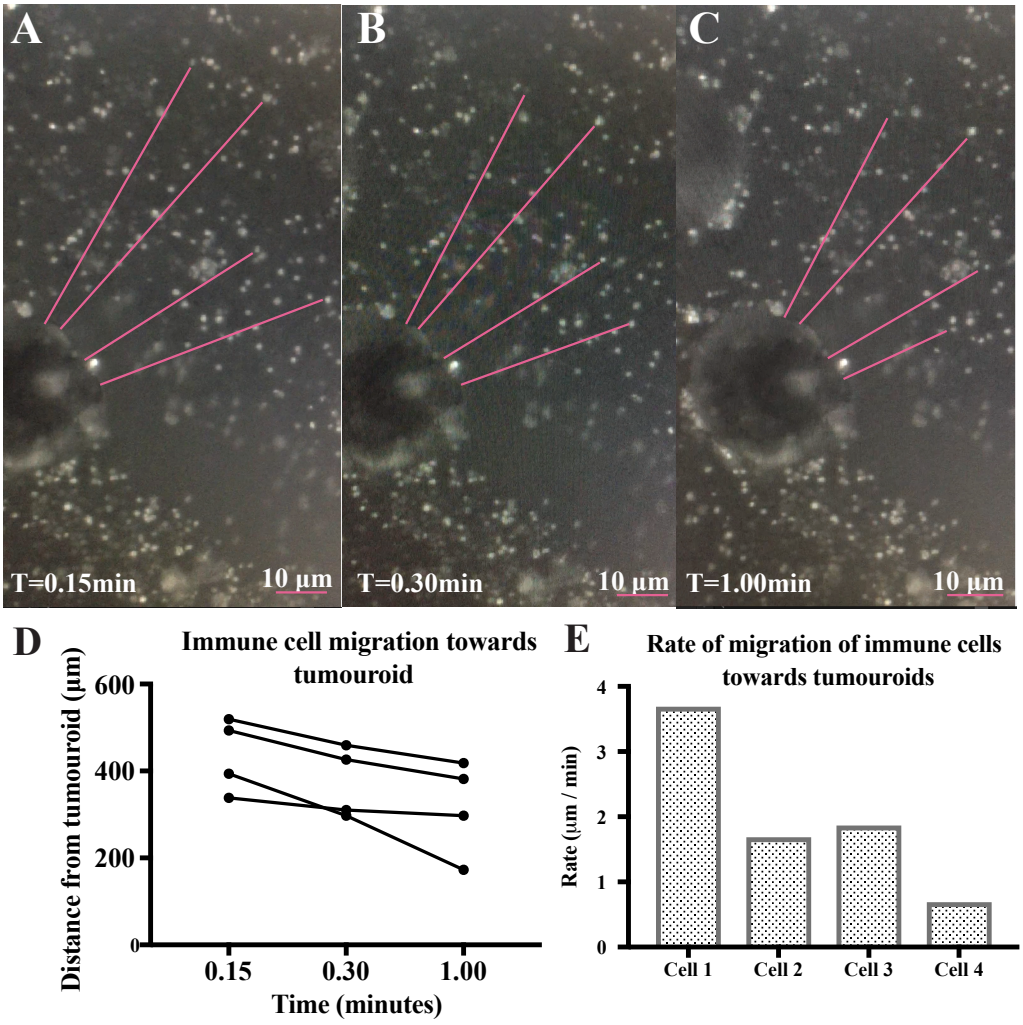


**Figure 4.1 Select lymphocytes home towards tumouroid through 3D-matrix. Autologous TILs cells were labelled with PI and visualised after 24 hours of co-culture.** "Still-shot" images taken on wide field microscope over a 1 minute time lapse at (**A**) 0.15 min (**B**) 0.30 min and (**C**) 1.00 min, scale bar=10 µm to depict distances travelled by immune cells, pink lines highlight 4 immune cells homing towards tumouroid. (**D**) Dot-plot depicting the quantified distance travelled (µm ) by 4 immune cells over 1 minute (**E**) Rate of migration of individual cells calculated as distance travelled (µm) over time (min), n=1.

The diameter of tumouroids was measured, as seen in **Figure 4.2**, highlighting if tumouroids have either: increased (grown), remained stagnant or decreased in size, the latter indicating cell death and disruption. Tumouroids alone had a mean diameter of 240 µm and this is comparable to tumouroids + CT TILs (mean: 242 ± 26.68 µm ) indicating that the CT TILs are not effective killers against IM tumouroids. IM TILs were more effective at reducing tumouroid diameter (mean: 142 ± 21.37 µm ). The distant liver lymphocytes, expanded from healthy normal liver, were able to reduce the diameter of the tumouroids by 50% (mean: 93 ± 13.53 µm ). Healthy

donor PBMCs, used as a positive control, were comparable to DL lymphocytes, confirming this effect. These were the first data to indicate that autologous TILs and tumouroids can be successfully co-cultured together and both qualitative and quantitative data can be extrapolated. However measuring diameter alone, as a read out of tumouroid death was not instructive enough in regards to specific killing. It was also too ambiguous, deciphering the difference between tumouroids being resistant to immune attack and growing (increase), being controlled by the lymphocytes and not growing (static) or killed by the lymphocytes and reducing in size. To address this further, an improved method to detect specific killing was developed.

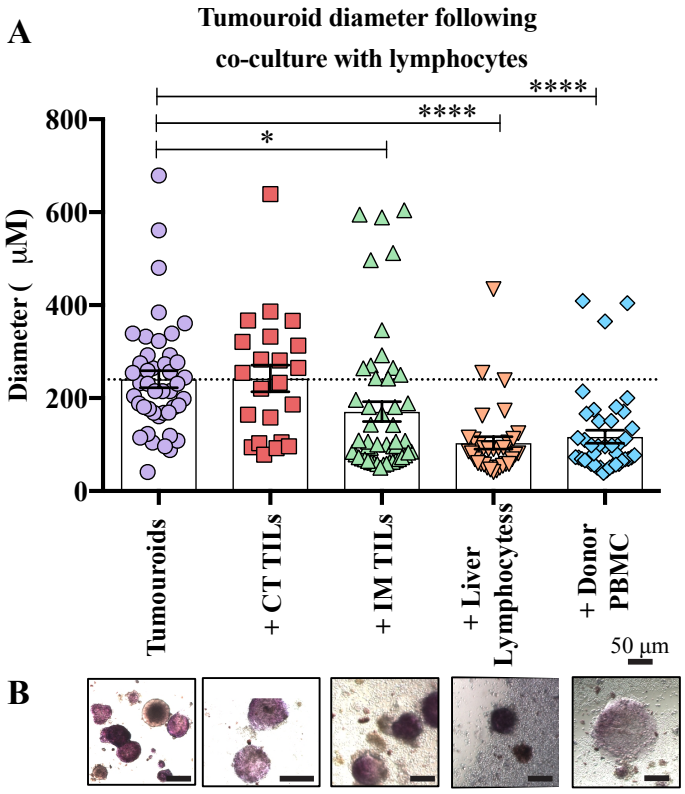


**Figure 4.2 Tumouroid death is induced by functional distant liver lymphocytes but not TILs.** Autologous tumouroids were co-cultured for 24 hours and stained with CTV to visualise the diameter of the tumouroid (**A**) Scatter-plot displaying diameter of tumouroids (µm) after exposure to lymphocytes expanded from different regions of the autologous tumour. Each individual dot represents one tumouroid, error bars represent SEM, n=20-50 tumouroids measured per condition, One-Way ANOVA, *p=0.041, ****p<0.0001 (**B**) Microscopy images taken for each condition after staining with CTV showing tumouroids after 24 hours of exposure to autologous TILs, scale bars = 50 µm, n=1.

Following this pilot experiment, I next approached this assay using live-imaging microscopy. The concept of using live imaging microscopy is to gain an understanding of the kinetic interaction of the TILs with tumouroids, and to decipher if TILs specifically interact with tumouroids. To achieve this, the wide-field Olympus IX3 microscope was used. PI was included in the assay to highlight target cell death (M. R. Jenkins *et al*., 2015). Lymphocytes were pre-labelled with a live cell-tracer dye Syto11 (Thermo Fisher Scientific, Massachusetts, US) that allowed tracking of the lymphocytes. PI was used, as a marker of cell death upon binding to the nuclear DNA and RNA. The assay ran for 24 hours and was imaged at 0, 4 and 24 hours, as seen in **Figure 4.3.**

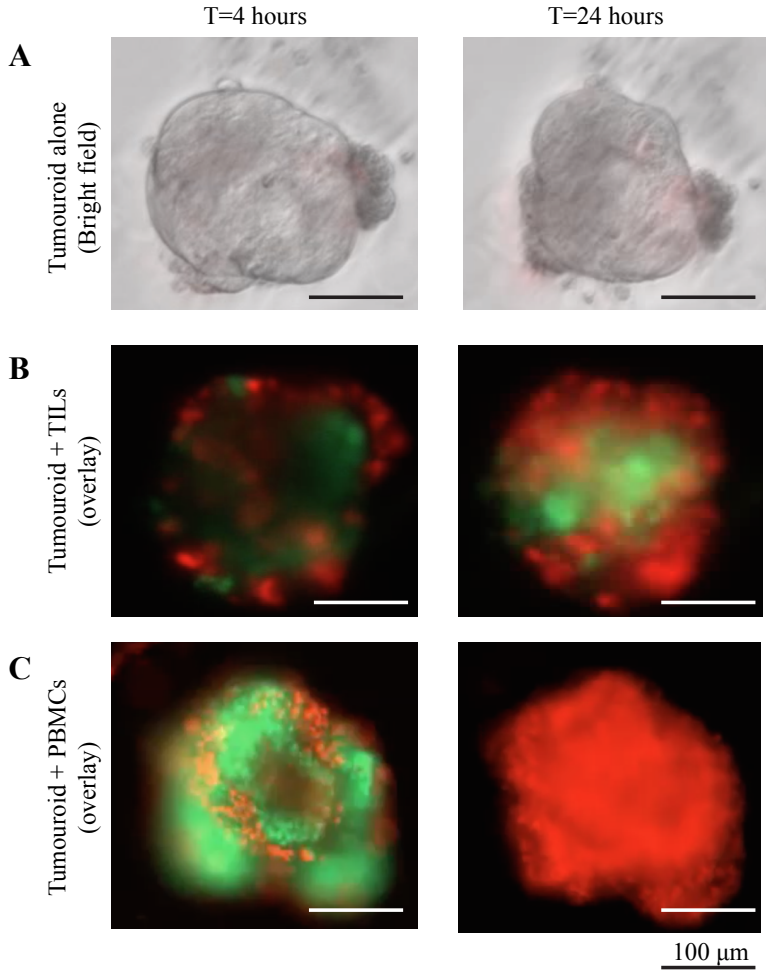


**Figure 4.3 Autologous TILs home to tumouroids and induce tumouroid death using wide field IX83 microscope.** "Still-shots" of patient-derived rectal cancer (RC) tumouroids that were co-cultured with autologous TILs and imaged at 4 and 24 hours (**A**) Bright-field images displaying tumouroid alone as negative control (**B**) Tumouroid + autologous TILs overlay of stained TILs (green) and dead cells (red) (**C**) Tumouroid + allogeneic PBMCs overlay. Scale bars=100 µm, images acquired at 20X magnification, n=1.

Live imaging microscopy provided more insight into the dynamic process of lymphocytes inducing cytotoxic death, particularly by acquiring time-lapse images, shown only as "still-shots" in **Figure 4.3**. In the live-imaging videos, it is evident that by 4 hours of co-culture, lymphocytes have already homed towards the tumouroid as indicated by the green flux that is observed. The red flush stained by PI is also evident at 4 hours on the exterior of the tumouroid and increases towards the centre of the tumouroid (**Figure 4.3B**). This is very obvious in the allogeneic PBMC condition (**Figure 4.3C**), where by 24 hours the entire tumouroid has become red. This is likely to be due to NK cells being present in the PBMC, due to alloreactivity of the

NK cells against the tumouroids in the absence of recipient MHC-I ligands (Ruggeri *et al*., 2002).

The wide field microscope used in the previous experiment provided a good platform to visualise the interaction between lymphocytes and the tumouroid. However, the resolution of the images was not ideal. Therefore, I developed a method to distinguish tumouroid cells dying or lymphocytes surrounding the tumouroid dying due to cytotoxic-induced cell death (CICD) (Chavez-Galan, Arenas-Del Angel, Zenteno, Chavez, & Lascurain, 2009). To gain better resolution, the same experiment was set up and acquired on the confocal SP5 microscope. Images were acquired at 0, 4, 8 and 20 hours as seen in **Figure 4.4**. This approach provided higher resolution images, where PI uptake can be associated to a more refined area than observed with the wide-field microscope (**Figure 4.3**). In this example, architectural disruption is more evident after tumouroids have been exposed to autologous TILs or allogeneic PBMCs as observed by tumouroid 'blebbing' seen on the exterior of the tumouroid (**Figure 4.3B-C**). Also observed in this experiment is the centre of the tumouroid appearing darker after lymphocyte exposure compared to tumouroid alone, indicating an increased optical density of cells likely to be due to apoptosis.

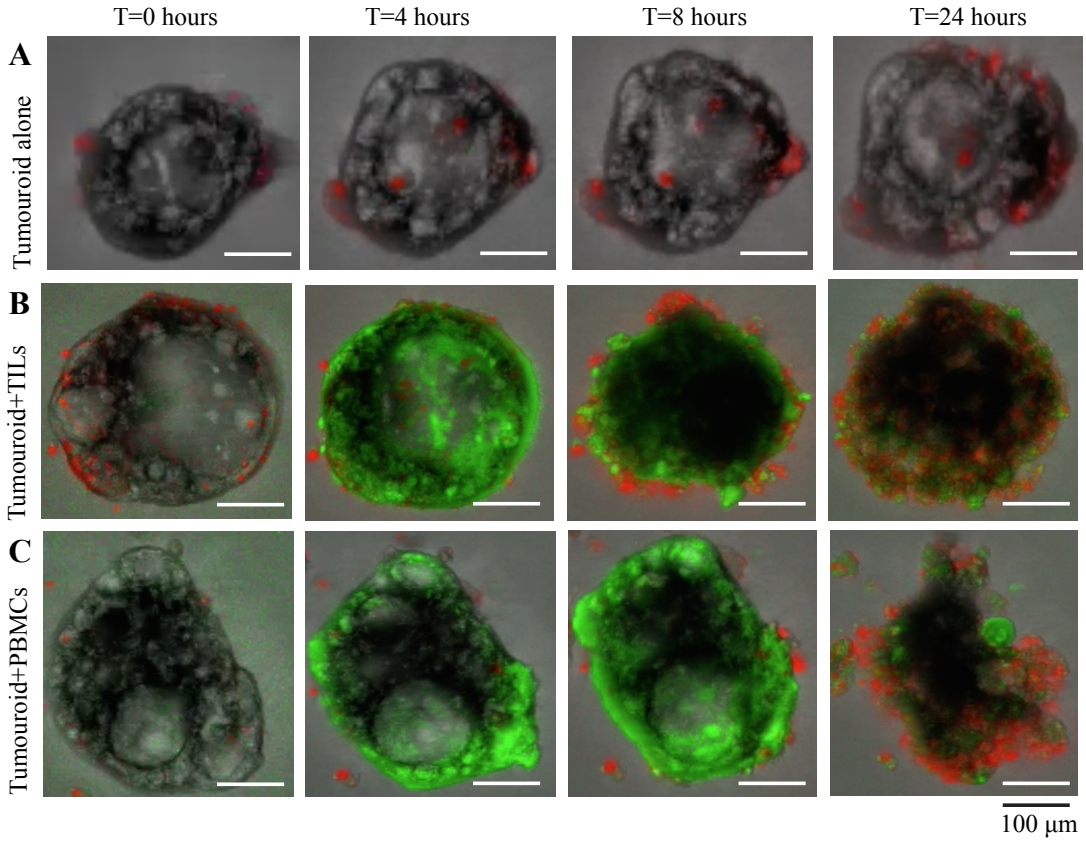


**Figure 4.4 Imaging of co-culture assay on confocal SP5 microscope provides better resolution than wide field microscope.** "Still shots" from time-lapse video of tumouroids at 0, 4, 8 and 24 hours hours taken on the confocal SP5 microscope. Green indicates Syto11 stained lymphocytes and red indicates cell death by PI uptake (**A**) Tumouroid alone (**B**) Tumouroid + autologous TILs and (**C**) Tumouroid + allogeneic PBMCs. Scale bars=100 µm, images acquired at 200X magnification, n=1.

Following these initial pilot experiments, a series of optimisation experiments were undertaken to optimise the platforms that included both wide field fluorescence and confocal microscopy. Additionally, titrations of lymphocyte concentrations were also optimised. Generally with immune co-culture assays, effector to target cell ratios are titrated in order to obtain a killing curve to determine the percentage of cytotoxicity. When passaging organoids, tumouroids are broken up to obtain a single cell suspension, but there are sometimes still cell clusters, and therefore calculating the effector: target (E:T) ratio is challenging. The tumouroids are seeded 7-10 days prior to conducting the co-culture and growth of tumouroids is not always uniform, despite attempting to seed the same number of cells. To overcome this, the numbers of tumouroids are counted prior to co-culture. It was estimated an tumouroid with an approximate

size of 50 μm consists of 300-500 single cells. There were a series of experiments carried out to achieve this titration as well as optimizing other aspects of the assay including cell tracer dyes and the microscopic platform, as seen in Table 4.1.

When optimising the assay on the Leica SP5 confocal microscope, some technical challenges were posed. For instance, it is important that there are not confounding factors that could contribute to cell death during the imaging process, as the output of this assay was measurement of cell death. One factor that was of concern when using confocal microscopy was the laser phototoxicity of the cells. As cells are rarely exposed to light, phototoxicity has the ability to affect cell viability. It is known that fluorescence excitation can cause phototoxicity to tissues and cells over time (Frigault, Lacoste, Swift, & Brown, 2009; Pattison & Davies, 2006). When imaging using the confocal microscope, images were acquired every hour to gain an understanding of the lymphocyte dynamics. However, it was evident in the negative control (tumouroids alone) that this constant acquisition on the confocal microscope caused some phototoxicity. This was especially noticed when there were multiple dyes being used to stain each component of the assay. Therefore, we decided to move back to the original platform, on the wide-field fluorescent microscope, for simplicity and with fewer exposure time points.

**Table 4.1. Series of experiments carried out to optimise various aspects of cytotoxic assay including titration of lymphocytes, cell-tracking dyes and the microscope.**

| Purpose | Effector cells | Lymph conc$^{n}$ | Control | Dyes | Platform |
|---|---|---|---|---|---|
| **Titration of lymphs** | Allogeneic PBMCs | $1x10^3$<br>$2\ x10^3$<br>$5\ x10^3$<br>$5\ x10^4$ | PI alone | Lymphs: Syto11 (5 µm) Tumouroid: Hoechst (0.5 µg/mL) Media: PI (100 µm) | Olympus IX3 |
| **Titration of lymphs, Syto11 and PI for Leica** | Autologous TILs | $5\ x10^3$<br>$1\ x10^4$<br>$25\ x10^4$<br>$1\ x10^5$<br>$2.5x10^5$ | Matrigel | Lymphs: Syto11 (5 µm) PI: 50, 100, 200 µm | Leica SP5 |
| **Titration of PI with tumouroids** | Allogeneic PBMC | $2.5x10^5$<br>$5\ x10^5$ | Tumouroid | Lymphs: Syto11 (5 µm) PI: 50, 100, 200µm | Leica SP5 |
| **Test MTS, MTT, Cell trace Glo** | Autologous TILs Allogeneic PBMCs | $2.5x10^5$ | No lymphs | Lymphs: Syto11 (5 µm) PI: 50 µm | Leica SP5 |
| **Titration of E:T** | Allogeneic PBMCs | $2\ x10^3$<br>$2\ x10^4$<br>$4\ x10^4$<br>$1\ x10^5$<br>$2x10^5$<br>$1x10^6$<br>$2x10^6$ | N/A | Lymphs: Syto11 (5 µm) | Leica SP5 |
| **Caspase 3/7 titration** | Allogeneic PBMC | $5x10^3$ | Tumouroid +caspase 3/7 | Caspase 3/7: pre-diluted | Leica SP5 |
| **Nuc-Red titration** | Autologous TILs | $1\ x10^4$<br>$1\ x10^5$<br>$2.5x10^5$<br>$5x10^5$<br>$1x10^6$<br>$2x10^6$ | N/A | Nuc-red: Pre-diluted | Leica SP5 |

Initial experiments to titrate E:T ratio included staining of the tumouroids with Hoechst 33342, which is a DNA-binding dye. In these experiments, a marker of apoptosis was used instead of PI, that is: Caspase-3/7 Green ReadyProbes® which binds to activated caspase 3, specifically detecting early apoptosis. To optimize the E:T ratios using this platform, 1:1, 5:1 and 10:1 were tested. This was acquired on the IX3 wide field microscope (Olympus) at 4, 8, 12 and 24 hours, as seen in **Figure 4.5**.

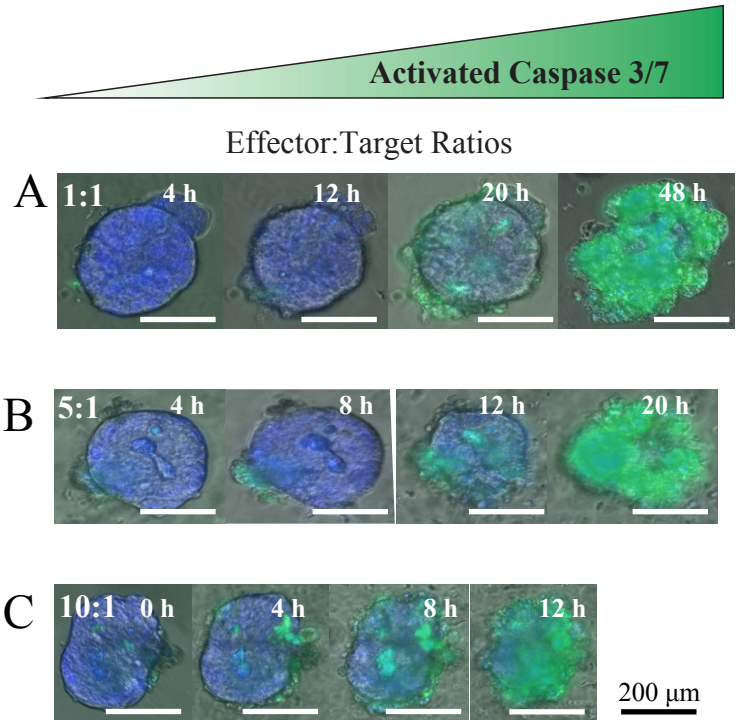


**Figure 4.5 Higher E:T ratio results in more rapid killing of tumouroids.** Rectal cancer tumouroids were used to optimise the E:T over time, Hoechst dye (blue) was used to stain the tumouroids and caspase 3/7 dye (green) was included in the media detecting cells undergoing early apoptosis. Images captured at 0, 4, 8, 12, 20 and 48 hours, E:T ratios are (**A**) 1:1 (**B**) 5:1 and (**C**) 10:1. Scale bars= 200 µm, images acquired at 20X magnification, n=1.

This was the first robust example of an effective E:T ratio. As can be seen in **Figure 4.5C**, when the effector to target ratio is increased to 10:1, tumouroids are rapidly killed by 12 hours. A second observation was that tumouroids at the edge of the matrigel, which is in a dome shape, as depicted in cartoon form in **Figure 4.6**, are the first tumouroids to be targeted by the lymphocytes. The tumouroids that are within the centre of the matrigel appear to take longer to be killed, as the lymphocytes have to penetrate further into the matrigel. Therefore, only tumouroids within 100 µm of the edge of the matrigel are routinely imaged. The ideal ratio of

E:T was found to be 10:1, and this was the ratio taken forward in the assay. Caspase 3/7 dye was used for titration only to detect specific apoptosis and therefore only PI was continued for use in subsequent acquisition of the assay.

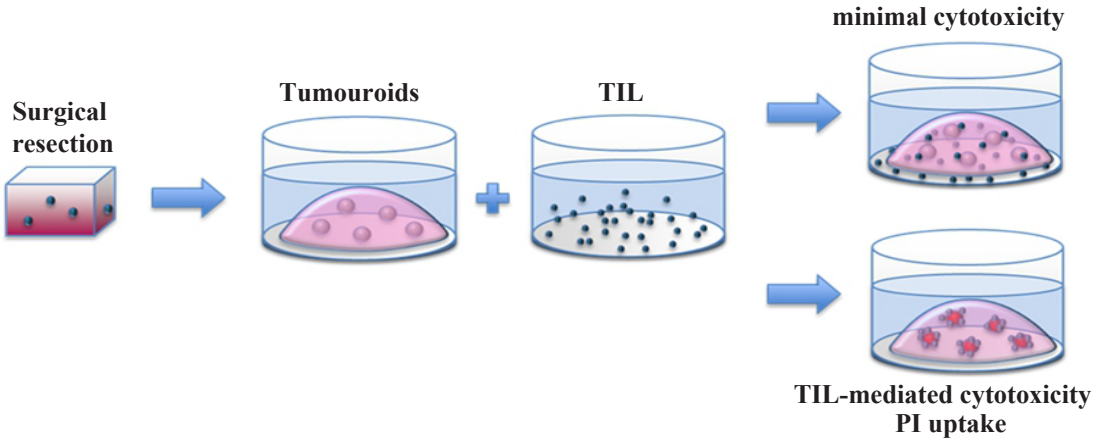


**Figure 4.6 Schematic diagram of processing tissue: from surgical resection to cytotoxic assay.** Following surgical resection or biopsy, tumouroids are established from viable tumour tissue and embedded in 3D matrigel. TILs are expanded from a separate piece of tumour tissue in recombinant human IL-2 (6,000 IU/mL). TILs are co-cultured with tumouroids, in the presence of PI and imaged on a wide-field fluorescence microscope for 48 hours. Uptake of PI by tumouroids indicates tumouroid death and TIL-mediated cytotoxicity. Lack of uptake of PI indicates minimal cytotoxicity and may be an indication of dysfunctional TILs or immunologically resistant tumouroids.

As previously mentioned, it was sometimes difficult to distinguish TILs from tumouroids when visualising the co-culture with wide-fide fluorescence microscopy. This was particularly apparent when the cells within the tumouroid start dying and it is complex to decipher if they are TILs sitting on top of the tumouroid or cells within the tumouroid itself. To make this distinction clearer, scanning electron microscopy was utilised. The experiment was set up where tumouroids were exposed to autologous TILs for 8 hours or not exposed to TILs at all. As seen in **Figure 4.7B**, following co-culture with autologous TILs, the surface of the tumouroid is completely disrupted compared to the smooth surface as seen in the tumouroid alone panel in **Figure 4.7A**. Lymphocytes are rendered pink and highlighted by pink arrows, and are evidently much smaller (≤10μm diameter) than tumouroids. Thus confirming that the cell death observed in the fluorescence microscopy images is more likely to be coming from the cells within the tumouroid rather than lymphocytes on the surface of the tumouroids. These qualitative data also highlight the E:T ratio being ideal, as this is reflective of 10:1 ratio and is in keeping with E:T ratio used in the CRA.

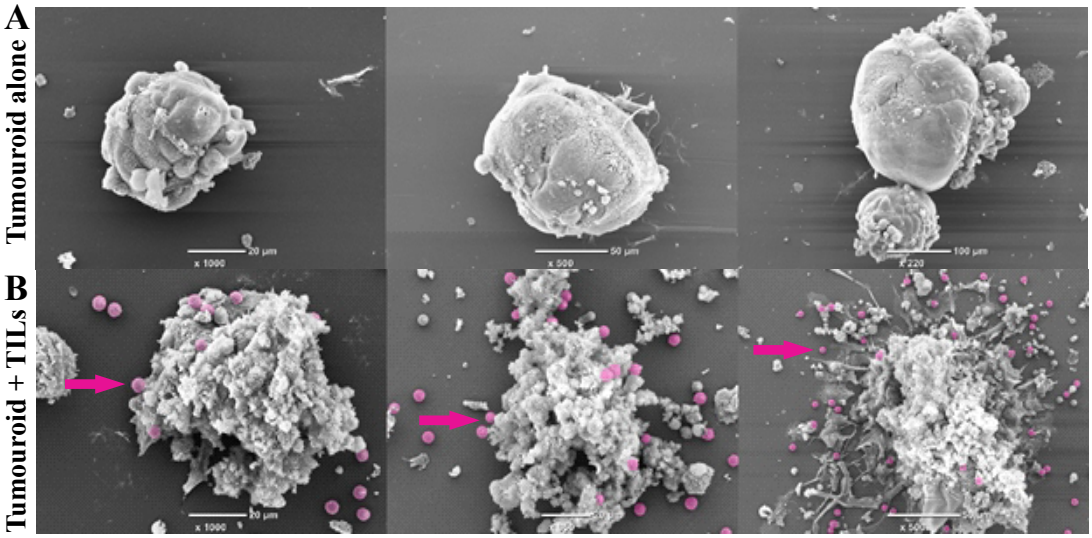


**Figure 4.7 Autologous TILs cause architectural disruption to tumouroids after co-culture.** Scanning electron micrographs showing tumouroid structure from three different patients (**A**) tumouroids cultured alone or (**B**) with autologous TILs at high concentration for 8 hours and then subjected to fixation and processing for SEM. As observed, there are morphological irregularities denoted by the ruffled surface in panel (**B**). Pink arrows highlight lymphocytes rendered in pink, providing a sense of size of the lymphocytes (<10 μm) compared to tumouroid, scale bar = 20, 50 and 100 μm, respectively.

### 4.4 Quantitation of the Cytotoxic Assay

Up to this point, most of the data collected to establish the protocol was qualitative, however there was a strong desire to configure a way to gain quantitative data from these experiments. As mentioned before, we established the protocol on the Olympus IX3 wide-field fluorescent microscope, imaging at least 10 tumouroids per well at the periphery of the matrigel. Selection of tumouroids was within 100 μm of the edge of the matrigel at time zero. Acquisition of these images was captured with the differential interference contrast (DIC) to visualise the tumouroid structure and then subsequently captured with the dsRed filter to detect PI uptake, as a measure of cell death. Sequential acquisition was every 2 hours for 48 hours. Once the assay had been completed, images were exported and converted to a tagged image filed format (TIFF) file. The subsequent data analysis pipeline was then completed using the National institutes of health (NIH) software ImageJ (**Chapter 2**).

First individual TIFF files were "stitched" together to create a time-lapse movie over 48 hours. To quantitate tumouroid death, each tumouroid within 100 μm of the matrigel edge, was selected and an area was drawn around it, as depicted with yellow circles in **Figure 4.8**. This

area was then copied to the dsRed channel to quantitate the mean fluorescent intensity (MFI) of PI uptake in that tumouroid.

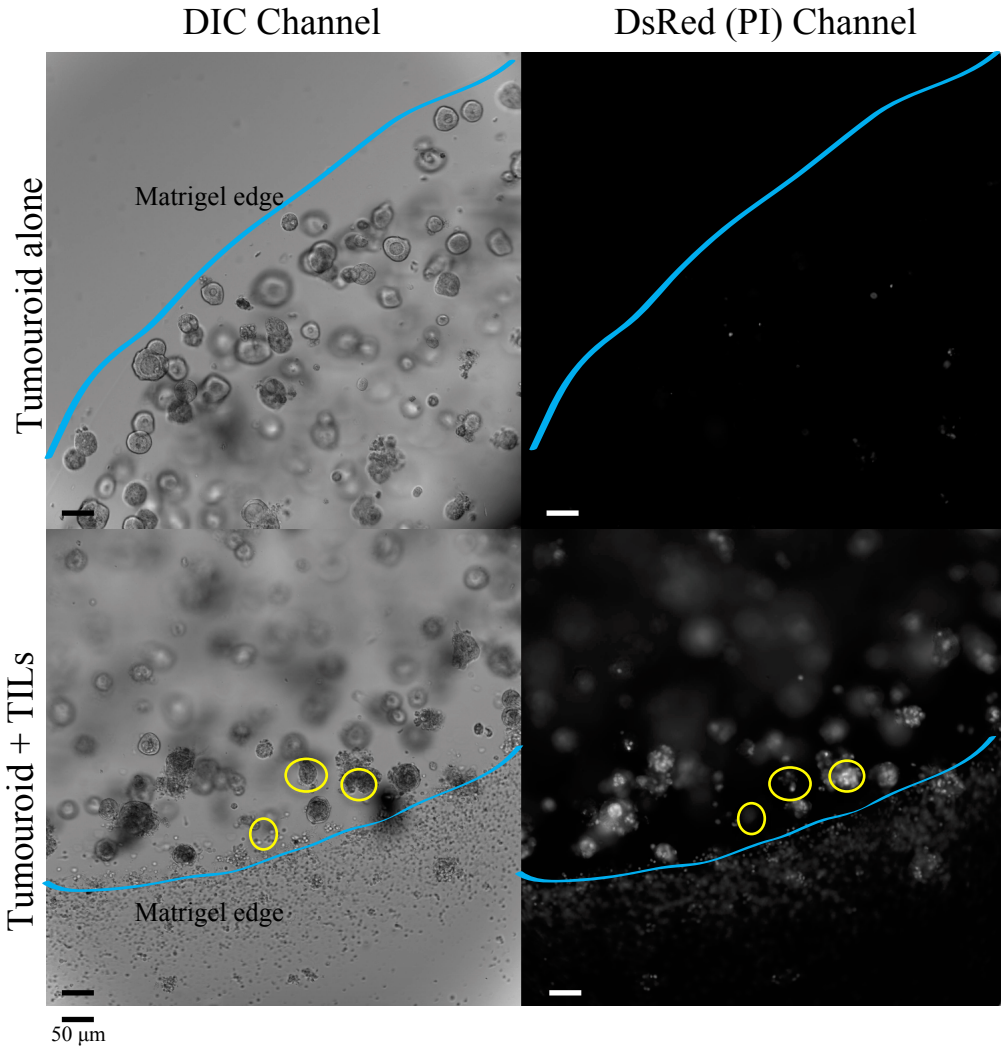


**Figure 4.8. Selection of tumouroids for quantitation of tumouroid death.** Tumouroids around the edge of the matrigel are selected for acquisition and quantitation using the DIC channel. These areas are then applied to DsRed channel and the MFI of PI uptake is then quantitated over time to obtain kinetic killing data as a measure of TIL-induced cytotoxicity. Scale bar = 50 µm.

The data obtained from this analysis provides kinetic information- where the same tumouroid is imaged for 48 hours. This then details the MFI of PI uptake over time and therefore tumouroid death over time, as seen in **Figure 4.9A**.

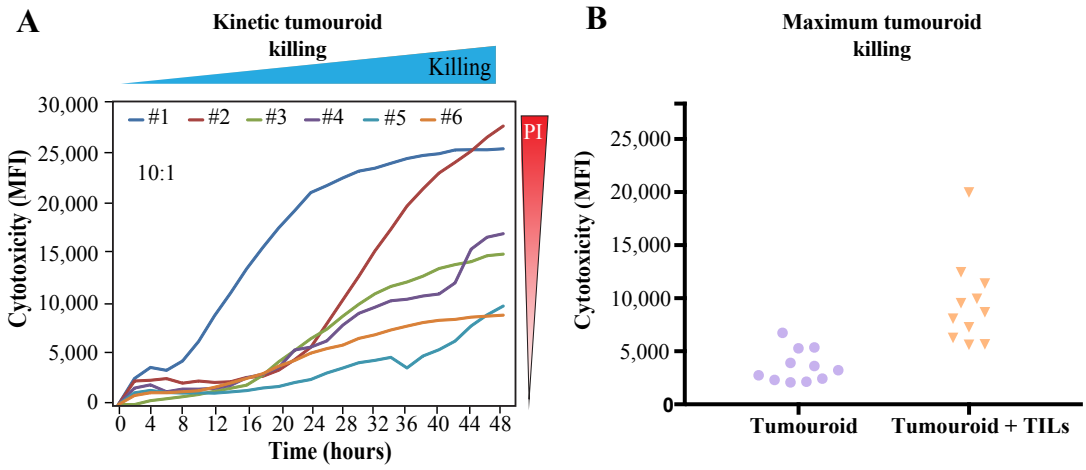


**Figure 4.9. Quantifying tumouroid death by kinetic and maximum analysis.** (**A**) XY-plot of rectal tumouroid death as measured by MFI of PI over time (hours). Heterogeneous killing of tumouroids by TILs. All experiments used 10:1 E:T ratio, lines represent the mean, n=6. (**B**) Scatter-plot of maximum MFI representing tumouroid killing. Background tumouroid death (purple circles) and tumouroid + TILs (orange triangles) at any time point during the co-culture, data representative of one experiment, individual dot represents one tumouroid, n=11 tumouroids per condition.

Additionally the maximum MFI value of each tumouroid was determined at any time point to obtain differences between test conditions as seen in **Figure 4.9B**. This is another representation of the data and allows statistical differences to be inferred between different test conditions.

To expand TILs from the tumour, viable tumour pieces were placed in complete media enriched with recombinant human IL-2, at 6,000 IU/mL. Expansion was continued for 7-10 days, whilst tumouroids were established. On the same day as the co-culture assay, TILs were phenotypically assessed using flow cytometry to understand the sub population frequencies post expansion including: CD4+, CD8+, T-regulatory cells, NK (CD56+) and NKT cells (CD56+ CD3+). Expression of activation markers was also confirmed including CD69, PD-1 and CD45RO. Through this analysis, a sense of immune frequencies present in the TIL culture were understood; however the whole TIL culture would mostly be used in the co-culture assay. To gain a deeper understanding of which sub population of TILs were most responsible for killing, TILs were separated by FACS into: CD8+/CD56-, CD8+/CD56+, CD4+ and CD56+/CD8- populations. This was done for three different RC patients, in three separate experiments, as seen in **Figure 4.10**.

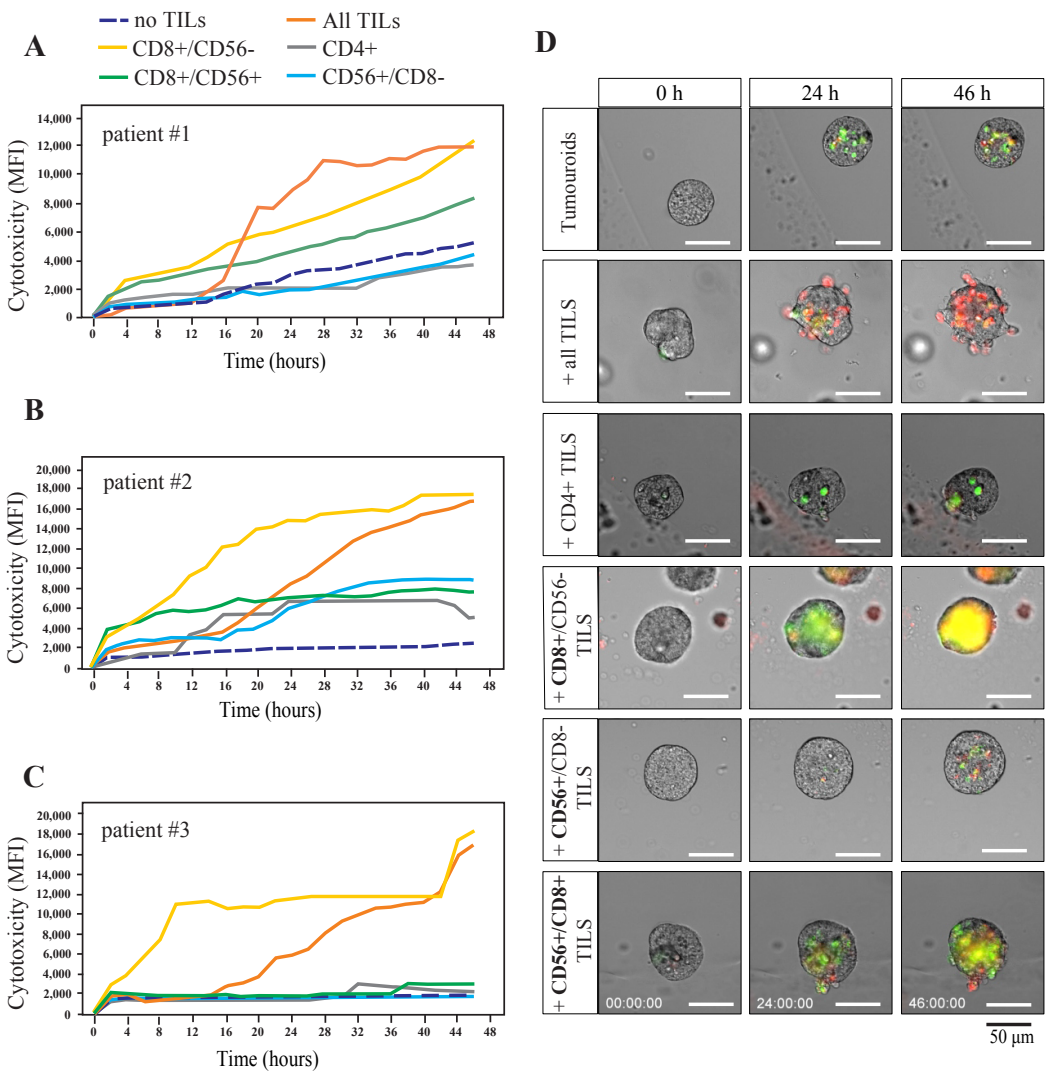


**Figure 4.10. CTL killing is mostly driven by cytotoxic CD8+ T-cell population.** Sub-populations of IL-2 expanded TILs were separated by FACS into CD8+/CD56- (yellow line), CD8+CD56+ (green line), CD4+ (grey line) and CD56+CD8- (blue line) populations and this was compared to all TILs (orange line) and tumouroids alone (dotted navy line). XY-plot showing MFI of PI uptake in tumouroids detailing kinetics of different TIL populations killing patient derived tumouroids over time (hours) in three different patients with RC (**A**) patient 1 (**B**) patient 2 and (**C**) patient 3. (**D**) Representative still shot images taken on Olympus IX3 wide-field fluorescent microscope at 0, 24 and 46 hours for tumouroid alone, all TILs and each sub-population separated by FACS. Caspase 3/7 dye (green) was used to document apoptosis and PI (red) was used to quantitate tumouroid death. Scale bars=50 µm, n=3.

From this experiment, the most prominent killing population found was CD8+ T-cells. In each patient, CD8+ T-cells had the most rapid onset of killing. The CD8+CD56+ frequency, which is likely to be NKT cells, is efficient at killing in 2/3 patients. Importantly the CD4+ population

did not induce cell death in the tumouroids, and the CD56+CD8-, likely to be NK cells did not have much effect. Alongside the CD8+ population, the condition that included all TILs was just as effective at inducing tumouroid death. It is likely that the combination of T-cells orchestrate tumouroid killing in unison, where the CD4+ helper T-cells likely produce cytokines to assist the CTL killing. This experiment also confirms that TIL killing is mostly CD8+ mediated, and that these CD8+ T cells are likely to be recognising tumour antigen.

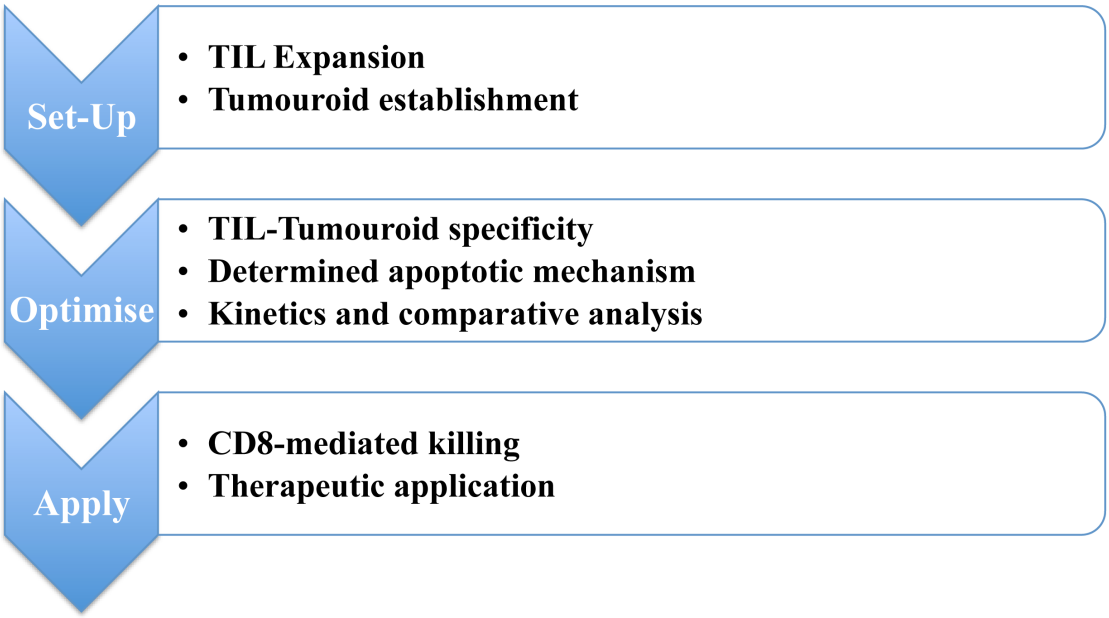


**Figure 4.11. Process of steps involved developing the cytotoxic assay.** In order to achieve an assay that can be used to address clinical questions regarding patient response, the initial set-up and optimisation steps must be achieved and this can then be applied to answer key biological and therapeutic questions.

The process of developing an assay involved many learning experiences including initial set up of tissue culture techniques, TIL expansion and tumouroid establishment from patient-derived material. Many optimising steps were required to determine if autologous tumouroids and TILs would specifically react in an *ex vivo* setting, and define an ideal setting to measure this. The mechanism of apoptosis was important to confirm this killing was inducing direct apoptosis and not just unspecific necrosis. Quantitating this to achieve kinetic and comparative analysis to determine differences between treatment conditions was essential. Determining this is mostly CD8+ mediated also validated the specificity of the assay. Finally optimising this assay to the point where key biological and therapeutic questions could be posed was the main objective. This assay could now be applied to start answering these questions.

## 4.5 Application Of The Cytotoxic Assay

The application that was envisioned for this assay, was the potential use of assessing CBI with patient derived TILs and tumouroids in the co-culture. We decided to target PD-1 and used the anti-PD-1 (αPD-1) checkpoint antibody Pembrolizumab (Keytruda®) and performed the experiment on three patient samples. We first assessed the basal levels of PD-1 expression on the expanded TILs by flow cytometry. The basal levels were 17.2%, 12.5% and 17.8% and following CD3/28 stimulation were 45.5%, 73.2% and 40.3% PD-1 positive on CD8+ cytotoxic T-cells, respectively (**Figure 4.12A-C**). Induction of PD-1 expression was achieved by stimulating the expanded TILs via the TCR using magnetic Dynabeads® human T-cell activator reagent targeting anti-CD3/28. These stimulated TILs were then taken into the cytotoxic assay. TILs were co-cultured with autologous tumouroids for 48 hours, and supernatants were taken at the endpoint of the assay (48 hours) and assessed by cytometric bead array (CBA). IFNγ and TNFα were assessed in each co-culture assay of each patient (**Figure 4.12D-F**), addition of αPD-1 (purple bars) showed a strong induction of both IFNγ and TNFα in all three patients, compared to no αPD-1 (blue bars).

In many functional immune cell assays, IFNγ is a typically a readout of effector function. However, what this experiment demonstrated was that assessment of cytokines does not always reflect the cytotoxic function. When analysing the cytotoxic assay co-culture (**Figure 4.12G-I**) without (blue bars) or with (purple bars) αPD-1, it can be seen that the response to CBI is heterogeneous between patients. When observing the responses individually, with patient 1 (**Figure 4.12G**), addition of aPD-1 rapidly enhances cytotoxic TIL function. However with patient 2 (**Figure 4.12H**) this does not occur until 8 hours, but eventually the TILs without aPD-1 reach the same cytotoxic effect. Finally, patient 3 (**Figure 4.12I**) there is no effect of αPD-1, highlighting the heterogeneity of response to CBI between patients. This experiment also emphasises the observation that measuring cytokine secretion alone does not always equate to the cytotoxic function, and therefore both measurements should ideally be assessed when determining TIL functionality.

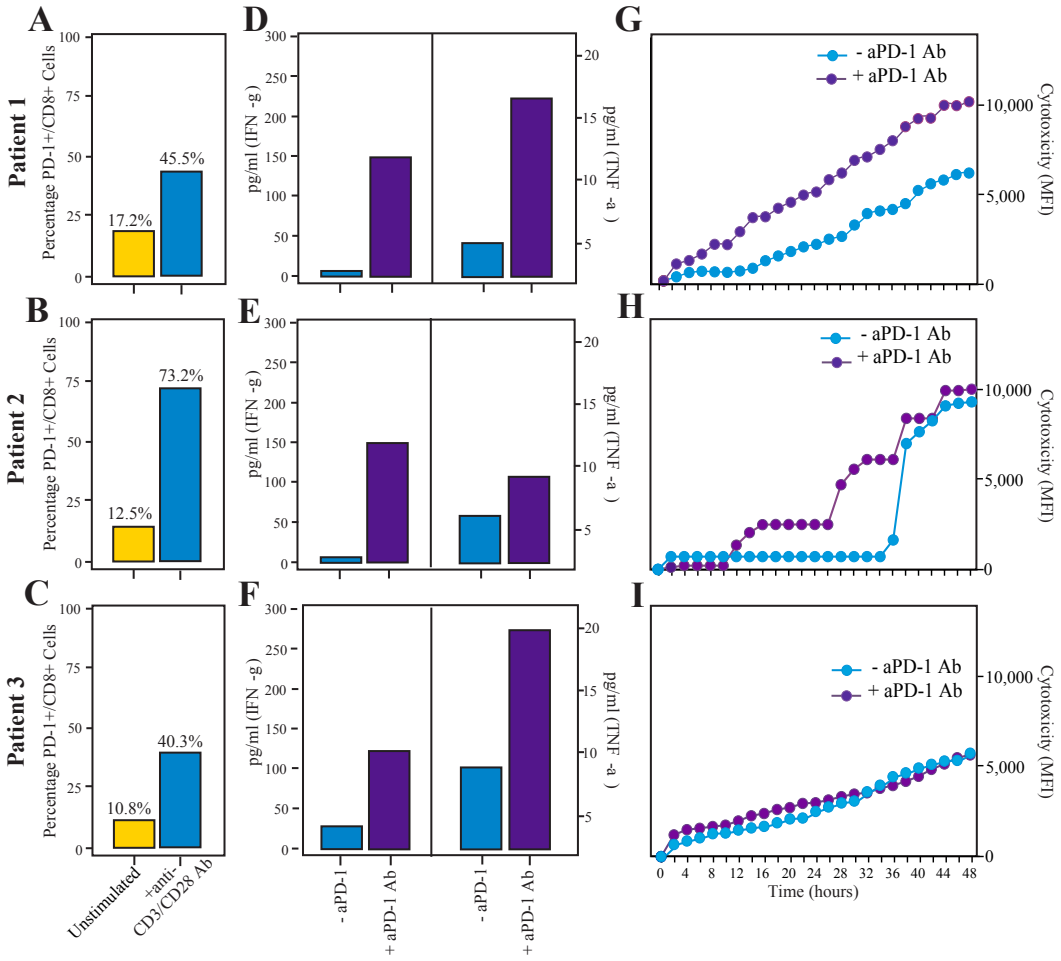


**Figure 4.12. PD-1 blockade results in heterogeneous responses between patients in cytotoxic assay co-culture. (A-C)** Bar graphs showing expanded TILs assessed for basal expression of PD-1 on CD8+ T-cells (yellow bars) and PD-1 expression following CD3/28 stimulation (blue bars) in three different RC patients (A, B, C, respectively). CD3/28 stimulated TILs were co-cultured with matched tumouroids and supernatant was assessed by CBA. IFNγ (right panel) and TNFα (left panel) secretion (pg/mL) was analysed without αPD-1 (blue bar) and with αPD-1 (purple bar) in three different patients. XY-plots show tumouroid killing by matched stimulated TILs without (blue) and with (purple) aPD-1 blockade, measuring MFI of PI uptake over time (hours). n=3 patients, conducted over three separate experiments.

The establishment of this assay was the first step in moving towards asking key immunological questions about patient-derived TILs and their function *ex vivo*. I therefore used this assay and additional techniques to evaluate the state of TILs in CRLM.

## 4.6 Assessment of TIL Function In CRLM

When this project was first designed, one of the main objectives was to compare the immune response at the primary site in the colon/rectum and the distal metastatic site in the liver. To address this question, we aimed not only to recruit patients with metachronous isolated liver metastasis, but also recruit patients with synchronous disease, where the primary and metastatic liver tumour are *in situ* and surgically resected simultaneously.

We recruited six patients that had synchronous surgical resections. Of the six patients, only one was successful in the generation of both tumouroids and TILs from each site, and we were able to utilise the cytotoxic assay to assess functional immune differences between these sites. In this proof of principle experiment, following expansion of TILs from both sites, on the day of the cytotoxic assay, the immune cells were assessed post expansion to determine different lymphocyte and T-cell subset frequencies as seen in **Figure 4.13**. T-cells are enriched in the expansion protocol and these frequencies are similar in the primary (blue bar) and liver met (yellow bar) tumours (**Fig. 4.13A**). T-helper cells (CD4+) are enriched from the primary tumour and cytotoxic T-cells (CD8+) are enriched from the met tumour (**Fig. 4.13B**). The CD8+ T-cells expanded from the met tumour have a more activated memory phenotype than those expanded from the primary tumour (**Fig. 4.13C**)

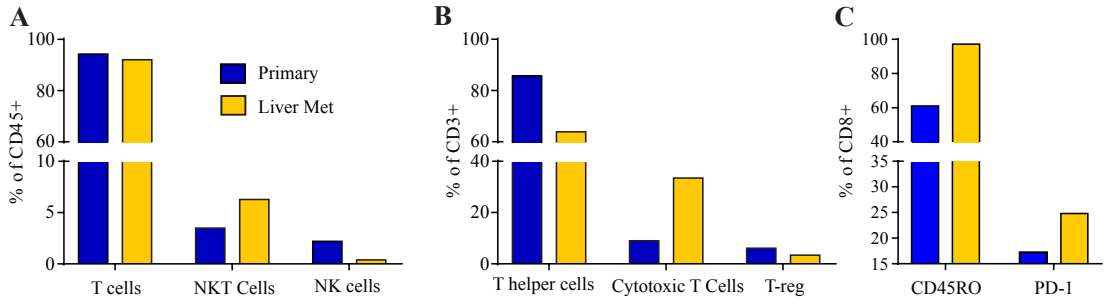


**Figure 4.13. TIL populations from different tumour sites have different phenotypes.** TILs were expanded from the primary tumour in the rectum (blue bars) and liver met (yellow bars) and assessed by flow cytometry (**A**) Bar plots showing TILs from one patient with synchronous primary rectal tumour and liver metastases analysed for sub-populations of lymphocytes, including T-cells (CD3+), NKT cells (CD3+CD56+) and NK cells (CD3-CD56+) (**B**) T cell subsets (T helper cells: CD4+, Cytotoxic T-cells (CD8+) and T-reg cells (CD25+Foxp3+) and (**C**) memory (CD45RO) and activation (PD-1) markers, n=1.

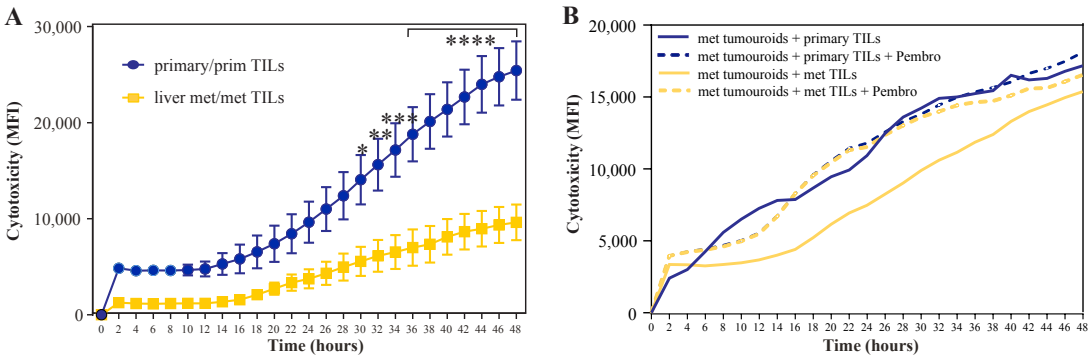


**Figure 4.14. TIL populations from different tumour sites have distinct killing capacity.** Pooled cytotoxicity data from tumouroids from two patients with synchronous primary rectal tumour and liver metastases challenged with (**A**) matched TILs expanded from the same (site) tumour are shown (**B**) The same samples with the addition of anti-PD-1 antibody (mean +/- SEM). $P < 0.05$ (*), $P < 0.01$ (**), $P < 0.001$ (***), $P < 0.0001$ (****); 2way ANOVA.

The function of these TILs was then investigated using the cytotoxic assay as seen in **Figure 4.14**. The first experiment was comparing the TILs ability to kill the tumouroids of the same origin (tumour). As can be seen in **Figure 4.14A**, primary TILs have the ability to kill matched primary tumouroids. However, the metastatic TILs have a reduced ability to do this. A cross over experiment was then done with (whole lines) or without (dotted lines) the addition of αPD-1. Primary tumour TILs were co-cultured with met tumouroids and met TILs were co-cultured with met tumouroids. As can be seen in **Figure 4.14B**, primary TILs have better killing efficacy than met TILs to the met tumouroids. This may imply that those TILs are the primary site are inherently more functional than those at the metastatic site. Interestingly, addition of αPD-1 rescues only the metastatic TIL function, and not the primary TILs. This may also be associated with the higher PD-1 expression on the met CD8+ TILs as seen in **Figure 4.14C**. So although the TILs at the metastatic site may not kill efficiently on their own, addition of αPD-1 rescues this function, also suggesting that they are not intrinsically dysfunctional.

To investigate this further in more patient samples, 4 CRLM patients were assessed using the cytotoxic co-culture assay. As seen in Figure **4.15A-B**, autologous TILs (red line) have the ability to induce tumouroid death 1-2 fold greater than background tumouroid death (purple line). However, unlike the anecdotal example in **Figure 4.12** where the TIL function was rescued with αPD-1, addition of αPD-1 in all patients assessed in **Figure 4.15A-B** did not enhance TIL function.

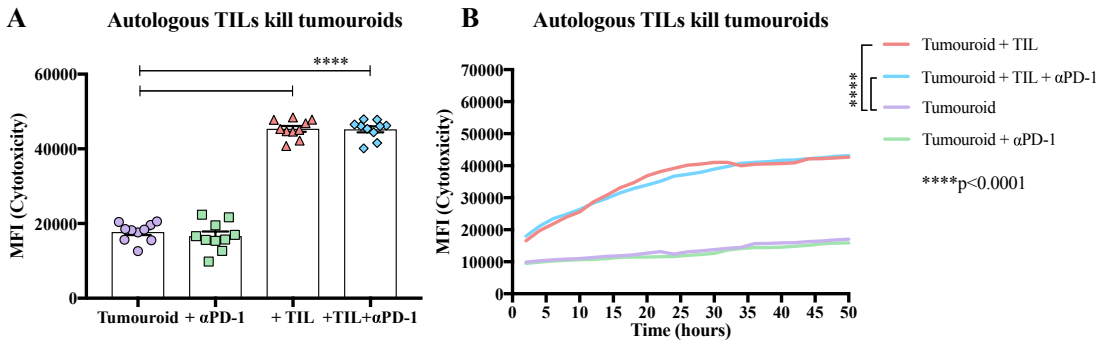


**Figure 4.15. Autologous T-cells induce killing in matched tumouroids, addition of checkpoint blockade does not enhance killing.** Patient-derived tumouroids were co-cultured with autologous IL-2 expanded TILs for 48 hours. (**A**) Bar-plot displaying mean maximum killing of tumouroids, each point represents the average of one tumouroid, error bars represent SEM (mean; one-way ANOVA ****p<0.001) (**B**) XY-plot describing kinetic data of tumouroid death by measure of MFI of PI uptake over time (hours), ANOVA ****p<0.001, n=4.

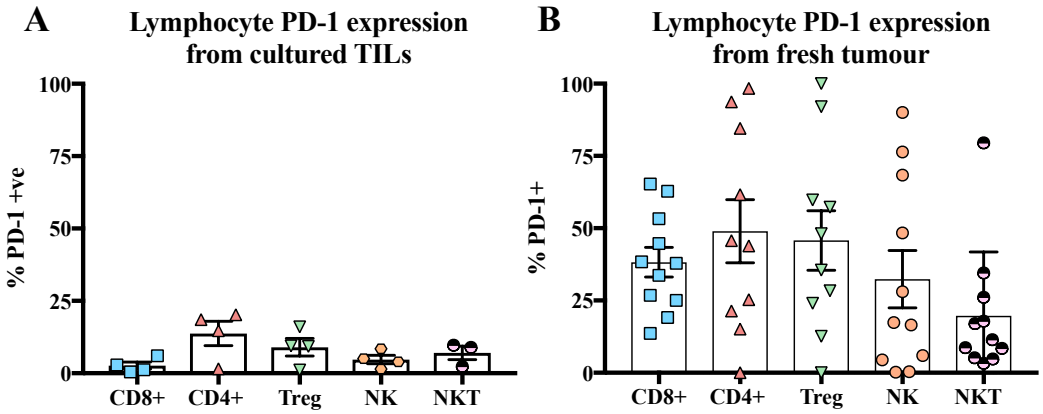


**Figure 4.16. PD-1 expression is lower on TILs expanded in culture compared to TILs freshly isolated from tumour of CRLM patients.** Bar-plots showing PD-1 expression on immune cell subsets of (**A**) TILs expanded from tumours of CRLM patients, error bars represent SEM, n=4 and (**B**) Freshly isolated TILs from tumours of CRLM patients, error bars represent SEM, n=11.

It may be possible that no effects were observed with addition of anti-PD-1 antibody due to low expression of PD-1 on immune cells. As seen in **Figure 4.16A**, lymphocyte PD-1 expression was below 25% on all subsets of immune cells. When this is compared to PD-1 expression on immune cells freshly isolated from tumours of CRLM patients as seen in **Figure 4.16B**, PD-1 expression is between 25-50% across all immune subsets. Therefore PD-1 expression on

immune cells is downregulated during culture. Although not included in this thesis, subsequent experiments to artificially induce PD-1 expression on expanded TILs used anti-CD3/28 stimulation, which did induce PD-1 expression. Another confounding factor of use of anti-PD-1 antibody in this assay was determination of PD-L1 expression on tumouroids. This was realised after completing these experiments, however it was found by a Ramsay laboratory member, that stimulation of tumouroids using IFNγ induced upregulation of PD-L1 on tumouroids in culture. Hence, the PD-1/PD-L1 axis should be present to see effects of blockade of this interaction, which may have been the reason no enhanced cytotoxic effects were observed. To assess phenotype of expanded TILs, a flow cytometry panel was used to determine the phenotype type of expanded TILs in culture.

The gating strategy to define populations of T-cells and gating for positive expression of surface markers is outlined in **Figure 4.17** in a representative sample. It can be observed that there is ~80% enrichment of T-cells in the expansion process. The proportions of CD8+/CD4+ T-cell ratio is similar to what is observed when assessing T-cell proportions from fresh tissue in CRLM, with a predominance of CD4+ T-helper cells. Expression levels of PD-1 on CD4+, CD8+ and T-reg cells was assessed by the positive percentage of each population, that was defined using an isotype control for the BV421 fluorophore.

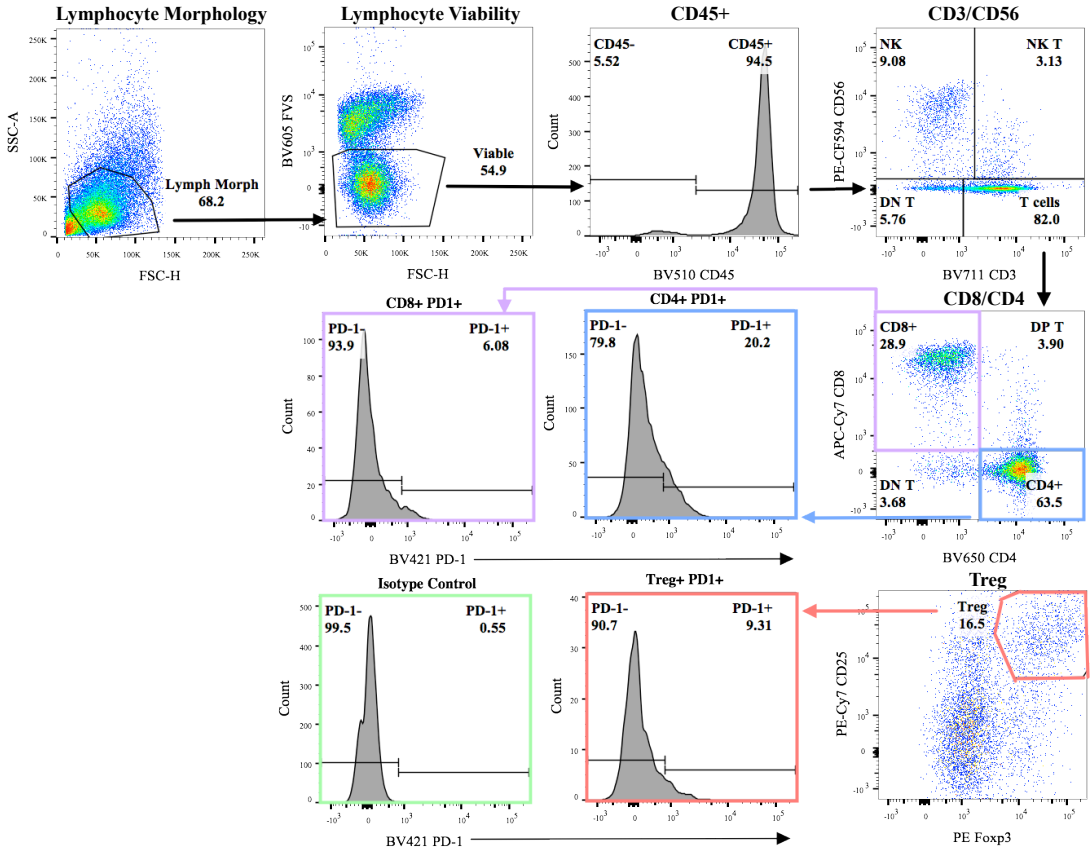


**Figure 4.17. Representative flow cytometry gating strategy of expanded TILs from patient tumour tissue.** Expanded TIL phenotype on the day of the cytotoxic assay. Lymphocytes are gated on morphology (SSC-A vs. FSC-H), viable cells using BV605 viability dye, BV510 CD45+. T-cells are gated on CD3+ T-cells and subpopulations defined by CD8+(purple) and CD4+ (blue) T-cells. T-regulatory cells (red) are defined by CD25+Foxp3+ staining. PD-1 expression levels were assessed on all sub-populations, using an isotype control (green) to define PD-1+ cells.

From the combined data analysis of the cytotoxic assay, it can be concluded that cytotoxic TIL function cannot generally be enhanced with addition of αPD-1. To investigate this on an individual basis, each patient assay was assessed, along with PD-1 expression levels, as seen in **Figure 4.18**. Patient 1 had the lowest expression levels of PD-1 on the entire T-cell population, and this was the only patient where the αPD-1 reduced the effect of TIL-mediated killing (**Fig 4.18A**). Patient 2 and 3 both had PD-1 expression levels of ~15%, αPD-1 did not enhance killing, but remained at a similar killing efficiency as TILs alone (**Fig. 4.18B-C**). Patient 4 had PD-1 expression levels of ~9%, and addition of αPD-1 only enhanced this effect slightly (**Fig. 4.18D**).

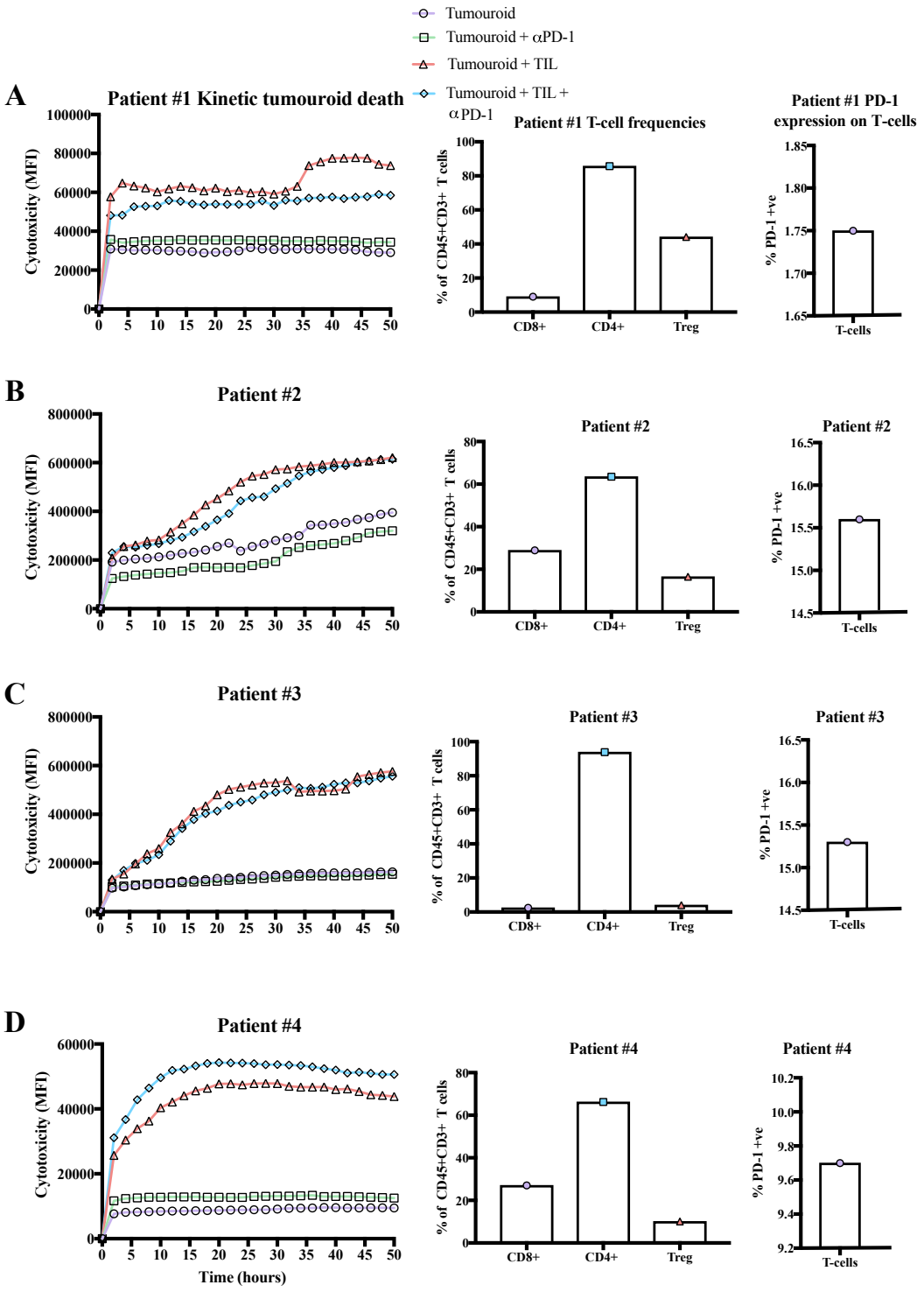


**Figure 4.18. TIL-mediated cytotoxicity in individual patients demonstrates killing, PD-1 expression on T-cells does not affect response to αPD-1.** XY-plot showing the mean kinetic data of tumouroid death by measuring MFI of PI uptake over time (hours). Bar-plots displaying the percentage of PD-1 expression on T-cells, CD8+, CD4+ and Treg by flow cytometry as gated in Figure 4.15. Individual data plotted for (**A**) Patient 1, (**B**) Patient 2, (**C**) Patient 3 and (**D**) Patient 4.

In addition to assessing immune function using the cytotoxic assay, supernatants were also taken over the time course of the assay to assess both cytokine and cytolytic molecule secretion. IFNγ production was increased when αPD-1 was added to the tumouroid + TILs and also TILs alone (**Fig. 4.19A**). Cytolytic molecules including granzyme B and FasL were also induced with the addition of αPD-1. However, the exclusive use of cytokine data as readout of cytotoxicity potential can be misleading, and should ideally be assessed alongside the cytotoxic data.

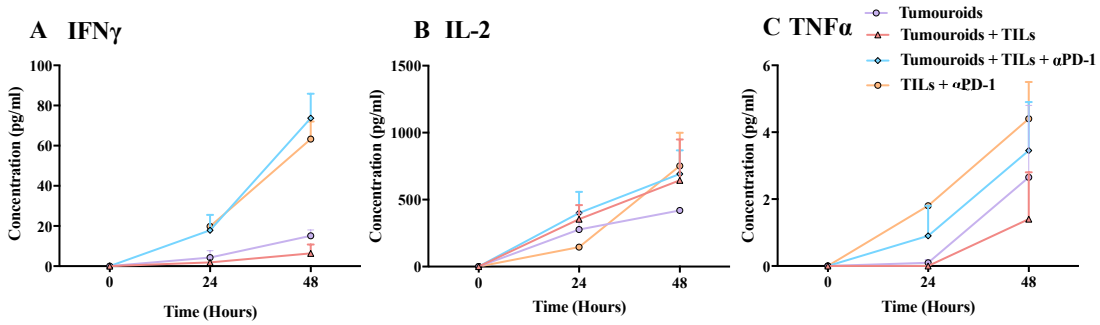


**Figure 4.19. Addition of anti-PD-1 induces cytokine secretion over time.** Autologous tumouroids and TILs were co-cultured and supernatants taken at 24 and 48 hours. CBA was performed to analyse the amount (pg/mL) of (**A**) IFNγ (**B**) IL-2 and (**C**) TNFα secreted over time. Mean +/- SEM, n=3

This *ex vivo* functional data provides insight into the biology of the TILs and their ability to respond to CBI. It is important to keep in mind that expanding the TILs in the presence of IL-2 and tumour may not be biologically optimal or reflect exactly what occurs *in vivo*. However, by expanding specific TILs and assessing their maximum function, we gain insights into the biology of these cells. Most importantly, it provides a platform to assess patient-derived samples, particularly assessing CBI, in a functional approach. To understand the *in situ* status of the immune response in patients with CRLM, I next assessed the frequency and phenotype of immune cells isolated fresh from the tissue.

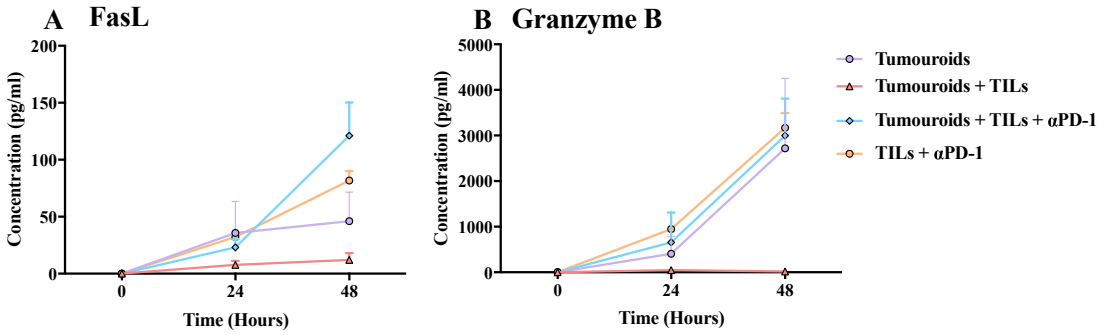


**Figure 4.20. Addition of anti-PD-1 induces cytolytic molecule secretion over time.** Autologous tumouroids and TILs were co-cultured and supernatants taken at 24 and 48 hours. CBA was performed to analyse the amount (pg/mL) of (**A**) FasL and (**B**) Granzyme B secreted over time. Mean +/- SEM, n=3.

### 4.7 Assessment of *in situ* TILs In CRLM

Flow cytometry was used to assess the frequency and phenotype of immune cells from within the TME in CRLM. Lymphocytes were freshly isolated from the resected specimen and stained on the same day. As seen in **Figure 4.21A** the predominant leukocyte population in both tumour and normal liver are T-cells. It can be observed that both NK and NK T-cells are significantly reduced in the tumour compared to normal liver tissue. Also reduced in the tumour are the MDSC population. When assessing the T-cell distribution in CRLM tumours as seen in **Figure 4.21B**, cytotoxic CD8+ T-cells are significantly reduced in the tumour compared to surrounding liver. Conversely, T-helper CD4+ cells are significantly increased in the tumour compared to surrounding liver. Of these CD4+ T-cells, ~16% are T-reg cells, that are more predominant in the tumour than in the surrounding liver. However, as can be seen in **Figure 4.21**, there is a broad range due to variability of patients and tumours.

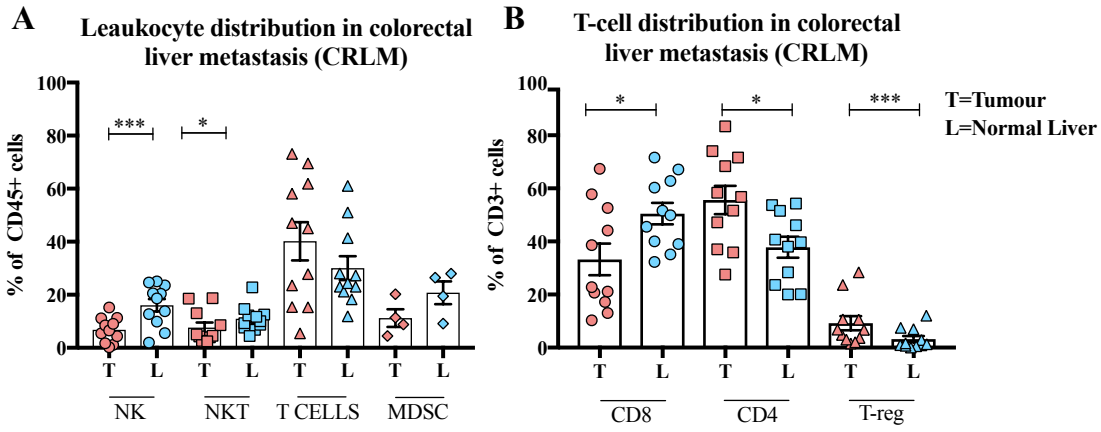


**Figure 4.21. Leukocyte distribution in CRLM involves T-cells that are mostly CD4+. Lymphocytes were freshly isolated from tissue and assessed using flow cytometry.** Bar-plots represent lymphocytes isolated from tumour (red) or normal distant liver (blue) detecting (**A**) the percentages CD45+ cells that are: NK cells (CD3-CD56+), NKT cells (CD3+CD56+), T-cells (CD3+) and MDSCs (CD45+HLA-DR-CD33+CD11b+). (**B**) T-cells are detected as a percentage of CD3+ cells including: Cytotoxic CD8+, T-helper CD4+ and T-reg cells (CD4+CD25+Foxp3+). Mean +/- SEM, n=11, Wilcoxon two-tailed t-test, *p=0.0021, ***p<0.0001.

Next I assessed the phenotype of these immune cells investigating markers of activation (PD-1), cytotoxicity (CD107a) and memory (CD45RO). As can be seen in **Figure 4.22**, PD-1 expression is prominent in all T-cells subsets within the tumour, and this is distinct from T-cells in the peripheral blood, demonstrating a local immune phenotype at the tumour site. Expression of PD-1 can indicate activation as well as exhaustion; the latter requires other transcription factor expression to confirm this, which was not included in this flow cytometry panel. Importantly expression of PD-1 indicates that these immune cells have the potential ability to bind anti-PD-1 antibody and perhaps respond to it.

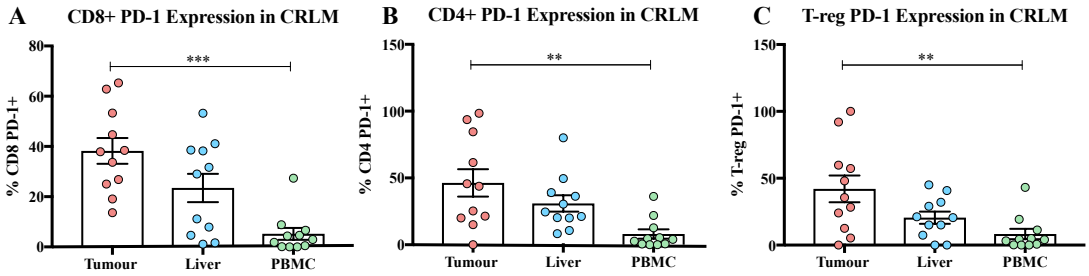


**Figure 4.22. PD-1 expression on lymphocytes is distinct in tissue compared to peripheral blood.** PD-1 expression was quantified as percentage positive on (**A**) Cytotoxic CD8+ (**B**) T-helper CD4+ T-cells and (**C**) T-regulatory cells, gating on the positive population as defined by an isotype control. This was assessed in lymphocytes from the tumour, liver and PBMCs. Mean +/- SEM, n=11, One-Way ANOVA (non-parametric) Friedman test, **p=0.0021, ***p=0.0002.

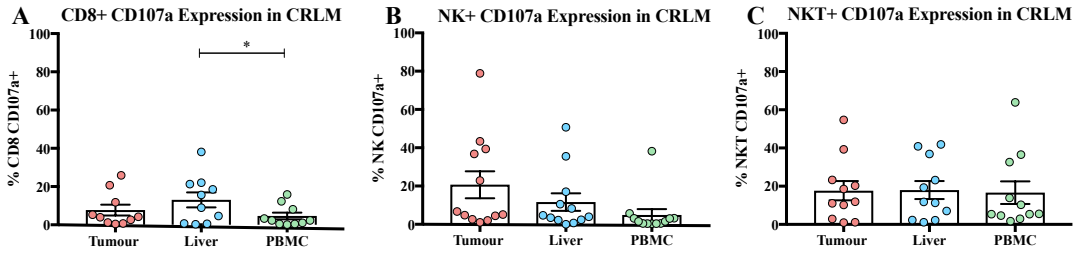


**Figure 4.23. CD107a expression on cytotoxic lymphocytes is reduced on CD8+ T-cells from the tumour.** CD107a expression was quantified as percentage positive on (**A**) Cytotoxic CD8+ (**B**) NK cells and (**C**) NKT cells, gating on the positive population as defined by an isotype control. This was assessed in lymphocytes from the tumour, liver and PBMCs. Mean +/- SEM, n=11, One-Way ANOVA (non-parametric) Friedman test, *p=0.03.

Next to assess the cytotoxicity of the cytotoxic lymphocytes in situ, CD107a expression was measured CD8+ cytotoxic T-cells, NK and NKT cells as seen in **Figure 4.23**. It can be seen that CD8+ T-cells in the tumour have reduced expression of CD107a compared to those in the liver, indicating a reduced "cytotoxic" phenotype in the tumour. Conversely NK cells in the tumour express more CD107a (**Fig. 4.23B**) and there is no difference in expression of CD107a between the tumour and liver in the NKT subset (**Fig. 4.23C**).

Finally to evaluate immune memory, CD45RO expression was interrogated as seen in **Figure 4.24**. Certainly expression of this marker is distinct in the tissue compared to the peripheral blood, which is expected as peripheral blood lymphocytes are more naïve. Expression of

CD45RO on CD4+, CD8+ T-cells and T-regulatory cells was higher in the tumour compared to the liver. These data indicate that these immune cells are antigen experienced in the tumour.

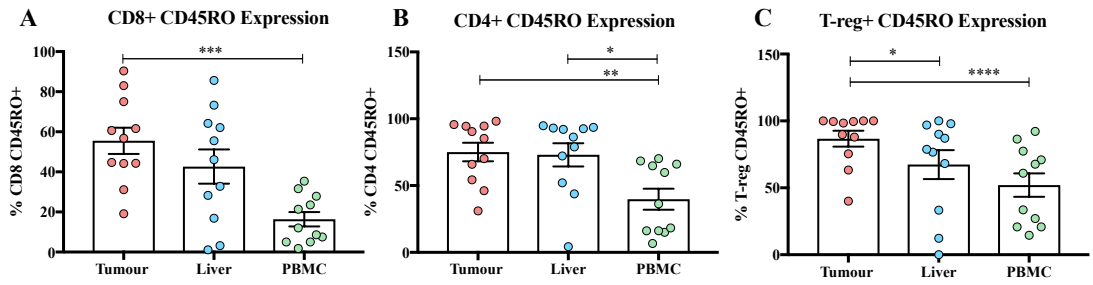


**Figure 4.24. Memory phenotype is distinct in the tissue compared to peripheral blood.** CD45RO expression was quantified as percentage positive on (**A**) Cytotoxic CD8+ (**B**) T-helper CD4+ T-cells and (**C**) T-regulatory cells, gating on the positive population as defined by an isotype control. This was assessed in lymphocytes from the tumour, liver and PBMCs. Mean +/- SEM, n=11, One-Way ANOVA (non-parametric) Friedman test, *p=0.03, **p=0.002, ***p=0.0002, ****<0.0001.

The phenotyping analysis provides a "snap-shot" insight into the *in situ* immune response at the tumour site, following surgical resection of the metastasis. What is evident from these data is that the cytotoxic immune infiltrate is reduced numerically and has a reduced cytotoxic function as assessed by CD107a expression. The CD8+ T-cells in the tumour also have an increased PD-1 expression, which could be targeted to restore cytotoxic function. The presence of T-regulatory cells that are both active and antigen experienced suggests these cells could play a role in suppressing effector function of the cytotoxic T-cells. The CD4+ T-cells also have this phenotype, however determining if the helper T-cells are Th1 or Th2 is beyond the scope of this flow cytometry panel. Using this flow cytometry panel, we can however conclude that within the tumours of CRLM, there is a reduced cytotoxic function and presence of T-regulatory cells that may contribute to a more immunosuppressive tumour microenvironment.

The disadvantage of using flow cytometry to assess freshly isolated lymphocytes is that the tissue is macroscopically segmented into tumour and normal liver. This method does not assess immune cells residing at particular areas within the tumour such as CT, IM and DL. To gain a sense of spatial location of infiltrating immune cells, multiplex immunohistochemistry (mIHC) was utilised to assess the location and frequency of the aforementioned immune subsets. This technique allows for detection of up to 7 cell surface markers on the same tissue section. This is unlike traditional chromogenic IHC where only one cell surface marker can be interrogated per section, requiring multiple sections to be used, or immunofluorescence (IF) that can be limited to fewer surface markers.

The advantage of opal is evaluation of multiple markers on the one cell, especially defining immune cells that require multiple surface markers. In this opal panel DAPI was used to stain and define all nucleated cells. Cytotoxic T-cells were defined using an antibody for CD8+ and T-helper cells were identified using an antibody for CD4+. T-regulatory cells were noted as CD4+ Foxp3+ nuclear stain. Antibodies targeting PD-1 on immune cells and PD-L1 on tumour/other cells were also included. Tumour cells were defined as DAPI+ and AE1/AE3+, a cytokeratin marker used in the pathological diagnosis of CRC. Tumour and stromal areas were defined using a classifier system in HALO (PerkinElmer) software; detailing the DAPI+AE1AE3+ tumour cells are tumour and normal surrounding liver.

When assessing the immune infiltrate in CRLM tumours using opal, there were no statistical differences observed between tumour and stromal infiltrate, as seen in **Figure 4.25**. This is different to the data generated using flow cytometry at the single cell level, where distinctions were observed. However, the advantage of using the opal technique details spatial location of immune cells to the tumour cells. Overall, the CD8+ T-cell cell infiltrate is low (<150 cells/$mm^2$) compared to published data by Galon *et al* where recurrent CRC patients had 150-250 cells/ $mm^2$ and non-recurrent patients 250-350 cells/ $mm^2$ (Galon *et al*., 2006).

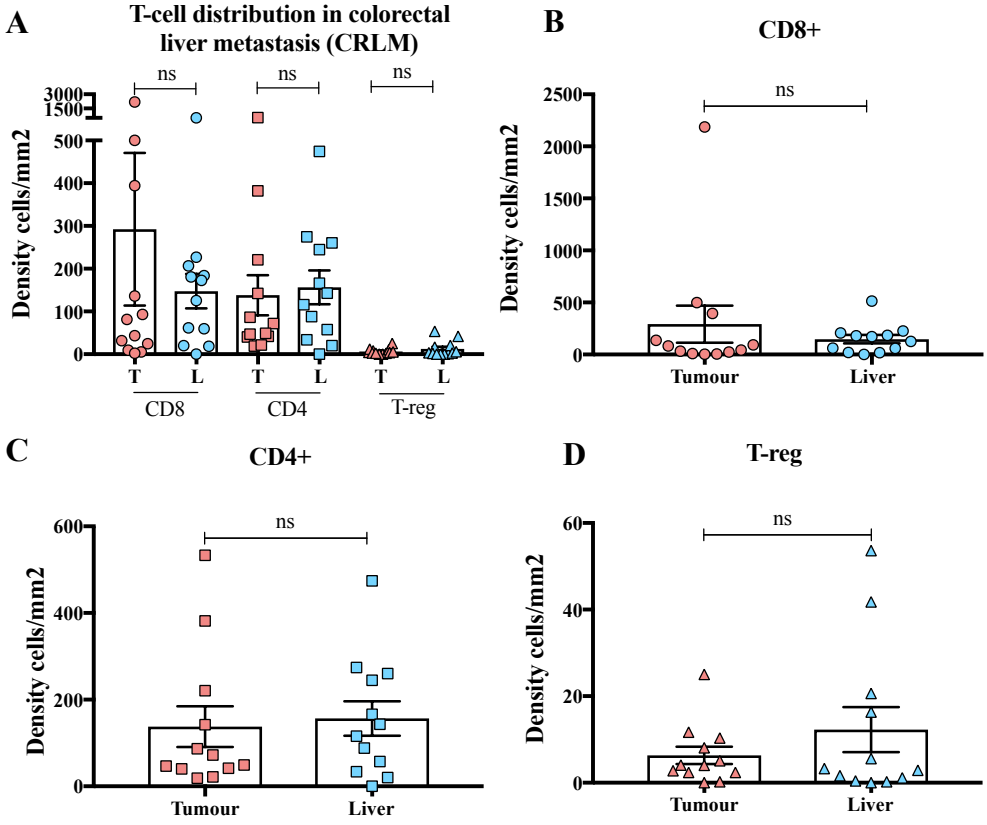


**Figure 4.25. Immune cell infiltrate in CRLM quantified using mIHC analysis does not show differences between tumour and stromal infiltrate.** Immune cells were identified using mIHC detailing CD8+, CD4+ and T-regulatory cells in the tumour and stromal regions of the tissue, quantified as cell count/mm$^2$. (**A**) Bar plots of all sub populations showing CD8+, CD4+ and T-reg populations in the tumour (red symbols) and surrounding liver (blue symbols). Individual bar plots of (**B**) CD8+ (**C**) CD4+ and (**D**) T-regulatory cell distribution in the tumour and surrounding liver per mm$^2$. Mean +/- SEM, n=12, paired Wilcoxon t-test.

To compare the differences observed between FACS and opal CD4:8 ratios were calculated from the T-cell frequencies of each method. As seen in Figure 4.26 there is not a significant difference when using either method with the exception of one outlier. Both methods provide complementary information; FACS provides single-cell protein expression of phenotypic markers and opal documents the spatial location of the immune cells in the context of tumour cells.

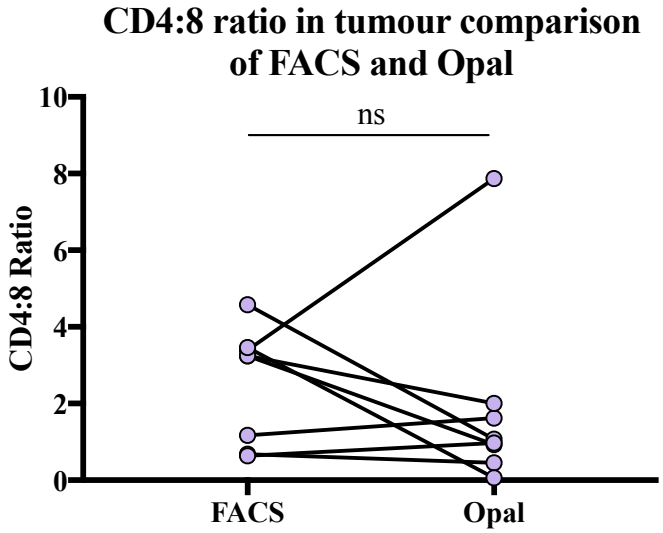


**Figure 4.26. CD4:8 ratio is similar when comparing TILs using FACS vs. Opal.** CD4:CD8 ratios were compared from FACS and opal analysis by dividing CD4+/CD8+ frequencies. n=8, paired two-tailed Wilcoxon test.

Expression of PD-1 on CD8+, CD4+ and T-reg cells was assessed, and no differences were observed between those immune cells in the tumour vs. liver (**Fig. 4.27)**. However there were more CD4+ T-cells expressing PD-1 than CD8+ and T-reg cells. There were some outlier tumours that had high expression of PD-1 on the immune cells, which could imply an immune suppressive TME.

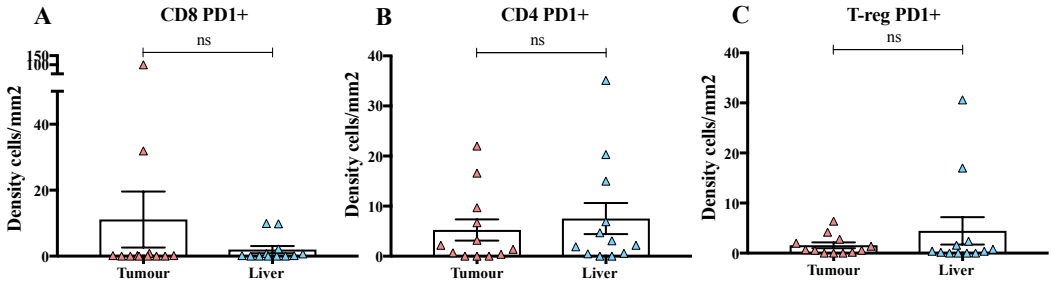


**Figure 4.27. No differential expression of PD-1 on immune cells from the tumour vs. stroma observed using multispectral analysis.** Immune cells were identified using multispectral IHC detailing CD8+, CD4+ and T-regulatory cells in the tumour and surrounding liver regions of the tissue, quantified as cell count/mm$^2$. Bar plots of PD-1 expression on (**A**) CD8+ (**B**) CD4+ and (**C**) T-regulatory cells in the tumour (red symbols) and stroma (blue symbols) of CRLM tumours per mm$^2$. Mean +/- SEM, n=12, paired Wilcoxon t-test.

One other advantage of using mIHC is the spatial location of immune cells relative to tumour cells that can be assessed. As seen in **Figure 4.28A**, CD8+ T-cells have a proximal distance of

117 µm to the tumour. It was observed that smaller micrometastases were surrounded by immune cells as seen in **Figure 4.28B**.

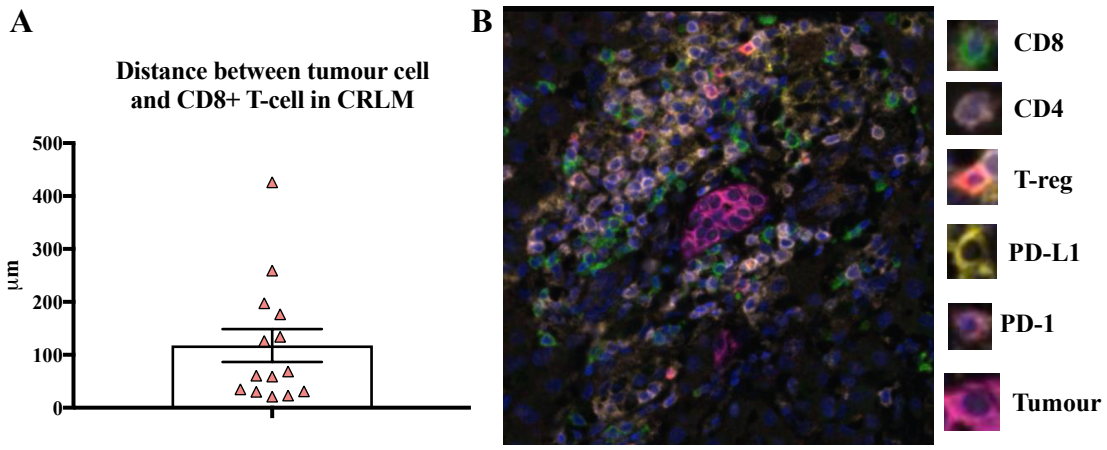


**Figure 4.28. CD8+ cell proximity to tumour cells is on average within 100 µm. (A)** Bar plot showing distance between tumour cells and CD8+ cytotoxic cells (µm), error bar represent SEM, n=14. (**B**) Representative image of tumour cells (magenta) surrounded by immune cells of different subtypes.

Unlike the micrometastases that were engulfed by immune cells, immune cell exclusion was observed in large areas of tumour. It can be seen in these large areas of tumour that the immune cells reside in the surrounding liver tissue, with a reduced frequency within the tumour cells. This implies that the TME is suppressing immune cell infiltration, and is therefore able to evade the immune response. It is particularly important to highlight the volume of tumour, which suggests that when a tumour increases in size, the immune response is unable to maintain control and tumour surpasses the ability of the immune response.

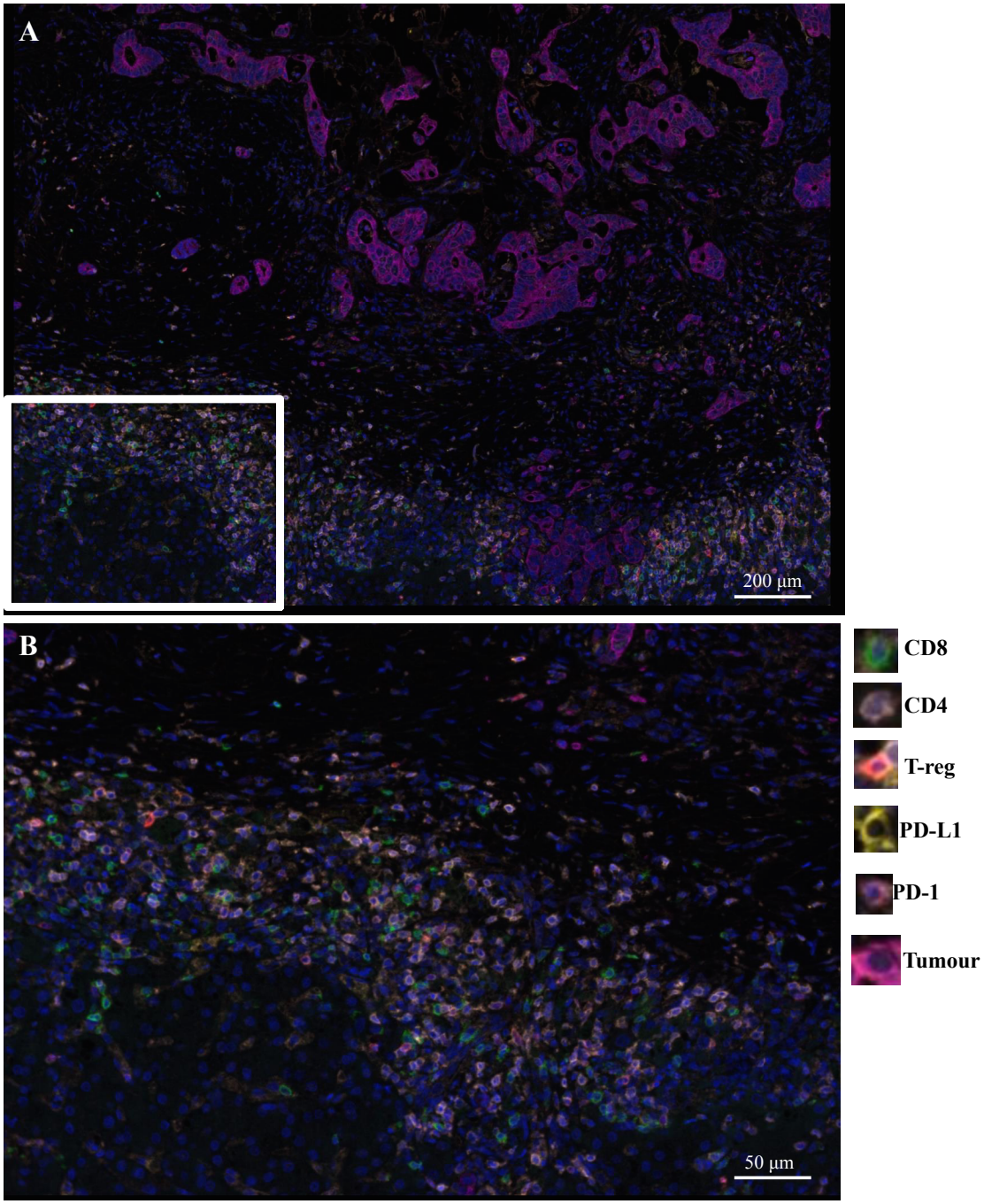


**Figure 4.29. Immune cell exclusion in the tumour of CRLM.** mIHC staining documenting immune cell exclusion including CD8+ T-cells within the tumour of CRLM at (**A**) 200 µm and (**B**) 50 µm.

## 4.8 Discussion

From the findings in **Chapter 3**, it is clear that the immune response at the primary site in mCRC patients has failed. Through failure of an effective immune response, the tumour has the ability to progress to metastatic sites. This is ultimately what causes death from the disease. To understand the immune response at the distant metastatic site, in this chapter, I sought out to assess the tumours from patients with CRLM. The initial design of this study was to compare the immune response in the primary tumour to the metastatic site in patients with synchronous disease. Unfortunately, due to limited patient numbers of synchronous presentation of disease, I was unable to undertake this. Instead, I assessed the immune response in CRLM tumours that presented following treatment of the primary tumour.

Compared to earlier stages of CRC (I-III), in metastatic stage IV CRC, TIL presence does not appear to improve survival. The disease progression at this stage is advanced and the impact of the immune response is limited. Evaluation of immune cell presence alone is not enough, and more in-depth assessment of TIL function should be considered.

In this chapter, I employed flow cytometry to assess immune cell frequency and phenotype in CRLM tumours. It was found that CRLM tumours had a reduced cytotoxic environment, with reduced NK, NKT cells and CD8+ T-cell infiltrate. Conversely, these tumours had an increased CD4+ frequency and determining if these CD4+ T-cells are Th1, Th2 or Th17 warrants further investigation. This would indicate whether the CD4+ immune cells promote or inhibit tumour progression in the TME. Fifteen per cent of this CD4+ T-cell population were T-regulatory cells, which is increased in the tumour compared to the liver. Thus it can be concluded the TME in CRLM tumours is more suppressed, with a reduced cytotoxic ability.

But does this reduction in cytotoxic T-cell frequency, described above, also equate to a reduced cytotoxic function? The *in situ* phenotype data suggest that CD8+ T-cells in the tumour have reduced cytotoxic function as measured by expression of degranulation marker CD107a. Additionally the CD8+ T-cells in the tumour have higher expression of PD-1 compared to distal normal liver and peripheral blood and this is the first indication that these cells may be exhausted. In order to determine their effector function, the cytotoxic assay developed in this chapter was used to assess TIL function in CRLM tumours, *ex vivo*.

TILs were expanded *ex vivo* from CRLM tumours and this was done in the presence of IL-2 and tumour pieces. Throughout this project there were a number of patient samples where the TILs failed to expand. Although not experimentally controlled, this observation provided some

insight, as it implies TILs from those samples have an inability to proliferate, even when provided with exogenous potent stimulation of IL-2. Proliferative non-responsiveness is a hallmark associated with exhaustion (Mueller *et al*., 1989). Other hallmarks of exhaustion include transcriptional reprogramming, expression of markers including PD-1, CTLA-4, Lymphocyte activation gene-3 (LAG-3) and T-cell immunoglobulin and mucin-domain containing-3 (TIM-3), altered metabolism and failure to produce Th1 secreted cytokines (Pauken & Wherry, 2015). It may be possible that due to heterogeneity of tumours, some tumour pieces may not have had any TIL and subsequent expansion did not occur. There were some patient samples where no TILs expanded, despite plating multiple tumour pieces. This observation highlights an inability of the TILs to proliferate and could be indicate dysfunction.

On the other hand, this expansion protocol also highlights the potential of immune function *ex vivo*. When one considers tumour growth *in vivo*, the ability of immune cells to function and control it is based on tumour volume and tumour-mediated immune inhibition. The ability of tumour cells to suppress TIL function can be through checkpoint mechanisms and soluble factors in the TME. Those TILs that did expand, in the absence of tumour growth and inhibition, *in vitro,* demonstrated that the immune cells are no longer suppressed. This is what is observed in those tumours where TIL expansion did occur, and highlights that some aspects of immune cell function is contextual.

Direct cytotoxic TIL function was then tested utilising the cytotoxic assay developed in this chapter. In all 4 CRLM patients assessed, the TILs were able to kill autologous tumouroids. However, it seems apparent that in the patient, these TILs were not able to control tumour growth *in situ*. This suggests that immune cells are likely to be inhibited in the immunosuppressive TME *in vivo*. Unlike the co-culture system *in vitro*, where tumour: immune cell ratio is accounted for, the tumour burden in the patient may be large. Therefore the shear volume of tumour is unable to be controlled by the TILs, and this contest is reversed *in vitro*. Additionally, the co-culture system does not have arterial or venous blood flow, thus trafficking immune cells that may play a role *in vivo* were not assessed here.

When assessing CBI using the co-culture assay none of the four patients tested demonstrated response to anti-PD-1. This was not altered by expression of PD-1 on the expanded TILs, with low-expressing PD-1 cells having a similar killing capacity as moderate PD-1 expressing cells. Clinically, only CRC patients who respond to CBI are those with microsatellite unstable tumours. The patients included in this cohort all had microsatellite stable tumours, and this may be explain why these TILs are unable to be therapeutically reinvigorated. Importantly, the

majority of CRC patients are MSS and thus do not respond to CBI and identifying why this is the case is really crucial to improving therapies. Only 4 patients with CRLM were assessed using the co-culture assay in this study, and increasing the sample size will be essential if we are to observe variations in response to CBI in rare patients.

In addition to live-cell imaging, TIL function was evaluated by measuring cytokine secretion in the supernatant of the co-culture. When tumouroid and TIL were cultured together there was minimal production of IFNγ and TNFα, however this was enhanced with addition of anti-PD-1. These data indicate that despite anti-PD-1 not affecting direct cytotoxic killing, it was able to induce TILs to secrete cytokine. Induction of Th1 cytokines can affect the TME by recruiting and activating more cytotoxic T-cells, improving tumour control but also increase PD-L1 expression on tumour cells (Barber *et al*., 2006).

The importance of these observations is that despite being MSS, the TILs from these patients have the capacity to function *ex vivo*. This probably reflects the ability of the tumour to suppress immune responses *in vivo*. Assessment of TIL function utilising the assay may provide another dimension to understand the dynamic biology of T-cells from solid tumours and how we can therapeutically enhance their function. Our assay has a clinical potential to study dynamic interactions between TIL and patient-derived tumouroids. This assay also has the capacity to test CBI in patient-derived material. In a different use, our assay has recently been used to test the efficacy of drugs in combination with chimeric antigen receptor (CAR) T-cells against patient derived tumours (Michie *et al*., 2019). Therefore, the application of the assay both clinically and scientifically can provide insight and be utilised as a platform to test therapeutics targeting immune responses. The tumours from MSS CRLM patients appear to have a reduced cytotoxic and enhanced suppressive phenotype. It is evident that patients with MSS tumours do not respond to current CBI. Thus, therapeutically, there should be a continued focus on altering the balance in the immune infiltrate to a more cytotoxic and reduced suppressive state.

# 5 MUCOSAL ASSOCIATED INVARIANT T-CELLS IN COLORECTAL LIVER METASTASIS (CRLM)

## 5.1 Introduction

In **Chapter 3** my results showed that TIL abundance is no longer predictive in primary CRC in patients with synchronous metastases. However, the presence of an immune infiltrate in colorectal tumours has been strongly associated with prognosis in earlier stages of disease (Pages *et al*., 2005). Our group and others have found that conventional CD8+ T-cells are the most significant population to correlate with prognosis in primary CRC tumours (Galon *et al*., 2006; Millen *et al*., 2016; Pages *et al*., 2009). The question then arises about the status of TILs in mCRC.

The most common site of metastatic spread in CRC is the liver (CRLM) (Nordlinger *et al*., 2013). The liver is an important organ for processing nutrients and clearing toxins and acts as an immunological organ, harbouring a high frequency and variety of immune cells (Racanelli & Rehermann, 2006). This is due to the continuous arterial and venous blood supply, 80% of which is delivered via the portal vein (Sheth & Bankey, 2001). This vein drains from the gut, bringing nutrients and pathogen-derived molecules directly to the liver. Due to the constant supply of antigen trafficking through the liver, the immune response balances immunity with tolerance (Racanelli & Rehermann, 2006). Both high blood flow and intrahepatic immune tolerance may underpin why CRC disseminates within the liver. Investigating the immune response in the setting of CRLM is therefore important to understand the steps involved in the progression of metastasis to this organ. Hence, the liver being a unique immunological site and the preference of CRC to disseminate indicates we need to explore this context in further detail.

The immune response in tumours is comprised of both innate and adaptive immune cells, the latter being extensively studied in the context of primary CRC (Galon *et al*., 2013; Naito *et al*., 1998; Ropponen *et al*., 1997). A novel cell type that bridges the innate and adaptive immune system are mucosal-associated invariant T-cells (MAIT cells), which have been recently defined as a subset of unconventional T-cells. The physiological and pathological roles of MAIT cells are still being elucidated. However, it is known that bacteria and some yeast activate MAIT cells via the MAIT cell TCR-MR1 axis (Gold *et al*., 2010; Le Bourhis *et al*., 2010). This TCR is restricted by the highly conserved molecule MR1 that captures a novel class of antigens that are released into the extracellular environment or can be found in the lumen of phagosomal compartments following microbe engulfment (McWilliam *et al*., 2016). This unique class of ligands belong to vitamin B antigens, and MAIT cell activation depends on recognition of the ligands bound to MR1. In this context, it is thought that MAIT cells play a protective role in

controlling bacterial infections, as the known ligand to activate MAIT cells is 5-OP-RU, a by-product of microbial riboflavin synthesis (Le Bourhis *et al*., 2013). Viruses including dengue, hepatitis C and influenza are also known to activate MAIT cells in a TCR-independent mechanism via cytokines including IL-12 and IL-18 (Loh *et al*., 2016; van Wilgenburg *et al*., 2016). During viral infections it has been found that peripheral MAIT cell frequencies are depleted, and this may increase host susceptibility to opportunistic bacterial infections, providing more evidence that MAIT cells play a protective role in this context (Ussher, Willberg, & Klenerman, 2018).

As MAIT cells reside within the mucosal tissue, it is thought that they may play an important role in patrolling the epithelial barrier interface. When the epithelial barrier is damaged, immune homeostasis is disrupted, with a high chance of microbial and resident lymphocyte interactions, possibly including MAIT cells. This has been highlighted in inflammatory bowel diseases (IBD), such as Crohn's disease (ChD) where high MAIT cell accumulation was detected in damaged ileum tissue compared to normal healthy tissue (Serriari *et al*., 2014).

Because MAIT cells reside in mucosal tissues, and play a role in IBD, there has been a particular interest to determine their role in CRC. When colorectal tumours develop, disruption to the epithelial barrier occurs, creating inflammation (Grivennikov *et al*., 2012; Peterson & Artis, 2014). As highlighted in **Chapter 1**, MAIT cells have been detected in colorectal tumours with reduced production of IFNγ (Sundstrom *et al*., 2015). The same observation was found in CRLM, with reduced MAIT cells in the tumour that were functionally impaired and unable to produce IFNγ. The conclusion from these studies was that MAIT cell effector function was suppressed in the TME. Additionally across all studies of patients with CRC MAIT cell frequency was not affected by chemotherapy, implying that MAIT cells are chemotherapy resistant (Shaler, Tun-Abraham, *et al*., 2017).

As well as being chemotherapy resistant (Dusseaux *et al*., 2011; Novak, Dobrovolny, Brozova, Novakova, & Kozak, 2016), the majority of MAIT cells have been reported as CD8+ (Gherardin, Souter, *et al*., 2018). We know from other studies that conventional CD8+ TILs in the primary and metastatic tumours of CRC patients correlate with a better OS (Kwak *et al*., 2016; Shibutani *et al*., 2018). As MAIT cells commonly express the CD8α receptor, it is very likely that MAIT cells are erroneously included in the quantification of CD8+ TILs. Therefore there is a sub population of CD8+ cells that has not been accounted for previously and this population warrants further investigation. As previously mentioned, MAIT cells in the primary tumour have been associated with a less favourable clinical outcome. Since MAIT cells are abundant in normal liver tissue I decided to investigate their role in CRLM, and when I

embarked on this study there were no publications addressing this matter.

In the current study, I investigated the presence and phenotype of MAIT cells within human CRLM, surrounding normal liver and peripheral blood. Using the patient-derived tumouroid model previously described, I investigated the function of MAIT cells in the setting of tumour immunity. I also explored the response of MAIT cells to CBI, to evaluate the therapeutic attributes and utility of these therapies in the context of mCRC.

**Hypothesis:**

MAIT cells are present within CRLM tumours due to their abundance in the liver**.**

**Aims:**

1. Investigate the functional capacity of MAIT cells in the context of colorectal cancer.
2. Determine the presence and abundance of MAIT cells in CRLM.

## 5.2 Patient Characteristics

To enrol patients to this study, I wrote the human ethics application and recruited patients with CRLM. Patients with CRLM were provided with informed consent and recruited to the study. On the day of the surgical operation, blood was drawn from the patients pre-incision for collection of PBMCs). After the specimen had been surgically removed from the patient, tumour and healthy liver pieces were dissected in theatre, or by a registered pathologist (to ensure that the surgical margins were not compromised). The tissue was then placed in ice-cold media and transferred to the laboratory for immediate processing. The patient characteristics are listed in **Chapter 2.**

## 5.3 MAIT Cells in the Context of Colorectal Cancer

To first determine if primary and metastatic tumours of CRC origin have the ability to express MR1, RNAseq was performed on tumour samples from CRLM patients. As seen in **Figure 5.1** MR1 expression was detectable in all samples tested, however expression was found to be heterogeneous across both primary and metastatic tumours. What these data demonstrate is the potential ability of tumours to express MR1, which may indicate a role of MAIT cell presence in these tumours.

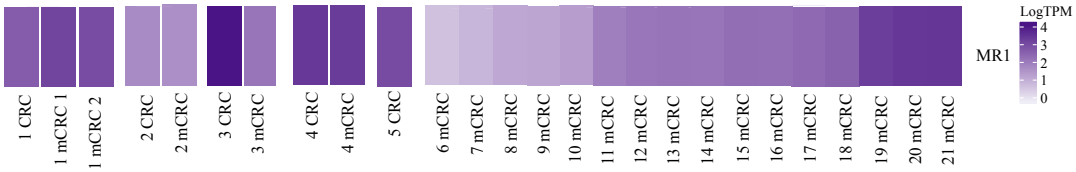


**Figure 5.1. MR1 expression in tumour tissue is heterogeneous in both primary and metastatic CRC.** RNA was isolated from primary (CRC) (CT) and metastatic (CRLM) (LT) tumours and sequenced using RNAseq. Samples are clustered based on location of tumour with shades of purple indicating the LogTPM expression change.

Due to MAIT cell abundance in the liver, MAIT cell presence in CRLM tumours was interrogated. The majority of MAIT cells are CD8+, suggesting that when conventional CD8+ T-cells are scored (e.g. for the Immunoscore™) it is highly likely that MAIT cells are included in this count. To address this question, using flow cytometry, I quantified MAIT cells as a proportion of the CD8+ population in the tumour and liver. As can be seen in **Figure 5.2** MAIT cells in the tumour comprise of ~20% of total CD8+ T-cells in the tumour and ~45% in the liver. This demonstrates that it is very likely that by scoring CD8+ T-cells, a substantial proportion of MAIT cells are included.

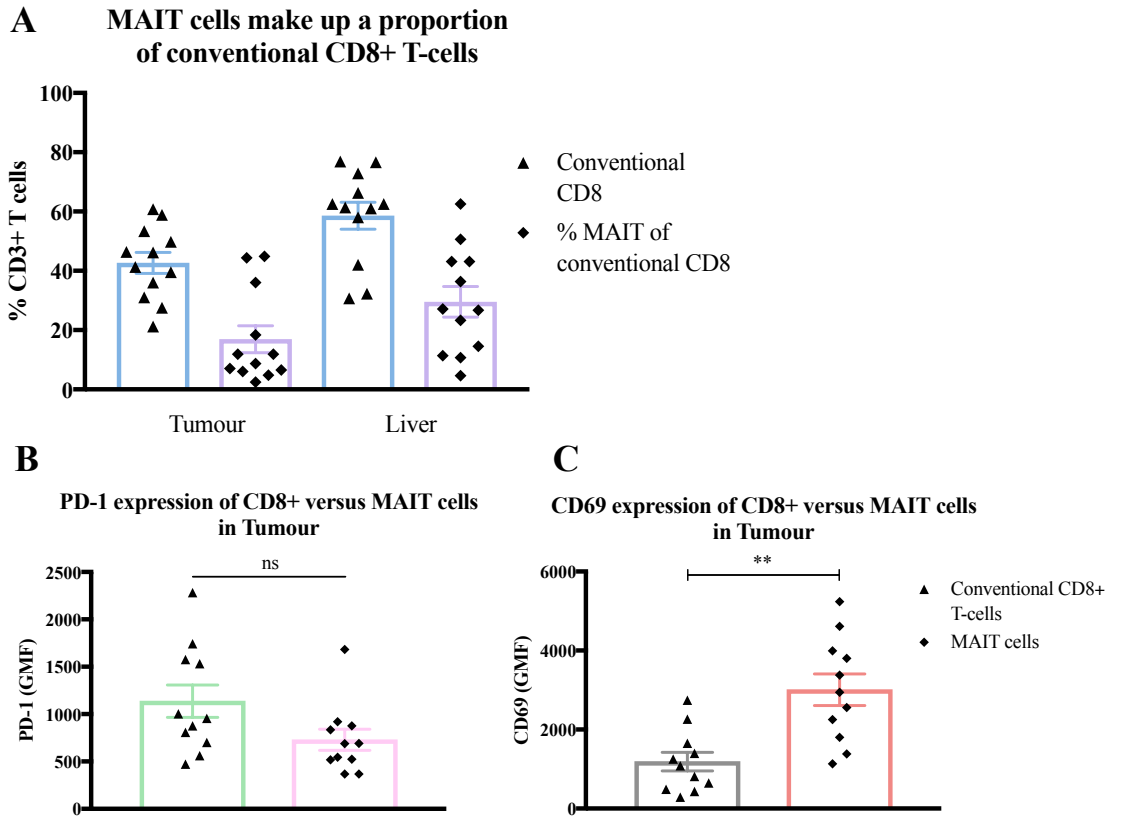


**Figure 5.2. MAIT cells account for a high proportion of CD8+ T-cells and show similar expression of PD-1. T-cells form the tumour and liver were quantitated using flow cytometry.** (**A**) Bar-graphs represent total CD8+ T-cells (blue) as proportion of CD3+ T-cells, MAIT cells (purple) shown as a proportion of CD8+ T-cells (**B**) Bar-graphs showing quantitation of PD-1 and (**C**) CD69 expression on only CD8+ T-cells and MAIT cells in the tumour, represented as GMF. Each data point represent individual patients samples, error bars represent SEM, n=11 CRLM patients, non-parametric One-Way ANOVA Friedman test, **p<0.0021.

To determine if MAIT cells are phenotypically different to conventional CD8+ T-cells, I compared expression of PD-1 and CD69. As seen in **Figure 5.2**, no significant difference is observed between PD-1 expression on MAIT cells and total CD8+ T-cells in the tumour. However, when assessing CD69 expression on conventional CD8+ T-cells and MAIT cells in the tumour, it can be seen that MAIT cells express significantly more CD69 compared to conventional CD8+ T-cells.

### 5.4 Detection of MAIT Cell Frequency Using Flow Cytometry

To determine the frequency of MAIT cells within CRLM patient samples, a flow-cytometry panel for MAIT cell detection was developed. This was initially optimised on healthy control PBMCs based on the gating strategy proposed by Sundström *et al* who detected MAIT cells in

primary CRC tumours (Sundstrom *et al*., 2015). Using this gating strategy MAIT cells were defined by excluding doublet cells, including viable, CD45+CD3+ T-cells with Vα7-2+ TCR expression and high expression of CD161. Included in this panel were CD8α+ and CD4+ markers, to define different subsets of MAIT cell populations. This panel was initially optimised and acquired on the BD FACSCanto™ and then subsequently acquired on the BD Fortessa™ as depicted in **Figure 5.3**.

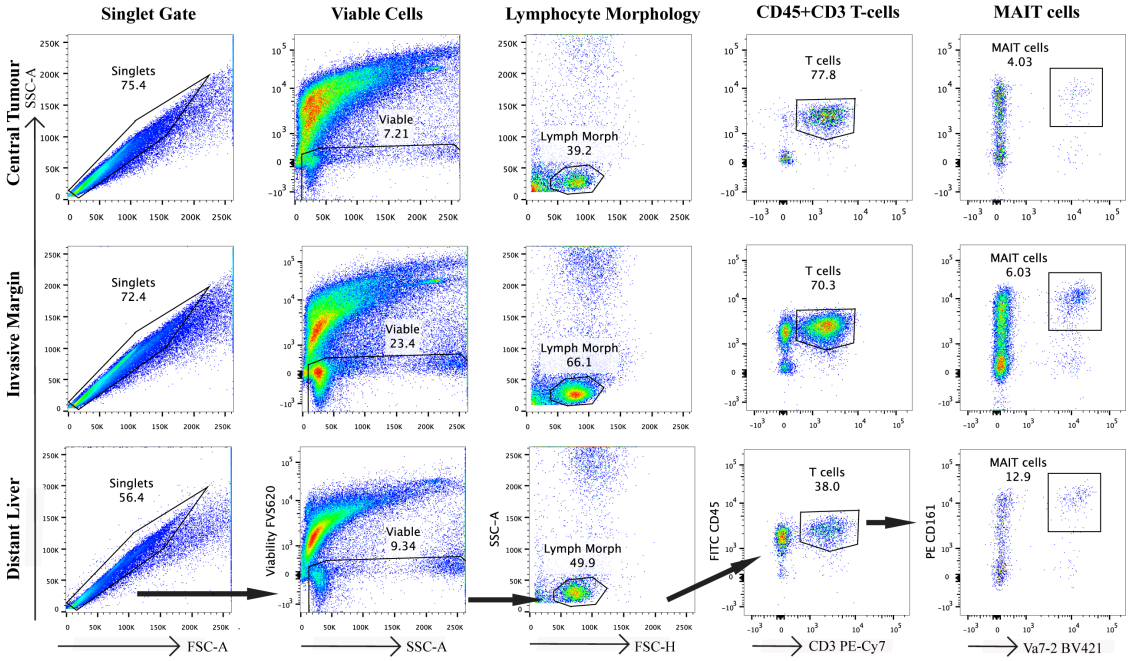


**Figure 5.3. Gating strategy used to define MAIT cells in different tissue regions. Single cell lymphocyte preparations from CT, IM and DL were acquired on a BD Fortessa™.** All events are gated on singlets to exclude doublet populations, viable cells using the cell fixable viability stain (FVS) 620, and lymphocyte morphology based on SSC-A v FSC-H, CD45+CD3+ double positive T-cells and co-expression of CD161 and Vα7-2 to define MAIT cells.

Following establishment of the MAIT cell flow cytometry panel, the first 13 patients were screened for MAIT cells within tumour tissue, liver tissue and PBMCs. After collection, tumour specimens were initially divided macroscopically into CT and IM sections and compared to distant liver (DL). This approach was designed based on the work of Galon *et al* documenting differential infiltration of TILs, in FFPE sections, at the CT and the IM (Galon *et al*., 2006). At the time, it was unknown if MAIT cells had the ability to infiltrate CRLM tumours, a question I considered required addressing.

However, due to the steep learning process of tissue processing, lack of tissue and low cell numbers, only 5/13 patients had paired datasets with both CT and IM analysed. Flow cytometric analysis was completed only on samples that had >1000 T-cells to increase statistical confidence.

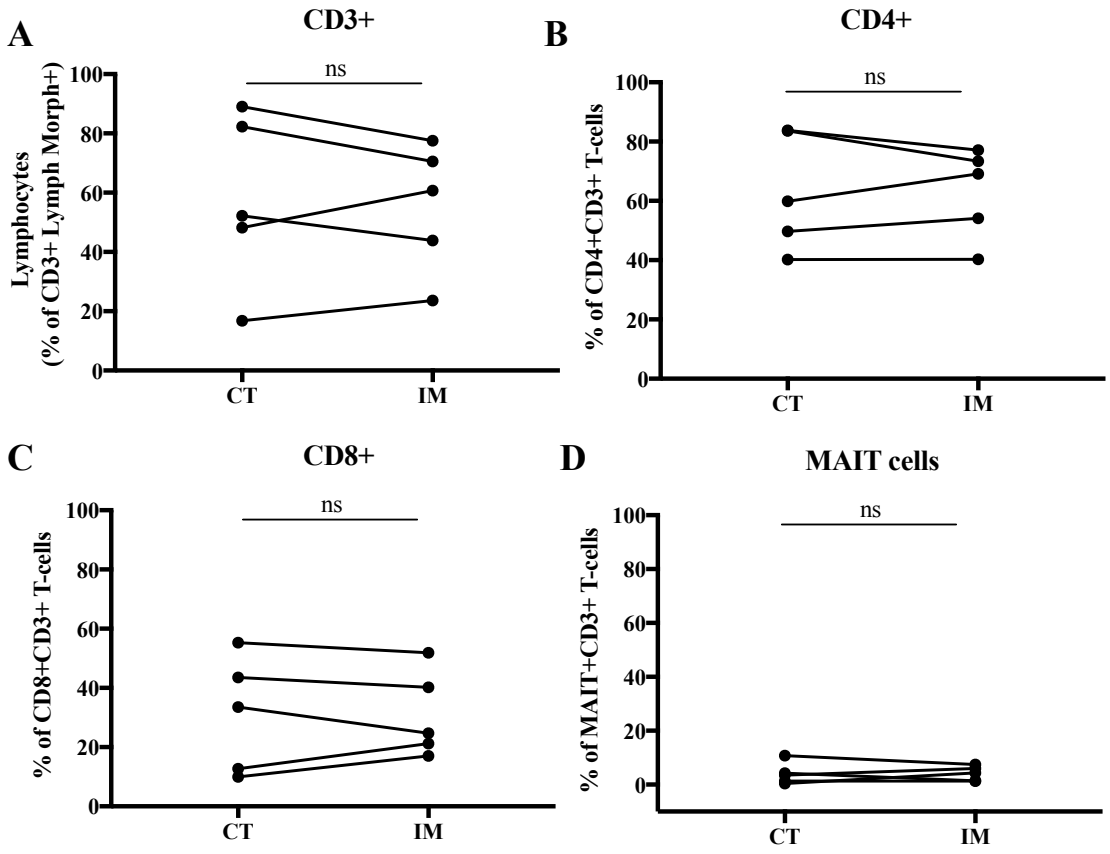


**Figure 5.4. No difference in degree of T-cell infiltration between the CT and IM regions in patients with CRLM.** Percentage of infiltrating T-cells was assessed in the CT and IM of patients with colorectal liver metastasis by flow cytometry. (**A**) CD3+ T-cells were assessed as a percentage of viable lymphocytes (**B**) CD4+ (**C**) CD8+ T-cells and (**D**) MAIT ($CD161^{high}V\alpha7.2+$) cells were assessed as a percentage of CD45+CD3+ T-cells. Each point represents an individual patient, n=5, paired Wilcoxon t-test, $p<0.05$.

When comparing T-cell infiltration in the tumour, there were no statistical differences between CT and IM, as seen in **Figure 5.4 A-D**. Therefore, all subsequent samples were only assessed comparing tumour and normal liver.

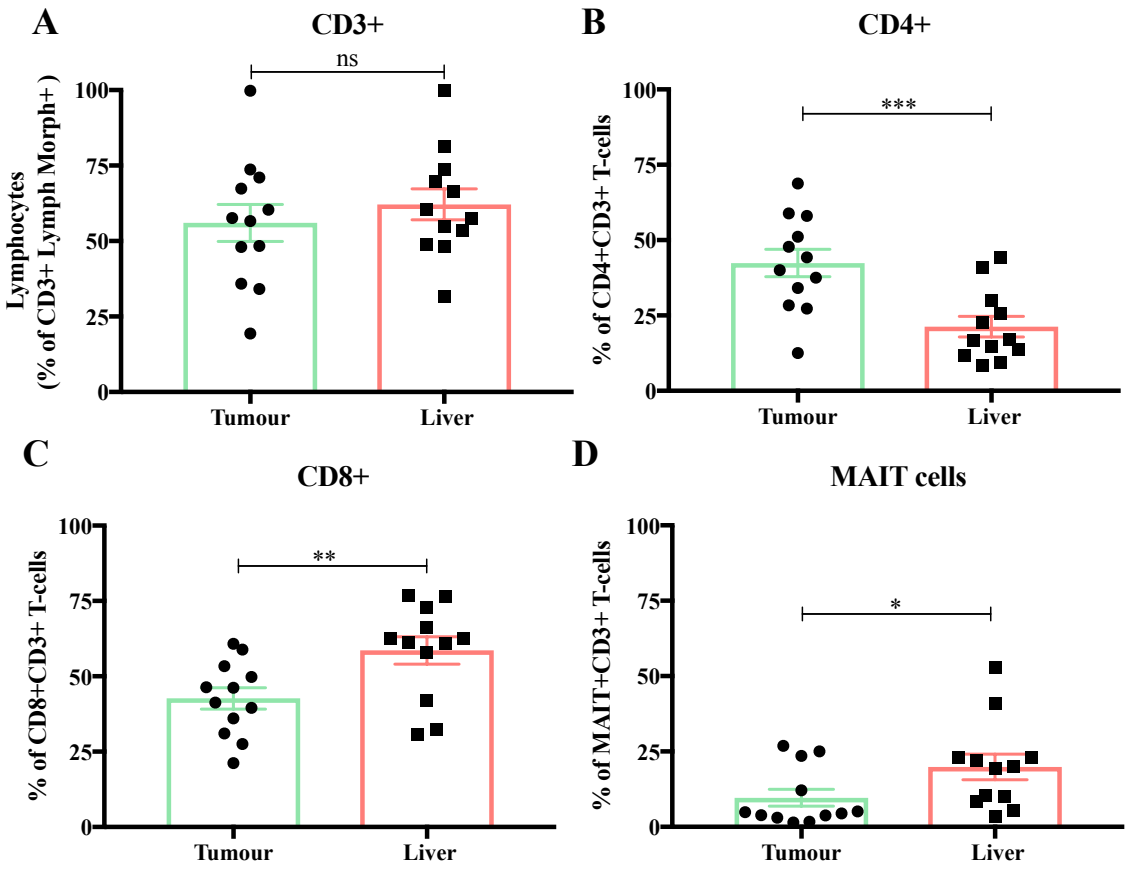


**Figure 5.5. Colorectal-liver tumours have increased T-helper (Th) and reduced cytotoxic lymphocytes including MAIT cells.** Lymphocytes from patients with CRLM were isolated from the tumour and liver as paired samples and analysed by flow cytometry. (**A**) CD3+ T-cells were assessed as a percentage of viable lymphocytes (**B**) CD4+ (**C**) CD8+ T-cells and (**D**) MAIT ($CD161^{high}V\alpha7.2+$) cells. Each point represents an individual patient as a paired samples, n=12 CRLM patients, error bars represent SEM, Wilcoxon paired t-test, (*p<0.01, **p<0.001, ***p<0.0001.

When using this approach to assess T-cell infiltrate, there was an increase of Th-CD4+ T-cells in the tumour compared to liver (mean 42.3% vs. 21.3%) (Fig. 5.5 B). The opposite is observed when quantifying cytotoxic CD8+ T-cells in the tumour compared to liver (mean 42.6% vs. 58.5%) (Fig. 5.5 C). When quantifying MAIT cells, a decrease is observed in the tumour compared to the liver tissue (mean 9.6% vs. 19.8%) (Fig. 5.5 D). These data highlight a reduction of cytotoxic immune cells within the tumour tissue compared to the surrounding liver tissue.

MAIT cell presence was then assessed in all patient samples, as seen in **Figure 5.6**. There was a significant reduction of MAIT cells in the tumour compared to the liver. It can be seen that the majority of samples have fewer MAIT cell infiltrate in the tumour (mean: 9.4%, lower 95% CI: 4.6, upper 95% CI: 14.3) than the liver tissue (mean: 20.3, lower 95% CI: 11.9, upper 95% CI: 28.7), with a wider spread. Interestingly, there are still some cases with a high percentage of MAIT cells infiltrating the tumour. Representative flow cytometry plots show the differences between a patient with low (**Fig. 5.6B**) and high (**Fig. 5.6C**) MAIT cell infiltration across both tumour and liver.

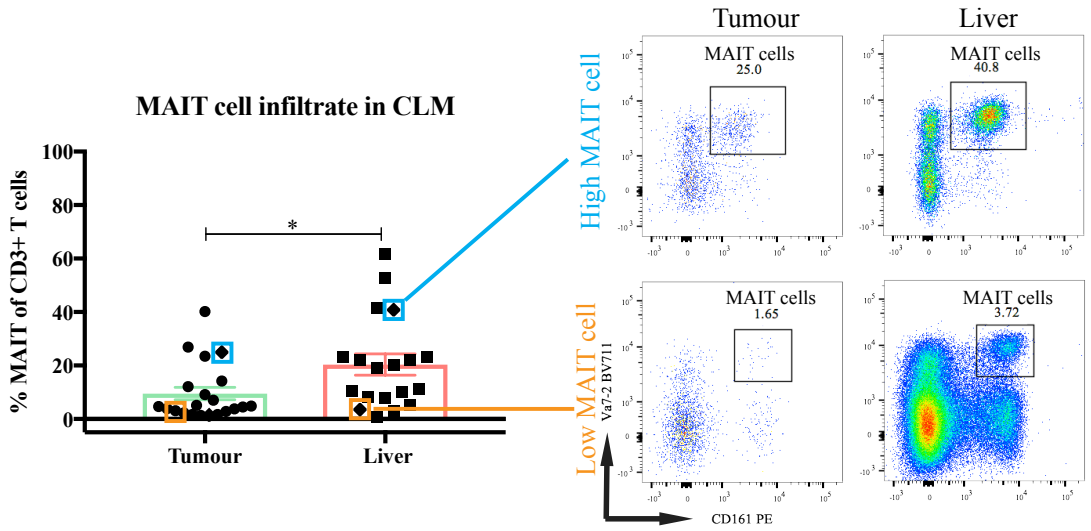


**Figure 5.6. MAIT cell infiltration in the tumour is generally reduced, but is individually heterogeneous.** All CRLM samples were combined (**A**) MAIT cell infiltration was significantly reduced in the tumour compared to the liver (*p<0.05). Representative flow cytometry plots of (**B**) a patient with low MAIT cell infiltrate (**C**) and high MAIT cell infiltrate in the tumour and liver. Each data point represents individual patient, n=24 CRLM patients, error bars are SEM, unpaired Mann-Whitney t-test, and p <0.05.

When this project started in October 2015, the widely accepted detection method for MAIT cells was the use of the surrogate markers: Vα7-2+, CD161$^{high}$ or IL-18Rα+. An MHC tetramer acts as a ligand to detect specific TCR and this is conjugated to a fluorophore to detect specific T-cell populations in lymphocyte samples. Therefore, the 5-OP-RU tetramer specific for the MAIT cell TCR was developed at the Peter Doherty Institute in Parkville, Melbourne (Reantragoon *et al.*, 2013). However, this was an in-house tetramer and was not publically available. Towards the end of 2016, the tetramer became publically available through the NIH tetramer facility in the United States of America. I obtained this reagent and incorporated it into the flow cytometry panel. There were some issues with staining using the tetramer, where flow

cytometry plots displayed a "smeared" appearance (**Fig. 5.7**) and had a less defined population compared to the surrogate marker detection Vα7-2+CD161$^{high}$. When comparing the detection methods in five samples, there were no differences observed. To ensure consistency across the cohort, I decided to continue detecting MAIT cells using the Vα7-2+CD161$^{high}$ method.

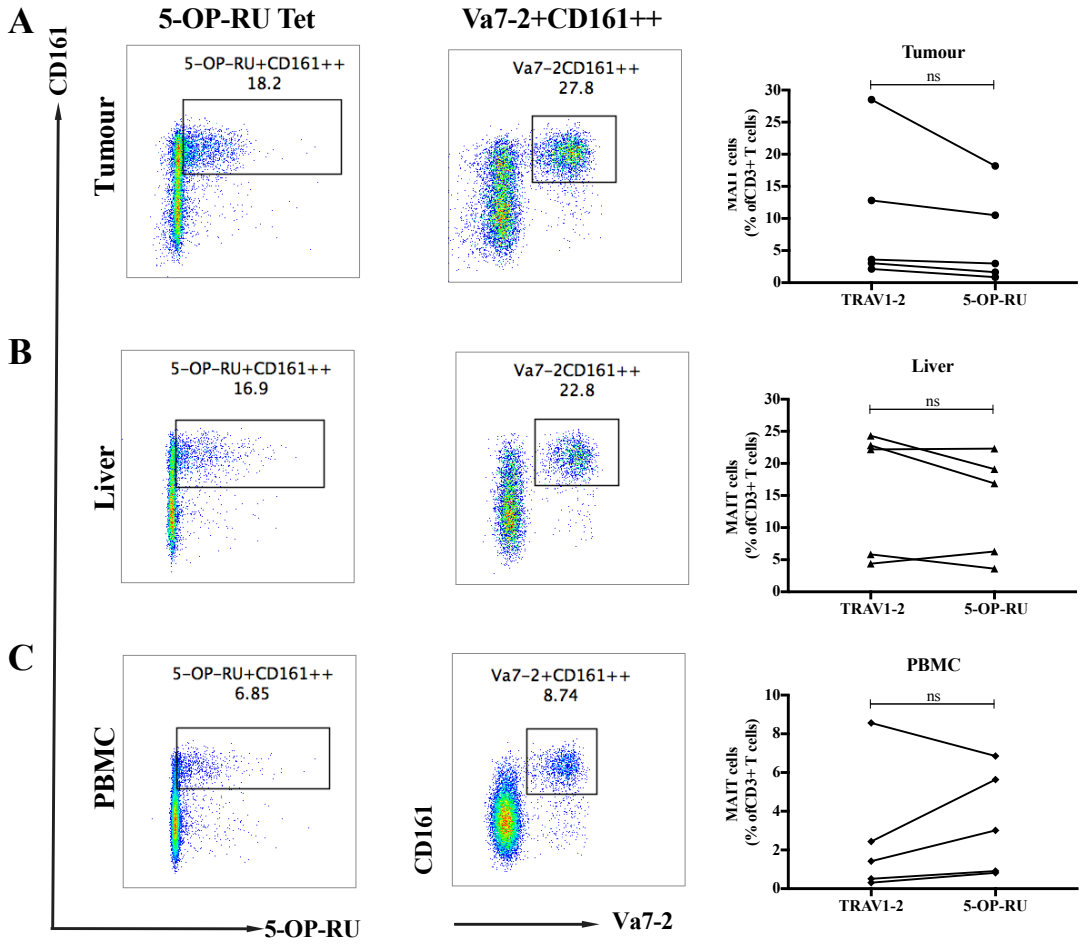


**Figure 5.7. Comparison of MAIT cell frequencies using surrogate markers and the 5-OP-RU tetramer.** Representative flow cytometry plots and quantitation of MAIT cell detection from (**A**) tumour, (**B**) liver and (**C**) PBMC. Two detection methods were directly compared: specific 5-OP-RU tetramer staining or surrogate marker detection Vα7-2+CD161$^{high}$. Each data point represent individual patients samples, n=5 CRLM patients, paired Wilcoxon t-test, $p<0.05$.

It is known that MAIT cells in the peripheral blood range from 1-10% of all T-cells in healthy donors, and a reduced frequency has been reported in patients with CRC (Gherardin, Loh, *et al.*, 2018; Ling *et al.*, 2016). In my quantitation of MAIT cells in the periphery of CRLM patients, I found no significant difference when compared to healthy donors (**Fig. 5.8C**). The range of MAIT cells in the periphery of CRLM patients was 0.1-7.5% of CD3+ T-cells compared to 0.1-

15.4% of healthy donor PBMCs. No statistical difference was observed when quantifying conventional CD8+ T-cells (**Fig. 5.8B**). However, there was a significant difference when assessing CD4+ T-cell frequencies (**Fig 5.8A**). This is a similar observation with a higher frequency of CD4+ T-cells infiltrating the tumour compared to the surrounding normal liver, indicating that these patients have a higher frequency of circulating and tumour infiltrating CD4+ T-cells.

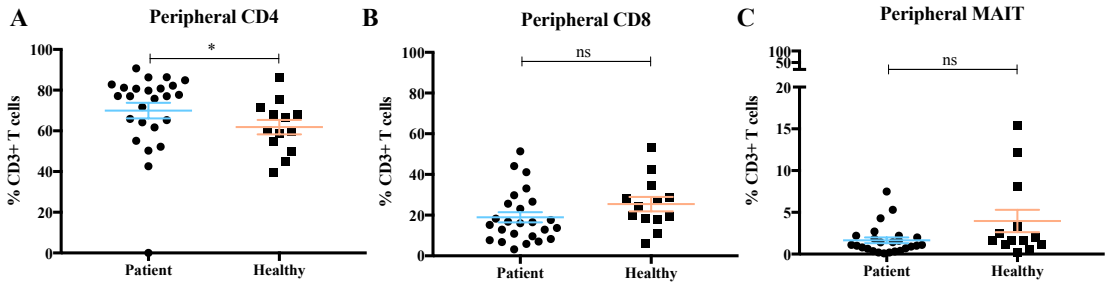


**Figure 5.8. Peripheral MAIT cell frequency in patient PBMCs is similar to healthy donor PBMC.** Peripheral T-cells were quantified by flow cytometry from CRLM patients (n=25) and healthy donors (n=13). (**A**) Peripheral CD4+ T-cells were significantly increased in CRLM patient blood compared to healthy donors (*$p<0.05$). No significant differences seen in (**B**) CD8+ or (**C**) MAIT cell frequencies. Each data point represent individual patients samples, error bars represent SEM, n=25 CRLM patients and n=13 healthy donors, unpaired Mann-Whitney t-test.

### 5.5 MAIT Cell Phenotype *In Situ* in Tumours from Patients with CRLM

In order to characterise MAIT cell phenotype in more detail, the activation profile of MAIT cells from the tumour; liver and peripheral blood was assessed by expression of PD-1, CD69, HLA-DR and CD45RO. As seen in **Figure 5.9**, MAIT cells express PD-1 and CD69, and this expression is distinct in the tissue compared to peripheral blood.

Similar to PD-1, another conventional T-cell activation marker is CD69. This indicates that the MAIT cells from the tumour and liver have a distinct phenotype than to that of peripheral blood.

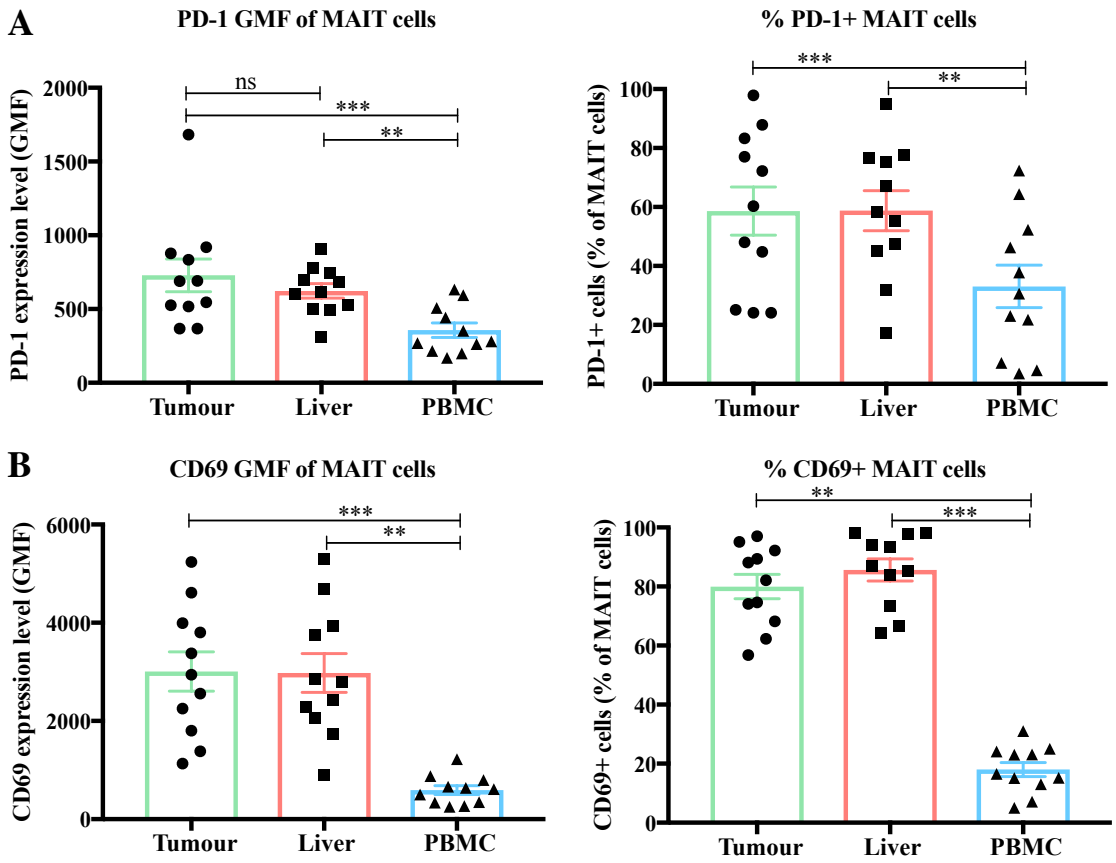


**Figure 5.9. MAIT cell PD-1 and CD69 expression is distinct in tissue compared to PBMCs.** Expression of PD-1 was assessed by flow cytometry on MAIT cells in the tumour, liver and PBMCs. Bar-plots represent expression of (**A**) PD-1 as the Geometric Mean Fluorescence (GMF) of MAIT cells and % PD-1+ MAIT cells and (**B**) CD69 as the GMF of MAIT cells and % CD69+ MAIT cells. Each data point represent individual patient samples, n=11 CRLM patients, error bars are SEM, One-Way ANOVA (nonparametric) Friedman's test, *p<0.03, **p<0.002, ***p<0.0002.

MAIT cells are known to express HLA-DR, which has been used to assess activation of the cells in the liver (X. Z. Tang *et al.*, 2013). The tumour and liver MAIT cells had a higher expression of HLA-DR than MAIT cells in the peripheral blood (**Fig. 5.10A**). Again, this suggests that MAIT cells in the tissue are activated. Finally to assess if MAIT cells have the capacity of memory, expression of the memory T-cell marker CD45RO was assessed. Across all sample types, MAIT cells expressed CD45RO (**Fig. 5.10B**), indicating that these MAIT cells have the capacity for memory.

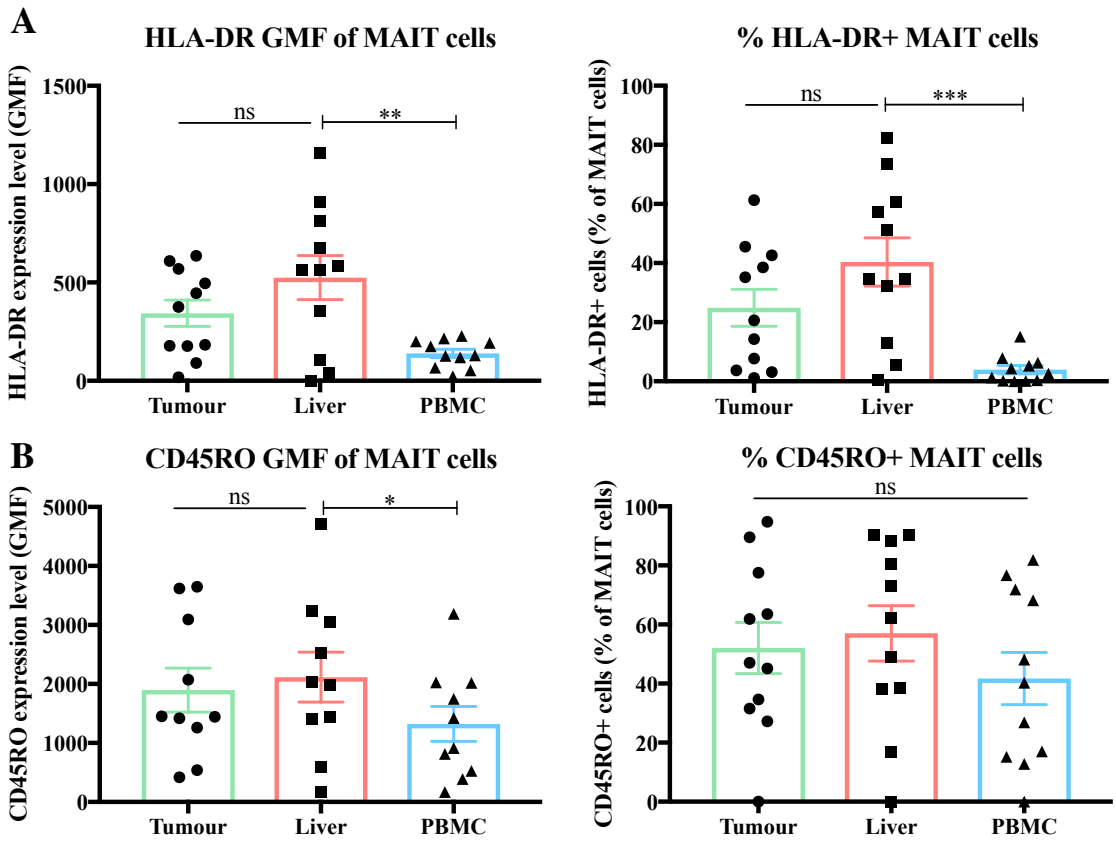


**Figure 5.10. HLA-DR and CD45RO expression on MAIT cells. Expression of HLA-DR and CD45RO was assessed by flow cytometry on MAIT cells in the tumour, liver and PBMCs.** Bar-plots represent expression (**A**) of HLA-DR as the Geometric Mean Fluorescence (GMF) of MAIT cells and % HLA-DR+ MAIT cells and (**B**) CD45RO as the GMF of MAIT cells and % CD45RO+ MAIT cells. Each data point represent individual patients samples, n=11 CRLM patients, error bars are SEM, One-Way ANOVA (nonparametric) Friedman's test, *p<0.03, **p<0.002, ***p<0.0002.

Collectively these phenotyping data demonstrate that the MAIT cells within the tissue are phenotypically distinct from MAIT cells in the peripheral blood. Some of the current published work only assesses peripheral MAIT cells, as access to tissue can be difficult. However, my results highlight the importance of assessing MAIT cells isolated from the tissue of interest to determine differential phenotypes.

### 5.6 Cytotoxic Capability of MAIT Cells Against Patient-Derived Tumouroids

Understanding the effector functions of MAIT cells against tumour cells was the main aim of this study. It is known that MAIT cells are specifically activated through the MAIT cell TCR/MR1 axis, when the ligand 5-OP-RU binds MR1; MAIT cells have the ability to induce cytotoxicity and produce cytokines (Corbett *et al*., 2014; Kjer-Nielsen *et al*., 2012). Previous studies have reported the ability of MAIT cells to detect and kill myeloma cell lines that have

been pulsed with 5-OP-RU, in an MR-1 dependant manner (Gherardin, Loh, *et al*., 2018). However, there have been no *in vivo* reports of tumours having the ability to present endogenous ligand and activate MAIT cells. It is plausible that mucosal tumours provide an environment, which attract and activate MAIT cells (Godfrey, Le Nours, Andrews, Uldrich, & Rossjohn, 2018). Hence, activated MAIT cells could have direct anti-tumour effector function or act within the TME as bystander immune cells secreting cytokines. As viruses can also activate MAIT cells in a TCR-independent manner, MAIT cell anti-tumour activity might also operate in a TCR-independent manner noting that they express a highly restricted TCR repertoire.

In order to understand MAIT cell interaction with tumour cells, the assay developed in **Chapter 4** was used to assess MAIT cell-mediated cytotoxicity. Patient-derived tumouroids were established *ex vivo* and co-cultured with allogeneic healthy donor MAIT cells. The first pilot experiment assessed MAIT cell ability to kill patient-derived tumouroids, and addressed two key questions: (1) Do MAIT cells kill tumouroids and (2) do tumouroids have the ability to present 5-OP-RU?

Purified expanded MAIT cells were obtained from Professor Dale Godfrey's laboratory at the Peter Doherty Institute. These healthy donor MAIT cells had been purified using the 5-OP-RU tetramer by FACS and expanded in the presence of 5-OP-RU, plate bound anti-CD3/28 antibodies and cytokines as described in **Chapter 2** and had been cryopreserved. A tumouroid line and expanded autologous TILs were established from a CRLM patient and used in the assay. To address the question of TCR/MR1-mediated activation of MAIT cells, 5-OP-RU soluble ligand was added to the culture to assess the ability of tumouroids to present ligand to MAIT cells.

Tumouroid death was assessed by uptake of PI, as a measure of cell death. As seen in **Figure 5.11A** autologous TILs co-cultured with tumouroids induced tumouroid death, with clear evidence of PI uptake. This also occured in the allogeneic purified MAIT cells however to a lesser degree. When kinetic killing was assessed in **Figure 5.11B**, MAIT cells (red line) were able to induce tumouroid death, which was enhanced with the addition of the ligand 5-OP-RU (orange line). However, MAIT cell killing was inferior to autologous TIL killing (green line), which had a greater killing capacity and enhanced kinetic killing.

When cytokine function was assessed, it was evident that, MAIT cells did not produce IFNγ when co-cultured with tumouroids alone, but did secrete IFNγ in the presence of 5-OP-RU (**Figure 5.11C**). In contrast, although the TILs were able to effectively kill the tumouroids as

seen in **Figure 5.11B**, TILs failed to produce IFNγ in the co-culture (<1 pg/mL at all time points) compared to MAIT cells and tumouroids + 5-OP-RU (>500 pg/mL at 4 hours) (**Figure 5.11D**). These data demonstrated that MAIT cells have the ability to kill patient-derived tumouroids, but to a lesser extent than patient-matched TILs.

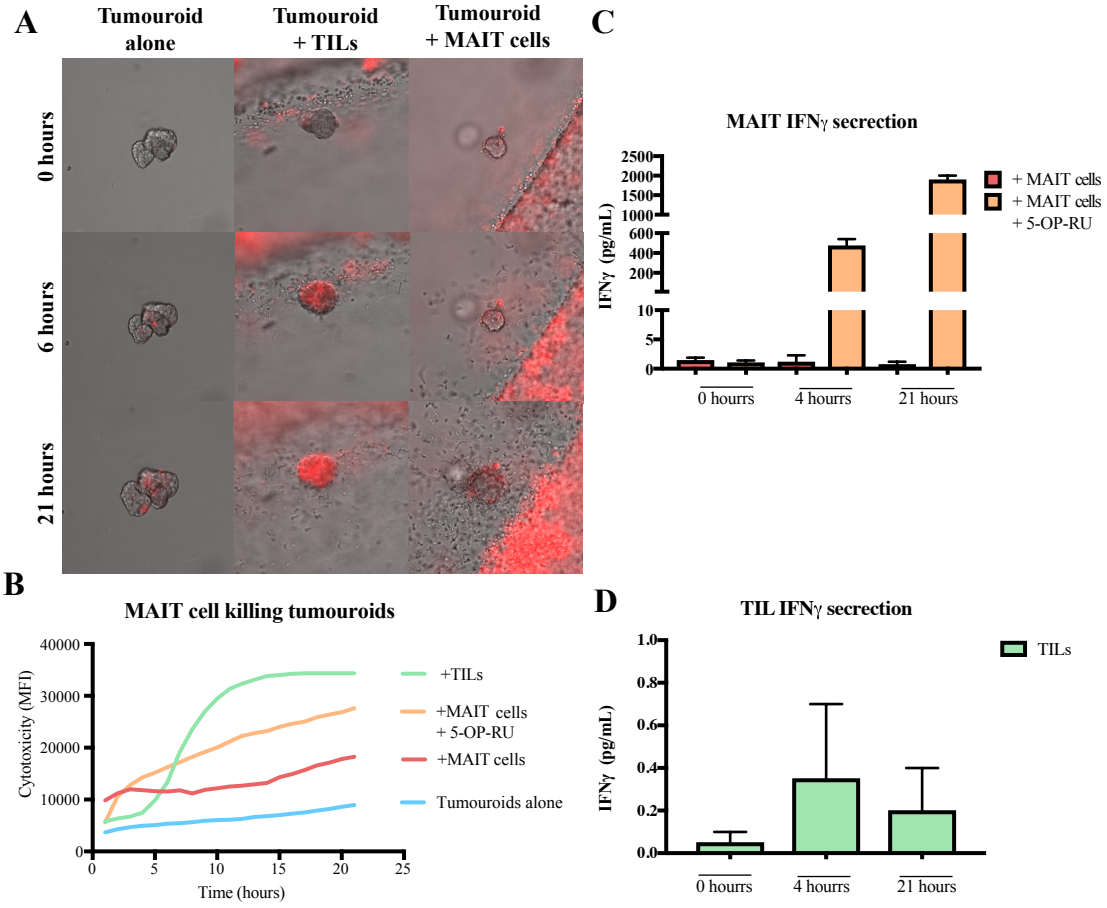


**Figure 5.11. Purified MAIT cells are able to kill tumouroids, but are inferior to autologous TILs.** Allogeneic purified expanded MAIT cells and autologous patient TILs were co-cultured with patient-derived tumouroids, respectively. (**A**) Representative images from differential interference contrast (DIC) live-imaging microscopy co-culture over 21 hours, showing PI uptake (red) in tumouroids. (**B**) XY-plot showing kinetic killing of tumouroids by quantitation of the MFI of PI uptake in tumouroids over time (hours) with immune cell co-culture, n=21 tumouroids measured per condition. Bar graphs show the amount of IFNγ secretion by (**C**) MAIT cells and (**D**) autologous TILs during co-culture, over 24 hours in pg/mL, representative of one experiment.

To build on the pilot experiment, the next questions addressed were: (1) Do MAIT cells have a bystander role by enhancing autologous TIL-mediated killing through cytokine secretion and (2) does addition of anti-PD-1 antibody enhance the effector function of MAIT cells? Therefore, to develop this assay in more depth, fresh healthy donor MAIT cells were used against patient-derived tumouroids. Ideally, patient-derived MAIT cells would be used with autologous tumouroids; however, the biggest challenge of these experiments was isolating sufficient quantities of MAIT cells from patients for functional experiments. Importantly, MAIT cells are not MHC-restricted and therefore, using allogeneic MAIT cells against patient-derived tumouroids did not induce human leukocyte antigen (HLA)-mismatch. Conversely, access to healthy donors and large amounts of blood was not a limitation in these assays.

Instead of using FACS to purify MAIT cells, healthy donor MAIT cells were enriched using Vα7-2+ magnetic separation kits from Stemcell technologies (Vancouver, Canada). In comparison to the pilot study (**Fig. 5.11**), this experiment used freshly isolated MAIT cells, which had not been expanded, activated, or cryopreserved. As with the pilot experiment, autologous IL-2 expanded TILs were used to directly compare the killing efficiency of TILs vs. MAIT cells. Addition of anti-PD-1 antibody was used as an experimental condition, to assess if MAIT cell or TIL killing was enhanced with CBI. A final condition was included, where MAIT cells and TILs were combined, to understand if MAIT cells played a bystander role to either enhance or hinder TIL function, through secretion of cytokines.

In this experiment (**Fig. 5.12A**), TILs alone (red line) proved to be the most efficient at killing tumouroids, and addition of anti-PD-1 (dotted red line) slightly decreased this efficiency. MAIT cells (green line) were able to induce tumouroid death, compared to tumouroid alone, but this effect was much less than with TILs. Addition of anti-PD-1 antibody (dotted green line) did not enhance the cytotoxicity. Addition of 5-OP-RU to the culture (blue line) improved MAIT cell killing, and this was the second experiment to show that tumouroids have the ability to present ligand and activate MAIT cells. Finally, when MAIT cells and TILs were combined at a 1:1 ratio with anti-PD-1 antibody (dotted purple line), this decreased the cytotoxic ability of the TILs. It cannot be determined from this experiment if this was due to MAIT cells alone or the addition of anti-PD-1 antibody as I did not include a MAIT cell + TIL only condition, due to limited cell numbers.

The maximum killing capacity was assessed at any given time point (**Fig. 5.12B**), and it showed that TILs alone had the most substantive cytotoxic effect when compared to background (mean MFI 2257 vs. 765.7). There was not a large difference observed with the addition of anti-PD-1 antibody (mean MFI MAIT cells 2257 vs. MAIT cells + anti-PD-1 antibody). Addition of 5-OP-

RU did not significantly enhance MAIT cell killing (**Fig. 12B**) In summary, MAIT cells alone were able to induce tumouroid death.

Finally, cytokine secretion in each condition was assessed including IFNγ (**Fig. 5.12C**) and TNFα (**Fig. 5.12D**). Interestingly, although MAIT cells + TILs + anti-PD-1 antibody did not have a significant effect in terms of cytotoxicity, there is an increased cytokine production of both IFNγ and TNFα (>1000 pg/mL). These quantities are comparable to MAIT cells + tumouroids + 5-OP-RU, indicating again that MAIT cells are robust producers of cytokines. This is again demonstrates that MAIT cells have the ability to act as bystanders and perhaps influence the TME.

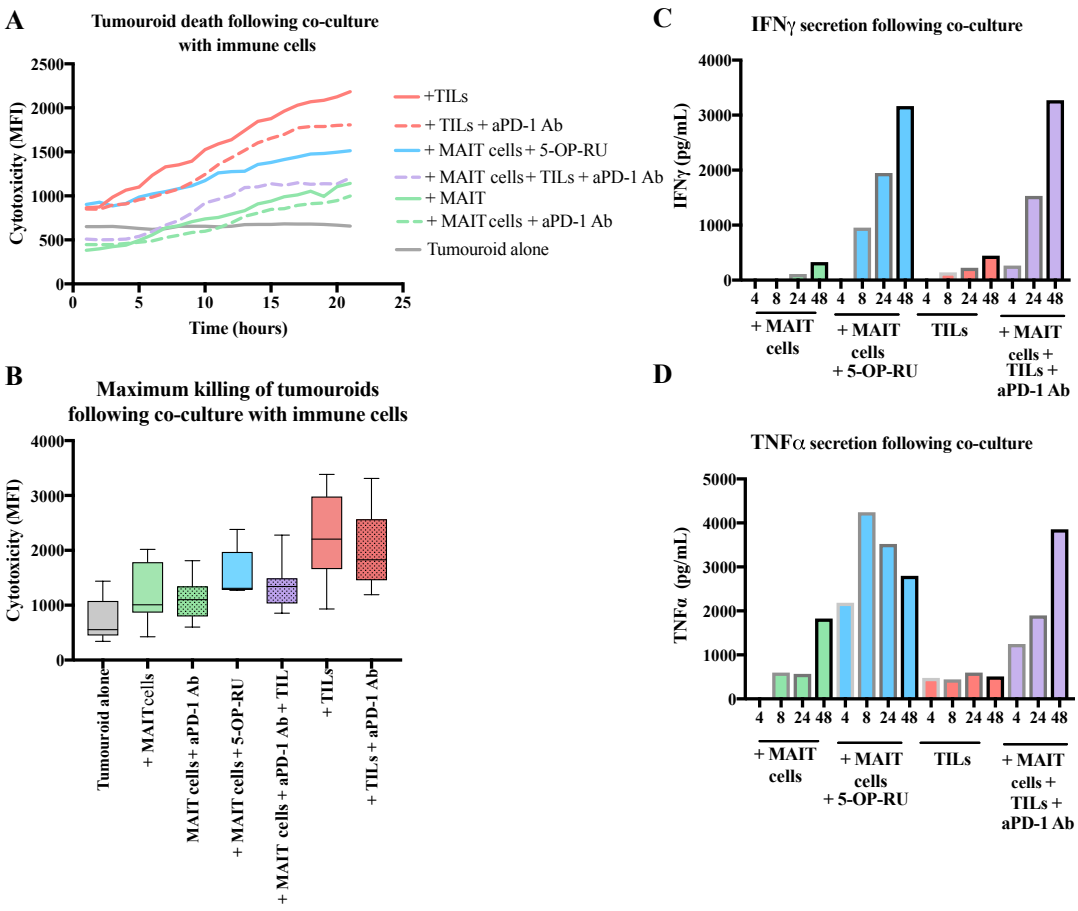


**Figure 5.12. Autologous TILs are more efficient inducers of tumouroid cytotoxicity than allogeneic MAIT cells. (A)** XY-plot showing kinetic killing of tumouroids by quantitation of cytotoxicity by MFI of PI uptake in tumouroids over time (hours). (**B**) Box and whisker plots of the maximum MFI of PI uptake over 48 hours in tumouroids following co-culture with immune cells including all conditions. (**C**) Bar graphs showing the amount of IFNγ and (**D**) TNFα secretion over 48 hours when immune cells and tumouroids were co-cultured, representative of one experiment.

The previous pilot experiments assessed peripheral MAIT cells in a 'resting' state. To assess the full cytotoxic potential of MAIT cells, I decided to compare stimulated and resting peripheral MAIT cells and their cytotoxic capabilities against patient-derived tumouroids. To do this, I adapted the MAIT cell stimulation protocol from Professor Godfrey's laboratory that is regularly used to expand pure populations of MAIT cells (Gherardin, Loh, *et al*., 2018). This stimulation protocol is described in **Chapter 2**, but briefly, plate-bound anti-CD3 and soluble anti-CD3/28 antibodies were used to stimulate MAIT cells that have been purified by FACS from healthy donor PBMCs. This expansion protocol included a combination of cytokines: IL-2, IL-7, IL-12, IL-15 and IL-18, and the stimulus 5-OP-RU. I decided to omit 5-OP-RU from this stimulation protocol, because I found in the pilot experiments that addition of 5-OP-RU did not improve cytotoxicity. Importantly, there is literature reporting that IL-7 is produced by hepatocytes in an inflammatory state, and that IL-7 can license MAIT cells through regulated TCR-mediated activation (X. Z. Tang *et al*., 2013). MAIT cells can also be activated by IL-15 and IL-18 and profoundly boosts their activation in concert with TCR ligation (Sattler, Dang-Heine, Reinke, & Babel, 2015). Therefore, I attempted to maximally stimulate these MAIT cells and assessed their full cytotoxic potential.

To investigate the phenotype of MAIT cells stimulated using this method, cells were assessed using flow cytometry and CBA. As seen in **Figure 5.13A-B**, both TCR stimulation alone and TCR + cytokine stimulation; resulted in a strong effector phenotype where nearly 100% of cells expressed CD69 and granzyme B. In comparison, IL-15/18 stimulation in the absence of TCR stimulation resulted in nearly all cells expressing the activation marker CD69, but only 31.4% of cells expressed granzyme B (**Fig. 5.13B**). When assessing the secreted cytokine as seen in **Figure 5.13C**, TCR + cytokine stimulation produced the most substantial amount of granzyme B. For subsequent experiments, anti-CD3/28 antibodies & cytokine stimulation were used to artificially activate MAIT cells, in order to study their interaction with patient-derived tumouroids in a fully activated state.

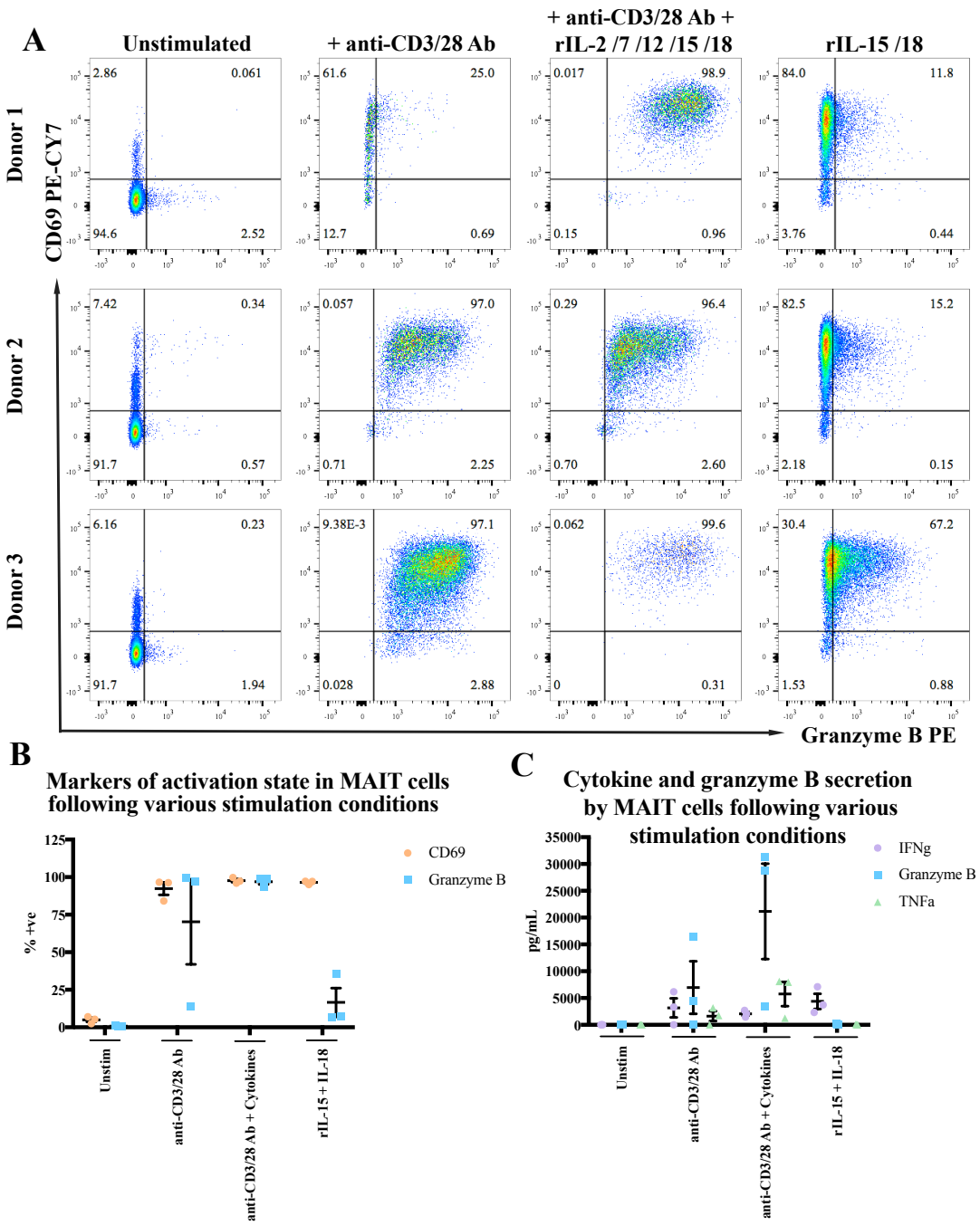


**Figure 5.13. Stimulation of peripheral MAIT cells via TCR and cytokines results in a cytotoxic phenotype.** MAIT cells were freshly isolated from healthy donors via FACS and stimulated with anti-CD3/28 antibody alone, anti-CD3/28 antibody + cytokines or IL15/18 only for 48 hours. (**A**) Representative flow cytometry plots from three donors following stimulation (**B**) Scatter-plots showing expression of CD69 (orange) and granzyme B (blue) following stimulation detected via flow cytometry. (**C**) Scatter-plots showing cytokine secretion in supernatant following stimulation measuring IFNγ (purple), granzyme B (blue) and TNFα (green). Each data point represents one healthy individual, n=3, representative of 1 experiment.

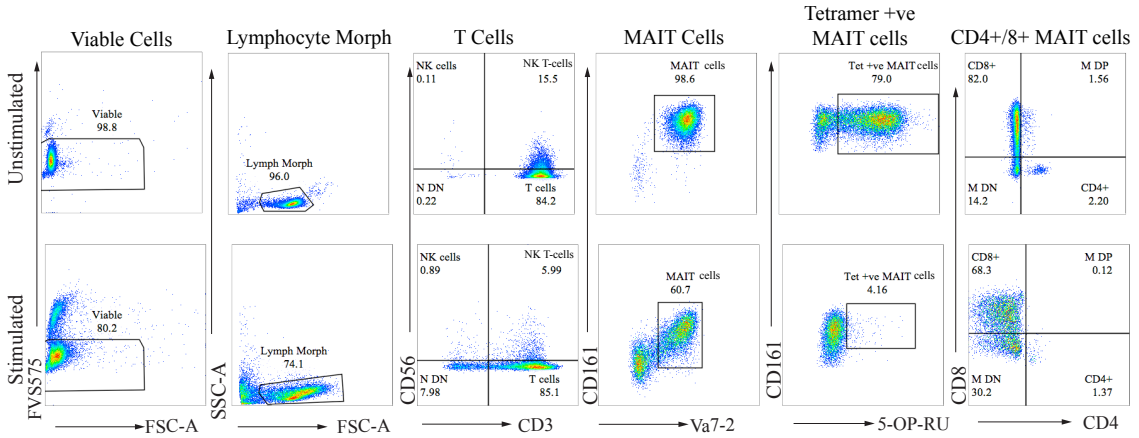


**Figure 5.14. MAIT cell stimulation induces activation phenotype.** Peripheral MAIT cells from healthy donors were freshly isolated by FACS and stimulated with anti-CD3/28 antibody and cytokine cocktail. Representative flow cytometry plots showing gating strategy of freshly isolated unstimulated MAIT cells (top) and stimulated MAIT cells (bottom).

To further investigate the functional phenotype of MAIT cells using this stimulation protocol, MAIT cells were isolated from three healthy donors and phenotypically assessed. **Figure 5.14** shows the phenotype of unstimulated vs. stimulated MAIT cells. As seen in **Figure 5.14**, following stimulation, MAIT cells were only detected by Vα7-2+ CD161$^{high}$ expression. MAIT cells could not be detected using 5-OP-RU tetramer (bottom panel **Fig. 5.14**), which was observed across all three donors. This was most likely due to occupation of the receptor by the soluble anti-CD3/28 antibody or alternatively downregulation of the receptor. I was confident it was not an artefact of staining, as the unstimulated MAIT cells were detected using the 5-OP-RU tetramer and stained simultaneously. In the example of **Figure 5.14**, it was also observed that the FACS isolation was not optimal, as only 63.8% were pure MAIT cells. This implied that the initial sort was not pure and likely had other T-cell populations that expanded during the stimulation. In both unstimulated and stimulated MAIT cells, CD8+ and DN populations were observed, with little to no CD4+ MAIT cell subpopulations. Upon stimulation it can be seen that MAIT cells upregulated PD-1 and CD69 expression (**Fig. 5.15**). Interestingly, in all experiments CD45RO downregulation was observed, why this occurs during activation is unknown and intriguing.

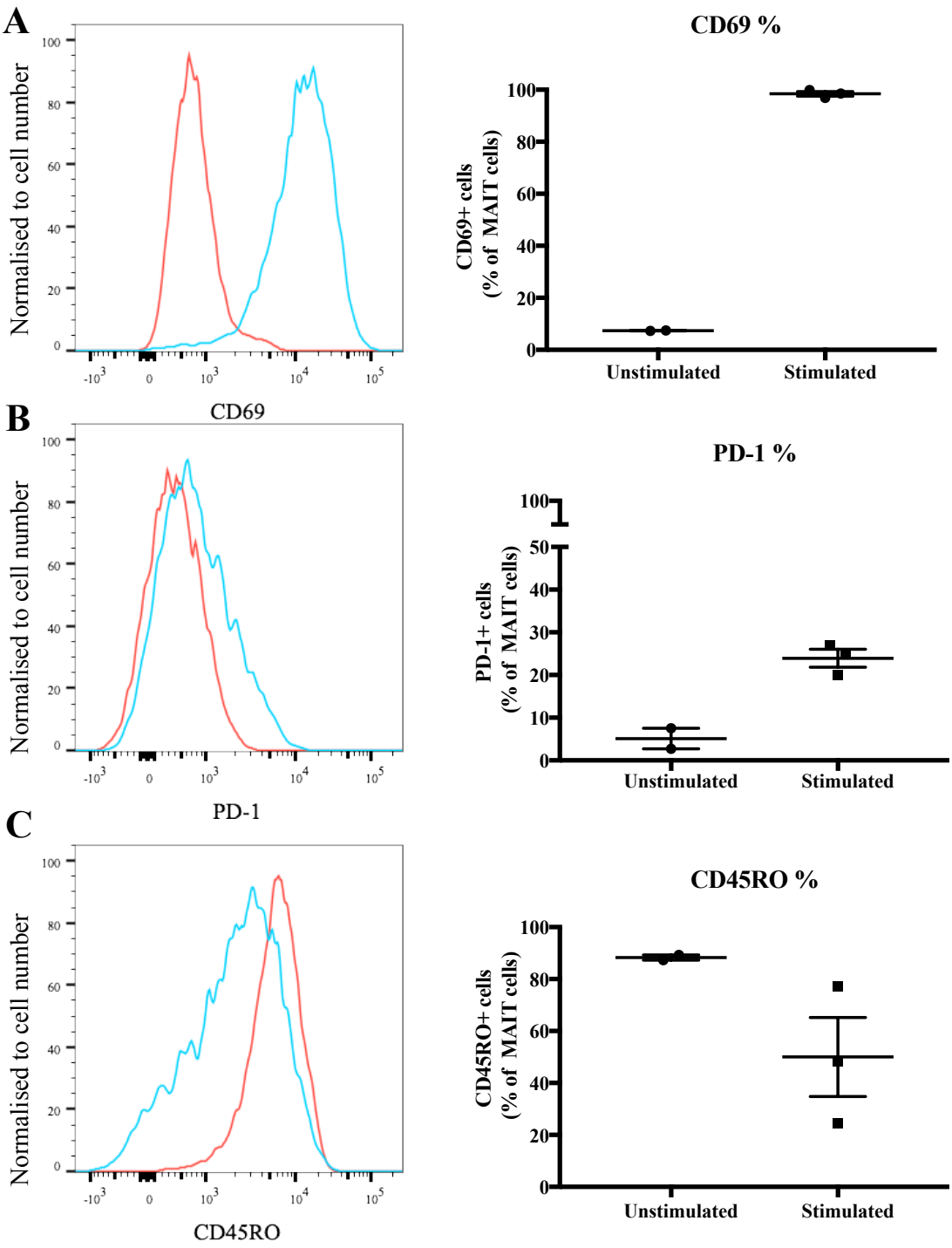


**Figure 5.15. MAIT cell stimulation induces an activation phenotype.** Peripheral MAIT cells from healthy donors were freshly isolated by FACS and stimulated with anti-CD3/28 antibody and cytokines. (**A**) Representative flow cytometry plots showed expression of CD69, (**B**) PD-1 and (**C**) CD45RO in unstimulated (red) and stimulated (blue) MAIT cells (**C**) Scatter plots showed quantitation of percentage of MAIT cells expressing CD69, PD-1 and CD45RO following stimulation. Each data point represents one healthy individual, n=2 (unstimulated) and 3 (stimulated).

To compare the killing capacity of unstimulated and stimulated MAIT cells against patient-derived tumouroids, a series of cytotoxic assays were performed. To determine if MAIT cells are activated via MR1 in this assay, anti-MR1 blocking antibody was used to determine the mechanism of activation. **Figure 16A** depicts the kinetic killing of tumouroids by unstimulated MAIT cells, which takes at least 20 hours to see any effects. As shown in **Figure 16B**, in the stimulated state, MAIT cell killing occurs rapidly within 10 hours and induces greater levels of cytotoxicity. Assessment of the maximum tumouroid death induced by MAIT cells is shown in **Figure 5.17**. Unstimulated MAIT cells were able to significantly kill tumouroids (mean MFI 1680, tumouroid alone vs. 5302, + MAIT cells), which demonstrated that MAIT cells have the capacity to kill tumouroids. Blocking MR1 did not alter this, suggesting that unstimulated MAIT cells have cytotoxic effect that is MR1-independent. Blocking PD-1 did not enhance MAIT cell killing. Compared to unstimulated MAIT cells, stimulating MAIT cells did not significantly enhance tumouroid killing. This effect was also MR-1 independent, and not affected by anti-PD-1 antibody. These data indicate that MAIT cells are able to kill tumouroids, in an MR-1 independent manner, and addition of anti-PD-1 antibody does not enhance killing.

To assess specificity of MAIT cell killing directed against tumouroids, normal liver organoids were established from normal liver tissue of a hepatocellular carcinoma (HCC) patient, by the Visvanathan laboratory. **Figure 5.17** highlighted that unstimulated and stimulated MAIT cells are able to kill normal liver organoids. Through which mechanism this occurs was unknown, as MAIT cell numbers were not sufficient for further validation.

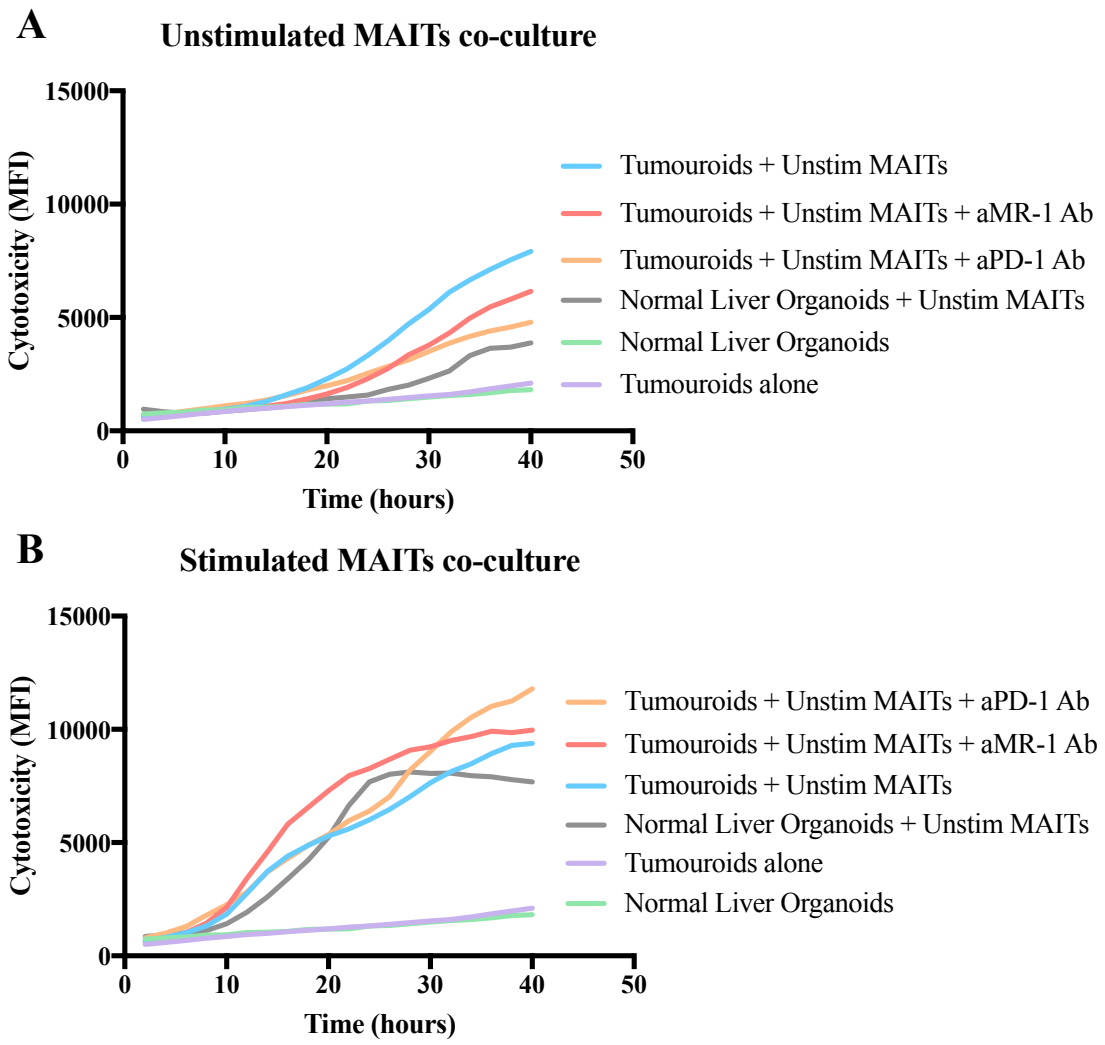


**Figure 5.16. Kinetic killing of tumouroids by MAIT cells is enhanced when pre-stimulated.** Unstimulated and stimulated MAIT cells were co-cultured with tumouroids for 40 hours. Cell death of tumouroids was assessed using MFI of PI uptake over time. XY-plot showing kinetic killing of tumouroids and normal liver organoids by unstimulated MAIT cells quantitating MFI of PI uptake in tumouroids over 40 hours in (**A**) unstimulated and (**B**) stimulated MAIT cells. Lines represent the mean of four healthy individuals, n=4 donors, 2 repeat experiments.

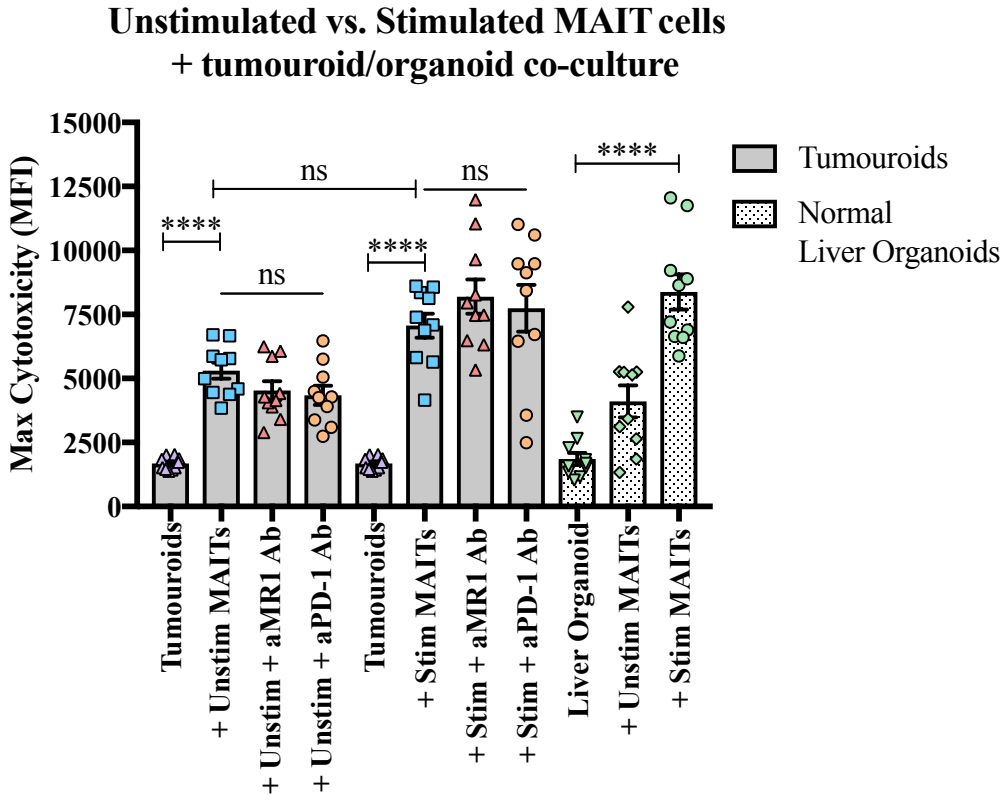


**Figure 5.17. MAIT cells kill in an MR-1 independent mechanism.** Unstimulated and stimulated MAIT cells were co-cultured with tumouroids (solid grey bars) or organoids (pattern bars) for 40 hours. Cell death of tumouroids was assessed by the maximum cytotoxicity (MFI of PI) at one time point over 40 hours. Bar graphs displaying the maximum fluorescence of tumouroid/organoid uptake at any given time point. Bar graphs displaying the maximum MFI (tumouroid death), over 30 hours, error bars represent SEM, one-way ANOVA, ****$p<0.0001$ n=4 MAIT cell donors, 2 repeat experiments.

All of these co-cultures used healthy-donor peripheral blood-derived MAIT cells and may not have been reflective of tissue-derived MAIT cells. Stimulation of peripheral MAIT cells was used as a surrogate to recapitulate the phenotype of tissue-derived MAIT cells. There were multiple attempts to culture tissue-derived MAIT cells from the tumour and liver, however following FACS sorting for purification, the cells were very sensitive and did not survive in culture. Although anecdotal, there was one patient where MAIT cells from the normal liver were successfully purified and expanded (using the aforementioned stimulation protocol). This expansion was for two weeks prior to being co-cultured with autologous tumouroids. This was the ideal co-culture experiment to assess autologous MAIT cell function, *ex vivo*. Addition of anti-PD-1 antibody was used to assess the response of tissue-derived MAIT cells with CBI. As shown in **Figure 5.18A-B**, the normal liver-derived MAIT cells were able to induce cytotoxicity of matched tumouroids. Addition of anti-PD-1 antibody did not enhance killing.

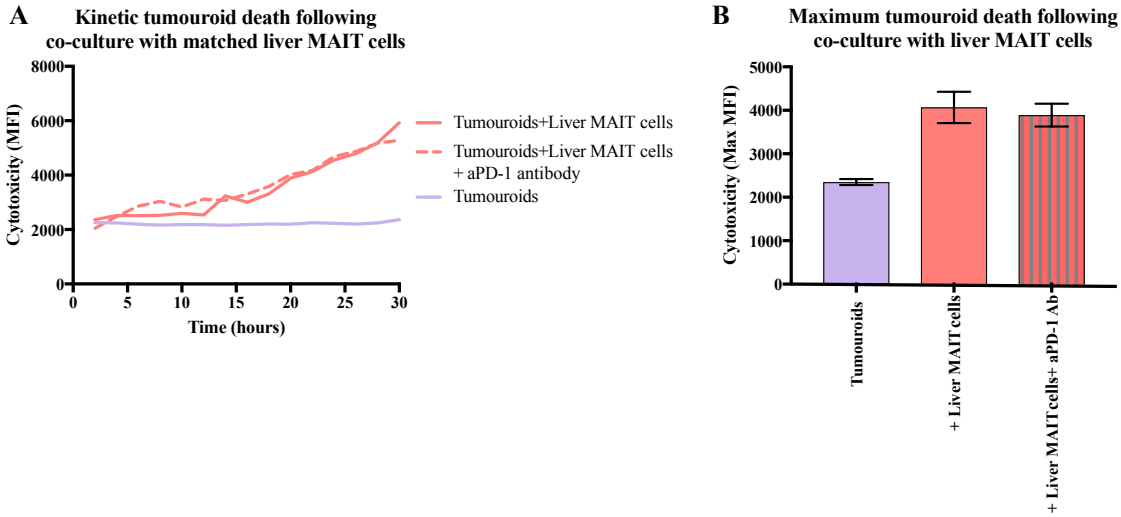


**Figure 5.18. Autologous liver-derived MAIT cells are able to effectively kill tumouroids *ex vivo*.** MAIT cells were isolated and expanded from normal-liver and co-cultured with matched autologous patient-derived tumouroids. (**A**) XY-plot showing kinetic killing of tumouroids by expanded normal liver-MAIT cells quantitating MFI of PI uptake in tumouroids over 30 hours (**B**) Bar graphs displaying the maximum MFI (tumouroid death), over 30 hours, error bars represent SEM.

From these cytotoxic data it can be concluded that tissue derived and expanded MAIT cells were able to kill patient-derived tumouroids *ex vivo*. Thus demonstrating the potential killing capability of MAIT cells, providing insight into their function. Understanding their phenotype *in situ* provided additional clues into their role in a pathological state.

In conclusion, I have found that both unstimulated and stimulated MAIT cells have the ability to kill patient-derived tumouroids, and are potent producers of IFNγ. This indicated that MAIT cells possess the capability to influence the TME under inflammatory conditions. MAIT cells isolated from tissue of CRLM patients are phenotypically distinct compared to peripheral MAIT cells, assessed by activation and memory markers. However, despite MAIT cells being activated in the tumour, they are reduced in frequency. Understanding why this is the case is yet to be clarified. These data contribute to the field of MAIT cells in the context of tumour immunity, to better understand their role in this pathological state.

## 5.7 Discussion

In a review of the literature documenting TILs in various tumour types, Pagès *et al* reported that in 98% of these studies, cytotoxic CD8+ T-cells were associated with a good prognosis. In contrast, other immune cells subsets were associated with either a good or poor prognosis depending on the method used or the cancer type (Pages *et al*., 2018). Therefore, it is clear that CD8+ T-cells play a role in controlling tumour progression, due to their cytotoxic ability. What the field has failed to recognise is that not all of the CD8+ T-cells accounted for are conventional CD8+ T-cells. Included in the assessment of CD8+ T-cells is the MAIT cell subset, where function in tumour immunity is less defined.

Approximately 80-90% of blood MAIT cells express either CD8αα homodimer or CD8αβ heterodimer. Therefore, MAIT cells are likely to be included in the quantitation of conventional CD8+ T-cells when assessing TILs especially in colorectal tumours and CRLM. Based on this information, it would also imply that CD8+ MAIT cells are associated with good prognosis in CRC in the primary tumour, stages I-III. However, in the more advanced stage of disease and at the metastatic site, it may not be the case. Assessment of MAIT cells as a proportion of CD8+ T-cells revealed that CD8+ T-cells comprise up to 50% of MAIT cells. Ongoing work in the lab, that is not part of this thesis, will confirm this using mIHC. This approach will provide more information about the spatial location of MAIT cells within and around the tumour and provide a more definitive proportion of MAIT cells of CD8+ T-cells compared to FACS assessment.

To understand the different phenotypes between conventional CD8+ T-cells and MAIT cells, expression levels of PD-1 and CD69 were compared. The expression of PD-1 on conventional CD8+ T-cells and MAIT cells was not significantly different and suggested that both cell populations may be exhausted. More importantly it indicates that expression of PD-1 by these cells could be therapeutically targeted with anti-PD-1 antibody. Hence, MAIT cells may represent an additional T-cell population that may respond the CBI, which has not been described previously. Conversely, CD69 expression is significantly higher on MAIT cells than conventional CD8+ T-cells and indicates activation. In recent years, CD69 is becoming more widely accepted as a tissue-residency marker, however assessment of the additional CD103+ marker would be required (Kumar *et al*., 2017). If it was the case, then it demonstrates that these MAIT cells in the TME are likely to be local tissue-resident cells from the liver. Whether MAIT cells are tissue resident T-cells or not is still contentious in the field (Booth *et al*., 2015; Voillet *et al*., 2018).

It is clear that MAIT cells make up a significant proportion of T-cell populations at mucosal sites in humans. The most abundant population of MAIT cells is found in the liver, and accounts for 20-40% of T-cells (Dusseaux *et al*., 2011). When assessing the frequency of these cells in CRLM, MAIT cell frequency was numerically reduced in the tumour compared to surrounding liver. There are two likely reasons for this: (1) MAIT cells are not tumour specific or (2) the TME is generally immunosuppressive, and results in a reduction of MAIT cell infiltration.

MAIT cells are known to be protective in bacterial infections, where they are able to kill bacterially infected cells in an MR1-dependant fashion (Kurioka *et al*., 2015; Le Bourhis *et al*., 2013). However MAIT cells also have the ability to produce pro-inflammatory cytokines independent of MR1, through IL-12 and IL-18 (Banki *et al*., 2019). In some tumours analysed, an increased (>20%) frequency of MAIT cells was observed. Understanding why these tumours had a high MAIT cell infiltrate warrants further investigation. The results from the functional cytotoxic assay show that peripheral MAIT cells were able to kill independent of MR1. Because killing is independent of MR-1, it suggests that MR-1 expression on tumour cells from patients may not be informative of MAIT cell presence, as may have been predicted. However, it is still unclear of the exact activation of killing in the *ex vivo* assay. Future work will be required to understand if both tumour tissue and tumouroids have protein expression of MR1 and activating NKG2D cell receptor ligands such as MICA/B, ULBP16 or Rae1 (Spear, Wu, Sentman, & Sentman, 2013). This is because MAIT cells are known to have NK cell receptors including inhibitory NKG2A and activating NKG2D receptors and cytotoxic effector function could be occurring through these pathways (Dusseaux *et al*., 2011). It is therefore unlikely that MAIT cells are tumour specific, but perhaps play a role as bystander cells within the TME.

Further studies to understand if MAIT cells kill tumour cells are required, to achieve more clarity on this question. This is of course a key question in the context of cancer therapy because if MAIT cells have the ability to kill tumour cells they may be good targets for immunotherapy. What sets my investigations apart from the aforementioned functional *in vitro* studies is the use of patient-derived tumouroids, which better recapitulate tumour cell heterogeneity compared to traditional cell lines (M. Fujii *et al*., 2016). The data generated from my collective cytotoxic experiments show that MAIT cells do have the capability to kill patient-derived tumouroids and this is without the inclusion of 5-OP-RU in the co-culture. This indicates that there is another mechanism of action that MAIT cells function through, independent of MR1.

The results of this thesis show that MAIT cells explored from the tissue displayed an activated state. Hence, artificial activation of peripheral MAIT cells would determine their maximal

functional capability. However, I was concerned that these polarised MAIT cells may have the ability to kill normal cells non-specifically. To address this concern, I included patient-derived normal liver organoids to assess specific tumour killing. Both unstimulated and stimulated MAIT cells did kill normal liver organoids. This is of some concern as use of MAIT cells therapeutically could cause damage to normal tissues. As the normal liver organoids were only derived from one patient, it is important to repeat this experiment, particularly using normal liver organoids from the same patient as the tumouroids used in the assay. The presented cytotoxic data are the first report that donor MAIT cells have the ability to kill patient-derived tumouroids. MAIT cells may be potentially considered for therapeutic use to kill tumour cells. One caveat of CAR T-cell therapy is the eligibility of patients to meet established criteria/measures for such therapy. This includes the requirement to provide sufficient amounts of blood for effective transduction of autologous CAR T-cells, which are then re-infused back into the patient. Patients are often unwell, may be lymphopenic and therefore not be able to be eligible for this therapy. The advantage of using MAIT CAR T-cells is that MAIT cells function independent of MHC-I and MAIT cells could be used allogeneically in this context (Godfrey *et al*., 2018).

To understand MAIT cell biology in the context of tumour, future studies will attempt to assess the *in situ* MAIT cell phenotype from tissue-derived cells using single-cell RNAseq. It will compare differential expression of immune markers on conventional CD8+ T-cells and MAIT cells derived from the tumour and liver. The initial RNAseq data from CRLM indicate that tumours from primary and metastatic CRC have the ability to express MR1. This requires further validation at the protein level. To further address MAIT cell presence in the tumour and surrounding liver, I plan to perform mIHC, to visualise where the MAIT cells are located within the TME. It is clear from the flow cytometry data that MAIT cells are present in tumours and some are at higher frequencies than others. Due to complete disruption of tissue using flow cytometry to assess MAIT cell phenotype at the single-cell level, we don't have the ability to visualise whether there is an accumulation in CT or IM. Therefore, using mIHC to address this will be highly informative.

In this chapter I was able to identify the ability of MAIT cells to kill tumouroids *ex vivo*. I also found that MAIT cells make up a significant proportion of conventional CD8+ T-cells, which have not been previously accounted for. MAIT cell frequency was reduced in the tumour, a finding that is consistent with the current literature. An activation phenotype of MAIT cells from the tumour and liver was observed. Due to the detected expression of PD-1 on MAIT cells, cytotoxic assays were designed to test if anti-PD-1 antibody enhanced MAIT cell effector function. From these experiments anti-PD-1 antibody did not enhance killing. The ability of

MAIT cells to rapidly secrete cytokines and cytotoxic molecules highlight that these cells could be used therapeutically (e.g. CAR-MAIT cells). Understanding their role in pathologies of the liver will contribute to the field of MAIT cell biology. Thus, understanding the biology of MAIT cells provides important insight into the potential of these cells therapeutically and to more precisely define the nature of TILs in mCRC.

## 6. DISCUSSION

Twenty years ago, diagnosis of Stage IV CRC was associated with <1% five-year survival (Jones *et al*., 2012; Rougier *et al*., 1995). Metastatic spread to the liver is common, and now, with advances in surgical technique and both neo-adjuvant and adjuvant chemotherapy, five-year survival of patients with colorectal liver metastasis is between 30-40% (Choti *et al*., 2002; Luca Vigano, 2012; Manfredi *et al*., 2006; Tomlinson JS1, 2007). However a significant proportion of these patients develop recurrence at some stage (D'Angelica *et al*., 1997; Tomlinson JS1, 2007) and most patients succumb to death as a result of their metastatic disease. This thesis seeks to identify why this might occur in the context of the innate and adaptive immune responses.

We know that TILs have prognostic significance in CRC, where a high TIL frequency is associated with improved survival (Galon *et al*., 2006; Pages *et al*., 2005; Pages *et al*., 2009; Pages *et al*., 2018; Smyrk, Watson, Kaul, & Lynch, 2001). The seminal work by Galon *et al*, confirmed that patients with CRC stratified by TNM staging alone had a stage-dependant reduced survival (I-IV). Stage IV had the worst DFS, which is unsurprising (Manfredi *et al*., 2006). However when those patients, who were TNM stage I-III were then stratified by infiltration of CD3+ T-cells, they had a different prognosis, regardless of TNM stage. Importantly, stage IV CRC patients stratified based on CD3+ T-cell alone did not show a statistically significant improved OS (Galon *et al*., 2006). Thus this work demonstrates that the immune response influences time to recurrence and overall survival in stage I-III CRC, but is less pronounced in metastatic stage IV CRC. Based upon these observations, I question what immunological factors might be involved in the progression of primary CRC to metastatic disease.

In **Chapter 3**, immunological factors were investigated in the context of the primary tumour, which had been surgically resected in patients who also had *de novo* mCRC. Included in this unique cohort of patients were patients with microsatellite unstable tumours. This MSI-H subgroup of patients is known to be unresponsive to conventional chemotherapy and have a worse outcome compared to stage I-III CRC patients (Goldstein *et al*., 2014; Koopman *et al*., 2009; Overman *et al*., 2017). There was no statistical difference in OS observed when comparing patients with MSI-H to MSS. To evaluate whether the immune response plays a role in OS of stage IV disease, cytotoxic CD8+ T-cell infiltration was assessed at the primary site. No difference was found in OS between high and low frequencies of CD8+ T-cells. These data suggest that the immune response in both primary and metastatic sites has failed. Verifying this view would involve assessment of the CD8+ T-cell infiltrate in matched distant metastatic tumours, however the clinical realities are completely consistent. It suggests that for the disease to progress to metastasis, the TILs in the primary tumour must be unable to control tumour growth.

Similarly at the metastatic site, upon dissemination, the tumour cells likely undergo immune evasion and maintain this through immunosuppression. This entire process supposedly occurs due to "aggressiveness" of the tumour through accumulation of genetic and epigenetic events as well as immune evasion and suppression (Dienstmann *et al*., 2017).

The tumour-intrinsic progression to metastasis, by definition, encompasses an immune evasive microenvironment. This can be through mechanisms including downregulation of immunogenic properties such as antigenic machinery including MHC-I (Becht, Giraldo, Dieu-Nosjean, Sautes-Fridman, & Fridman, 2016). Tumour cells can impede the immune response through checkpoint inhibitory mechanisms including the PD-1/PD-L1 axis. In **Chapter 3**, I found that immune evasion by these proposed mechanisms in the primary tumour did not correlate with survival. Tumour PD-L1 expression of >1% did not influence OS, and highlights that other immune evasion mechanisms must be at play. Investigating the distant metastatic tumours would be of interest, to assess if PD-L1 expression is present. Not only is it the tumour-mediated immunosuppression in the TME but activated APCs also have the ability to express PD-L1. Evaluation of infiltrating immune cells showed PD-L1 expression on immune cells was present. Despite high expression of PD-L1 on these cells, this property did not correlate with OS.

Evaluation of MHC-I expression would also provide valuable insight into other immune escape mechanisms by the tumour cells and should be explored in future studies. Finally to investigate the oncogenic properties of the tumour, whole exome sequencing (WES) should be done for both primary and metastatic tumours. Of particular interest would be the TGF-β pathway. Increased levels of TGF-β can lead to immune evasion and promotion of T-cell exclusion from tumours (Tauriello *et al*., 2018). Of course there could be another mechanism the tumour cells operate to evade the immune response and progress to metastasis.

The other component of metastatic progression is the possibility of T-cell dysfunction in the tumour of either primary or metastatic lesions in patients with mCRC. This is because the tumour has progressed to a clinically detectable stage indicating that is has bypassed elimination and equilibrium phases, directed by immune cells. As observed in **Chapter 3**, despite some tumours having a high quantity of CD8+ T-cells, this did not affect OS, yet these immune cells are still present in the tumours. If these T-cells are present, what then is their purpose and indeed are they functional?

To address the state of TIL function, now in the metastatic lesion, **Chapter 4** investigates the immune milieu in CRLM tumours. The axis of T-cell activation and exhaustion is intertwined. Immune checkpoints exist to reduce autoimmunity and maintain T-cell homeostasis. But this

mechanism can be hijacked by tumours to evade immune surveillance (Keir, Butte, Freeman, & Sharpe, 2008). When T-cells are in a chronic state of activation, also known as anergy this can produce a phenotype of "functionally exhausted" T-cells. Exhausted T-cells fail to function normally with reduced production of effector cytokines, reduced ability to proliferate, metabolic changes and reprogramming of transcription factors (Ahmadzadeh *et al*., 2009). Expression of PD-1 can indicate activation in the early stages of T-cell activity and later exhaustion in the chronically stimulated stage of T-cell activity. When evaluating PD-1 expression on CD4+, CD8+ and T-regulatory T-cells from CRLM, PD-1 expression was higher in the tumour compared to normal liver and peripheral T-cells. This is a similar finding to initial reports of TILs in melanoma having high PD-1 expression in the tumour compared to surrounding tissue and peripheral blood (Ahmadzadeh *et al*., 2009). This is the first indication these TILs are potentially dysfunctional, however additional evaluation of transcription factors such as NFAT, BLIMP-1, T-BET and EOMES would provide insight into the transcriptional reprogramming of these cells to confidently render them dysfunctional. Functional studies assessing the ability of the freshly isolated TILs to produce IFNγ and IL-2 as well as their proliferative capacity from the tumour would also be informative of this phenotype.

To more directly address this function dynamically, we developed the cytotoxic assay. This was designed to address quality over quantity of the TILs and interrogate the function of these immune cells. In **Chapter 4**, assessment of TILs from CRLM demonstrated the ability of these TILs to kill autologous tumouroids suggesting that these TILs are not terminally exhausted. However, although the TILs used were directly isolated *ex vivo*, they were subsequently expanded in presence of IL-2 and tumour debris as a source of tumour antigen. A common feature of dysfunctional TILs is their inability to proliferate. When given the opportunity of expansion *in vitro*, all of the TILs assessed with the cytotoxic assay had the ability to proliferate. As recorded in the results, there were many patient-TIL samples that failed to expand in culture. This could be attributed to the area of the tumour section, which may have been necrotic or may simply not have had enough immune cells to expand. However this was accounted for in our protocol, with multiple cultures established with a tumour fragment provided. Sometimes heterogeneity of the tumour fragment would be observed where only a few wells would proliferate. But in those tumours where no TIL proliferation occurred, the autologous tumouroids established would grow rapidly. Although these observations are at present anecdotal findings and not experimentally controlled, it does suggest that the TILs are likely under tumour control *in vivo* and unable to function normally. When removed from this TME and then provided with the opportunity to proliferate in culture, TILs are functional without the constant competition of tumour cells with potential inhibitory mechanisms at play. Nevertheless, they may not have been tumour specific as others have found many TILs are bystanders (Simoni *et al*., 2018).

To assess if these expanded TILs could be enhanced with the addition of CBI, anti-PD-1 blockade was evaluated in the context of the immune co-culture, *ex vivo*. It is important to note that in these studies, all patients assessed had microsatellite stable tumours, which are known to not respond to CBI. PD-1 expression was confirmed by flow cytometry, however compared to *in situ* expression levels on T-cells from CRLM of 15-75%, expanded TILs ranged from 0-15%. PD-L1 expression was also evaluated on the culture tumouroids, with no endogenous expression. Following stimulation with IFNγ, upregulation of MHC-I and PD-L1 can be observed. Unfortunately this methodology was only realised after completing the CRLM cytotoxic assay co-culture experiments. Therefore, it may be possible that without PD-L1 expression, addition of anti-PD-1 antibody will not affect killing, because the axis is not present to manipulate. Future experiments will therefore aim to include these conditions to account for PD-L1.

There is growing evidence to suggest that those TILs that are unable to exert effector functions, and are not rescued by CBI, are therefore intrinsically dysfunctional. Comprehensive rescue of function by CBI was observed only in one MSS rectal cancer sample, which demonstrates that some MSS tumours have the ability to respond (Kong, 2018). Those tumours with immune cells that do not kill and cannot be rescued by CBI therefore exhibit dysfunction. Whether or not this is reversible is a pressing area that should be focused on in the field.

One final measurement of TIL function utilised in the assay was production of cytokines secreted into the supernatant. Of particular interest is production of IFNγ and TNFα as effector cytokines. Tumouroids and TILs alone produced minimal IFNγ levels (<20 pg/mL) however the addition of anti-PD-1 antibody increased this a modest two to three-fold over time. These data indicate that although the TILs are able to kill the tumouroid as seen in the cytotoxic assay, there is an inability to produce robust levels of IFNγ. However, despite not observing an improved killing capacity, an induction of IFNγ production is observed with the addition of anti-PD-1. This phenomenon has been documented previously, where cytotoxic lymphocytes that lacked perforin-dependent machinery were unable to kill target cells. Instead these cytotoxic lymphocytes entered a state of hypersecretion of inflammatory cytokines including IFNγ production (M. R. Jenkins *et al*., 2015). Therefore this state is what was observed with the addition of anti-PD-1 antibody, where no enhanced killing was observed but enhanced secretion of IFNγ occurred. In the context of the TME this is not ideal as IFNγ can induce PD-L1 expression on tumour cells. This phenomenon has been demonstrated in recent experiments in the Ramsay lab where tumouroids and TILs were co-cultured together and secreted IFNγ by the TILs resulted in PD-L1 expression on the tumouroids. Perhaps these are some of the mechanisms at play by which CBI is not effective in

MSS tumours, as it creates a more immune-evasive phenotype rather than a direct enhancement of a cytotoxic environment.

Collectively these data presented in **Chapter 4** suggest that the metastatic site has an infiltration of CD3+ T-cells. The majority of these cells are CD4+ and the T-reg population (CD4+Foxp3+) is also increased in the tumour compared to 'normal' liver. Cytotoxic NK, NKT and CD8+ T-cells are reduced in the tumour compared to liver, but are nonetheless still present and remain unable to exert effector functions *in situ*. A recent study by Scheper *et al* documented a limited number of tumour-reactive TCR clones of CD8+ T-cell infiltrating the tumour. Therefore, despite high numbers of TILs there may only be a select few TCR clones that react to the tumour specifically. Such observations firstly highlight the concept of quantity versus quality, that despite high numbers of TILs it does not indicate they are tumour specific and functional. Secondly, it suggests T-cells present that are not tumour specific are likely to play a bystander role. Simoni *et al* recently investigated this concept, where they identified CD39+ as a marker of tumour-specific T-cells. It was discovered that CD8+ T-cells infiltrated lung and CRC tumours and only those that were not tumour specific and were CD39- lacked hallmarks of chronic antigen stimulation, classifying them as bystanders (Simoni *et al*., 2018). Bystander cells are therefore not tumour specific, but they nonetheless have the ability to infiltrate the tumour and contribute to the TME. It would seem that discerning the exact role bystander cells play is just as important as interrogating the tumour specific cells.

One type of non-classical CD8+ T-cell is a MAIT cell (Gherardin, Souter, *et al*., 2018). This is a cell population that is beginning to be accounted for in CRC. It is possible that MAIT cells also play a bystander role in the TME. MAIT cells are abundant in the liver, comprising between 30-50% of T-cells. The role of MAIT cells in the context of tumour is gradually being uncovered. A recent publication by Shaler *et al* found that MAIT cells in CRLM were reduced in the tumour and functionally impaired with reduced IFNγ production (Shaler, Tun-Abraham, *et al*., 2017). I confirmed this with my findings of MAIT cells being reduced in the tumour of CRLM compared to surrounding normal liver, outlined in **Chapter 5**. Some patient tumours harboured more MAIT cells than others. Interrogating why some tumours had high MAIT infiltrate would be of benefit to understand whether they are functional or not. It is plausible that bacterial ligands may be present in context with the tumour, due to the tissue (e.g. vessels) disruption by tumour growth. To address this; tumours could be probed for 16S rRNA genes, which can detect bacterial gene sequences and could provide insight into reasons MAIT cells may be present. In this context, MAIT cells would be considered bystanders within the TME. Once again, it is unlikely that MAIT cells are specific for tumour cells, but these data suggest that MAIT cells still have the ability to infiltrate and may influence the TME.

What was determined from the evaluation of MAIT cells in the tumour was the majority of MAIT cells were CD8+ and this is a sub-population of CD8+ cells that have not been previously accounted for. MAIT cell PD-1 expression was comparable between the tumour and liver and, therefore, in this context they are likely to be activated rather than exhausted as those MAIT cells in the liver are presumed to be normal. Expression of CD69 on MAIT cells was also comparable between the tumour and liver, but most importantly, MAIT cells in the tissue are distinct from those in the peripheral blood.

When assessing the ability of donor peripheral MAIT cells to kill tumouroids *in vitro*, utilising the cytotoxic assay, unstimulated MAIT cells were able to kill tumouroids. This was independent of MR1, and the mechanism of recognition and inducing cytotoxicity is still unknown. MAIT cells are also known to have NK cell receptors (Gherardin, Souter, *et al*., 2018), which have not been investigated in this study, but should be in the future. Determining the role of this previously undefined population of CD8+ T-cells is still yet to be determined. This is a population that is abundant in the liver and needs to be functionally understood in the context of tumours arising in the liver.

## 6.1 SUMMARY

CRC that has metastasised is the most advanced stage of the disease. Only 20% of patients are deemed resectable at time of diagnosis (Manfredi *et al*., 2006). Even though surgical resection offers improved five-year survival, recurrence frequently occurs. Understanding the progression of disease from the primary tumour to the metastatic lesion is critical to improve clinical management of these patients.

From this body of work, it is apparent that advanced CRC disease in the metastatic setting has progressed beyond immune control. Determining the mechanism of progression from primary to metastatic lesions highlights targetable stages in this sequence. In the primary tumour of *de novo* mCRC patients, CD8+ T-cells do not offer a survival benefit indicating an inability to control tumour growth.

In the metastatic tumours that have progressed to the liver, the immune context is tipped towards a suppressive phenotype, with a reduced infiltration of cytotoxic T-cells. In a milieu such as this, immune-mediated tumour control is impeded with these suppressive factors at play. Assessing the cytotoxic capability of TILs provides functional assessment and demonstrates that some of these TILs are able to mount a cytotoxic response, when removed from the immunosuppressive

environment *ex vivo*. This further highlights the influence of tumour control over the immune response.

Finally this work has identified a novel subset of CD8+ T-cells that were not previously accounted for in the context of the Immunoscore, quantifying conventional CD8+ T-cells. This subset of cells known as MAIT cells are abundant in the liver and have the capacity to kill patient-derived tumouroids *ex vivo*, highlighting them as a cell type that may potentially be targeted immunotherapeutically.

Improving patient outcome in the setting of metastasis is challenging, yet this work highlights some avenues to pursue in the context of immunotherapies in patients with CRLM.

## 6.2 FUTURE DIRECTIONS

### 6.2.1 Interrogating the Specificity of Infiltrating CD8+ T-cells

Since its fruition, the concept of this study has been to interrogate the difference between quantity and quality of TILs. The Immunoscore does not inform the quality of the TILs. It informs clinicians of prognosis but does not actually guide therapeutic options. As I found in **Chapter 3**, despite the number of TILs being present it does not equate to tumour control or survival advantage in the metastatic setting of CRC. Currently the field defines a solid tumour as either 'hot' or 'cold' in regards to immune infiltrate. However the quality of the TILs in terms of their effector function really needs to be taken into account. Additionally their tumour specificity also needs to be considered, as with recent studies it is apparent that only a small proportion of TILs are actually tumour reactive. This approach from a clinical perspective would involve phenotyping the TIL from patients using high-throughput analysis including mass cytometry (CyTOF), where >30 parameters can be assessed in one sample, such a technique is feasible to achieve rapid results following surgerySequencing TCR's from patient tumours would also provide insight into tumour-reactive T-cells, however this may take analytical time and would be expensive. Tumouroid and immune cell co-cultures such as the one we've developed is a novel platform to investigate the dynamic interactions between immune cells and tumouroids. Transcriptomic sequencing of the immune cells and tumouroids after co-culture would further highlight transcriptional reprogramming the immune and tumour cells undergo, after exposure to one another. This would perhaps highlight pathways of immune-resistance and immune evasion by tumour cells and thus pathways that could be targeted therapeutically.

### 6.2.2 Therapeutic Strategies to Improve Immunogenicity of Tumours

Currently in the immuno-oncology field, the focus is targeting the immune cells to exert effector functions. This is still important but imperative that the field focuses on increasing the

immunogenicity of the tumour. We must not forget the importance of chemotherapy and radiotherapy to achieve this. Destruction of the tumour cells via these therapies exposes the immune cells to neoantigens and improves immunogeneic responses. However these therapies should also not be considered to be mutually exclusive. Combination therapies of immune checkpoints in line with chemotherapy and/or radiotherapy may see improved efficacy of both of these treatments. Another avenue to increase immunogenicity of the tumour is the use of vaccines against tumour cells to prime the immune response. Vaccines such as DNA-based vaccines are currently in trials including MYPHISMO as Peter MacCallum Cancer Centre. Again these approaches may not have been effective as single agents, but now in the era of CBI these approaches are potentially more efficacious. First boosting the immune response with a vaccine, and then having checkpoint blockade antibodies to ensure immune evasion by the tumour cells does not occur, theoretically should enhance efficacy.

Finally, we are now in an era where CAR T-cells have been approved by the federal drug association (FDA) and are being used in the clinic for haematological malignancies. Strong efforts are now being pursued to improve efficacy of these therapies in the solid tumour setting. Therefore utilising other endogenous immune cells that may not be tumour specific, but classify, as bystander cells should be exploited. This has been addressed in the efficacy of CAR T-cell therapy in combination with inhibitors of apoptosis protein (IAP) antagonists. This combination enhanced tumour death by sensitising tumour cells to TNFα, resulting in indirect bystander killing (Michie *et al*., 2019).

### 6.2.3 Utilising Bystander Immune Cells Therapeutically

Bystander cells are those cells that are present within the tumour but are not exclusively tumour reactive. That isn't to say they do not influence to TME, and they likely have the ability to do this by secreting cytokines. One kind of potential bystander cell within the TME of CRLM tumours are MAIT cells. The abundance of MAIT cells in both the liver and peripheral blood and the ability of these cells to rapidly secrete cytokine and have cytotoxic function make them attractive cells to therapeutically target. MAIT cells may indeed be ideal CAR T-cells for these reasons. The other advantage of these cells is they do not function through MHC-I, but are restricted to MR1 and this means that if used as a CAR T-cell, healthy donors of MAIT cells that can function in an allogeneic setting (Godfrey *et al*., 2018). Embarking on their use therapeutically requires further investigation and this stems from understanding their role in the TME, which this body of work has contributed to.

## 6.3 CONCLUDING SUMMARY

Patients with advanced stage CRC have a significantly poorer prognosis compared to those patients with earlier stage CRC. Therefore, investigating the biology of these tumours both at the primary and metastatic site is integral to improve therapeutic options. In the era of immunotherapies, understanding the immune response is key to gain insight into these dynamic immune interactions occurring during tumour progression. What this body of work has found is that tumours in the advanced setting of CRC have evaded the immune response. This is evidenced by the findings that cytotoxic CD8+ T-cell infiltrate in primary tumours of *de novo* mCRC patients no longer affects OS, as what is observed in earlier stages of CRC. The immune context at the metastatic site in CRLM tumours is angled towards an immunosuppressive phenotype and reduced cytotoxic immune environment. Thus indicating these tumours have the ability to suppress the effector function of immune cells, and the TME is immunosuppressive. Efforts in altering this balance should therefore be made, with focus on counteracting the suppressive immune cells and improving the immunogenicity of tumours so they are more recognisable by the cytotoxic immune cells. Targeting other immune cells that can rapidly respond within the TME is another strategy that should be focused on, particularly in the era of CAR T-cell therapy. Improving knowledge of these immune responses in mCRC patients is crucial to improving treatment options and clinical outcome.

## 7. BIBLIOGRAPHY


Abraham, C., & Cho, J. H. (2009). Inflammatory bowel disease. *N Engl J Med, 361*(21), 2066-2078. doi:10.1056/NEJMra0804647

Ahmadzadeh, M., Johnson, L. A., Heemskerk, B., Wunderlich, J. R., Dudley, M. E., White, D. E., & Rosenberg, S. A. (2009). Tumor antigen-specific CD8 T cells infiltrating the tumor express high levels of PD-1 and are functionally impaired. *Blood, 114*(8), 1537-1544. doi:10.1182/blood-2008-12-195792

Alexander, J., Watanabe, T., Wu, T. T., Rashid, A., Li, S., & Hamilton, S. R. (2001). Histopathological identification of colon cancer with microsatellite instability. *Am J Pathol, 158*(2), 527-535. doi:10.1016/S0002-9440(10)63994-6

Alitalo, K., Winqvist, R., Lin, C. C., de la Chapelle, A., Schwab, M., & Bishop, J. M. (1984). Aberrant expression of an amplified c-myb oncogene in two cell lines from a colon carcinoma. *Proc Natl Acad Sci U S A, 81*(14), 4534-4538.

Alroy, I., & Yarden, Y. (1997). The ErbB signaling network in embryogenesis and oncogenesis: signal diversification through combinatorial ligand-receptor interactions. *FEBS Lett, 410*(1), 83-86.

Alsaab, H. O., Sau, S., Alzhrani, R., Tatiparti, K., Bhise, K., Kashaw, S. K., & Iyer, A. K. (2017). PD-1 and PD-L1 Checkpoint Signaling Inhibition for Cancer Immunotherapy: Mechanism, Combinations, and Clinical Outcome. *Front Pharmacol, 8*, 561. doi:10.3389/fphar.2017.00561

Altman, J. B., Benavides, A. D., Das, R., & Bassiri, H. (2015). Antitumor Responses of Invariant Natural Killer T Cells. *J Immunol Res, 2015*, 652875. doi:10.1155/2015/652875

Andre, T., Bensmaine, M. A., Louvet, C., Francois, E., Lucas, V., Desseigne, F., . . . de Gramont, A. (1999). Multicenter phase II study of bimonthly high-dose leucovorin, fluorouracil infusion, and oxaliplatin for metastatic colorectal cancer resistant to the same leucovorin and fluorouracil regimen. *J Clin Oncol, 17*(11), 3560-3568. doi:10.1200/JCO.1999.17.11.3560

Andre, T., Boni, C., Mounedji-Boudiaf, L., Navarro, M., Tabernero, J., Hickish, T., . . . Multicenter International Study of Oxaliplatin/5-Fluorouracil/Leucovorin in the Adjuvant Treatment of Colon Cancer, I. (2004). Oxaliplatin, fluorouracil, and leucovorin as adjuvant treatment for colon cancer. *N Engl J Med, 350*(23), 2343-2351. doi:10.1056/NEJMoa032709

Aparicio, S., Hidalgo, M., & Kung, A. L. (2015). Examining the utility of patient-derived xenograft mouse models. *Nat Rev Cancer, 15*(5), 311-316. doi:10.1038/nrc3944

Atreya, I., & Neurath, M. F. (2008). Immune cells in colorectal cancer: prognostic relevance and therapeutic strategies. *Expert Rev Anticancer Ther, 8*(4), 561-572. doi:10.1586/14737140.8.4.561

Baker, S. J., Fearon, E. R., Nigro, J. M., Hamilton, S. R., Preisinger, A. C., Jessup, J. M., . . . Vogelstein, B. (1989). Chromosome 17 deletions and p53 gene mutations in colorectal carcinomas. *Science, 244*(4901), 217-221.

Balch, C. M., Riley, L. B., Bae, Y. J., Salmeron, M. A., Platsoucas, C. D., von Eschenbach, A., & Itoh, K. (1990). Patterns of human tumor-infiltrating lymphocytes in 120 human cancers. *Arch Surg, 125*(2), 200-205.

Balkwill, F., & Mantovani, A. (2001). Inflammation and cancer: back to Virchow? *Lancet, 357*(9255), 539-545. doi:10.1016/S0140-6736(00)04046-0

Banki, Z., Krabbendam, L., Klaver, D., Leng, T., Kruis, S., Mehta, H., . . . Klenerman, P. (2019). Antibody opsonization enhances MAIT cell responsiveness to bacteria via a TNF-dependent mechanism. *Immunol Cell Biol*. doi:10.1111/imcb.12239

Barber, D. L., Wherry, E. J., Masopust, D., Zhu, B., Allison, J. P., Sharpe, A. H., . . . Ahmed, R. (2006). Restoring function in exhausted CD8 T cells during chronic viral infection. *Nature, 439*(7077), 682-687. doi:10.1038/nature04444

Becht, E., Giraldo, N. A., Dieu-Nosjean, M. C., Sautes-Fridman, C., & Fridman, W. H. (2016). Cancer immune contexture and immunotherapy. *Curr Opin Immunol, 39*, 7-13. doi:10.1016/j.coi.2015.11.009

Benson, A. B., 3rd, Venook, A. P., Al-Hawary, M. M., Cederquist, L., Chen, Y. J., Ciombor, K. K., . . . Freedman-Cass, D. A. (2018). NCCN Guidelines Insights: Colon Cancer, Version 2.2018. *J Natl Compr Canc Netw, 16*(4), 359-369. doi:10.6004/jnccn.2018.0021

Bilchik, A. J., Poston, G., Adam, R., & Choti, M. A. (2008). Prognostic variables for resection of colorectal cancer hepatic metastases: an evolving paradigm. *J Clin Oncol, 26*(33), 5320-5321. doi:10.1200/JCO.2008.18.3152

Biron, C. A., Nguyen, K. B., Pien, G. C., Cousens, L. P., & Salazar-Mather, T. P. (1999). Natural killer cells in antiviral defense: function and regulation by innate cytokines. *Annu Rev Immunol, 17*, 189-220. doi:10.1146/annurev.immunol.17.1.189

Blank, C., Brown, I., Peterson, A. C., Spiotto, M., Iwai, Y., Honjo, T., & Gajewski, T. F. (2004). PD-L1/B7H-1 inhibits the effector phase of tumor rejection by T cell receptor (TCR) transgenic CD8+ T cells. *Cancer Res, 64*(3), 1140-1145.

Blansfield, J. A., Beck, K. E., Tran, K., Yang, J. C., Hughes, M. S., Kammula, U. S., . . . Sherry, R. M. (2005). Cytotoxic T-lymphocyte-associated antigen-4 blockage can induce autoimmune hypophysitis in patients with metastatic melanoma and renal cancer. *J Immunother, 28*(6), 593-598.

Boland, C. R., & Goel, A. (2010). Microsatellite instability in colorectal cancer. *Gastroenterology, 138*(6), 2073-2087 e2073. doi:10.1053/j.gastro.2009.12.064

Booth, J. S., Salerno-Goncalves, R., Blanchard, T. G., Patil, S. A., Kader, H. A., Safta, A. M., . . . Sztein, M. B. (2015). Mucosal-Associated Invariant T Cells in the Human Gastric Mucosa and Blood: Role in Helicobacter pylori Infection. *Front Immunol, 6*, 466. doi:10.3389/fimmu.2015.00466

Boyle, P., & Langman, J. S. (2000). ABC of colorectal cancer: Epidemiology. *BMJ, 321*(7264), 805-808.

Brennan, P. J., Brigl, M., & Brenner, M. B. (2013). Invariant natural killer T cells: an innate activation scheme linked to diverse effector functions. *Nat Rev Immunol, 13*(2), 101-117. doi:10.1038/nri3369

Brunner, K. T., Mauel, J., Cerottini, J. C., & Chapuis, B. (1968). Quantitative assay of the lytic action of immune lymphoid cells on 51-Cr-labelled allogeneic target cells *in vitro*; inhibition by isoantibody and by drugs. *Immunology, 14*(2), 181-196.

Bubenik, J. (2003). Tumour MHC class I downregulation and immunotherapy (Review). *Oncol Rep, 10*(6), 2005-2008.

Burnet, F. M. (1970). The concept of immunological surveillance. *Prog Exp Tumor Res, 13*, 1-27.

Burnet, M. (1957). Cancer; a biological approach. I. The processes of control. *Br Med J, 1*(5022), 779-786.

Cady, B., Jenkins, R. L., Steele, G. D., Jr., Lewis, W. D., Stone, M. D., McDermott, W. V., . . . Linehan, D. C. (1998). Surgical margin in hepatic resection for colorectal metastasis: a critical and improvable determinant of outcome. *Ann Surg, 227*(4), 566-571.

Cancer, A. J. C. o. (2010). *Colon and Rectum Cancer Staging*. Retrieved from https://cancerstaging.org/references-tools/quickreferences/Documents/ColonSmall.pdf

Chambers, A. F., Groom, A. C., & MacDonald, I. C. (2002). Dissemination and growth of cancer cells in metastatic sites. *Nat Rev Cancer, 2*(8), 563-572. doi:10.1038/nrc865

Chang, G. J., Rodriguez-Bigas, M. A., Skibber, J. M., & Moyer, V. A. (2007). Lymph node evaluation and survival after curative resection of colon cancer: systematic review. *J Natl Cancer Inst, 99*(6), 433-441. doi:10.1093/jnci/djk092

Chavez-Galan, L., Arenas-Del Angel, M. C., Zenteno, E., Chavez, R., & Lascurain, R. (2009). Cell death mechanisms induced by cytotoxic lymphocytes. *Cell Mol Immunol, 6*(1), 15-25. doi:10.1038/cmi.2009.3

Choti, M. A., Sitzmann, J. V., Tiburi, M. F., Sumetchotimetha, W., Rangsin, R., Schulick, R. D., . . . Cameron, J. L. (2002). Trends in long-term survival following liver resection for hepatic colorectal metastases. *Ann Surg, 235*(6), 759-766.

Coquet, J. M., Chakravarti, S., Kyparissoudis, K., McNab, F. W., Pitt, L. A., McKenzie, B. S., . . . Godfrey, D. I. (2008). Diverse cytokine production by NKT cell subsets and identification of an IL-17-producing CD4-NK1.1- NKT cell population. *Proc Natl Acad Sci U S A, 105*(32), 11287-11292. doi:10.1073/pnas.0801631105

Corbett, A. J., Eckle, S. B., Birkinshaw, R. W., Liu, L., Patel, O., Mahony, J., . . . McCluskey, J. (2014). T-cell activation by transitory neo-antigens derived from distinct microbial pathways. *Nature, 509*(7500), 361-365. doi:10.1038/nature13160

Cox, A. D., Fesik, S. W., Kimmelman, A. C., Luo, J., & Der, C. J. (2014). Drugging the undruggable RAS: Mission possible? *Nat Rev Drug Discov, 13*(11), 828-851. doi:10.1038/nrd4389

D'Angelica, M., Brennan, M. F., Fortner, J. G., Cohen, A. M., Blumgart, L. H., & Fong, Y. (1997). Ninety-six five-year survivors after liver resection for metastatic colorectal cancer. *J Am Coll Surg, 185*(6), 554-559.

D'Incecco, A., Andreozzi, M., Ludovini, V., Rossi, E., Capodanno, A., Landi, L., . . . Cappuzzo, F. (2015). PD-1 and PD-L1 expression in molecularly selected non-small-cell lung cancer patients. *Br J Cancer, 112*(1), 95-102. doi:10.1038/bjc.2014.555

de Gramont, A., Figer, A., Seymour, M., Homerin, M., Hmissi, A., Cassidy, J., . . . Bonetti, A. (2000). Leucovorin and fluorouracil with or without oxaliplatin as first-line treatment in advanced colorectal cancer. *J Clin Oncol, 18*(16), 2938-2947. doi:10.1200/JCO.2000.18.16.2938

Deb, S., Xu, H., Tuynman, J., George, J., Yan, Y., Li, J., . . . Fox, S. B. (2014). RAD21 cohesin overexpression is a prognostic and predictive marker exacerbating poor prognosis in KRAS mutant colorectal carcinomas. *Br J Cancer, 110*(6), 1606-1613. doi:10.1038/bjc.2014.31

Dienstmann, R., Vermeulen, L., Guinney, J., Kopetz, S., Tejpar, S., & Tabernero, J. (2017). Consensus molecular subtypes and the evolution of precision medicine in colorectal cancer. *Nat Rev Cancer, 17*(4), 268. doi:10.1038/nrc.2017.24

Dijkstra, K. K., Cattaneo, C. M., Weeber, F., Chalabi, M., van de Haar, J., Fanchi, L. F., . . . Voest, E. E. (2018). Generation of Tumor-Reactive T Cells by Co-culture of Peripheral Blood Lymphocytes and Tumor Organoids. *Cell, 174*(6), 1586-1598 e1512. doi:10.1016/j.cell.2018.07.009

Dinh, T. A., Rosner, B. I., Atwood, J. C., Boland, C. R., Syngal, S., Vasen, H. F., . . . Burt, R. W. (2011). Health benefits and cost-effectiveness of primary genetic screening for Lynch syndrome in the general population. *Cancer Prev Res (Phila), 4*(1), 9-22. doi:10.1158/1940-6207.CAPR-10-0262

Dolcetti, R., Viel, A., Doglioni, C., Russo, A., Guidoboni, M., Capozzi, E., . . . Boiocchi, M. (1999). High prevalence of activated intraepithelial cytotoxic T lymphocytes and increased neoplastic cell apoptosis in colorectal carcinomas with microsatellite instability. *Am J Pathol, 154*(6), 1805-1813. doi:10.1016/S0002-9440(10)65436-3

Dong, H., Strome, S. E., Salomao, D. R., Tamura, H., Hirano, F., Flies, D. B., . . . Chen, L. (2002). Tumor-associated B7-H1 promotes T-cell apoptosis: a potential mechanism of immune evasion. *Nat Med, 8*(8), 793-800. doi:10.1038/nm730

Dorner, B. G., Smith, H. R., French, A. R., Kim, S., Poursine-Laurent, J., Beckman, D. L., . . . Yokoyama, W. M. (2004). Coordinate expression of cytokines and chemokines by NK cells during murine cytomegalovirus infection. *J Immunol, 172*(5), 3119-3131.

Duan, M., Goswami, S., Shi, J. Y., Wu, L. J., Wang, X. Y., Ma, J. Q., . . . Gao, Q. (2019). Activated and Exhausted MAIT Cells Foster Disease Progression and Indicate Poor Outcome in Hepatocellular Carcinoma. *Clin Cancer Res*. doi:10.1158/1078-0432.CCR-18-3040

Dunn, G. P., Bruce, A. T., Ikeda, H., Old, L. J., & Schreiber, R. D. (2002). Cancer immunoediting: from immunosurveillance to tumor escape. *Nat Immunol, 3*(11), 991-998. doi:10.1038/ni1102-991

Dusseaux, M., Martin, E., Serriari, N., Peguillet, I., Premel, V., Louis, D., . . . Lantz, O. (2011). Human MAIT cells are xenobiotic-resistant, tissue-targeted, CD161hi IL-17-secreting T cells. *Blood, 117*(4), 1250-1259. doi:10.1182/blood-2010-08-303339

Fearon, D. T., & Locksley, R. M. (1996). The instructive role of innate immunity in the acquired immune response. *Science, 272*(5258), 50-53.

Fearon, E. R., & Vogelstein, B. (1990). A genetic model for colorectal tumorigenesis. *Cell, 61*(5), 759-767.

Ferlazzo, G., Tsang, M. L., Moretta, L., Melioli, G., Steinman, R. M., & Munz, C. (2002). Human dendritic cells activate resting natural killer (NK) cells and are recognized via the NKp30 receptor by activated NK cells. *J Exp Med, 195*(3), 343-351.

Ferrara, N., Gerber, H. P., & LeCouter, J. (2003). The biology of VEGF and its receptors. *Nat Med, 9*(6), 669-676. doi:10.1038/nm0603-669

Finley, G. G., Schulz, N. T., Hill, S. A., Geiser, J. R., Pipas, J. M., & Meisler, A. I. (1989). Expression of the myc gene family in different stages of human colorectal cancer. *Oncogene, 4*(8), 963-971.

Folprecht, G., Gruenberger, T., Bechstein, W. O., Raab, H. R., Lordick, F., Hartmann, J. T., . . . Kohne, C. H. (2010). Tumour response and secondary resectability of colorectal liver metastases following neoadjuvant chemotherapy with cetuximab: the CELIM randomised phase 2 trial. *Lancet Oncol, 11*(1), 38-47. doi:10.1016/S1470-2045(09)70330-4

Fong, Y., Cohen, A. M., Fortner, J. G., Enker, W. E., Turnbull, A. D., Coit, D. G., . . . Brennan, M. F. (1997). Liver resection for colorectal metastases. *J Clin Oncol, 15*(3), 938-946. doi:10.1200/JCO.1997.15.3.938

Fong, Y., Fortner, J., Sun, R. L., Brennan, M. F., & Blumgart, L. H. (1999). Clinical score for predicting recurrence after hepatic resection for metastatic colorectal cancer: analysis of 1001 consecutive cases. *Ann Surg, 230*(3), 309-318; discussion 318-321.

Forde, P. M., Chaft, J. E., Smith, K. N., Anagnostou, V., Cottrell, T. R., Hellmann, M. D., . . . Pardoll, D. M. (2018). Neoadjuvant PD-1 Blockade in Resectable Lung Cancer. *N Engl J Med, 378*(21), 1976-1986. doi:10.1056/NEJMoa1716078

Freeman, G. J., Long, A. J., Iwai, Y., Bourque, K., Chernova, T., Nishimura, H., . . . Honjo, T. (2000). Engagement of the PD-1 immunoinhibitory receptor by a novel B7 family member leads to negative regulation of lymphocyte activation. *J Exp Med, 192*(7), 1027-1034.

Fridman, W. H., Pages, F., Sautes-Fridman, C., & Galon, J. (2012). The immune contexture in human tumours: impact on clinical outcome. *Nat Rev Cancer, 12*(4), 298-306. doi:10.1038/nrc3245

Friedl, P., & Wolf, K. (2003). Tumour-cell invasion and migration: diversity and escape mechanisms. *Nat Rev Cancer, 3*(5), 362-374. doi:10.1038/nrc1075

Frigault, M. M., Lacoste, J., Swift, J. L., & Brown, C. M. (2009). Live-cell microscopy - tips and tools. *J Cell Sci, 122*(Pt 6), 753-767. doi:10.1242/jcs.033837

Fujii, M., Shimokawa, M., Date, S., Takano, A., Matano, M., Nanki, K., . . . Sato, T. (2016). A Colorectal Tumor Organoid Library Demonstrates Progressive Loss of Niche Factor Requirements during Tumorigenesis. *Cell Stem Cell, 18*(6), 827-838. doi:10.1016/j.stem.2016.04.003

Fujii, S., Shimizu, K., Smith, C., Bonifaz, L., & Steinman, R. M. (2003). Activation of natural killer T cells by alpha-galactosylceramide rapidly induces the full maturation of dendritic cells *in vivo* and thereby acts as an adjuvant for combined CD4 and CD8 T cell immunity to a coadministered protein. *J Exp Med, 198*(2), 267-279. doi:10.1084/jem.20030324

Galon, J., Angell, H. K., Bedognetti, D., & Marincola, F. M. (2013). The continuum of cancer immunosurveillance: prognostic, predictive, and mechanistic signatures. *Immunity, 39*(1), 11-26. doi:10.1016/j.immuni.2013.07.008

Galon, J., Costes, A., Sanchez-Cabo, F., Kirilovsky, A., Mlecnik, B., Lagorce-Pages, C., . . . Pages, F. (2006). Type, density, and location of immune cells within human colorectal

tumors predict clinical outcome. *Science, 313*(5795), 1960-1964. doi:10.1126/science.1129139
Galon, J., Fridman, W. H., & Pages, F. (2007). The adaptive immunologic microenvironment in colorectal cancer: a novel perspective. *Cancer Res, 67*(5), 1883-1886. doi:10.1158/0008-5472.CAN-06-4806
Garcia-Lora, A., Algarra, I., & Garrido, F. (2003). MHC class I antigens, immune surveillance, and tumor immune escape. *J Cell Physiol, 195*(3), 346-355. doi:10.1002/jcp.10290
Gatalica, Z., Snyder, C., Maney, T., Ghazalpour, A., Holterman, D. A., Xiao, N., . . . Hamid, O. (2014). Programmed cell death 1 (PD-1) and its ligand (PD-L1) in common cancers and their correlation with molecular cancer type. *Cancer Epidemiol Biomarkers Prev, 23*(12), 2965-2970. doi:10.1158/1055-9965.EPI-14-0654
Gayowski, T. J., Iwatsuki, S., Madariaga, J. R., Selby, R., Todo, S., Irish, W., & Starzl, T. E. (1994). Experience in hepatic resection for metastatic colorectal cancer: analysis of clinical and pathologic risk factors. *Surgery, 116*(4), 703-710; discussion 710-701.
Gerosa, F., Baldani-Guerra, B., Nisii, C., Marchesini, V., Carra, G., & Trinchieri, G. (2002). Reciprocal activating interaction between natural killer cells and dendritic cells. *J Exp Med, 195*(3), 327-333.
Gherardin, N. A., Loh, L., Admojo, L., Davenport, A. J., Richardson, K., Rogers, A., . . . Godfrey, D. I. (2018). Enumeration, functional responses and cytotoxic capacity of MAIT cells in newly diagnosed and relapsed multiple myeloma. *Sci Rep, 8*(1), 4159. doi:10.1038/s41598-018-22130-1
Gherardin, N. A., McCluskey, J., Rossjohn, J., & Godfrey, D. I. (2018). The Diverse Family of MR1-Restricted T Cells. *J Immunol, 201*(10), 2862-2871. doi:10.4049/jimmunol.1801091
Gherardin, N. A., Souter, M. N., Koay, H. F., Mangas, K. M., Seemann, T., Stinear, T. P., . . . Godfrey, D. I. (2018). Human blood MAIT cell subsets defined using MR1 tetramers. *Immunol Cell Biol, 96*(5), 507-525. doi:10.1111/imcb.12021
Gilboa, E. (1999). The makings of a tumor rejection antigen. *Immunity, 11*(3), 263-270.
Girardi, M., Oppenheim, D. E., Steele, C. R., Lewis, J. M., Glusac, E., Filler, R., . . . Hayday, A. C. (2018). Pillars Article: Regulation of Cutaneous Malignancy by gammadelta T Cells. Science. 2001. 294: 605-609. *J Immunol, 200*(9), 3031-3035.
Gismondi, A., Stabile, H., Nisti, P., & Santoni, A. (2015). Effector Functions of Natural Killer Cell Subsets in the Control of Hematological Malignancies. *Front Immunol, 6*, 567. doi:10.3389/fimmu.2015.00567
Godfrey, D. I., Le Nours, J., Andrews, D. M., Uldrich, A. P., & Rossjohn, J. (2018). Unconventional T Cell Targets for Cancer Immunotherapy. *Immunity, 48*(3), 453-473. doi:10.1016/j.immuni.2018.03.009
Gold, M. C., Cerri, S., Smyk-Pearson, S., Cansler, M. E., Vogt, T. M., Delepine, J., . . . Lewinsohn, D. M. (2010). Human mucosal associated invariant T cells detect bacterially infected cells. *PLoS Biol, 8*(6), e1000407. doi:10.1371/journal.pbio.1000407
Goldstein, J., Tran, B., Ensor, J., Gibbs, P., Wong, H. L., Wong, S. F., . . . Overman, M. J. (2014). Multicenter retrospective analysis of metastatic colorectal cancer (CRC) with high-level microsatellite instability (MSI-H). *Ann Oncol, 25*(5), 1032-1038. doi:10.1093/annonc/mdu100
Grady, W. M., & Carethers, J. M. (2008). Genomic and epigenetic instability in colorectal cancer pathogenesis. *Gastroenterology, 135*(4), 1079-1099. doi:10.1053/j.gastro.2008.07.076
Green, M. R., Monti, S., Rodig, S. J., Juszczynski, P., Currie, T., O'Donnell, E., . . . Shipp, M. A. (2010). Integrative analysis reveals selective 9p24.1 amplification, increased PD-1 ligand expression, and further induction via JAK2 in nodular sclerosing Hodgkin lymphoma and primary mediastinal large B-cell lymphoma. *Blood, 116*(17), 3268-3277. doi:10.1182/blood-2010-05-282780
Greenman, C., Stephens, P., Smith, R., Dalgliesh, G. L., Hunter, C., Bignell, G., . . . Stratton, M. R. (2007). Patterns of somatic mutation in human cancer genomes. *Nature, 446*(7132), 153-158. doi:10.1038/nature05610

Grivennikov, S. I., Wang, K., Mucida, D., Stewart, C. A., Schnabl, B., Jauch, D., . . . Karin, M. (2012). Adenoma-linked barrier defects and microbial products drive IL-23/IL-17-mediated tumour growth. *Nature, 491*(7423), 254-258. doi:10.1038/nature11465

Gryfe, R., Kim, H., Hsieh, E. T., Aronson, M. D., Holowaty, E. J., Bull, S. B., . . . Gallinger, S. (2000). Tumor microsatellite instability and clinical outcome in young patients with colorectal cancer. *N Engl J Med, 342*(2), 69-77. doi:10.1056/NEJM200001133420201

Guinney, J., Dienstmann, R., Wang, X., de Reynies, A., Schlicker, A., Soneson, C., . . . Tejpar, S. (2015). The consensus molecular subtypes of colorectal cancer. *Nat Med, 21*(11), 1350-1356. doi:10.1038/nm.3967

Gumperz, J. E., Miyake, S., Yamamura, T., & Brenner, M. B. (2002). Functionally distinct subsets of CD1d-restricted natural killer T cells revealed by CD1d tetramer staining. *J Exp Med, 195*(5), 625-636.

Habr-Gama, A., Perez, R. O., Nadalin, W., Sabbaga, J., Ribeiro, U., Jr., Silva e Sousa, A. H., Jr., . . . Gama-Rodrigues, J. (2004). Operative versus nonoperative treatment for stage 0 distal rectal cancer following chemoradiation therapy: long-term results. *Ann Surg, 240*(4), 711-717; discussion 717-718.

Halama, N., Michel, S., Kloor, M., Zoernig, I., Benner, A., Spille, A., . . . Jaeger, D. (2011). Localization and density of immune cells in the invasive margin of human colorectal cancer liver metastases are prognostic for response to chemotherapy. *Cancer Res, 71*(17), 5670-5677. doi:10.1158/0008-5472.CAN-11-0268

Hassett, M. J., Uno, H., Cronin, A. M., Carroll, N. M., Hornbrook, M. C., Fishman, P., & Ritzwoller, D. P. (2017). Survival after recurrence of stage I-III breast, colorectal, or lung cancer. *Cancer Epidemiol, 49*, 186-194. doi:10.1016/j.canep.2017.07.001

Hellmann, M. D., Ciuleanu, T. E., Pluzanski, A., Lee, J. S., Otterson, G. A., Audigier-Valette, C., . . . Paz-Ares, L. (2018). Nivolumab plus Ipilimumab in Lung Cancer with a High Tumor Mutational Burden. *N Engl J Med, 378*(22), 2093-2104. doi:10.1056/NEJMoa1801946

Herbst, R. S., Soria, J. C., Kowanetz, M., Fine, G. D., Hamid, O., Gordon, M. S., . . . Hodi, F. S. (2014). Predictive correlates of response to the anti-PD-L1 antibody MPDL3280A in cancer patients. *Nature, 515*(7528), 563-567. doi:10.1038/nature14011

Hidalgo, M., Amant, F., Biankin, A. V., Budinska, E., Byrne, A. T., Caldas, C., . . . Villanueva, A. (2014). Patient-derived xenograft models: an emerging platform for translational cancer research. *Cancer Discov, 4*(9), 998-1013. doi:10.1158/2159-8290.CD-14-0001

Hillingso, J. G., & Wille-Jorgensen, P. (2009). Staged or simultaneous resection of synchronous liver metastases from colorectal cancer--a systematic review. *Colorectal Dis, 11*(1), 3-10. doi:10.1111/j.1463-1318.2008.01625.x

House, A. K., & Watt, A. G. (1979). Survival and the immune response in patients with carcinoma of the colorectum. *Gut, 20*(10), 868-874.

Hurwitz, H., Fehrenbacher, L., Novotny, W., Cartwright, T., Hainsworth, J., Heim, W., . . . Kabbinavar, F. (2004). Bevacizumab plus irinotecan, fluorouracil, and leucovorin for metastatic colorectal cancer. *N Engl J Med, 350*(23), 2335-2342. doi:10.1056/NEJMoa032691

Ionov, Y., Peinado, M. A., Malkhosyan, S., Shibata, D., & Perucho, M. (1993). Ubiquitous somatic mutations in simple repeated sequences reveal a new mechanism for colonic carcinogenesis. *Nature, 363*(6429), 558-561. doi:10.1038/363558a0

Ishida, Y., Agata, Y., Shibahara, K., & Honjo, T. (1992). Induced expression of PD-1, a novel member of the immunoglobulin gene superfamily, upon programmed cell death. *EMBO J, 11*(11), 3887-3895.

Janeway, C. A., Jr., & Medzhitov, R. (2002). Innate immune recognition. *Annu Rev Immunol, 20*, 197-216. doi:10.1146/annurev.immunol.20.083001.084359

Jass, J. R. (1986). Lymphocytic infiltration and survival in rectal cancer. *J Clin Pathol, 39*(6), 585-589.

Jenkins, M. R., Rudd-Schmidt, J. A., Lopez, J. A., Ramsbottom, K. M., Mannering, S. I., Andrews, D. M., . . . Trapani, J. A. (2015). Failed CTL/NK cell killing and cytokine

hypersecretion are directly linked through prolonged synapse time. *J Exp Med, 212*(3), 307-317. doi:10.1084/jem.20140964

Jenkins, R. W., Aref, A. R., Lizotte, P. H., Ivanova, E., Stinson, S., Zhou, C. W., . . . Barbie, D. A. (2018). *Ex vivo* Profiling of PD-1 Blockade Using Organotypic Tumor Spheroids. *Cancer Discov, 8*(2), 196-215. doi:10.1158/2159-8290.CD-17-0833

Jess, T., Rungoe, C., & Peyrin-Biroulet, L. (2012). Risk of colorectal cancer in patients with ulcerative colitis: a meta-analysis of population-based cohort studies. *Clin Gastroenterol Hepatol, 10*(6), 639-645. doi:10.1016/j.cgh.2012.01.010

Jones, R. P., Vauthey, J. N., Adam, R., Rees, M., Berry, D., Jackson, R., . . . Malik, H. Z. (2012). Effect of specialist decision-making on treatment strategies for colorectal liver metastases. *Br J Surg, 99*(9), 1263-1269. doi:10.1002/bjs.8835

June, C. H., Bluestone, J. A., Nadler, L. M., & Thompson, C. B. (1994). The B7 and CD28 receptor families. *Immunol Today, 15*(7), 321-331. doi:10.1016/0167-5699(94)90080-9

Kabbinavar, F., Hurwitz, H. I., Fehrenbacher, L., Meropol, N. J., Novotny, W. F., Lieberman, G., . . . Bergsland, E. (2003). Phase II, randomized trial comparing bevacizumab plus fluorouracil (FU)/leucovorin (LV) with FU/LV alone in patients with metastatic colorectal cancer. *J Clin Oncol, 21*(1), 60-65. doi:10.1200/JCO.2003.10.066

Kane, M. F., Loda, M., Gaida, G. M., Lipman, J., Mishra, R., Goldman, H., . . . Kolodner, R. (1997). Methylation of the hMLH1 promoter correlates with lack of expression of hMLH1 in sporadic colon tumors and mismatch repair-defective human tumor cell lines. *Cancer Res, 57*(5), 808-811.

Karimi, M. A., Lee, E., Bachmann, M. H., Salicioni, A. M., Behrens, E. M., Kambayashi, T., & Baldwin, C. L. (2014). Measuring cytotoxicity by bioluminescence imaging outperforms the standard chromium-51 release assay. *PLoS One, 9*(2), e89357. doi:10.1371/journal.pone.0089357

Kataoka, K., Shiraishi, Y., Takeda, Y., Sakata, S., Matsumoto, M., Nagano, S., . . . Ogawa, S. (2016). Aberrant PD-L1 expression through 3'-UTR disruption in multiple cancers. *Nature, 534*(7607), 402-406. doi:10.1038/nature18294

Keir, M. E., Butte, M. J., Freeman, G. J., & Sharpe, A. H. (2008). PD-1 and its ligands in tolerance and immunity. *Annu Rev Immunol, 26*, 677-704. doi:10.1146/annurev.immunol.26.021607.090331

Kekelidze, M., D'Errico, L., Pansini, M., Tyndall, A., & Hohmann, J. (2013). Colorectal cancer: current imaging methods and future perspectives for the diagnosis, staging and therapeutic response evaluation. *World J Gastroenterol, 19*(46), 8502-8514. doi:10.3748/wjg.v19.i46.8502

Kim, K. A., Kakitani, M., Zhao, J., Oshima, T., Tang, T., Binnerts, M., . . . Tomizuka, K. (2005). Mitogenic influence of human R-spondin1 on the intestinal epithelium. *Science, 309*(5738), 1256-1259. doi:10.1126/science.1112521

Kim, K. J., Li, B., Winer, J., Armanini, M., Gillett, N., Phillips, H. S., & Ferrara, N. (1993). Inhibition of vascular endothelial growth factor-induced angiogenesis suppresses tumour growth *in vivo*. *Nature, 362*(6423), 841-844. doi:10.1038/362841a0

Kinzler, K. W., & Vogelstein, B. (1996). Lessons from hereditary colorectal cancer. *Cell, 87*(2), 159-170.

Kjer-Nielsen, L., Corbett, A. J., Chen, Z., Liu, L., Mak, J. Y., Godfrey, D. I., . . . Eckle, S. B. (2018). An overview on the identification of MAIT cell antigens. *Immunol Cell Biol, 96*(6), 573-587. doi:10.1111/imcb.12057

Kjer-Nielsen, L., Patel, O., Corbett, A. J., Le Nours, J., Meehan, B., Liu, L., . . . McCluskey, J. (2012). MR1 presents microbial vitamin B metabolites to MAIT cells. *Nature, 491*(7426), 717-723. doi:10.1038/nature11605

Koh, C., Freeman, V, Gormly, K, O'Rourke, N, Lee, P, Luck, A, Yan, T. (2017). *MNG14: Which patients with resectable synchronous or metachronous metastatic colon or rectal cancer are suitable for curative surgery?* Retrieved from https://wiki.cancer.org.au/australiawiki/index.php?oldid=173107

Kong, J. G., GG & Millen, RM, Roth, S., Xu,H..L., Neeson, P.N., Darcy, P.K., Kershaw, M.H., Sampurno, S., Malaterre, J., Liu, D.S., Pham, T., Wang, M., Huang, Y., Visvanathan,

K., McCormick, J., Lynch, A.C., Warrier, S., Michael, M., Desai, J., Murray, W., Mitchell, C., Ngan, S., Phillips, W.A., Heriot, A.G., Ramsay, R.G. . (2018). Tumor Infiltrating Lymphocyte Function Predicts Response to Neoadjuvant Chemoradiotherapy in Locally Advanced Rectal Cancer. *Journal of Clinical Oncology Precision Oncology, Accepted*.

Koopman, M., Kortman, G. A., Mekenkamp, L., Ligtenberg, M. J., Hoogerbrugge, N., Antonini, N. F., . . . van Krieken, J. H. (2009). Deficient mismatch repair system in patients with sporadic advanced colorectal cancer. *Br J Cancer, 100*(2), 266-273. doi:10.1038/sj.bjc.6604867

Kowanetz, M., Zou, W., Gettinger, S. N., Koeppen, H., Kockx, M., Schmid, P., . . . Hegde, P. S. (2018). Differential regulation of PD-L1 expression by immune and tumor cells in NSCLC and the response to treatment with atezolizumab (anti-PD-L1). *Proc Natl Acad Sci U S A, 115*(43), E10119-E10126. doi:10.1073/pnas.1802166115

Kumar, B. V., Ma, W., Miron, M., Granot, T., Guyer, R. S., Carpenter, D. J., . . . Farber, D. L. (2017). Human Tissue-Resident Memory T Cells Are Defined by Core Transcriptional and Functional Signatures in Lymphoid and Mucosal Sites. *Cell Rep, 20*(12), 2921-2934. doi:10.1016/j.celrep.2017.08.078

Kurioka, A., Ussher, J. E., Cosgrove, C., Clough, C., Fergusson, J. R., Smith, K., . . . Klenerman, P. (2015). MAIT cells are licensed through granzyme exchange to kill bacterially sensitized targets. *Mucosal Immunol, 8*(2), 429-440. doi:10.1038/mi.2014.81

Kwak, Y., Koh, J., Kim, D. W., Kang, S. B., Kim, W. H., & Lee, H. S. (2016). Immunoscore encompassing CD3+ and CD8+ T cell densities in distant metastasis is a robust prognostic marker for advanced colorectal cancer. *Oncotarget, 7*(49), 81778-81790. doi:10.18632/oncotarget.13207

Le Bourhis, L., Dusseaux, M., Bohineust, A., Bessoles, S., Martin, E., Premel, V., . . . Lantz, O. (2013). MAIT cells detect and efficiently lyse bacterially-infected epithelial cells. *PLoS Pathog, 9*(10), e1003681. doi:10.1371/journal.ppat.1003681

Le Bourhis, L., Martin, E., Peguillet, I., Guihot, A., Froux, N., Core, M., . . . Lantz, O. (2010). Antimicrobial activity of mucosal-associated invariant T cells. *Nat Immunol, 11*(8), 701-708. doi:10.1038/ni.1890

Le, D. T., Uram, J. N., Wang, H., Bartlett, B. R., Kemberling, H., Eyring, A. D., . . . Diaz, L. A., Jr. (2015). PD-1 Blockade in Tumors with Mismatch-Repair Deficiency. *N Engl J Med, 372*(26), 2509-2520. doi:10.1056/NEJMoa1500596

Leach, D. R., Krummel, M. F., & Allison, J. P. (1996). Enhancement of antitumor immunity by CTLA-4 blockade. *Science, 271*(5256), 1734-1736.

Leporrier, J., Maurel, J., Chiche, L., Bara, S., Segol, P., & Launoy, G. (2006). A population-based study of the incidence, management and prognosis of hepatic metastases from colorectal cancer. *Br J Surg, 93*(4), 465-474. doi:10.1002/bjs.5278

Ling, L., Lin, Y., Zheng, W., Hong, S., Tang, X., Zhao, P., . . . Jiang, Y. (2016). Circulating and tumor-infiltrating mucosal associated invariant T (MAIT) cells in colorectal cancer patients. *Sci Rep, 6*, 20358. doi:10.1038/srep20358

Linnekamp, J. F., Hooff, S. R. V., Prasetyanti, P. R., Kandimalla, R., Buikhuisen, J. Y., Fessler, E., . . . Medema, J. P. (2018). Consensus molecular subtypes of colorectal cancer are recapitulated in *in vitro* and *in vivo* models. *Cell Death Differ, 25*(3), 616-633. doi:10.1038/s41418-017-0011-5

Linsley, P. S., Brady, W., Grosmaire, L., Aruffo, A., Damle, N. K., & Ledbetter, J. A. (1991). Binding of the B cell activation antigen B7 to CD28 costimulates T cell proliferation and interleukin 2 mRNA accumulation. *J Exp Med, 173*(3), 721-730.

Linsley, P. S., Clark, E. A., & Ledbetter, J. A. (1990). T-cell antigen CD28 mediates adhesion with B cells by interacting with activation antigen B7/BB-1. *Proc Natl Acad Sci U S A, 87*(13), 5031-5035.

Liotta, L. A., & Kohn, E. C. (2001). The microenvironment of the tumour-host interface. *Nature, 411*(6835), 375-379. doi:10.1038/35077241

Loh, L., Wang, Z., Sant, S., Koutsakos, M., Jegaskanda, S., Corbett, A. J., . . . Kedzierska, K. (2016). Human mucosal-associated invariant T cells contribute to antiviral influenza

immunity via IL-18-dependent activation. *Proc Natl Acad Sci U S A, 113*(36), 10133-10138. doi:10.1073/pnas.1610750113

Luca Vigano, N. R., Alessandro Ferrero, Serena Langella, Elisa Sperti, and Lorenzo Capussotti. (2012). Evolution of Long-Term Outcome of Liver Resection for Colorectal Metastases: Analysis of Actual 5-Year Survival Rates over Two Decades. *Annals of Surgical Oncology, 19*, 2035–2044. doi:10.1245/s10434-011-2186-1

Maas, M., Beets-Tan, R. G., Lambregts, D. M., Lammering, G., Nelemans, P. J., Engelen, S. M., . . . Beets, G. L. (2011). Wait-and-see policy for clinical complete responders after chemoradiation for rectal cancer. *J Clin Oncol, 29*(35), 4633-4640. doi:10.1200/JCO.2011.37.7176

Maker, A. V., Ito, H., Mo, Q., Weisenberg, E., Qin, L. X., Turcotte, S., . . . D'Angelica, M. I. (2015). Genetic evidence that intratumoral T-cell proliferation and activation are associated with recurrence and survival in patients with resected colorectal liver metastases. *Cancer Immunol Res, 3*(4), 380-388. doi:10.1158/2326-6066.CIR-14-0212

Manfredi, S., Lepage, C., Hatem, C., Coatmeur, O., Faivre, J., & Bouvier, A. M. (2006). Epidemiology and management of liver metastases from colorectal cancer. *Ann Surg, 244*(2), 254-259. doi:10.1097/01.sla.0000217629.94941.cf

Martin, E., Treiner, E., Duban, L., Guerri, L., Laude, H., Toly, C., . . . Lantz, O. (2009). Stepwise development of MAIT cells in mouse and human. *PLoS Biol, 7*(3), e54. doi:10.1371/journal.pbio.1000054

Martin, R., Paty, P., Fong, Y., Grace, A., Cohen, A., DeMatteo, R., . . . Blumgart, L. (2003). Simultaneous liver and colorectal resections are safe for synchronous colorectal liver metastasis. *J Am Coll Surg, 197*(2), 233-241; discussion 241-232. doi:10.1016/S1072-7515(03)00390-9

Matzinger, P. (1994). Tolerance, danger, and the extended family. *Annu Rev Immunol, 12*, 991-1045. doi:10.1146/annurev.iy.12.040194.005015

Maughan, T. S., Adams, R. A., Smith, C. G., Meade, A. M., Seymour, M. T., Wilson, R. H., . . . Investigators, M. C. T. (2011). Addition of cetuximab to oxaliplatin-based first-line combination chemotherapy for treatment of advanced colorectal cancer: results of the randomised phase 3 MRC COIN trial. *Lancet, 377*(9783), 2103-2114. doi:10.1016/S0140-6736(11)60613-2

McWilliam, H. E., Eckle, S. B., Theodossis, A., Liu, L., Chen, Z., Wubben, J. M., . . . Villadangos, J. A. (2016). The intracellular pathway for the presentation of vitamin B-related antigens by the antigen-presenting molecule MR1. *Nat Immunol, 17*(5), 531-537. doi:10.1038/ni.3416

Medico, E., Russo, M., Picco, G., Cancelliere, C., Valtorta, E., Corti, G., . . . Bardelli, A. (2015). The molecular landscape of colorectal cancer cell lines unveils clinically actionable kinase targets. *Nat Commun, 6*, 7002. doi:10.1038/ncomms8002

Mendelsohn, J., & Baselga, J. (2000). The EGF receptor family as targets for cancer therapy. *Oncogene, 19*(56), 6550-6565. doi:10.1038/sj.onc.1204082

Michie, J., Beavis, P. A., Freeman, A. J., Vervoort, S. J., Ramsbottom, K. M., Narasimhan, V., . . . Oliaro, J. (2019). Antagonism of IAPs Enhances CAR T-cell Efficacy. *Cancer Immunol Res*. doi:10.1158/2326-6066.CIR-18-0428

Millen, R., Malaterre, J., Cross, R. S., Carpinteri, S., Desai, J., Tran, B., . . . Ramsay, R. G. (2016). Immunomodulation by MYB is associated with tumor relapse in patients with early stage colorectal cancer. *Oncoimmunology, 5*(7), e1149667. doi:10.1080/2162402X.2016.1149667

Mitry, E., Fields, A. L., Bleiberg, H., Labianca, R., Portier, G., Tu, D., . . . Rougier, P. (2008). Adjuvant chemotherapy after potentially curative resection of metastases from colorectal cancer: a pooled analysis of two randomized trials. *J Clin Oncol, 26*(30), 4906-4911. doi:10.1200/JCO.2008.17.3781

Mlecnik, B., Bindea, G., Angell, H. K., Maby, P., Angelova, M., Tougeron, D., . . . Galon, J. (2016). Integrative Analyses of Colorectal Cancer Show Immunoscore Is a Stronger Predictor of Patient Survival Than Microsatellite Instability. *Immunity, 44*(3), 698-711. doi:10.1016/j.immuni.2016.02.025

Mlecnik, B., Tosolini, M., Charoentong, P., Kirilovsky, A., Bindea, G., Berger, A., . . . Galon, J. (2010). Biomolecular network reconstruction identifies T-cell homing factors associated with survival in colorectal cancer. *Gastroenterology, 138*(4), 1429-1440. doi:10.1053/j.gastro.2009.10.057

Mlecnik, B., Van den Eynde, M., Bindea, G., Church, S. E., Vasaturo, A., Fredriksen, T., . . . Galon, J. (2018). Comprehensive Intrametastatic Immune Quantification and Major Impact of Immunoscore on Survival. *J Natl Cancer Inst, 110*(1). doi:10.1093/jnci/djx123

Morris, E. J., Forman, D., Thomas, J. D., Quirke, P., Taylor, E. F., Fairley, L., . . . Poston, G. (2010). Surgical management and outcomes of colorectal cancer liver metastases. *Br J Surg, 97*(7), 1110-1118. doi:10.1002/bjs.7032

Motzer, R. J., Tannir, N. M., McDermott, D. F., Aren Frontera, O., Melichar, B., Choueiri, T. K., . . . CheckMate, I. (2018). Nivolumab plus Ipilimumab versus Sunitinib in Advanced Renal-Cell Carcinoma. *N Engl J Med, 378*(14), 1277-1290. doi:10.1056/NEJMoa1712126

Mueller, D. L., Jenkins, M. K., & Schwartz, R. H. (1989). Clonal expansion versus functional clonal inactivation: a costimulatory signalling pathway determines the outcome of T cell antigen receptor occupancy. *Annu Rev Immunol, 7*, 445-480. doi:10.1146/annurev.iy.07.040189.002305

Murphy, K. M., Zhang, S., Geiger, T., Hafez, M. J., Bacher, J., Berg, K. D., & Eshleman, J. R. (2006). Comparison of the microsatellite instability analysis system and the Bethesda panel for the determination of microsatellite instability in colorectal cancers. *J Mol Diagn, 8*(3), 305-311. doi:10.2353/jmoldx.2006.050092

Nahas, C. S. R., Nahas, S. C., Ribeiro-Junior, U., Bustamante-Lopez, L., Marques, C. F. S., Pinto, R. A., . . . Cecconello, I. (2017). Prognostic factors affecting outcomes in multivisceral en bloc resection for colorectal cancer. *Clinics (Sao Paulo), 72*(5), 258-264. doi:10.6061/clinics/2017(05)01

Naito, Y., Saito, K., Shiiba, K., Ohuchi, A., Saigenji, K., Nagura, H., & Ohtani, H. (1998). CD8+ T cells infiltrated within cancer cell nests as a prognostic factor in human colorectal cancer. *Cancer Res, 58*(16), 3491-3494.

Nguyen, T. A., Yin, T. I., Reyes, D., & Urban, G. A. (2013). Microfluidic chip with integrated electrical cell-impedance sensing for monitoring single cancer cell migration in three-dimensional matrixes. *Anal Chem, 85*(22), 11068-11076. doi:10.1021/ac402761s

Nordlinger, B., Guiguet, M., Vaillant, J. C., Balladur, P., Boudjema, K., Bachellier, P., & Jaeck, D. (1996). Surgical resection of colorectal carcinoma metastases to the liver. A prognostic scoring system to improve case selection, based on 1568 patients. Association Francaise de Chirurgie. *Cancer, 77*(7), 1254-1262.

Nordlinger, B., Sorbye, H., Glimelius, B., Poston, G. J., Schlag, P. M., Rougier, P., . . . Federation Francophone de Cancerologie, D. (2008). Perioperative chemotherapy with FOLFOX4 and surgery versus surgery alone for resectable liver metastases from colorectal cancer (EORTC Intergroup trial 40983): a randomised controlled trial. *Lancet, 371*(9617), 1007-1016. doi:10.1016/S0140-6736(08)60455-9

Nordlinger, B., Sorbye, H., Glimelius, B., Poston, G. J., Schlag, P. M., Rougier, P., . . . Federation Francophone de Cancerologie, D. (2013). Perioperative FOLFOX4 chemotherapy and surgery versus surgery alone for resectable liver metastases from colorectal cancer (EORTC 40983): long-term results of a randomised, controlled, phase 3 trial. *Lancet Oncol, 14*(12), 1208-1215. doi:10.1016/S1470-2045(13)70447-9

Nott, L., Khattak, M, Price, T, Townsend, A, Cancer Council Australia Colorectal Cancer Guidelines Working Party. (2017). *Clinical practice guidelines for the prevention, early detection and management of colorectal cancer*. Retrieved from Sydney, Australia: https://wiki.cancer.org.au/australia/Guidelines:Colorectal_cancer/Systemic_chemotherapy_first-line_treatment

Novak, J., Dobrovolny, J., Brozova, J., Novakova, L., & Kozak, T. (2016). Recovery of mucosal-associated invariant T cells after myeloablative chemotherapy and autologous

peripheral blood stem cell transplantation. *Clin Exp Med, 16*(4), 529-537. doi:10.1007/s10238-015-0384-z

Nozaki, K., Mochizuki, W., Matsumoto, Y., Matsumoto, T., Fukuda, M., Mizutani, T., . . . Nakamura, T. (2016). Co-culture with intestinal epithelial organoids allows efficient expansion and motility analysis of intraepithelial lymphocytes. *J Gastroenterol, 51*(3), 206-213. doi:10.1007/s00535-016-1170-8

Okano, K., Maeba, T., Moroguchi, A., Ishimura, K., Karasawa, Y., Izuishi, K., . . . Maeta, H. (2003). Lymphocytic infiltration surrounding liver metastases from colorectal cancer. *J Surg Oncol, 82*(1), 28-33. doi:10.1002/jso.10188

Ong, M. L., & Schofield, J. B. (2016). Assessment of lymph node involvement in colorectal cancer. *World J Gastrointest Surg, 8*(3), 179-192. doi:10.4240/wjgs.v8.i3.179

Overman, M. J., McDermott, R., Leach, J. L., Lonardi, S., Lenz, H. J., Morse, M. A., . . . Andre, T. (2017). Nivolumab in patients with metastatic DNA mismatch repair-deficient or microsatellite instability-high colorectal cancer (CheckMate 142): an open-label, multicentre, phase 2 study. *Lancet Oncol, 18*(9), 1182-1191. doi:10.1016/S1470-2045(17)30422-9

Padman, S., Padbury, R., Beeke, C., Karapetis, C. S., Bishnoi, S., Townsend, A. R., . . . Price, T. J. (2013). Liver only metastatic disease in patients with metastatic colorectal cancer: impact of surgery and chemotherapy. *Acta Oncol, 52*(8), 1699-1706. doi:10.3109/0284186X.2013.831473

Pages, F., Berger, A., Camus, M., Sanchez-Cabo, F., Costes, A., Molidor, R., . . . Galon, J. (2005). Effector memory T cells, early metastasis, and survival in colorectal cancer. *N Engl J Med, 353*(25), 2654-2666. doi:10.1056/NEJMoa051424

Pages, F., Kirilovsky, A., Mlecnik, B., Asslaber, M., Tosolini, M., Bindea, G., . . . Galon, J. (2009). In situ cytotoxic and memory T cells predict outcome in patients with early-stage colorectal cancer. *J Clin Oncol, 27*(35), 5944-5951. doi:10.1200/JCO.2008.19.6147

Pages, F., Mlecnik, B., Marliot, F., Bindea, G., Ou, F. S., Bifulco, C., . . . Galon, J. (2018). International validation of the consensus Immunoscore for the classification of colon cancer: a prognostic and accuracy study. *Lancet, 391*(10135), 2128-2139. doi:10.1016/S0140-6736(18)30789-X

Pardoll, D. M. (2012). The blockade of immune checkpoints in cancer immunotherapy. *Nat Rev Cancer, 12*(4), 252-264. doi:10.1038/nrc3239

Patel, S. P., & Kurzrock, R. (2015). PD-L1 Expression as a Predictive Biomarker in Cancer Immunotherapy. *Mol Cancer Ther, 14*(4), 847-856. doi:10.1158/1535-7163.MCT-14-0983

Pattison, D. I., & Davies, M. J. (2006). Actions of ultraviolet light on cellular structures. *EXS*(96), 131-157.

Pauken, K. E., & Wherry, E. J. (2015). Overcoming T cell exhaustion in infection and cancer. *Trends Immunol, 36*(4), 265-276. doi:10.1016/j.it.2015.02.008

Peggs, K. S., Quezada, S. A., Korman, A. J., & Allison, J. P. (2006). Principles and use of anti-CTLA4 antibody in human cancer immunotherapy. *Curr Opin Immunol, 18*(2), 206-213. doi:10.1016/j.coi.2006.01.011

Pegram, H. J., Andrews, D. M., Smyth, M. J., Darcy, P. K., & Kershaw, M. H. (2011). Activating and inhibitory receptors of natural killer cells. *Immunol Cell Biol, 89*(2), 216-224. doi:10.1038/icb.2010.78

Peper, J. K., Schuster, H., Loffler, M. W., Schmid-Horch, B., Rammensee, H. G., & Stevanovic, S. (2014). An impedance-based cytotoxicity assay for real-time and label-free assessment of T-cell-mediated killing of adherent cells. *J Immunol Methods, 405*, 192-198. doi:10.1016/j.jim.2014.01.012

Peterson, L. W., & Artis, D. (2014). Intestinal epithelial cells: regulators of barrier function and immune homeostasis. *Nat Rev Immunol, 14*(3), 141-153. doi:10.1038/nri3608

Porru, M., Pompili, L., Caruso, C., Biroccio, A., & Leonetti, C. (2018). Targeting KRAS in metastatic colorectal cancer: current strategies and emerging opportunities. *J Exp Clin Cancer Res, 37*(1), 57. doi:10.1186/s13046-018-0719-1

Quill, H., & Schwartz, R. H. (1987). Stimulation of normal inducer T cell clones with antigen presented by purified Ia molecules in planar lipid membranes: specific induction of a long-lived state of proliferative nonresponsiveness. *J Immunol, 138*(11), 3704-3712.

Racanelli, V., & Rehermann, B. (2006). The liver as an immunological organ. *Hepatology, 43*(2 Suppl 1), S54-62. doi:10.1002/hep.21060

Reantragoon, R., Corbett, A. J., Sakala, I. G., Gherardin, N. A., Furness, J. B., Chen, Z., . . . Kjer-Nielsen, L. (2013). Antigen-loaded MR1 tetramers define T cell receptor heterogeneity in mucosal-associated invariant T cells. *J Exp Med, 210*(11), 2305-2320. doi:10.1084/jem.20130958

Ribas, A., Camacho, L. H., Lopez-Berestein, G., Pavlov, D., Bulanhagui, C. A., Millham, R., . . . Gomez-Navarro, J. (2005). Antitumor activity in melanoma and anti-self responses in a phase I trial with the anti-cytotoxic T lymphocyte-associated antigen 4 monoclonal antibody CP-675,206. *J Clin Oncol, 23*(35), 8968-8977. doi:10.1200/JCO.2005.01.109

Roda, J. M., Joshi, T., Butchar, J. P., McAlees, J. W., Lehman, A., Tridandapani, S., & Carson, W. E., 3rd. (2007). The activation of natural killer cell effector functions by cetuximab-coated, epidermal growth factor receptor positive tumor cells is enhanced by cytokines. *Clin Cancer Res, 13*(21), 6419-6428. doi:10.1158/1078-0432.CCR-07-0865

Ropponen, K. M., Eskelinen, M. J., Lipponen, P. K., Alhava, E., & Kosma, V. M. (1997). Prognostic value of tumour-infiltrating lymphocytes (TILs) in colorectal cancer. *J Pathol, 182*(3), 318-324. doi:10.1002/(SICI)1096-9896(199707)182:3<318::AID-PATH862>3.0.CO;2-6

Rougier, P., Milan, C., Lazorthes, F., Fourtanier, G., Partensky, C., Baumel, H., & Faivre, J. (1995). Prospective study of prognostic factors in patients with unresected hepatic metastases from colorectal cancer. Fondation Francaise de Cancerologie Digestive. *Br J Surg, 82*(10), 1397-1400.

Ruggeri, L., Capanni, M., Urbani, E., Perruccio, K., Shlomchik, W. D., Tosti, A., . . . Velardi, A. (2002). Effectiveness of donor natural killer cell alloreactivity in mismatched hematopoietic transplants. *Science, 295*(5562), 2097-2100. doi:10.1126/science.1068440

Ryan, J. E., Warrier, S. K., Lynch, A. C., & Heriot, A. G. (2015). Assessing pathological complete response to neoadjuvant chemoradiotherapy in locally advanced rectal cancer: a systematic review. *Colorectal Dis, 17*(10), 849-861. doi:10.1111/codi.13081

Sato, T., van Es, J. H., Snippert, H. J., Stange, D. E., Vries, R. G., van den Born, M., . . . Clevers, H. (2011). Paneth cells constitute the niche for Lgr5 stem cells in intestinal crypts. *Nature, 469*(7330), 415-418. doi:10.1038/nature09637

Sato, T., Vries, R. G., Snippert, H. J., van de Wetering, M., Barker, N., Stange, D. E., . . . Clevers, H. (2009). Single Lgr5 stem cells build crypt-villus structures *in vitro* without a mesenchymal niche. *Nature, 459*(7244), 262-265. doi:10.1038/nature07935

Sattler, A., Dang-Heine, C., Reinke, P., & Babel, N. (2015). IL-15 dependent induction of IL-18 secretion as a feedback mechanism controlling human MAIT-cell effector functions. *Eur J Immunol, 45*(8), 2286-2298. doi:10.1002/eji.201445313

Segal, N. H., Parsons, D. W., Peggs, K. S., Velculescu, V., Kinzler, K. W., Vogelstein, B., & Allison, J. P. (2008). Epitope landscape in breast and colorectal cancer. *Cancer Res, 68*(3), 889-892. doi:10.1158/0008-5472.CAN-07-3095

Serriari, N. E., Eoche, M., Lamotte, L., Lion, J., Fumery, M., Marcelo, P., . . . Treiner, E. (2014). Innate mucosal-associated invariant T (MAIT) cells are activated in inflammatory bowel diseases. *Clin Exp Immunol, 176*(2), 266-274. doi:10.1111/cei.12277

Shaler, C. R., Choi, J., Rudak, P. T., Memarnejadian, A., Szabo, P. A., Tun-Abraham, M. E., . . . Haeryfar, S. M. M. (2017). MAIT cells launch a rapid, robust and distinct hyperinflammatory response to bacterial superantigens and quickly acquire an anergic phenotype that impedes their cognate antimicrobial function: Defining a novel mechanism of superantigen-induced immunopathology and immunosuppression. *PLoS Biol, 15*(6), e2001930. doi:10.1371/journal.pbio.2001930

Shaler, C. R., Tun-Abraham, M. E., Skaro, A. I., Khazaie, K., Corbett, A. J., Mele, T., . . . Haeryfar, S. M. M. (2017). Mucosa-associated invariant T cells infiltrate hepatic metastases in patients with colorectal carcinoma but are rendered dysfunctional within and adjacent to tumor microenvironment. *Cancer Immunol Immunother*. doi:10.1007/s00262-017-2050-7

Shankaran, V., Ikeda, H., Bruce, A. T., White, J. M., Swanson, P. E., Old, L. J., & Schreiber, R. D. (2001). IFNgamma and lymphocytes prevent primary tumour development and shape tumour immunogenicity. *Nature, 410*(6832), 1107-1111. doi:10.1038/35074122

Sheth, K., & Bankey, P. (2001). The liver as an immune organ. *Curr Opin Crit Care, 7*(2), 99-104.

Shibutani, M., Maeda, K., Nagahara, H., Fukuoka, T., Matsutani, S., Kashiwagi, S., . . . Ohira, M. (2018). A comparison of the local immune status between the primary and metastatic tumor in colorectal cancer: a retrospective study. *BMC Cancer, 18*(1), 371. doi:10.1186/s12885-018-4276-y

Silberhumer, G. R., Paty, P. B., Temple, L. K., Araujo, R. L., Denton, B., Gonen, M., . . . Fong, Y. (2015). Simultaneous resection for rectal cancer with synchronous liver metastasis is a safe procedure. *Am J Surg, 209*(6), 935-942. doi:10.1016/j.amjsurg.2014.09.024

Simoni, Y., Becht, E., Fehlings, M., Loh, C. Y., Koo, S. L., Teng, K. W. W., . . . Newell, E. W. (2018). Bystander CD8(+) T cells are abundant and phenotypically distinct in human tumour infiltrates. *Nature, 557*(7706), 575-579. doi:10.1038/s41586-018-0130-2

Sinicrope, F. A., Rego, R. L., Halling, K. C., Foster, N., Sargent, D. J., La Plant, B., . . . Witzig, T. E. (2006). Prognostic impact of microsatellite instability and DNA ploidy in human colon carcinoma patients. *Gastroenterology, 131*(3), 729-737. doi:10.1053/j.gastro.2006.06.005

Smith, F. M., Wiland, H., Mace, A., Pai, R. K., & Kalady, M. F. (2014). Clinical criteria underestimate complete pathological response in rectal cancer treated with neoadjuvant chemoradiotherapy. *Dis Colon Rectum, 57*(3), 311-315. doi:10.1097/DCR.0b013e3182a84eba

Smyrk, T. C., Watson, P., Kaul, K., & Lynch, H. T. (2001). Tumor-infiltrating lymphocytes are a marker for microsatellite instability in colorectal carcinoma. *Cancer, 91*(12), 2417-2422.

Smyth, M. J., & Trapani, J. A. (2001). Lymphocyte-mediated immunosurveillance of epithelial cancers? *Trends Immunol, 22*(8), 409-411.

Song, L., Asgharzadeh, S., Salo, J., Engell, K., Wu, H. W., Sposto, R., . . . Metelitsa, L. S. (2009). Valpha24-invariant NKT cells mediate antitumor activity via killing of tumor-associated macrophages. *J Clin Invest, 119*(6), 1524-1536. doi:10.1172/JCI37869

Spear, P., Wu, M. R., Sentman, M. L., & Sentman, C. L. (2013). NKG2D ligands as therapeutic targets. *Cancer Immun, 13*, 8.

Stewart, B. W., Wild, C. P. (2014a). *World Cancer Report 2014*. Retrieved from

Stewart, B. W., Wild, C. P. (2014b). *World Cancer Report 2014*. Retrieved from

Stingl, J., Eaves, C. J., Zandieh, I., & Emerman, J. T. (2001). Characterization of bipotent mammary epithelial progenitor cells in normal adult human breast tissue. *Breast Cancer Res Treat, 67*(2), 93-109.

Stolk, D., van der Vliet, H. J., de Gruijl, T. D., van Kooyk, Y., & Exley, M. A. (2018). Positive & Negative Roles of Innate Effector Cells in Controlling Cancer Progression. *Front Immunol, 9*, 1990. doi:10.3389/fimmu.2018.01990

Sugawara, S., Takeda, K., Lee, A., & Dennert, G. (1993). Suppression of stress protein GRP78 induction in tumor B/C10ME eliminates resistance to cell mediated cytotoxicity. *Cancer Res, 53*(24), 6001-6005.

Sundstrom, P., Ahlmanner, F., Akeus, P., Sundquist, M., Alsen, S., Yrlid, U., . . . Quiding-Jarbrink, M. (2015). Human Mucosa-Associated Invariant T Cells Accumulate in Colon Adenocarcinomas but Produce Reduced Amounts of IFN-gamma. *J Immunol, 195*(7), 3472-3481. doi:10.4049/jimmunol.1500258

Supernat, A., Lapinska-Szumczyk, S., Sawicki, S., Wydra, D., Biernat, W., & Zaczek, A. J. (2012). Deregulation of RAD21 and RUNX1 expression in endometrial cancer. *Oncol Lett, 4*(4), 727-732. doi:10.3892/ol.2012.794

Talmadge, J. E., & Fidler, I. J. (2010). AACR centennial series: the biology of cancer metastasis: historical perspective. *Cancer Res, 70*(14), 5649-5669. doi:10.1158/0008-5472.CAN-10-1040

Tang, F., & Zheng, P. (2018). Tumor cells versus host immune cells: whose PD-L1 contributes to PD-1/PD-L1 blockade mediated cancer immunotherapy? *Cell Biosci, 8*, 34. doi:10.1186/s13578-018-0232-4

Tang, X. Z., Jo, J., Tan, A. T., Sandalova, E., Chia, A., Tan, K. C., . . . Bertoletti, A. (2013). IL-7 licenses activation of human liver intrasinusoidal mucosal-associated invariant T cells. *J Immunol, 190*(7), 3142-3152. doi:10.4049/jimmunol.1203218

Tauriello, D. V. F., Palomo-Ponce, S., Stork, D., Berenguer-Llergo, A., Badia-Ramentol, J., Iglesias, M., . . . Batlle, E. (2018). TGFbeta drives immune evasion in genetically reconstituted colon cancer metastasis. *Nature, 554*(7693), 538-543. doi:10.1038/nature25492

Terme, M., Ullrich, E., Aymeric, L., Meinhardt, K., Desbois, M., Delahaye, N., . . . Zitvogel, L. (2011). IL-18 induces PD-1-dependent immunosuppression in cancer. *Cancer Res, 71*(16), 5393-5399. doi:10.1158/0008-5472.CAN-11-0993

Thibodeau, S. N., Bren, G., & Schaid, D. (1993). Microsatellite instability in cancer of the proximal colon. *Science, 260*(5109), 816-819.

Thornton, M., Aslam, M. A., Tweedle, E. M., Ang, C., Campbell, F., Jackson, R., . . . Boyd, M. T. (2013). The unfolded protein response regulator GRP78 is a novel predictive biomarker in colorectal cancer. *Int J Cancer, 133*(6), 1408-1418. doi:10.1002/ijc.28137

Tilloy, F., Treiner, E., Park, S. H., Garcia, C., Lemonnier, F., de la Salle, H., . . . Lantz, O. (1999). An invariant T cell receptor alpha chain defines a novel TAP-independent major histocompatibility complex class Ib-restricted alpha/beta T cell subpopulation in mammals. *J Exp Med, 189*(12), 1907-1921.

Timmermann, B., Kerick, M., Roehr, C., Fischer, A., Isau, M., Boerno, S. T., . . . Schweiger, M. R. (2010). Somatic mutation profiles of MSI and MSS colorectal cancer identified by whole exome next generation sequencing and bioinformatics analysis. *PLoS One, 5*(12), e15661. doi:10.1371/journal.pone.0015661

Tomlinson JS1, J. W., DeMatteo RP, Fong Y, Kornprat P, Gonen M, Kemeny N, Brennan MF, Blumgart LH, D'Angelica M. (2007). Actual 10-year survival after resection of colorectal liver metastases defines cure. *Journal of Clinical Oncology, 25*(29), 4575-4580.

Topalian, S. L., Hodi, F. S., Brahmer, J. R., Gettinger, S. N., Smith, D. C., McDermott, D. F., . . . Sznol, M. (2012). Safety, activity, and immune correlates of anti-PD-1 antibody in cancer. *N Engl J Med, 366*(26), 2443-2454. doi:10.1056/NEJMoa1200690

Townsend, S. E., & Allison, J. P. (1993). Tumor rejection after direct costimulation of CD8+ T cells by B7-transfected melanoma cells. *Science, 259*(5093), 368-370.

Tranchart, H., Chirica, M., Faron, M., Balladur, P., Lefevre, L. B., Svrcek, M., . . . Paye, F. (2013). Prognostic impact of positive surgical margins after resection of colorectal cancer liver metastases: reappraisal in the era of modern chemotherapy. *World J Surg, 37*(11), 2647-2654. doi:10.1007/s00268-013-2186-3

Tumeh, P. C., Harview, C. L., Yearley, J. H., Shintaku, I. P., Taylor, E. J., Robert, L., . . . Ribas, A. (2014). PD-1 blockade induces responses by inhibiting adaptive immune resistance. *Nature, 515*(7528), 568-571. doi:10.1038/nature13954

Tziris, N., Dokmetzioglou, J., Giannoulis, K., Kesisoglou, I., Sapalidis, K., Kotidis, E., & Gambros, O. (2008). Synchronous and metachronous adenocarcinomas of the large intestine. *Hippokratia, 12*(3), 150-152.

UK, C. R. (2019). Worldwide cancer statistics. Retrieved from https://www.cancerresearchuk.org/health-professional/cancer-statistics/worldwide-cancer

Ussher, J. E., Willberg, C. B., & Klenerman, P. (2018). MAIT cells and viruses. *Immunol Cell Biol, 96*(6), 630-641. doi:10.1111/imcb.12008

Van Cutsem, E., Cervantes, A., Adam, R., Sobrero, A., Van Krieken, J. H., Aderka, D., . . . Arnold, D. (2016). ESMO consensus guidelines for the management of patients with metastatic colorectal cancer. *Ann Oncol, 27*(8), 1386-1422. doi:10.1093/annonc/mdw235

Van Cutsem, E., Lenz, H. J., Kohne, C. H., Heinemann, V., Tejpar, S., Melezinek, I., . . . Ciardiello, F. (2015). Fluorouracil, leucovorin, and irinotecan plus cetuximab treatment and RAS mutations in colorectal cancer. *J Clin Oncol, 33*(7), 692-700. doi:10.1200/JCO.2014.59.4812

van Wilgenburg, B., Scherwitzl, I., Hutchinson, E. C., Leng, T., Kurioka, A., Kulicke, C., . . . Klenerman, P. (2016). MAIT cells are activated during human viral infections. *Nat Commun, 7*, 11653. doi:10.1038/ncomms11653

Vandeweyer, D., Neo, E. L., Chen, J. W., Maddern, G. J., Wilson, T. G., & Padbury, R. T. (2009). Influence of resection margin on survival in hepatic resections for colorectal liver metastases. *HPB (Oxford), 11*(6), 499-504. doi:10.1111/j.1477-2574.2009.00092.x

Vasen, H. F., Watson, P., Mecklin, J. P., & Lynch, H. T. (1999). New clinical criteria for hereditary nonpolyposis colorectal cancer (HNPCC, Lynch syndrome) proposed by the International Collaborative group on HNPCC. *Gastroenterology, 116*(6), 1453-1456.

Vassiliou, I., Arkadopoulos, N., Theodosopoulos, T., Fragulidis, G., Marinis, A., Kondi-Paphiti, A., . . . Smyrniotis, V. (2007). Surgical approaches of resectable synchronous colorectal liver metastases: timing considerations. *World J Gastroenterol, 13*(9), 1431-1434.

Veluchamy, J. P., Spanholtz, J., Tordoir, M., Thijssen, V. L., Heideman, D. A., Verheul, H. M., . . . van der Vliet, H. J. (2016). Combination of NK Cells and Cetuximab to Enhance Anti-Tumor Responses in RAS Mutant Metastatic Colorectal Cancer. *PLoS One, 11*(6), e0157830. doi:10.1371/journal.pone.0157830

Verneris, M. R., Karimi, M., Baker, J., Jayaswal, A., & Negrin, R. S. (2004). Role of NKG2D signaling in the cytotoxicity of activated and expanded CD8+ T cells. *Blood, 103*(8), 3065-3072. doi:10.1182/blood-2003-06-2125

Vogelstein, B., Fearon, E. R., Hamilton, S. R., Kern, S. E., Preisinger, A. C., Leppert, M., . . . Bos, J. L. (1988). Genetic alterations during colorectal-tumor development. *N Engl J Med, 319*(9), 525-532. doi:10.1056/NEJM198809013190901

Voillet, V., Buggert, M., Slichter, C. K., Berkson, J. D., Mair, F., Addison, M. M., . . . Prlic, M. (2018). Human MAIT cells exit peripheral tissues and recirculate via lymph in steady state conditions. *JCI Insight, 3*(7). doi:10.1172/jci.insight.98487

von Roon, A. C., Reese, G., Teare, J., Constantinides, V., Darzi, A. W., & Tekkis, P. P. (2007). The risk of cancer in patients with Crohn's disease. *Dis Colon Rectum, 50*(6), 839-855. doi:10.1007/s10350-006-0848-z

Wagner, P., Koch, M., Nummer, D., Palm, S., Galindo, L., Autenrieth, D., . . . Weitz, J. (2008). Detection and functional analysis of tumor infiltrating T-lymphocytes (TIL) in liver metastases from colorectal cancer. *Ann Surg Oncol, 15*(8), 2310-2317. doi:10.1245/s10434-008-9971-5

Wang, M., Zhao, X. R., Wang, P., Li, L., Dai, Y., Huang, H., . . . Shen, G. X. (2007). Glucose regulated proteins 78 protects insulinoma cells (NIT-1) from death induced by streptozotocin, cytokines or cytotoxic T lymphocytes. *Int J Biochem Cell Biol, 39*(11), 2076-2082. doi:10.1016/j.biocel.2007.05.022

Weber, J. C., Bachellier, P., Oussoultzoglou, E., & Jaeck, D. (2003). Simultaneous resection of colorectal primary tumour and synchronous liver metastases. *Br J Surg, 90*(8), 956-962. doi:10.1002/bjs.4132

Welfare, A. I. o. H. a. (2014). Cancer in Australia: an overview, 2014. *Cancer series no. 78.* Retrieved from https://canceraustralia.gov.au/affected-cancer/cancer-types/bowel-cancer/bowel-cancer-statistics

Williams, D. S., Bird, M. J., Jorissen, R. N., Yu, Y. L., Walker, F., Zhang, H. H., . . . Burgess, A. W. (2010). Nonsense mediated decay resistant mutations are a source of expressed

mutant proteins in colon cancer cell lines with microsatellite instability. *PLoS One, 5*(12), e16012. doi:10.1371/journal.pone.0016012
Williams, S. A., Anderson, W. C., Santaguida, M. T., & Dylla, S. J. (2013). Patient-derived xenografts, the cancer stem cell paradigm, and cancer pathobiology in the 21st century. *Lab Invest, 93*(9), 970-982. doi:10.1038/labinvest.2013.92
Wood, L. D., Parsons, D. W., Jones, S., Lin, J., Sjoblom, T., Leary, R. J., . . . Vogelstein, B. (2007). The genomic landscapes of human breast and colorectal cancers. *Science, 318*(5853), 1108-1113. doi:10.1126/science.1145720
Wortzel, R. D., Philipps, C., & Schreiber, H. (1983). Multiple tumour-specific antigens expressed on a single tumour cell. *Nature, 304*(5922), 165-167.
Wright, C. M., Dent, O. F., Barker, M., Newland, R. C., Chapuis, P. H., Bokey, E. L., . . . Macdonald, G. A. (2000). Prognostic significance of extensive microsatellite instability in sporadic clinicopathological stage C colorectal cancer. *Br J Surg, 87*(9), 1197-1202. doi:10.1046/j.1365-2168.2000.01508.x
Wu, J., & Lanier, L. L. (2003). Natural killer cells and cancer. *Adv Cancer Res, 90*, 127-156.
Xu, H., Balakrishnan, K., Malaterre, J., Beasley, M., Yan, Y., Essers, J., . . . McKay, M. J. (2010). Rad21-cohesin haploinsufficiency impedes DNA repair and enhances gastrointestinal radiosensitivity in mice. *PLoS One, 5*(8), e12112. doi:10.1371/journal.pone.0012112
Yoong, K. F., & Adams, D. H. (1998). Interleukin 2 restores CD3-zeta chain expression but fails to generate tumour-specific lytic activity in tumour-infiltrating lymphocytes derived from human colorectal hepatic metastases. *Br J Cancer, 77*(7), 1072-1081.
Young, J., Simms, L. A., Biden, K. G., Wynter, C., Whitehall, V., Karamatic, R., . . . Jass, J. R. (2001). Features of colorectal cancers with high-level microsatellite instability occurring in familial and sporadic settings: parallel pathways of tumorigenesis. *Am J Pathol, 159*(6), 2107-2116. doi:10.1016/S0002-9440(10)63062-3
Zabijak, L., Attencourt, C., Guignant, C., Chatelain, D., Marcelo, P., Marolleau, J. P., & Treiner, E. (2015). Increased tumor infiltration by mucosal-associated invariant T cells correlates with poor survival in colorectal cancer patients. *Cancer Immunol Immunother, 64*(12), 1601-1608. doi:10.1007/s00262-015-1764-7
Zdanov, S., Mandapathil, M., Abu Eid, R., Adamson-Fadeyi, S., Wilson, W., Qian, J., . . . Khleif, S. N. (2016). Mutant KRAS Conversion of Conventional T Cells into Regulatory T Cells. *Cancer Immunol Res, 4*(4), 354-365. doi:10.1158/2326-6066.CIR-15-0241
Zeman, M., Maciejewski, A., Poltorak, S., & Kryj, M. (2013). Evaluation of outcomes and treatment safety of patients with metastatic colorectal cancer to the liver with estimation of prognostic factors. *Pol Przegl Chir, 85*(6), 333-339. doi:10.2478/pjs-2013-0050